

BIODYNAMIC RESPONSES OF THE SEATED OCCUPANTS TO MULTI-AXIS WHOLE-BODY VIBRATION

Santosh Chary Mandapuram

A Thesis
In
The department
of
Mechanical and Industrial Engineering

Presented in Partial fulfillment of the requirements
for the Degree of Doctor of Philosophy at
Concordia University
Montreal, Quebec, Canada

November, 2012.

©Santosh Chary Mandapuram, 2012.

CONCORDIA UNIVERSITY
SCHOOL OF GRADUATE STUDIES

This is to certify that the thesis prepared

By: **Santosh Chary Mandapuram**

Entitled: **Biodynamic Responses of the Seated Occupants to Multi-Axis Whole-Body Vibration**

and submitted in partial fulfillment of the requirements for the degree of

DOCTOR OF PHILOSOPHY (Mechanical Engineering)

complies with the regulations of the university and meets the accepted standards with respect to originality and quality.

Signed by the final examining committee:

_____	Chair
Dr. Elektorowicz	
_____	External examiner
Dr. Mansfield	
_____	External to program
Dr. Bagchi	
_____	Examiner
Dr. Gouw	
_____	Examiner
Dr. Su	
_____	Thesis Co-Supervisor
Dr. Rakheja	
_____	Thesis Co-Supervisor
Dr. Boileau	

Approved by _____
Dr. Ali Dolatabadi, Graduate Program Director

November 29, 2012

Dr. Robin A. L. Drew, Dean of faculty
Faculty of Engineer & Computer Science

ABSTRACT

“Biodynamic Responses of the Seated Occupants to Multi-Axis Whole-Body Vibration”

Santosh Chary Mandapuram, Ph. D.
Concordia University, 2012.

Occupational on-road and off-road vehicle operators are exposed to low frequency whole-body vibration (WBV) of comprehensive magnitudes, and have shown a high prevalence of back disorders. Characterisation of seated body biodynamics response is considered vital for assessing potential injury risks of WBV and for developing effective biomechanical models for integration in the primary and secondary suspension design processes. The seated body biodynamic responses to single axis vibration have been investigated widely under vertical axis and a few under individual horizontal axis. The responses to simultaneous three-axis vibration, as encountered during vehicle driving, however, have been investigated in two recent studies. In this dissertation research, the biodynamic responses of seated body exposed to single as well as multiple axis vibration are characterised in terms of the apparent mass (APMS), vibration power absorbed (VPA) and seat-to-head vibration transmissibility (STHT) responses with both hands and back supports. The APMS responses are characterised considering two-driving-points formed by the buttocks-pan and upper-body backrest interfaces to fully describe the body-seat interactions. This study proposes a method to determine the total seated body APMS response from the forces measured at the two-driving points. Furthermore, it is shown that the commonly used frequency-response-function (H_I), would suppress the contributions of the cross-axis responses under uncorrelated simultaneous multi-axis excitations. Consequently an alternative frequency response estimator (H_v) is applied for analyses of responses to uncorrelated multi-axis. The results obtained, clearly revealed the contributions of cross-axis responses, which were not

evident in the reported responses derived using H_1 function estimator. Further, it is shown that the total response along an axis can be estimated from super position of the direct and cross-axis response components along the same axis.

The seat-to-head vibration (STHT) transmissibility responses are also obtained so as to obtain additional target functions for defining the biodynamic models. The STHT responses also revealed considerable coupling effects of multi-axis vibration, when H_v function estimator is applied. The total VPA of the body under multi-axis is further derived considering the power absorption attributed to cross-axis body responses. A methodology is proposed to derive frequency-weightings similar to those in ISO 2631-1 using the absorbed power responses. Thus derived weightings based on total responses of the seated body under multi-axis uncorrelated vibration, are proposed to better evaluate the vibration exposure risk due to the whole-body multi-axis vibration. The results of the study suggest that the frequency-weightings derived for the back supported postures differ substantially from the current standardised weighting. The current weighting is thus believed to be applicable only for back unsupported sitting conditions.

ACKNOWLEDGEMENTS

My affectionate appreciations to my family: mother, father and sisters who have been supportive in my endeavors, all throughout. I am thankful to my wife for bearing with me during thesis writing phase.

I am sincerely grateful to my supervisors, Dr. Rakheja and Dr. Boileau, for their continued guidance and encouragement throughout the course of this research and during the preparation of this thesis.

My appreciations to following who have contributed greatly for this research:

Dr. Dong from NIOSH (National Institute of Occupational safety and Health, USA), for his technical inputs.

Dr. Maeda and Dr. Shibata for their lab facility and hosting me at JNIOOSH (National Institute of Occupational safety and Health, Japan).

Professor Dickey for his lab facility, hosting me and his help during my preliminary experiments in his lab at University of Guelph, Ontario.

Dr. Marcotte from IRSST (Institut de recherche Robert-Sauvé en santé et en sécurité du travail).

Mr. Esteves and Mr. Juras, members and staff for their assistance at CONCAVE (Concordia centre for Advanced Vehicle Engineering) Research Centre, Concordia University.

My special appreciations to friends who voluntarily participated in my experiments and students who were hired for experiments in Japan.

Last but not the least, I am thankful to my friends and well wishers for their positive energy during this thesis.

CONTENTS

ABSTRACT	iii
ACKNOWLEDGEMENTS	v
TABLE OF CONTENTS	vi
LIST OF FIGURES	ix
LIST OF TABLES	xvi
CHAPTER 1 INTRODUCTION AND SCOPE OF DISSERTATION	
1.1 INTRODUCTION	1
1.2 REVIEW OF RELEVANT LITERATURE	3
1.2.1 Vehicle vibration environment	5
1.2.2 Biodynamic measures and measurement methods	7
1.2.3 Characterisation of seated body biodynamic responses	12
1.2.4 Biodynamic responses to Multi-axis WBV	28
1.2.5 Biodynamic modelling	33
1.3 SCOPE AND OBJECTIVES OF DISSERTATION RESEARCH	35
1.4 ORGANIZATION OF THE DISERTATION	36
CHAPTER 2 CHARACTERIZATION OF SEATED BODY BIODYNAMIC RESPONSES TO MULTI-AXIS VIBRATION	
2.1 GENERAL	38
2.2 RESPONSES OF SEATED OCCUPANTS UNDER SINGLE AND DUAL AXIS HORIZONTAL VIBRATION	38
2.3 BIODYNAMIC RESPONSES TO UNCORRELATED FORE-AFT AND VERTICAL WHOLE-BODY VIBRATION	44
2.4 BIODYNAMIC RESPONSES OF SEATED BODY TO THREE TRANSLATIONAL AXIS VIBRATION	46
2.5 ABSORBED POWER ANALYSES TO MULTI-AXIS VIBRATION	47
2.6 ABSORBED POWER BASED FREQUENCY WEIGHTINGS	47
CHAPTER 3 APPARENT MASS AND SEAT TO HEAD TRANSMISSIBILITY RESPONSES OF SEATED OCCUPANTS UNDER SINGLE AND DUAL AXIS HORIZONTAL VIBRATION	
3.1 INTRODUCTION	49
3.2 METHODS	53
3.2.1 Exposure conditions and subjects	53
3.2.2 Data acquisition and analyses	55
3.2.3 Total Seatpan APMS response	57
3.2.4 Normalisation factors	60
3.2.5 Relationship between responses to single- and dual-axis vibration	63
3.3 RESULTS	65
3.3.1 Apparent mass responses	69
3.3.2 Seat-to-head-transmissibility responses	73
3.3.3 Effect of hands position	76

3.3.4	Effect of back support	79
3.3.5	Effect of excitation magnitude	82
3.4	DISCUSSIONS	82
CHAPTER 4	ANALYSES OF BIODYNAMIC RESPONSES OF SEATED OCCUPANTS TO UNCORRELATED FORE-AFT AND VERTICAL WHOLE-BODY VIBRATION	
4.1	INTRODUCTION	88
4.2	METHOD	93
4.3	DATA ANALYSIS	96
4.3.1	Analyses of biodynamic responses to multi-axis vibration	97
4.3.2	PSD method of analysis	101
4.3.3	H _v Estimator	101
4.4	NORMALISATION FACTORS	102
4.5	RESULTS	103
4.6	DISCUSSIONS	114
4.6.1	Effects of supports	116
4.6.2	Vibration magnitude effect	118
4.7	CONCLUSIONS	119
CHAPTER 5	APPARENT MASS AND HEAD VIBRATION TRANSMISSION RESPONSES OF SEATED BODY TO THREE TRANSLATIONAL AXIS VIBRATION	
5.1	INTRODUCTION	120
5.2	METHOD	124
5.3	DATA ANALYSIS	126
5.3.1	Analyses of biodynamic responses to three-axis vibration	126
5.4	APMS NORMALISATION FACTORS	128
5.5	RESULTS	129
5.6	DISCUSSIONS	137
5.6.1	Effect of three-axis vibration	138
5.6.2	Effects of supports	140
5.7	CONCLUSIONS	142
CHAPTER 6	ENERGY ABSORPTION OF SEATED BODY EXPOSED TO SINGLE AND THREE-AXIS WHOLE BODY VIBRATION	
6.1	INTRODUCTION	144
6.2	METHOD	148
6.3	DATA ANALYSIS	149
6.3.1	Analyses of absorbed power responses to three-axis vibration	151
6.3.2	Estimation of power absorbed under vehicular vibration	153
6.4	RESULTS	155
6.5	RELATIVE VPA CHARACTERISTICS UNDER VEHICULAR VIBRATION	161
6.6	DISCUSSION	163
6.7	CONCLUSIONS	167

CHAPTER 7	ENERGY ABSORPTION OF SEATED OCCUPANTS EXPOSED TO HORIZONTAL VIBRATION AND ROLE OF BACK SUPPORT	
7.1	INTRODUCTION	168
7.2	METHOD	173
7.3	ANALYSIS OF ABSORBED POWER	176
7.4	RESULTS AND DISCUSSIONS	181
7.4.1	Normalization of the measured absorbed power response	187
7.4.2	Effect of vibration magnitude	188
7.4.3	Effect of posture	191
7.4.4	Effect of seat height	194
7.5	DISCUSSIONS IN VIEW OF THE REPORTED RESULTS	195
7.5.1	A Discussion on Frequency-Weighting of Vibration Power Absorption (VPA)	196
7.6	CONCLUSIONS	200
CHAPTER 8	CONCLUSIONS AND RECOMMENDATIONS FOR FUTURE WORK	
8.1	MAJOR CONTRIBUTIONS OF THE DISSERTATION RESEARCH	203
8.2	MAJOR CONCLUSIONS	203
8.3	RECOMMENDATIONS FOR THE FUTURE WORK	205
REFERENCES		207

LIST OF FIGURES

<p>Figure 1.1: Comparisons of mean normalized vertical apparent mass and seat-to-head transmissibility magnitudes of the seated body exposed to vertical vibration: (a) No back support; (b) vertical back support; and (c) inclined back support. , normalized <i>APMS</i>; , <i>STHT</i>.</p>	11
<p>Figure 1.2: (a) vertical apparent mass magnitude responses of subjects within three different body mass range; and (b) normalised APMS responses.</p>	22
<p>Figure 1.3: Influence of back support on the seat-to-head acceleration transmissibility, and apparent mass under vertical vibration.</p>	25
<p>Figure 1.4: Influence of magnitude of back support condition on apparent mass responses of seated body to different magnitudes of fore-aft vibration: (a) no back support and (b) back support.</p>	25
<p>Figure 2.1: (a) Schematic of the test seat with force plate serving as the seat pan; and (b) reaction forces at the seat-pan result in the cancellation of force at the seat-pan: f_{p_x} is the measured force at the seat-pan, f_{px} and f_{bx} are the actual forces at seat-pan and backrest interfaces, respectively.</p>	39
<p>Figure 2.2: Schematic representation of the two-input-and-single-output model of the biodynamic functions under mutually uncorrelated fore-aft and lateral vibration.</p>	42
<p>Figure 3.1: (a) Schematic of the test seat with force plate serving as the seatpan: f'_{px} and f_{bx} are forces measured at the seatpan and backrest, respectively, and f_{px} is the total force; (b) Experimental setup showing the subject seated with back supported posture and the locations of force-plates.</p>	57
<p>Figure 3.2: Mean measured fore-aft backrest and seatpan APMS, and corrected-seatpan APMS magnitude and phase responses of occupants seated with back support and exposed to fore-aft vibration of 0.25 m/s^2 rms acceleration magnitude.</p>	59
<p>Figure 3.3: Comparison of reported APMS magnitude of subjects seated with a back support and exposed to fore-aft vibration, and the corrected APMS in the present study (0.25 m/s^2).</p>	60
<p>Figure 3.4: Comparisons of mean APMS magnitude and phase responses to single- and dual-axis fore-aft and lateral vibration (No back support; hands in lap; single axis: $a_x=a_y=0.4 \text{ m/s}^2$; dual-axis: $a_x=a_y=0.28 \text{ m/s}^2$).</p>	70
<p>Figure 3.5: Comparisons of mean APMS magnitude and phase responses to single- and dual-axis fore-aft and lateral vibrations (Back support; hands in lap; single axis: $a_x=a_y=0.4 \text{ m/s}^2$; dual-axis: $a_x=a_y=0.28 \text{ m/s}^2$).</p>	71
<p>Figure 3.6: Comparisons of mean backrest APMS magnitude and phase responses to single- and dual-axis fore-aft and lateral vibrations (hands in lap; single axis: $a_x=a_y=0.4 \text{ m/s}^2$; dual-axis: $a_x=a_y=0.28 \text{ m/s}^2$).</p>	73

Figure 3.7: Comparisons of mean cross-axis APMS responses obtained at the seatpan along fore-aft (M_{xy}) and lateral (M_{yx}) axis (single axis vibration: $a_x=a_y=0.4$ m/s ²): (a) No back support; (b) Back support.	73
Figure 3.8: Comparisons of mean STHT magnitude and phase responses to single and dual-axis fore-aft and lateral vibrations (No back support; hands in lap; single axis: $a_x=a_y=0.4$ m/s ² ; dual-axis: $a_x=a_y=0.28$ m/s ²).	74
Figure 3.9: Comparisons of mean STHT magnitude responses to single and dual-axis fore-aft and lateral vibrations (Back support; hands in lap; single axis: $a_x=a_y=0.4$ m/s ² ; dual-axis: $a_x=a_y=0.28$ m/s ²).	75
Figure 3.10: Comparisons of mean seatpan APMS responses of occupants seated with hands in lap and hands on steering wheel (No back support; dual-axis: $a_x=a_y=0.28$ m/s ²).	76
Figure 3.11: Comparisons of mean total and backrest APMS responses of occupants seated with hands in lap and hands on steering wheel to: (a) fore-aft; and (b) lateral vibration (Back support; dual-axis vibration: $a_x=a_y=0.28$ m/s ²).	77
Figure 3.12: Comparisons of mean STHT responses of the occupants seated with hands in lap and hands on steering wheel (dual-axis: $a_x=a_y=0.28$ m/s ²): (a) No back support and (b) Back support.	79
Figure 3.13: Comparisons of mean (a) total APMS and (b) STHT responses of occupants seated with back unsupported (NB) and supported (B0), and hands in lap (HL) and hands on steering wheel (HS) under dual axis vibration ($a_x=a_y=0.28$ m/s ²).	80
Figure 3.14: Comparison of normalized total APMS and STHT measures of occupants seated with hands in lap and exposed to dual-axis vibration ($a_x=a_y=0.28$ m/s ²): (a) No back support and (b) Back support.	81
Figure 3.15: Comparisons of estimated and measured fore-aft and lateral STHT responses to dual-axis vibration: (a) fore-aft; and (b) lateral (No back support; $a_x=a_y=0.28$ m/s ²).	86
Figure 4.1: Schematic illustration of the sitting postures realised by the subjects during the vibration exposure; (a) No back support but hands supported, NB-HS; (b) No back support and hands in lap, NB-HL; (c) Back supported and hands on steering wheel, B0-HS; and (d) Back supported but hands in lap, B0-HL.	95
Figure 4.2: Schematic illustration of the direct and cross-axis responses developed during single-input and multiple-output (SIMO) system under single vibration.	98
Figure 4.3: Comparisons of the direct and cross-axis seat-to-head-transmissibility (STHT) magnitude responses of a subject (S1) seated with no back support and hands in lap posture (NB-HL) derived using H_1 and H_v methods under single axis vibration: (a) fore-aft vibration; and (b) vertical vibration.	104
Figure 4.4: Comparisons of the single subject's (S1) APMS and STHT magnitude responses to single and dual (xz) axis vibrations. (seated with back support and hands in lap posture, B0-HL) H_v ; H_1 ; direct, and H_1 cross axis single axis vibration (H_1).	105
Figure 4.5: Comparisons of the single subject's (S2) APMS and STHT magnitude responses to single and dual (xz) axis vibrations. (seated with back support and hands in lap).	105

- Figure 4.6: Comparisons of the mean fore-aft and vertical APMS and STHT magnitude responses under single and dual axis vibrations. (seated without back support and hands in lap posture, NB-HL) ——— dual-axis (H_v); ——— dual-axis (H_1); - - - - - direct and ——— cross axis single axis vibration. 106
- Figure 4.7: Comparisons of the mean fore-aft and vertical APMS and STHT magnitude responses under single and dual axis vibrations. (seated with back support and hands in lap posture, B0-HL) ——— dual-axis (H_v); ——— dual-axis (H_1); - - - - - direct and ——— cross axis single axis vibration. 107
- Figure 4.8: The effect of hands support on the fore-aft seat-to-head-transmissibility (STHT) and apparent mass (APMS) responses under dual-axis vibration derived using H_v estimator. (a) without back support, NB and (b) with back supported posture, B0; Vibration magnitude 0.28 m/s^2 along each axis) - - - - - Hands in lap, HL; and ——— Hands on steering wheel, HS. 110
- Figure 4.9: The effect of hands support on the fore-aft backrest apparent mass (APMS) responses of the seated occupant seated with back supported (B0) posture derived using H_v estimator. (Vibration magnitude 0.28 m/s^2 along each axis) - - - - - Hands in lap, HL and ——— Hands on steering wheel, HS. 112
- Figure 4.10: The effect of back support in terms of mean seat-to-head-transmissibility (STHT) and apparent mass (APMS) responses of the seated occupants derived using H_v estimators under single and dual-axis vibration with hands in lap posture. - - - - - NB, single axis (H_1); ——— NB, dual axis (H_v); - - - - - B0, single axis (H_1); ——— B0, dual axis (H_v). 113
- Figure 4.11: Effect of vibration magnitude on the direct and cross-axis seat-to-head-transmissibility (STHT) responses of seated occupants without back support (NB) and exposed to single axis fore-aft and vertical vibration derived using H_1 estimator. - - - - - 0.25 m/s^2 ; ——— 0.40 m/s^2 . 113
- Figure 4.12: The effect of vibration magnitude on the fore-aft and vertical seat-to-head-transmissibility (STHT) responses of the seated occupants with hands in lap (HL) derived using H_v estimator. (a) without back support, NB; (b) with back support, B0. - - - - - dual-axis (0.4 m/s^2); ——— dual-axis (0.58 m/s^2). 114
- Figure 5.1: (a) Schematic of the test seat with force plate serving as the seatpan and backrest; (b) Experimental setup showing the subject seated with back supported posture and the locations of force-plates. 126
- Figure 5.2: The mean direct and cross-axis seat-to-head-transmissibility (STHT) magnitude responses of the occupants seated without back support and hands in lap posture under single axis fore-aft, lateral and vertical axis of 0.4 m/s^2 rms vibration magnitude. 130
- Figure 5.3: Comparison of the mean seat-to-head-transmissibility (STHT) magnitudes obtained with the H_1 and H_v methods of the seated occupants seated with the hands in lap and exposed to single ($a_x=a_y=a_z=0.4 \text{ m/s}^2$) and three-axis ($a_x=a_y=a_z=0.23 \text{ m/s}^2$); (a) No back support and (b) Vertical back support. 131
- Figure 5.4: Comparisons of mean apparent mass (APMS) and seat-to-head-transmissibility (STHT) magnitude responses to single and three-axis fore-aft, lateral and vertical vibration of the occupants seated without and with back support and hands in lap; three-axis vibration ($a_x=a_y=a_z=0.23 \text{ m/s}^2$). 132

Figure 5.5: Comparisons of mean backrest and pan apparent mass (APMS) magnitude responses to single and three-axis fore-aft, lateral and vertical vibration with hands in lap; single axis: $a_x=0.4\text{ m/s}^2$; three-axis ($a_x=a_y=a_z=0.23\text{ m/s}^2$).	134
Figure 5.6: Comparisons of mean apparent mass (APMS) and seat-to-head-transmissibility (STHT) magnitude responses to three-axis fore-aft, lateral and vertical vibration of the occupants seated with hands in lap and on steering wheel and no back support; three-axis vibration ($a_x=a_y=a_z=0.23\text{ m/s}^2$).	135
Figure 5.7: Comparisons of mean apparent mass (APMS) and seat-to-head-transmissibility (STHT) magnitude responses to three-axis fore-aft, lateral and vertical vibration of the occupants seated with hands in lap and on steering wheel and vertical back support; three-axis vibration ($a_x=a_y=a_z=0.23\text{ m/s}^2$).	136
Figure 6.1: (a) Schematic of the test seat with force plate serving as the seatpan and backrest; (b) Experimental setup showing the subject seated with back supported posture and the locations of force-plates.	149
Figure 6.2: Computation of power absorbed by the seated body under three-axis vibration.	153
Figure 6.3: The rms acceleration spectra of selected vehicles.	154
Figure 6.4: Comparisons of the mean absorbed power responses of 9 subjects seated without the back support (<i>NB</i>) and exposed to single axis fore-aft, lateral and vertical vibration of rms acceleration magnitudes 0.25 and 0.40 m/s^2 .	156
Figure 6.5: Comparisons of the mean absorbed power responses of occupants seated with back support (<i>B0</i>) and exposed to single axis fore-aft, lateral and vertical vibration of rms acceleration magnitudes 0.25 and 0.40 m/s^2 .	156
Figure 6.6: Comparisons of the mean absorbed power responses of occupants seated with and without back support and exposed to single axis fore-aft, lateral and vertical vibration of rms acceleration magnitude 0.40 m/s^2 .	157
Figure 6.7: The mean absorbed power responses of the subjects along the fore-aft (<i>x</i>), lateral (<i>y</i>) and vertical (<i>z</i>) axis, and the total absorbed power when exposed to three-axis whole-body vibration (a) No back support- <i>NB</i> ; (b) Vertical back support- <i>B0</i> .	158
Figure 6.8: Comparisons of the absorbed power responses of the seated occupants exposed to single- and three-axis whole-body vibration of identical effective magnitude of 0.4 m/s^2 : (a) No back support- <i>NB</i> ; and (b) Vertical back support- <i>B0</i> .	158
Figure 6.9: Comparisons of the total absorbed power responses of the seated occupant exposed to three-axis whole-body vibration of rms acceleration of 0.4 and 0.7 m/s^2 : (a) No back support- <i>NB</i> ; (b) Vertical back support- <i>B0</i> .	160
Figure 6.10: Comparison of the total <i>VPA</i> responses of occupants seated without and with back support and exposed to three-axis vibration of magnitude 0.4 m/s^2 .	160
Figure 6.11: Estimated <i>VPA</i> values along fore-aft, lateral and vertical axis in the vehicles based on the measured vibration at the seat location.	162

Figure 6.12: Relationship between the total average vibration power absorption and the overall rms acceleration due to vibration spectra of selected vehicles.	163
Fig. 7.1: Schematic illustrations of the three different sitting postures used in the study under fore-aft (x -axis) vibration. (NB - No back support; Wb0 - Vertical back support; WbA - Inclined back support).	174
Figure 7.2: Arrangement of the test seat on the horizontal vibration platform for measurement of the responses under y -axis excitation.	175
Figure 7.3: Comparison of absorbed power magnitude responses measured at the seat pan of eight subjects seated with NB (no back support), Wb0 (vertical back support) and WbA: (inclined back support) postures, and exposed to 1 m/s^2 rms acceleration along the fore-aft (x) and lateral (y) directions (seat height H_1).	183
Figure 7.4: Comparison of absorbed power magnitude responses measured at the backrest of eight subjects seated with Wb0 (vertical back support) and WbA (inclined back support) postures, and exposed to 1 m/s^2 rms acceleration along the fore-aft (x) and lateral (y) directions (seat height H_1).	184
Figure 7.5. Mean across subjects ($n=8$) absorbed power characteristics measured at the seat pan under different magnitudes of excitation 0.5 and 1.0 m/s^2 rms, and, NB (no back support) and WbA (inclined back support) postures, along fore-aft (x) and lateral (y) vibration.	189
Figure 7.6. Mean across subjects ($n=8$) absorbed power characteristics measured at the backrest under different magnitudes of excitation 0.5 and 1.0 m/s^2 rms, and Wb0: (vertical back support) and WbA (inclined back support) postures: a) fore-aft (x) vibration; b) lateral (y) vibration.	192
Figure 7.7. Mean absorbed power characteristics ($n=8$) measured at the seat pan under NB (no back support) Wb0 (vertical back support) and WbA (inclined back support) postures (excitation magnitude – 1.0 m/s^2 rms): a) fore-aft (x) vibration; b) lateral (y) vibration.	193
Figure 7.8: Comparison of mean absorbed power response ($n=8$) measured at the seat pan and the backrest under fore-and-aft (x) vibration (WbA - inclined back supported posture, Seat height- H_1).	194
Figure 7.9: Comparisons of weighting filter magnitudes derived from mean absorbed power responses corresponding to NB (no back support), Wb0 (vertical back support) and WbA: (inclined back support) postures (a) Fore-aft (x) vibration; and (b) Lateral vibration.	198

LIST OF TABLES

Table 1.1: Magnitudes of frequency-weighted rms accelerations due to vibration measured along the fore-aft and lateral and vertical axis, on the seats of agricultural/forestry tractors.	7
Table 1.2: Frequency ranges of predominant vibration of wheeled off-road vehicles.	7
Table 1.3: Summary of experimental conditions employed in studies reporting driving-point biodynamic responses of seated human body to vertical vibration.	14-16
Table 1.4: Summary of experimental conditions employed in studies reporting biodynamic responses of seated human body to fore-aft vibration.	17
Table 1.5: Summary of experimental conditions employed in studies reporting biodynamic responses of seated human body to lateral vibration.	18
Table 1.6: Summary of experimental conditions employed in studies reporting seat-to-head transmissibility (STHT) of seated human body to vertical vibration.	19
Table 1.7: Grouping of factors affecting the biodynamic responses of the seated body exposed to WBV.	20
Table 1.8: Reported resonance frequencies observed in APMS responses of seated occupant exposed to horizontal WBV.	21
Table 3.1: Normalization factors (% of body mass), based on anthropometry.	62
Table 3.2: Statistical significance (p -values) of hands support attained from ANOVA performed on the seatpan APMS and STHT magnitude responses to single-axis fore-aft and lateral vibration under different conditions (back support: NB and B0; vibration magnitude: 0.25 and 0.4 m/s ²)	67
Table 3.3: Statistical significance (p -values) of back support attained from ANOVA performed on the seatpan APMS and STHT magnitude data under different conditions (back support: NB and B0; hands support: HL and HS; vibration magnitude: 0.25 and 0.4 m/s ² ; vibration direction: fore-aft and lateral; number of vibration axis: single and dual-axis)	68
Table 3.4: Frequencies (Hz) corresponding to important peak magnitudes observed in the mean APMS and STHT responses of seated occupants exposed to single axis horizontal vibration.	72
Table 4.1: Normalization factors (% of body mass supported by the seatpan and back support derived from the anthropometric data). No back support but hands	103

supported, NB-HS; no back support and hands in lap, NB-HL; back supported and hands on steering wheel, B0-HS and back supported but hands in lap, B0-HL.

Table 4.2: <i>p</i> -values illustrating the effect of the method of analysis (H_1 vs H_v) on the seat-to-head-transmissibility (STHT) and apparent mass (APMS) magnitudes under dual-axis vibration. (NB - no back support; B0- with back support)	108
Table 4.3: Frequencies corresponding to peak magnitudes in the seat-to-head-transmissibility (STHT) and apparent mass (APMS) responses of seated occupants to single (H_1) and dual-axis (H_v) vibrations. (No back support but hands supported, NB-HS; no back support and hands in lap, NB-HL; Back supported and hands on steering wheel, B0-HS and Back supported but hands in lap, B0-HL).	108
Table 4.4: <i>p</i> -values illustrating the effect of dual-axis vibration (single vs dual-axis vibration) in the seat-to-head-transmissibility (STHT) and apparent mass (APMS) magnitudes derived using H_1 and H_v methods. NB- no back support and B0- with back support.	109
Table 4.5: <i>p</i> -values illustrating the effect of hands support (HL vs HS) in the seat-to-head-transmissibility (STHT) and apparent mass (APMS) magnitudes derived using H_v estimator under dual-axis vibration. NB- no back support and B0- with back support.	111
Table 4.6: <i>p</i> -values illustrating the effect of back support (NB vs B0 posture) in the seat-to-head-transmissibility (STHT) and apparent mass (APMS) magnitudes derived using H_v estimator under dual-axis vibration. NB- no back support and B0- with back support.	117
Table 5.1: Summary of the broadband vibration magnitudes employed in this study.	125
Table 6.1: The total average power absorption of the seated occupant exposed to single and combined fore-aft, lateral and vertical-axis whole-body vibration of different magnitudes.	159
Table 6.2: The total <i>VPA</i> of the seated body exposed to combined fore-aft, lateral and vertical axis vibration along with the % of <i>VPA</i> along each axis of excitation.	159
Table 6.3: Constant α and exponent β values derived for the average total power relationship between average total power of the body seated with and without a back support and the rms acceleration of the single and combined fore-aft, lateral and vertical axis vibration: NB-No back support; B0: Vertical back support.	161
Table 7.1: Magnitudes of frequency weighted rms accelerations due to vibration measured along the <i>x</i> -, <i>y</i> - and <i>z</i> - axis on the seats of the heavy vehicles [31,135-138].	169

Table 7.2: Test matrix	176
Table 7.3: p -values attained from single and two-factor ANOVA performed on the seat pan absorbed power magnitude under fore-aft vibration.	185
Table 7.4: p -values attained from single and two-factor ANOVA performed on the seat pan absorbed power magnitude under lateral vibration.	186
Table 7.5: Effect of posture shown by the p -values derived from single-factor ANOVA performed on the seat pan absorbed power magnitude data under Fore-and-aft and lateral excitations.	186
Table 7.6: The total absorbed power measured at the seat pan and the backrest, under the influence of various unsupported and supported back postures, and magnitudes of vibration at seat height 425mm.	187
Table 7.7: Constant and exponent values for different excitation and postural conditions.	190
Table 7.8: Comparisons of the weighting values obtained in this study with the W_d -weighting defined in ISO-2631-1.	199

Chapter 1

INTRODUCTION AND SCOPE OF DISSERTATION

1.1 INTRODUCTION

Operators of the road and off-road vehicles are constantly exposed to low frequency whole-body vibration (WBV) of comprehensive magnitudes arising from tire/track-terrain interactions. Epidemiological studies have shown a high prevalence of back disorders such as disc degeneration, sciatica and muscular symptoms, among the occupational vehicle drivers exposed to whole-body vibration [1]. Occupational exposure to WBV is thus known to cause discomfort, annoyance, and health and safety risks. The development of effective seated-body biomechanical models for applications in suspension and seating designs require thorough understanding and characterization of biodynamic responses of the body to realistic vehicular WBV exposures and sitting postures. The biodynamic responses of the seated human body exposed to WBV have been widely studied under broad ranges of vibration and postural conditions, which are expressed in terms of: (i) force-motion relations at the seat-buttock driving-point, namely, apparent mass (*APMS*), driving-point mechanical impedance (*DPMI*) or absorbed power (*P_{ABS}*); and (ii) functions describing the flow of vibration through the body, such as seat-to-head vibration transmissibility (*STHT*) or body segments vibration transmissibility. The vast majority of the studies have focussed on vertical vibration biodynamics under wide range of experimental conditions since vehicle vibration are considered to be dominant along the vertical axis. These have provided considerable knowledge on the movement and mechanical properties of the body exposed to WBV, the influences of posture and vibration-related variables, resonance frequencies and probable modes of vibration, potential injury mechanisms and frequency-weightings for exposure assessments [e.g., 2-16].

A large number of work vehicles also transmit substantial magnitudes of fore-aft (x) and lateral (y) vibration in addition to the vertical (z) vibration [17,18]. However, relatively fewer studies have investigated biodynamic responses under horizontal vibration [e.g.,2,3]. The seated body responses to simultaneous three-axis vibration, which is more representative of vehicular vibration environment, have been investigated in even fewer recent studies. The reported studies did not reveal the coupled effects of three-axis vibration in the measured biodynamic responses, even though notable magnitudes of cross-axis responses have been observed under single axis vibration [e.g., 19-21]. The studies under single axis vibration have further suggested that body constraints such as back and hands supports, tend to alter the fore-aft, vertical and pitch motions of the upper body and may thus influence the biodynamic behaviour of the seated body. The combined effects of the back and hands supports, which are more representative of the occupational drivers postures, however, have not been considered under three-axis vibration.

The STHT measure has been suggested to have greater emphasis of the lower inertia components of the seated occupants while the APMS relates to the global seated body response. It is however desirable to characterise the seated body biodynamics in terms of both the measures to facilitate biodynamic model development and to enhance understanding of the seated body response to multi-axis vibration [4]. Furthermore, the frequency weightings defined in the International standards are applicable to assess the hazards and discomfort from fore-aft, lateral and vertical WBV [5-7]. These standards, however, suggest similar weightings for both the fore-aft and lateral vibration, while for the back supported posture, the magnitudes of biodynamic responses under fore-aft vibration are notably different compared to those under lateral vibration.

In this study, the biodynamic responses of the seated body are characterised under single (x , y and z), dual (xy and xz) and combined three-axis (xyz) whole-body vibration. The responses are derived in terms of both the APMS and STHT properties of the subjects seated with both hands and back supports. Furthermore, the APMS responses are characterised considering two-driving-points formed by the buttocks-pan and upper-body backrest interfaces. The measured data are analysed using an alternative frequency response estimator H_v considering the uncorrelated nature of the multi-axis vibration, as opposed to the commonly used H_l function estimator, which would suppress the contributions of the cross-axis responses under uncorrelated multi-axis excitations. Furthermore, this study suggests that the total response along an axis can be estimated from superposition of the direct and cross-axis response components along the same axis. The power absorbed by the seated body is further evaluated under single as well as multi-axis vibration. A methodology is proposed to derive frequency-weightings on the absorbed power responses.

1.2 REVIEW OF RELEVANT LITERATURE

Drivers of heavy road and off-road vehicles are occupationally exposed to considerable levels of translational as well as rotational ride vibration. The seated occupant's perception and sensation of vibration is directly associated with the ride vibration environment of the vehicle. Many studies have been performed on human subjects to quantify vibration comfort boundaries and assessment guidelines [8]. Although, there is no general method of assessment due to highly complex nature of human response to vibration, somewhat similar methods have been used to evaluate the human tolerance and acceptance of vibrations. These methods can be classified in different groups depending on their measurement techniques: (i) subjective ride measurements involving selected subjects; (ii) repetitive shake table tests using synthesised harmonic vibration

[e.g.,4]; (iii) shake table tests using stimulus representing the realistic road measured vibration environment; and (iv) measurement of ride environment and vibration exposure in vehicles under normal operating conditions [e.g.,8].

Apart from the comfort and perception, the occupational WBV exposure has been associated with an array of health disorders among the exposed drivers. Epidemiology studies have established strong correlations between the WBV and spine deformities among the drivers [22-24]. The data from these epidemiological studies, however, is not likely to yield a definite dose-effect relationship [25]. Characterisation of biodynamic responses of the seated body exposed to vibration is thus considered vital for building an understanding of mechanical responses of the biological system. The biodynamic responses could yield mechanical properties of the body such as resonance frequencies and deflection models, and frequency-weightings for assessing the exposure risk. Furthermore, the biodynamic responses form the essential basis for deriving biomechanical models of the seated body for design of anthropo-dynamic manikins for efficient assessment of suspension seats, ad for applications in seating and suspension design.

International standard ISO 2631-1 [6], defines frequency-weighting functions to account for variations in human sensitivity to vibration frequency, for vibration applied individually along three translational and three rotational axes. This standard suggests similar weightings for the vibration along the fore-aft and the lateral axis, which is likely true with the unsupported back postures. A back support, however, tends to alter the mechanical properties of the body, particularly along the fore-aft and vertical axis [2,3]. The human body seated with a back support exhibits greater sensitivity to higher frequency vibration along the fore-aft axis compared to that observed with unsupported back postures [2,3]. It has been suggested that vibration energy absorbed by the human body, attributed to visco-elastic properties of the body, may be a better

measure of the potential injury risk, since it is a measure of the stress and strain rate [9,13]. A few studies have characterised the vibration absorption properties of the seated body to vibration along the individual axis. The applicability of the responses in deriving frequency-weightings for assessing the injury risks, however, has been attempted only in a few studies on WBV [13] and hand transmitted vibration [26].

1.2.1 Vehicle vibration environment

The human occupants response and perception to vibration is directly associated with nature of the ride vibration of the vehicle with greater emphasis being placed on the magnitude of vibration. The characterisation of vibration environment thus forms the foremost task. Majority of the off-road vehicles are designed without wheel suspension. The ride behaviour of such vehicles is thus characterised by the response of a lightly damped system, where the damping arises from the tires alone. The modern industrial vehicles employed in construction and service sectors, however, are designed with primary suspension in order to obtain higher speeds, which tend to contribute to higher magnitudes of vibration along all the translational and rotational axes [17]. A large number of analytical and experimental studies have been performed to define ride vibration levels as functions of various design and operating factors of on-road and off-road vehicles [17,18,27-30]. These studies have clearly shown that a number of off-road vehicles could improve greater magnitudes of fore-aft and lateral vibration.

The ranges of vibration of urban buses, forklift trucks and side-walk snow-ploughs along the vertical, lateral, longitudinal, roll and pitch axes, under wide range of operating conditions, have been reported in [31]. For off-road tractors with implements or when ploughing, harrowing or drilling, the magnitudes of frequency-weighted longitudinal and lateral vibration could be either comparable to or exceed those of the vertical vibration [22,31-33]. The relatively low flexibility of tires of off-road vehicles coupled with high location of the operator, and presence of

localized slopes and cross-slopes in the terrain, contribute to considerable motions at the operators' location along the x - and y - axes. The relative magnitudes of horizontal vibration, however, would depend upon the type of vehicle and the task performed. Studies have reported high incidence of disorders among off-road vehicle drivers, being nearly 2-4 times higher than that among the crane operators (on-road) [22], which in-part may be attributed to higher vibration along x - and y - axes.

The agricultural and forestry vehicles have been most widely studied with respect to their ride vibration and safety and occupational diseases due to WBV exposure are found to be the highest among such vehicle drivers [18, 22,29,30]. The suspensions and tires properties, apart from the vehicles weights and dimensions of vehicles, strongly affect the nature of transmitted vibration. However, the primary focus of these studies has been limited to vertical vibration, which is further applied in development of effective seat-suspension design [28,32,34]. Such vehicles cause appreciable frequency-weighted magnitudes of vibration transmitted to the driver seat along the longitudinal and lateral axes. This is evident from the reported data summarised in Table 1.1, where a_{wx} , a_{wy} and a_{wz} denote the frequency-weighted accelerations along x -, y - and z -axis, respectively. The reported data suggest that the magnitudes of horizontal vibrations are significant when compared to those in the vertical direction, particularly for the harrowing and ploughing tasks. These suggest that characterisation of human responses to fore-aft and lateral vibration is equally important. Furthermore, the biodynamic responses of the seated body need to be defined under simultaneously applied multi-axis vibration. The predominant vibrations of wheeled off-road vehicles are observed to occur at low frequencies up to nearly 5 Hz, as illustrated in Table 1.2.

Table 1.1: Magnitudes of frequency-weighted rms accelerations due to vibration measured along the fore-aft and lateral and vertical axis, on the seats of agricultural/forestry tractors [22,33,35].

Operation/task	a_{wx} (m/s ²)	a_{wy} (m/s ²)	a_{wz} (m/s ²)
Tractor off-road	0.2-1.8	0.5-1.7	1.2-3
Tractor ploughing	0.3-1.3	0.2-0.6	0.3-0.59
Tractor Harrowing	0.2-0.69	0.2-0.8	0.38-0.96
Band excavator harrowing	0.2-2.6	0.2-1.0	0.3-1.4
Band excavator ploughing	0.5-1.3	0.3-1.3	0.4-1.0
Fork-lift truck (off-road)	0.10-0.90	0.10-2.5	0.5-1.6

Table 1.2: Frequency ranges of predominant vibration of wheeled off-road vehicles [36].

Vibration-axis	Frequency range (Hz)
Fore-aft (x)	2.0-4.5
Lateral (y)	≈1.0
Vertical (z)	2.0-3.5

1.2.2 Biodynamic measures and measurement methods

The biodynamic responses of the seated body to whole-body vibration have been expressed in terms of two broad functions: (i) ‘to-the-body’ response function describing the force-motion relation at the point of entry of vibration or the driving-point; and (ii) ‘through-the-body’ response function that describes the flow of source vibration to a particular location of the body [14]. The ‘to-the-body’ response function has been presented in terms of three inter-related force-motion relations: (i) driving-point mechanical impedance (*DPMI*) relating the dynamic force developed at the driving-point between the vibrating surface and the body with the driving-point velocity; (ii) apparent mass (*APMS*) relating the driving-point dynamic force with acceleration at the interface; and (iii) vibration energy absorbed by the body. Under random vibration, the force-motion relations (*DPMI* and *APMS*) are derived from [15]:

$$Z(j\omega) = S_{Fv} / S_v$$

$$M(j\omega) = S_{F_a} / S_a \quad (1.1)$$

Where $Z(j\omega)$ and $M(j\omega)$ are the complex *DPMI* and *APMS* response functions, respectively, corresponding to excitation frequency ω . S_{F_a} and S_{F_v} are the cross-spectral density force measured at the driving-point and the acceleration a and velocity v , respectively. S_a and S_v are acceleration and velocity auto spectral densities, respectively.

The *APMS* responses are known to yield lesser variability in the primary resonant frequency compared to that observed from the *DPMI* responses [14]. Both the *APMS* and *DPMI* functions are also related in the following manner:

$$Z(j\omega) = j\omega.M(j\omega) \quad (1.2)$$

The *APMS* or *DPMI* functions characterize the biodynamic response or properties of the human body exposed to vibration, but cannot be applied for quantifying the vibration exposure which is related to both the intensity and the exposure duration. The acceleration due to source vibration, on the other hand, is considered to represent the vibration hazard. The vibration power absorbed by the exposed body that combines both the vibration hazard and the biodynamic properties has been proposed to assess the effects of WBV. The measure is derived from the dynamic force and velocity at the driving point. The absorbed power thus relates to dissipation of energy attributed to relative motions of the tissues, muscles and skeletal system, which under prolonged exposures could lead to physical damages in the musculoskeletal system [9,16]. The vibration power absorbed by the vibration-exposed seated body $P_a(\omega)$ is thus expressed as the real part of the cross-spectrum between the force and velocity signals, such that [12,26]:

$$P_a(\omega) = \text{Re}[S_{F_v}] \quad (1.3)$$

Where Re designates the real component. Moreover, unlike the APMS or DPMS, the absorbed power can be used to estimate the cumulative energy dissipated by the exposed body over a given duration. This measure may thus facilitate assessment of effects of exposure duration apart from the intensity of vibration. The vibration power absorbed by the body can also be evaluated using an indirect method. It has been shown that total power, \bar{P} transferred is directly related to the APMS response [12]:

$$\bar{P} = \int_0^{\infty} \frac{\text{Im}[M^*(j\omega)]}{\omega} S_a(\omega) d\omega \quad (1.4)$$

Where ‘ Im ’ designate the imaginary component, $M^*(j\omega)$ is the conjugate of the complex APMS function, and \bar{P} is the total power absorbed by the seated body.

The ‘through-the-body’ response function is used to characterize the transmission of vibration to different segments of the body, and is defined as the ratio of acceleration due to transmitted vibration to that of the source vibration. The vibration transmission characteristics are derived from transfer function given by:

$$T_k(j\omega) = \frac{S_{a_k a}}{S_a} \quad (1.5)$$

Where $S_{a_k a}$ is the cross-spectral density of acceleration a_k measured at a particular location k on the body and the source vibration a , both being in the same direction. $T_k(j\omega)$ is the ‘through-the-body’ transfer function or vibration transmissibility of the location along a given direction. Owing to complexities associated with mounting of sensors on the skin, the vibration transmitted to the head is commonly measured to describe the transmission of vibration through the body. This method reduces the variability due to skin effects by employing either helmet or bite-bar mounted sensors [37]. The ‘through-the-body’ biodynamic responses are generally expressed by vibration transmitted along two- or more-axes, even though the source vibration

occurs along a single axis [19,20,40]. It has been suggested that the both driving-point and transmissibility functions need to be measured simultaneously in order to better understand the seated body responses and to develop reliable models [38]. The measurements of two functions under carefully controlled identical conditions and same subjects could yield considerable insight into relationship between the two functions.

A few studies have reported either both the functions, measured either simultaneously or sequentially [14,40-46], while, only two studies have explored the relationship between the two measures. A single study explored the relationship using simple vertical biodynamic models [14], and another study attempted the relationships through simultaneous measurements of the two functions for the body seated with and without a back support and exposed to vertical vibration [47]. Figure 1.1 illustrates the comparisons of the mean normalized *APMS* and *STHT* magnitude responses of the seated body with none, vertical and inclined back supports. The mean normalized *APMS* and *STHT* responses showed good agreements in terms of the primary resonances, irrespective of the back support condition, while considerable differences were observed between the normalized *APMS* and *STHT* magnitudes. Such differences between the two measures have also been reported from responses attained from biodynamic model [44]. The differences could be attributed to nonlinearities in the biodynamic functions, and far greater variability observed in the *STHT* responses reported in various studies, which can be mostly attributed to variations in the measurement systems used in different studies and involuntary head movements under vibration [4,46].

The studies concluded that the ‘through-the-body’ responses emphasize the biodynamic responses corresponding to higher vibration modes compared to the *APMS* responses [47,48]. This may partly be attributed to reduced contributions of the resonant oscillations of the low-

inertia body substructures to the driving-point. The transmissibility measures may thus be considered more appropriate for describing biodynamic responses to higher frequency vibration, and development of higher order models. However, no attempts have been made in establishing such relations for the biodynamic measures of the seated body exposed to horizontal or multi-axis vibration.

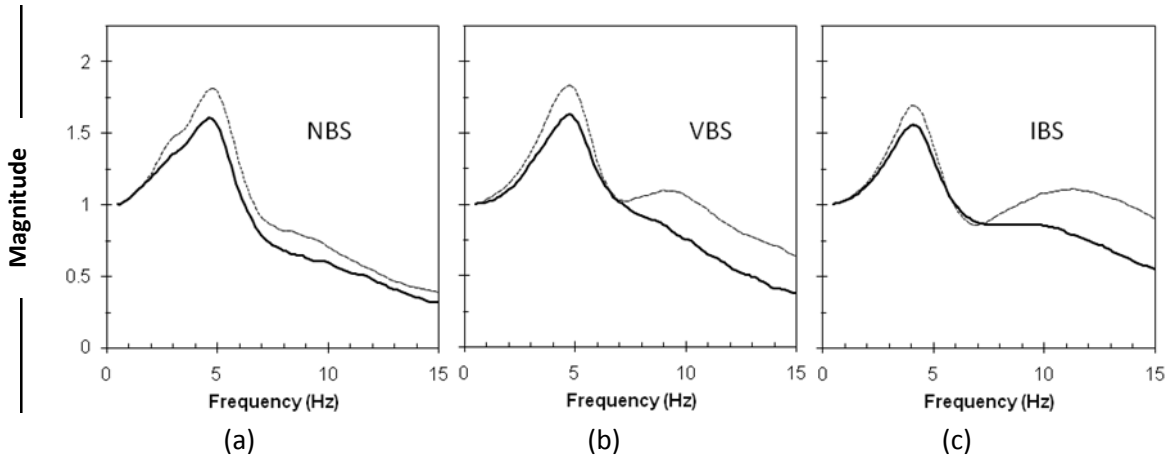


Figure 1.1: Comparisons of mean normalized vertical apparent mass and seat-to-head transmissibility magnitudes of the seated body exposed to vertical vibration: (a) No back support; (b) vertical back support; and (c) inclined back support. (—, normalized APMS; ·····, STHT [48]).

The STHT responses, in-general, exhibit far greater variability compared to the APMS, which is attributed to its higher sensitivity to variations in a wide variety of independent parameters, including the dynamic properties of the head acceleration measurement system, subject characteristics and experimental conditions [19,20]. The STHT and normalized APMS responses under vertical whole-body vibration correlate well in terms of peak magnitudes and corresponding frequencies. The effect of a back support is greatly emphasized in the vertical STHT responses compared to that observed in the APMS responses [48].

Only a single study has obtained the vibration transmissibility measures along three translational and rotational axes, under uncoupled fore-aft, lateral and vertical WBV [19,20]. The

measurements were obtained using accelerometers mounted on a bite-bar held in the mouth of the subjects instead of measurements on the head. The study considered back supported postures, while the hands were placed on the thighs, which is not representative of the typical vehicle driving condition. A need to characterize biodynamic responses of the seated body assuming representative driving postures and exposed to multi-axis vibration thus exists. Furthermore, it is desirable to conduct simultaneous measurements at the two driving-points, the seat-pan and the backrest, to characterize the responses.

The vast majority of the studies have investigated the to-the-body and through-the-body biodynamic functions under vertical WBV. These have been applied to derive different biodynamic models of the seated body including lumped-parameter, multi-body dynamic and finite element models [e.g., 42,49,50]. The lumped parameter models have also been applied for design of suspension seats in an attempt to reduce the magnitudes of vertical vibration experienced by the operator. The vast number of off-road vehicles, however, also impose comparable magnitudes of vibration along the horizontal axes (x and y), while only a few studies have characterised biodynamic response under x - and y - axis vibrations.

1.2.3 Characterisation of seated body biodynamic responses

Considerable efforts have been made to characterise the seated occupants responses to whole-body vibration in the laboratory. Numerous experiments have been performed to derive the biodynamic response functions namely, the apparent mass, seat-to-head vibration transmissibility and absorbed power to characterise human system behaviour, under varying independent variables such as type and magnitude of vibration, sitting posture and hands and back supports.

Tables 1.3 to 1.5 summarise the different experimental conditions considered in studies reporting ‘to-the-body’ biodynamic responses to vertical (z), fore-aft (x) and lateral (y) vibration respectively. From the tables, it is evident that the majority of the studies have considered responses to vertical vibration alone and relatively a fewer studies have measured the biodynamic response to single axis horizontal vibration. The responses to simultaneous dual or multi-axis vibration have been reported in even fewer recent studies [51-53]. The ‘through-the-body’ biodynamic responses have also been characterised in relatively fewer studies, while the vast majority have considered only vertical vibration. These studies have also employed widely different experimental conditions, as seen in Table 1.6. Considerable differences in the magnitudes of ‘to-the-body’ and ‘through-the-body’ responses reported in different studies have been observed [8,19,20]. These differences are attributable to nonlinear dependence of the biodynamic responses on various contributory factors, which may be grouped under subject anthropometry, sitting posture, nature of WBV and support conditions, as summarized in Table 1.7. The differences in the measured responses, which may also be partly, attributed to difference in the test conditions considered in different studies. The data reported in various studies are reviewed and discussed in the following sections to reveal the role of particular contributing factors, which in some cases appear to be contradictory. This may in-part be attributed to coupled effects of a number of factors exist.

Table 1.3: Summary of experimental conditions employed in studies reporting driving-point biodynamic responses of seated human body to vertical vibration.

Lead Author	n (gender)	Mass (kg) (mean)	Sitting conditions Posture; Back support	Excitation			Function Reported
				Type	Frequency (Hz)	Magnitude ² (m/s ² rms)	
Coermann [41]	8 (M)	70-99.5 (86.2)	Erect, relaxed; None	sine	1-20	Up to 0.5 g peak	Median MI ³ magnitude and phase
Edwards [54]	2 (M)	77.7-84 (81)	Upright;	sine	1-20	0.2, 0.35, 0.5 g peak	MI magnitude and phase (individuals)
Vykukal [55]	4 (M)	68-83 (75.8)	NR ⁶ ; NR	sine	2.5-20	0.4g peak (1, 2.5, 4 g bias)	MI magnitude and phase (n=1)
Vogt [56]	10 (M)	NR (80)	Erect; NR	sine	2-15	0.5g peak (1, 2, 3 g bias)	MI magnitude and phase
Suggs [57]	11 (M)	58-90 (73.6)	Upright; None	sine	1.75-10	1.25 mm peak displacement	Mean MI magnitude and phase
Miwa [58]	20 (M)	50-76 ² (60.8)	Erect, Relaxed; None	sine	3-200	0.1 g rms	Mean MI magnitude and phase
Mertens [59]	6(M) 3(F)	57-90 (66.8 ³)	Upright; NR	sine	2-20	0.4 g rms (1 to 4 g bias)	Mean MI magnitude and phase
Sandover [60]	6 (M)	52.7-87.2		Random	1-25	1	Individual AM ⁴ magnitude and phase
Donati [61]	15(M)	49-74 (62.9)	Upright, Hands on SW; None	Random sine	1-10	1.6	Mean MI magnitude and phase
Fairley [62]	8 (M)	57-85 (71.8)	Normal; None	Random	0.25-20	0.25-2.0	Individual AM magnitude and phase
Hinz [4]	4 (M)	56-83 (71.2)	Erect; NR ⁵	sine	2-12	1.5 and 3.0	Mean AM magnitude and phase
Fairley [63]	1 (M)	63	Normal; None	Random	0.25-20	1.0	AM magnitude & phase
Failrley [64]	24 (M ¹) 24(F ¹) 12(C ¹)	NR (63.1 ⁵)	Erect, tense; None	Random	0.25-20	1.0	Mean normalized AM magnitude
Mansfield [65]	12 (M)	60-85 (68.3)	Upright; None	Random	0.5-20	0.25-2.5	Individual AM magnitude
Matsumoto [66]	8 (M)	63-83	Normal; None	Random	0.5-20	1.0	Individual AM magnitude and phase

Table 1.3: Summary of experimental conditions employed in studies reporting driving-point biodynamic responses of seated human body to vertical vibration (Continued)

Lead Author	n (gender)	Mass (kg) (mean)	Sitting conditions Posture; Back support	Excitation			Function Reported
				Type	Frequency (Hz)	Magnitude ² (m/s ² rms)	
Kitazaki [67]	8 (M)	NR (74.6)	Normal, Slouched; None	Random	0.5-30	1.7	Mean normalized AM magnitude
Wu [68]	6 (M)	58-73 (64.2)	Erect; None	Random	0.5-20	1.0 and 2.0	Mean AM magnitude and phase
Boileau [69]	6 (M)	70-81 (75.4)	Erect, relaxed, slouched; None, Vertical, Inclined-14°	Sine Random	0.625-10	1, 1.5, 2.0 weighted	Mean MI magnitude and phase
Holmlund [70]	3 (M)	74 (74)	Erect, Relaxed; None	Field	1-20	NR	Individual MI magnitude
Mansfield [46]	12 (M)	60-85 (68.3)	Upright; None	Random	2-20	0.25-2.5	Median normalized AM ⁴ magnitude
Holmlund [71]	15(M) 15(F)	55-92 (74) 54-93 (66)	Erect, Relaxed; None	sine	2-100	0.5, 0.7, 1.0, 1.4	Mean MI magnitude and phase
Nawayseh [72]	12 (M)	57-106 (74.6)	Upright, 4 thigh support; None	Random	0.25-25	0.125, 0.25, .625, 1.25	Median AM magnitude and phase
Mansfield [10]	11(M) 13(F)	72-96(81) 54-79 (67)	Upright; None	Random	2-20	0.5, 1.0, 1..5	Median AM magnitude
Rakheja [73]	12(M) 12(F)	58-100 (78.5) 48-111 (64)	Relaxed; Automotive, 13° pan, 24° backrest	Random	0.5-40	0.25, 0.5, 1.0	Mean AM magnitude and phase
Matsumoto [74]	8(M)	64-87 (73)	Upright, Tense buttock; None	Random	2-20	0.35-1.4	Median normalized AM magnitude and phase
Mansfield [75]	12(M)	NR (75.4)	Upright; None, Vertical	Random	1-20	0.2, 1.0, 2.0	Normalized AM magnitude & individual phase
Hinz [76]	23 (M) 22 (F)	58-106 (NR) 51.5-84 (NR)	Relaxed; Automotive. 16° pan, 16° backrest	Random	1-35	0.3 weighted	Mean normalized AM magnitude and phase
Nawayseh [21]	12 (M)	62-106 (77.2)	Upright. – 4 thigh supports; Vertical	Random	0.25-20	0.125, 0.25, 0.625, 1.25	Median AM magnitude
Wang [77]	13 (M) 14 (F)	47.4-110.5 (70.8)	Upright, Hands on lap & SW; None, Vertical, Inclined	Random	0.5-40	0.5, 1.0	Mean AM magnitude and phase

Table 1.3: Summary of experimental conditions employed in studies reporting driving-point biodynamic responses of seated human body to vertical vibration (Continued)

Lead Author	n (gender)	Mass (kg) (mean)	Sitting conditions Posture; Back support	Excitation			Function Reported
				Type	Frequency (Hz)	Magnitude ² (m/s ² rms)	
Maeda [78]	12 (M)	NR (65.8)	NR; None	Random	1-20	1.0	Median AM magnitude and phase
Mansfield [79]	12 (M)	NR (65.8)	Upright; None	Random sine	1-40	1.0 .2-.5 weighted	Median normalized AM magnitude and phase
Kim [42]	5 (M)	89.8-98.7 (80.7)	Upright; None	Random	1-50	1.0	Mean AM magnitude and phase
Mansfield [79]	12 (M)	NR (63.8)	Upright/ twisted; None, Vertical	Random	1-20	0.4	Median normalized AM magnitude
Nawayseh [80]	12 (M)	65-103 (76.5)	Upright, 4 pan angles; Vertical	Random	0.5-15	0.125, 0.25, 0.625	Median AM magnitude
Huang [81]	14 (M)	NR (70.3)	Various postures; None	Random	0.5-20	0.25, 2	Median normalized AM magnitude and phase
Hinz [52]	13 (M)	61.3-103.6 (79.3)	Upright, Hands on bar; None	Random	0.25-30	0.25, 1.0, 2.0	Mean AM magnitude
Mansfield [83]	12 (M)	NR(79.1)	Upright; None, vertical	Random	2-20	1.0	Median AM magnitude
Mansfield [51]	15 (M)	NR(64.3)	Upright; None, vertical	Random	1-20	0.4, .8	Median AM magnitude
Patra [82]	9 (M) 9 (M) 9 (M)	50-60 (55.7) 70-80 (75.2) 93-107 (98)	Upright, Hands on lap & SW; None, Inclined	Random	0.5-20	0.5,1.0, 2.0	Mean AM magnitude and phase for 3 mass groups
Wang [47]	12(M)	66.4-99.6 (77.3)	Relaxed, Hands on lap &-SW; None, Vertical, Inclined	Random	0.5-15	0.5,1.0, 1.5	Mean AM magnitude and phase

¹M – male, F- female, C -children; ² Magnitude in m/s² rms unless stated; ³MI – Mechanical impedance; ⁴AM – Apparent mass; ⁵Estimated; ⁶NR-Not reported

Table 1.4: Summary of experimental conditions employed in studies reporting biodynamic responses of seated human body to fore-aft vibration.

Lead Author	n (gender)	Mass -kg (mean)	Sitting conditions		Excitation		Function Reported
			Posture; Back support	Type	Frequency (Hz)	Magnitude (m/s ²)	
Fairley [2]	8 (M)	57-85 (65.7)	Upright; None, Vertical	Random	0.25-20	0.5, <u>1.0</u> , 2 rms	Mean AM magnitude and individual AM phase
Holmlund [84]	15(M) 15(F)	55-93 (75) 54-76 (63)	Upright, erect/ relaxed; None	Discrete sine	1.13-80	0.25, <u>1.0</u> , 1.4 rms	Mean MI magnitude and phase
Mansfield [85]	15(M) 15(F)	(75.8) ⁴ (62.0)	Upright, Arms folded; None	Random	1.5-20	.25, .5, <u>1.0</u> rms	Median AM normalized magnitude
Holmlund [86]	15(M) 15(F)	55-93 (75) 54-76 (63)	Upright, - erect/ relaxed; None	Discrete sine	2-100	0.25, <u>1.0</u> , 1.4 rms	Mean MI magnitude and phase
Holmlund [70]	3 (M)	74 ¹	Upright, - erect/ relaxed; None	In-vehicle	-	NR	Mean MI magnitude only
Manadpuram [3]	8 (M)	59-92 (71.2)	Upright, -relaxed; None, Vertical Inclined	Random	0.5-10	0.25, <u>0.5</u> , <u>1.0</u> rms	Mean AM magnitude and phase
Nawayseh [87]	12 (M)	56-87 (77.5)	Upright – different thigh contact; None	Random	0.25-20	0.125, 0.25, 0.5, <u>1.0</u> 1.25 rms	Median AM magnitude and phase
Hinz [54]	13 (M)	61.3-103.6 (79.3)	Upright, Hands on a bar; None	Random	0.25-30	0.25, 1.0, 2 rms	Mean AM magnitude
Mansfield [93]	15 (M)	(64.3) ⁴	Upright; None, Vertical	Random	1-20	<u>0.4</u> rms	Median AM magnitude Median AM magnitude & phase (back support only)
Stein [50]	1 (M)	77.1	Upright, relaxed, Hands on a bar; Lumbar region contact	Random	0.3-30	<u>2.03</u> rms	AM magnitude and phase
Mansfield [51]	15 (M)	(64.3) ⁴	Upright, relaxed; None, Vertical	Random	1-20	0.4, <u>0.8</u> rms	Median AM magnitude

Table 1.5: Summary of experimental conditions employed in studies reporting biodynamic responses of seated human body to lateral vibration.

<i>Lead Author</i>	<i>n</i> <i>(gender)</i>	<i>Mass -kg</i> <i>(mean)</i>	<i>Sitting conditions</i>	<i>Excitation</i>			<i>Function Reported</i>
			<i>Posture; Back support</i>	Type	Frequency (Hz)	Magnitude Range (m/s ²)	
Fairley [2]	8 (M)	57-85 (65.7)	Upright; None, Vertical	Random	0.25-20	0.5, <u>1.0</u> , 2 rms	Mean AM ³ magnitude and individual AM phase
Holmlund [84]	15(M) 15(F)	55-93 (75) 54-76 (63)	Upright, erect/relaxed; None	Discrete sine	1.13-80	0.25, 0.5, <u>1.0</u> , 1.4 rms	Mean MI ² magnitude and phase
Mansfield [85]	15(M) 15(F)	(75.8) ⁴ (62.0)	Upright, Arms folded; None	Random	1.5-20	.25, .5, 1.0 rms	Median AM normalized magnitude
Holmlund [86]	15(M) 15(F)	55-93 (75) 54-76 (63)	Upright, erect/relaxed; None	Discrete sine	2-100	0.25, 0.5, <u>1.0</u> , 1.4 rms	Mean MI magnitude and phase
Holmlund [70]	3 (M)	74 ¹	Upright, erect/relaxed; None	In-vehicle	-	NR	Mean MI magnitude only
Manadpuram [3]	8 (M)	59-92 (71.2)	Upright, relaxed; None, Vertical, Inclined	Random	0.5-10	0.25, <u>0.5</u> , 1.0 rms	Mean AM magnitude and phase
Hinz [54]	13 (M)	61.3-103.6 (79.3)	Upright, Hands on a bar; None	Random	0.25-30	0.25, 1, 2 rms	Mean AM magnitude
Mansfield [93]	15 (M)	(64.3) ⁴	Upright; None, Vertical	Random	1-20	<u>0.4</u> rms	Median AM magnitude Median AM magnitude & phase (back support only)
Mansfield [51]	15 (M)	(64.3) ⁴	Upright, relaxed; None, Vertical	Random	1-20	0.4, <u>0.8</u> rms	Median AM magnitude

Table 1.6: Summary of experimental conditions employed in studies reporting seat-to-head transmissibility (STHT) of seated human body to vertical vibration.

<i>Lead Author</i>	<i>n</i> (gender)	<i>Mass -kg</i> (mean)	<i>Excitation</i>			Function Reported
			Type	Frequency (Hz)	Selected magnitudes (m/s ²)	
Coermann [41]	1 (M)	84	sine	1-20	< 0.5 g peak	Magnitude
Mertens [59]	6 (M) 3 (F)	57-90	sine	2-20	4.85 m/s ² rms	Mean magnitude and phase
Griffin [88]	18(M) 18(F)	NR	sine	1-100	NR	Mean magnitude
Hinz [4]	4(M)	56-83 (71)	sine	2-12	1.5 m/s ² rms	Mean magnitude and phase
Paddan [19]	12(M)	58-81 (70.8)	random	Up to 25 Hz	1.75 m/s ² rms	Individual magnitude; phase (n=1; 80 kg)
Zimmermann [89]	30 (M)	(77.6)	sine	4.5-16	1.0 m/s ² rms	Mean magnitude
Kitazaki [49]	8 (M)	(74.6)	random	0.5-35	1.7 m/s ² rms	Mean magnitude
Wu [68]	6 (M)	58-73 (64.2)	random	0.625-20	1.0 m/s ² rms	
Hinz [91]	39(M)	NR	random; (1-4 Hz)	1-20	0.7, 1.0 and 1.4 m/s ² rms - weighted	Mean magnitude and phase (Hands on steering wheel)
Kim [42]	5 (M)	65.7-98.7	random	1-50	1.0 m/s ² rms	Mean magnitude
Wang [37]	12 (M)	66.4-99.6 (77.3)	random	0.5-15	0.25, 0.5, 1.0 m/s ² rms	Median magnitude

Table 1.7: Grouping of factors affecting the biodynamic responses of the seated body exposed to WBV.

Anthropometry	Sitting Posture	Vibration	Support
Body mass Build Height Gender	Sitting erect Sitting slouched Muscle tension	Type (sine, random) Direction Intensity Frequency	Back support Back rest orientation Pan orientation Seat height Feet support Hands support

Despite the variability in the measured responses, the reported data under vertical WBV generally show primary response peak around 5 Hz, often referred to as the primary resonant frequency of the seated body [46,73,92]. The reported data also suggest secondary resonances in the 8-13 Hz range [48,82]. Considerable differences, however, exist in the resonance frequencies under horizontal vibration (Table 1.8). The *APMS* responses obtained under fore-aft and lateral vibration, revealed primary resonance frequencies near 0.7 Hz in both directions, when seated with unsupported back, with secondary modes near 2.5 and 2 Hz along the *x*- and *y*-axis, respectively [2,3]. The first mode was attributed to pitching and swaying of the upper body under *x*- and *y*-axis vibration, while the secondary modes were believed to be associated with horizontal motions of the musculoskeletal structure. Lee and Pradko [16] identified these frequencies near 1.3 Hz under *x*-axis and 0.6 and 1.8 Hz in the *y*-axis. Mansfield and Maeda [51] measured the *APMS* under single and multiple axis vibration in the 1-20 Hz range, and reported median resonance frequencies of less than 1.0 and near 1.75 Hz corresponding to *x*- and *y*-axis vibration, respectively. Irrespective of the axis of vibration, an increase in the excitation magnitude consistently revealed a decrease in the response peak magnitude and the corresponding resonant frequency [51,52]. Such non-linear behaviour has been interpreted as a non-linear softening effect in the muscle tension under increasing intensity of vibration [4,77,93,94].

Table 1.8: Reported resonance frequencies observed in APMS responses of seated occupant exposed to horizontal WBV.

Author	Posture (Backrest)	Resonant frequencies (Hz)			
		<i>Fore-aft APMS</i>		<i>Lateral APMS</i>	
		<i>Seatpan</i>	<i>Backrest</i>	<i>Seatpan</i>	<i>Backrest</i>
Fairley [2]	None Vertical	0.7, 2.5 3.5	- NR	0.7, 1.5 1.5	-
Mansfield [85]	None	3, 5	-	2.3, 5	-
Mandapuram [3]	None Vertical Inclined	0.7, 2.8, 4.75 3.3-5.4 2.7-4.1	- 1.25-2, 4-4.45 1-1.12, 2.6-4, 7-8	0.7, 2 0.9-2.1, 6 0.9-2.1, 6	1 1
Nawayseh [87,97]	None Vertical	1, 1-3, 3-5 2-4	- <2, 3-5	NR	- NR
Hinz [4]	None	2.18-2.9	-	1.37-2.04	-
Mansfield [93]	None Vertical	2-3 3.5	- NR	1.75 1.75	NR
Mansfield [51]	None Vertical	NR 4	- NR	1.5-1.75 2	NR

The biodynamic responses measured under single axis WBV exposures have consistently revealed strong effect of body mass and build [73,75,77]. A larger body mass causes greater contact area and uniform contact force at the driving points, which could considerably alter the ‘to-the-body’ biodynamic responses of the seated body [87]. The reported studies, invariably, show larger scatter in the *APMS* magnitude response, particularly in the low frequency range, which is attributed to body mass variations. The *APMS* responses are thus generally normalised with respect to the mass supported by the seat or the *APMS* magnitude at a low frequency, which greatly suppresses the scatter at the low frequencies [46,64,78]. The normalisation, however, cannot eliminate the important effect of the body mass [80]. Figure 1.2 (a) presents the mean *APMS* magnitude response of subjects within three different body mass ranges (near 55, 75 and 98 kg) exposed to vertical vibration [77]. The mean normalised responses, derived from the reported data, are presented in Figure

1.2 (b). The comparison suggests that normalisation eliminates the data scatter at low frequencies but alters the essential response trends at frequencies near primary resonance and beyond, which may make the interpretations more demanding. A number of studies have shown significant positive correlation between vertical *APMS* magnitude and body mass at frequencies up to and slightly above the primary resonance [77,82].

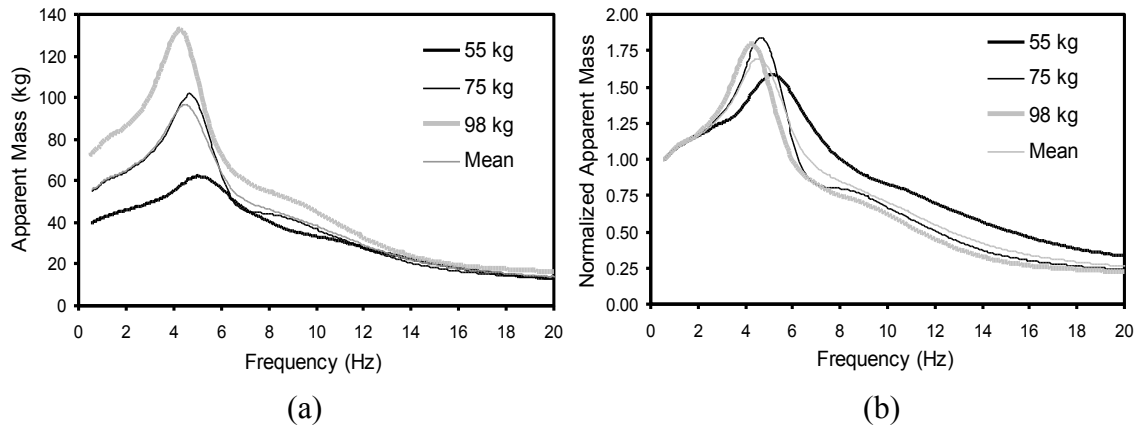


Figure 1.2: (a) vertical apparent mass magnitude responses of subjects within three different body mass range [77]; and (b) normalised APMS responses.

A linear dependence of the *APMS* magnitude on the body mass has been reported with various seat support conditions, including flat and inclined pan, and two hands position (on lap and on steering wheel) [43]. The power absorbed by the body, attributed to vertical WBV, has also been positively correlated with the body mass [13]. A positive linear correlation through a series of linear regression analyses, have been reported between the body mass and the total absorbed power, of the subjects seated with different body support conditions, including different back supports, hands positions, and seat heights [19]. A few studies have identified that the body mass effect is coupled with other contributing factors [82]. The effect of body mass on vibration transmissibility measures have been reported in only a few studies under vertical vibration. These show somewhat contradictory effects of body mass.

The vast majority of the studies report either mean or median biodynamic responses of a subject sample with considerably different masses. The mean or median responses thus do not permit the analyses of individual contributing factors, which are strongly coupled with the body mass effects. However, few studies have attempted to isolate the body mass effect from other factors by considering subjects within a narrow body mass range or by grouping the data under different mass groups [8, 37, 96, 97]. The low frequency and peak *APMS* magnitudes have been reported to increase with body mass, while the corresponding frequency decreases, as seen in Figure 1.2 (a) [77,82]. The fore-aft cross-axis *APMS* response magnitudes measured at the back support under vertical vibration, grouped within different mass groups, also revealed positive correlations with the body mass, as it was observed for the vertical responses measured at the seat pan [96].

A few studies have also investigated the gender effect on biodynamic responses of seated subjects under WBV exposures. However, the results appear to be contradictory. Some studies observed the gender effect to be insignificant under vertical vibration exposures [64,73,97]. A few studies under horizontal exposures, on the other hand, have revealed significant gender effect in terms of vibration power absorbed, and suggested that greater power absorption magnitudes of the females may be attributed to their greater fat to muscle mass proportions [13,64]. These studies, however, have considered male and female subjects of significantly different body masses, the findings may thus be biased due to coupled body mass effects. Another study investigated the gender effect by considering male and female subjects of comparable body masses, and concluded negligible gender effect on measured vertical *APMS* responses [77].

The seat geometry, back support, hands and feet positions have been identified to alter muscles tension and postural stresses, and thereby the biodynamic responses to vibration. An inclined backrest is known to support a greater portion of the trunk weight, which can reduce the compressive force between the trunk and the pelvis, and thereby intradiscal pressure [23,99]. The vast majority of the studies on experimental biodynamics have considered subjects seated without a back support, while the back supported sitting posture, a representative sitting condition in majority of the vehicles, constitutes multiple driving-points, where vibration enters the body at the buttocks, hands, feet and the back.

Only a few studies have investigated the effect of back support on the biodynamic responses of the seated body to vertical and horizontal vibration. These studies revealed a significant reduction in inter-subject variability, attributed to stabilised upper body [19, 20, 39]. Similar decrease in variability has also been reported with increase in the seat pan angle [80]. Compared to the APMS, even fewer studies have explored the effects of back support on the *STHT* responses [47,77]. Figure 1.3 illustrates the effect of back support on the mean measured *APMS* and *STHT* magnitudes under vertical vibration [99]. The results show that an inclined back support yields lower primary frequency and the corresponding magnitude, while it emphasises the response around the secondary resonance frequency. The influences of back support on the vibration transmitted to the head have also been investigated under vertical, horizontal, roll, pitch and yaw WBV, applied independently [19,20,101]. The *APMS* responses to horizontal vibration have also consistently shown the strong effects of the back support, as seen in Figure 1.4 for fore-aft vibration. The show that with addition of a backrest causes the fore-aft and lateral modes 1.5 and 3.5 Hz, respectively to converge to single modes 2.7-5.4 and 0.9 Hz, respectively [2-5]. The effects of back support on the absorbed

power responses under vertical and horizontal WBV have also been reported in a few studies [3,12].

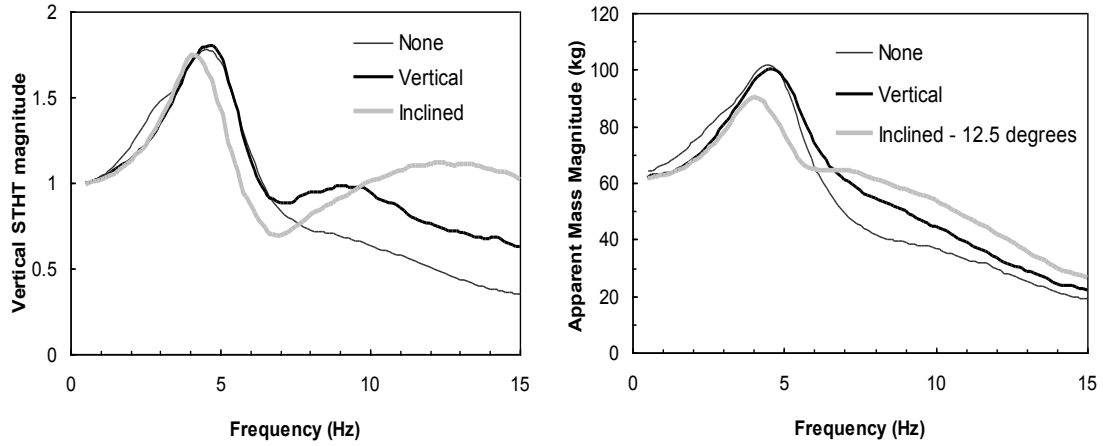


Figure 1.3: Influence of back support on the seat-to-head acceleration transmissibility, and apparent mass under vertical vibration. [47].

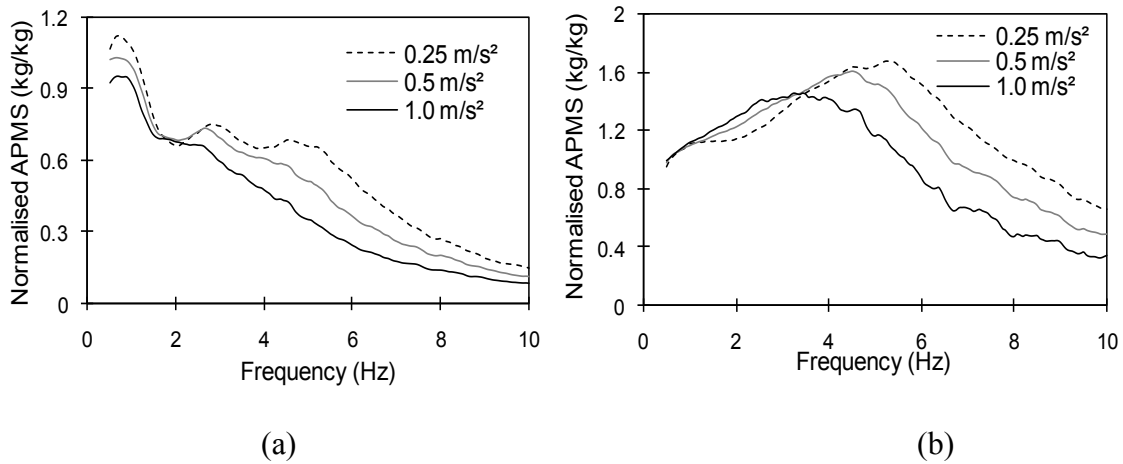


Figure 1.4: Influence of magnitude of back support condition on apparent mass responses of seated body to different magnitudes of fore-aft vibration: (a) no back support and (b) back support [3].

The *STHT* responses obtained under horizontal vibration revealed considerably different peaks and corresponding frequencies from those observed from the *APMS* studies. The *STHT* magnitude peaks occurred near 3 and 1.5 Hz under fore-aft and lateral vibration, respectively, when sitting with back unsupported posture [20]. The responses with back

supported postures showed an additional peak in fore-aft *STHT* near 8 Hz, with the primary peak shifting up to 2 Hz. Similar differences have also been observed in vertical *APMS* and *STHT* responses. This may in-part be caused by differences in subjects considered for measurements of the two responses. A thorough analysis of simultaneously measured *STHT* and *APMS* responses may help to better characterise the total biodynamic response of the seated body.

The measured responses to single axis vibration have also shown notable cross-axis responses, particularly in the presence of a back support. Exposure to vertical vibration is known to yield considerable fore-aft and pitch motions of the upper-body [34], which are known to instigate considerable dynamic interactions with the back support. Such interactions have been investigated in a few studies by measuring the responses at the back support [52, 60]. Such forces are significantly higher along fore-aft axis, and have been observed to increase with the inclination of the back support, suggesting greater coupling between the vertical and fore-aft responses.

The seat height may also affect the biodynamic responses, and the effect could be coupled with the feet position. An increase in the seat height, or lowering the footrest height, may lead to feet hanging postures. The feet position also substantially affects the biodynamic response, as it is known to affect the body mass supported by the seat pan, contact with the thighs, pelvic orientation and the upper-body posture [2]. Majority of the studies have considered the feet supported on the vibrating platform, while a few have considered adjustable footrest. The effect of minimum, maximum, average thigh contact and legs hanging postures, realised by variation of the footrest height, have been investigated under vertical and fore-aft vibration [21,47].

The biodynamic studies have mostly considered seated body with hands in lap or on thighs or arms folded across chest, which is not considered representative of the vehicle driving postures. It has been suggested that placing the hands on the thighs may help dampen the higher modes of vibration [66]. Relatively a fewer studies have considered the seated subjects with hands on a bar or a steering column [37,52,73,77]. The vibrating hand support (steering column) would represent another source of vibration to the body or an additional driving-point. The hands on steering column or a bar is known to reduce the proportion of body weight on the seat pan, and may cause greater reaction force at the upper body in the presence of back support [77,102]. It is also reported to cause stiffening of the body, and alter the pelvic orientation, which has been shown to effect the biodynamic responses [24,102,103] The effect of hands on the steering wheel has been observed on the biodynamic responses of seated body with back supported postures exposed to vertical vibration alone [77, 82]. The effect of hands position on the absorbed power under vertical vibration was also observed to be significant for back unsupported, vertical and inclined back support [12]. Unlike the *APMS* responses, the effect of hands position was observed to be more pronounced on the vertical and fore-aft STHT responses, for the no back support condition [62]. Sitting without a back support and hands on the steering wheel resulted in greater magnitudes of vertical head vibration in the 3-10 Hz range, while the effects were notable at frequencies above the primary resonance for the back supported postures. Such interactions could be significant particularly under fore-aft vibration, which are yet to be explored.

The significant effect of hands position has been reported in a single study in terms of *APMS* of the body seated on a cushioned seat and exposed to fore-aft vibration [50]. The study, however, measured the driving-point force at the seat base, assuming negligible

contribution of the seat cushion. The peak *APMS* with hands on steering wheel was nearly twice that obtained with hands in lap, when the steering wheel was close to the seat. The frequency corresponding to the peak was also observed to be considerably higher than that with hands in lap. The effect of hands position has been identified to be strongly coupled with many other factors, such as backrest inclination, seat height and pelvic orientation, and further investigations are needed to identify the contributions of the hands position.

The absorbed power responses of seated human body exposed to single axis WBV, have been investigated under continuous sinusoidal and random vibration considering both supported and unsupported back postures [3,12,13,104]. The reported P_a spectra generally exhibit peaks at frequencies that are comparable to those of the *APMS* magnitude peaks. The absorbed power response of the body increases nearly quadratically with the acceleration magnitude. The studies have also shown important influences of variations in the sitting posture and seat geometry factors (seat height, footrest position, hands position, back support and seat pan angle) on the absorbed power response of the seated human occupants exposed to vertical WBV [11, 19]. The effects of such factors on the absorbed power under horizontal vibration have not been adequately addressed.

The knowledge of the role of the contributing factors suggests that it is essential to consider, constrained conditions of the seating postures, body mass and vibration related factors to obtain biodynamic responses of the seated occupants under multi-axis vibration exposures, which are more representative of the vehicle vibration environments.

1.2.4 Biodynamic responses to Multi-axis WBV

The vehicle vibration environment is multi-directional. The biodynamic responses of the seated human body to multi-axis vibration are thus vital to enhance knowledge on mechanical properties of the body under realistic vehicular vibration. These would help

obtain improved frequency-weightings and biodynamic models for applications in seating design.

Recent developments in multi-axis vibration platforms have permitted characterization of biodynamic responses of the seated body to simultaneously applied dual- and three-axis translational vibration. The APMS responses of the seated body to multi-axis translational vibration have been reported in three recent studies [51-53], while one was limited to dual-axis vibration applied along xz and yz axes [93]. The STHT responses of the seated body to multi-axis vibration have been reported only in a single study [53]. The reported studies have considered different sitting conditions involving either back support [51,52] or hands support [52]. The response characterizations involving combined hands and back supports, representative of driving condition, has not yet been attempted. Furthermore, the reported studies were conducted under un-correlated multi-axis vibration, which may not be representative of realistic vehicle vibration. The ride vibration of vehicles, invariably, exhibit strongly coupled vertical-pitch, vertical-roll and roll-lateral vibration modes [e.g., 39,105]. The reported studies have derived biodynamic responses using the H_1 frequency response function method involving cross-spectrum of the response and excitation variables. This approach would suppress the cross-axis response and thus the coupled effects of uncorrelated multi-axis vibration. The reported studies have thus invariably shown that biodynamic responses to dual or three-axis translational vibration are quite comparable to those measured under single axis vibration. Considering that single axis vibration yields notable magnitudes of cross-axis response components, the above-stated finding of the reported studies would be highly questionable.

Mansfield and Maeda [51,93] measured APMS responses of 15 male subjects seated with and without a vertical back support and hands in lap while exposed to single-, dual- and three-axis WBV. The study employed broad band random vibration in the 1-20 Hz frequency range (rms acceleration = 0.4, 0.6 and 0.8 m/s²). The study reported both the direct and cross-axis APMS responses derived from the forces and accelerations measured at the seat pan. The application of vibration above 1.0 Hz, however, did not permit the responses corresponding to primary resonances, which are known to occur below 1 Hz under fore-aft and lateral vibration in the absence of a back support.

Hinz et al.[52], in a similar manner measured the APMS responses of seated human to single and multi-axis WBV. The subjects were seated without a back support and hands supported on a handle-bar, while exposed to broad band random vibration in the 0.25 to 30Hz. Different magnitudes of vibration were synthesized so as to achieve comparable over all rms acceleration due to single, dual and three-axis vibration. The study reported only direct seat-pan APMS, while the cross-axis APMS was not reported. Both the studies reported the relative lower APMS magnitudes and the corresponding frequencies under multi-axis vibration when compared to those under single axis vibration. The multi-axis vibration effect was similar to that observed with increase in single axis vibration magnitude.

The responses to single-axis vibration along the vertical and fore-aft axes, on the other hand, have shown considerable saggital-plane motions (vertical, fore-aft and pitch) of the upper body suggesting coupled effects of vertical and fore-aft vibration [96, 100], reporting STHT responses to single axis vibration have observed multi-axis motions of the upper body [19, 106].

The direct and cross-axis *APMS* responses to dual axis vibration applied along x - y , y - z and x - z axes have also been measured for subjects seated with and without vertical back support [93]. The study revealed that fore-aft and lateral *APMS* responses to combined x - y vibration were quite similar to those attained under respective single-axis vibration. The vertical *APMS* responses to coupled x - z and y - z axes vibration were also comparable with those measured under z -axis vibration. The data also showed considerable magnitudes of fore-aft and vertical cross-axis *APMS* under individual z - and x -axis motions, similar to those presented under vertical vibration alone [21,96]. The results suggest that the direct and cross-axis *APMS* responses to dual axis vibration occur at a slightly lower frequency compared to those to single-axis vibration, which may be partly attributed to relatively higher resultant magnitudes of two-axis vibration compared to that of the single-axis vibration employed in the study [93]. The relatively poor frequency resolution of 0.25 Hz used in the study, however, would make it difficult to establish definite trends.

Hinz et al. [52] also reported slightly lower mean peak fore-aft and lateral *APMS* magnitudes under dual-axis (xy) vibration coupled to that obtained under x -axis vibration, while the corresponding frequency was similar for the single as well as dual axis vibration. Similar effect was also observed in the responses to combined x - and z - axes (xz) vibration reported by Qui and Griffin [107], which showed decreasing peak vertical *APMS* magnitude and the corresponding frequency under increasing x -axis vibration, and vice-versa. Furthermore, it was difficult to establish definite trends in the primary peak frequencies due to relatively poor frequency resolution used in the above studies, 0.25 Hz and 0.39 Hz. The peak fore-aft and lateral *APMS* magnitudes under 3 axis vibrations, however, were observed to be higher for the low excitation level but similar to the single-axis response under the

higher excitation [51]. The effect of multiple axis vibration was observed to be statistically significant on the vertical *APMS* response. Peak vertical *APMS* magnitude and the corresponding frequency were observed to be lower under three-axis excitations compared to the vertical axis alone, as reported by Mansfield and Maeda [51]. The two studies, however, employed different magnitudes of excitations. While Mansfield and Maeda [51] considered identical magnitudes of vibration along each axis, Hinz et al [52,53] employed identical effective magnitudes of single and three-axis vibration.

The lack of coupling effects of multi-axis vibration may be attributed to two factors. Firstly, the H_l frequency response function estimator used in the reported studies tends to suppress the cross-axis components under uncorrelated multi-axis vibration [15]. Secondly, the *APMS* response measured at the seat pan may not entirely reflect the contributions of coupled upper-body motions. The measurements of *APMS* at the seat back and *STHT* may reveal the coupled effects of multi-axis vibration. The *STHT* responses under multi-axis vibration have been reported in a single study by Hinz et al [53]. The study reported translational and rotational *STHT* responses of the occupants seated without a back support and hands supported on a handle bar under single (x, y, z) and three (xyz) axis vibration. The results revealed definite differences between the single and multi-axis responses compared to those observed in the *APMS* responses. This would suggest greater coupling effects of multi-axis vibration on the upper-body movements, which may not be entirely captured by the driving-point measures. A study on hand-arm biodynamics has suggested that the three-axis vibration biodynamic response may be estimated from summation of the direct- and cross-axis components measured under single-axis vibration [109]. Alternatively, the H_v frequency

response function estimator could be employed to analyse the responses to uncorrelated multi-axis vibration [108].

1.2.5 Biodynamic modelling

The measured biodynamic responses have been extensively interpreted to gain understanding of the human responses to vibration and identification of potential injury mechanisms attributed to prolonged occupational exposure to whole-body vibration. In combination with the experimental studies, the biodynamical models could serve as powerful tools for the analysis of the effects of vibration exposure on health and comfort, and for design of seats and seating supports. The validity of a biodynamic model, however, strongly relies upon defining reliable target biodynamic responses. The non-linearity and complexity of the human system, attributed to various individual- (body mass, build, physical fitness), posture- (seat, supports, muscles tension and sitting conditions) and vibration- (type, magnitude and frequency) related factors [e.g., 58,67,75,111], however, pose difficult challenges for identifying target responses for model development.

The properties, identified from the measured biodynamic responses, under single axis studies, have been applied to formulate various mechanical-equivalent models [e.g., 42,49,50]. These models have been used for developing anthropometric manikins for efficient evaluations of suspension seats coupled with the human occupant, without the stigma of ethical issues in human vibration testing [112]. The properties and biodynamic response prediction abilities of various lumped-parameter models have been thoroughly reviewed in [113,114]. The models are generally formulated using linear elements to satisfy target biodynamic response(s) of the seated human body under WBV exposures, obtained under particular posture and vibration conditions. The contributions due to nonlinearity in the

biodynamic responses are ignored due to the associated complexities. The broad applicability of the models therefore necessitates that the target biodynamic response functions be established over the most practical ranges of whole-body vibration excitation and postural conditions [58,67,75,77,111].

The applications of biodynamic mechanical-equivalent models and anthropo-dynamic manikins, however, seem to have met limited success thus far. The majority of the models are built on the basis of human responses to only single axis (vertical) WBV exposures. However, exposures to significant vibration levels along horizontal axes are believed to cause shear stresses in the spine [115], which could form a major causative factor with regard to the injury-risk. This is also reflected by the recommended additional weighting of 1.4 on the horizontal vibration exposure in ISO-2631-1 (1997) [6]. The biodynamic models reporting responses to horizontal vibration, however, have not yet been formulated, with the exception of a simple lumped-parameter model reported by Mansfield [85]. Moreover, the validity of the vertical FE and MBD models has been demonstrated only under limited conditions.

There is a need for developing models based on the multiple target functions (APMS and STHT) defined for specific body mass ranges and sitting conditions. It is thus desirable to define target STHT and APMS response functions to more realistic three-axis vibration that would serve as essential basis for deriving mechanical-equivalent models of the seated body.

1.3 SCOPE AND OBJECTIVES OF DISSERTATION RESEARCH

The control of potential health risks associated with WBV exposure necessitates a thorough understanding of human response to realistic multi-axis vibration and design of interventions in the form of effective vibration attenuation devices. The design of such devices requires integration of the biodynamic models of the human body to the system design. From the literature, it is evident that the models developed thus far have met limited success in the design process and in deriving proven anthropo-dynamic manikins. Furthermore, the biodynamic responses and the models often offer only limited applications under representative vehicular environments. It is further evident that the biodynamic responses are strongly dependent not only on the anthropometry but also on various seat design and postural factors.

The model development have mostly considered the biodynamic responses to vertical vibration alone, even though a large number of off-road vehicles impose considerable horizontal vibration, which are either comparable to or greater than the magnitudes of vertical vibration. The characterisation of biodynamic responses to multi-axis WBV under representative vehicle driving postures could not only provide the knowledge on human response behaviour but also serve as the desired target functions for development of effective models. The conditions must include the representative back support in consideration of typical seat geometry and hands on the steering wheel or a control stick. Furthermore, such responses could provide considerable insight into the coupling effects of various vibration modes and cross-axis biodynamic responses.

The proposed dissertation research is primarily motivated by the need to characterise biodynamic responses of the seated body under representative multi-axis vibration to

contribute to target APMS and STHT response functions for developing reliable biodynamic models of the seated body. The primary objective of the proposed research thus involves characterisation of biodynamic responses to multi-axis vibration along the translational axes, including the coupling effect. The specific goals of the proposed research are listed below, which also describe the major contributions of the dissertation research:

- a) Characterise biodynamic responses of seated human subjects exposed to single, dual and three-axis translational vibrations in terms of both the ‘to-the-body’ and ‘through-the-body’ response functions;
- b) Characterise the upper body-backrest interactions under single, dual and three-axis vibration;
- c) Investigate an alternate method of analysis for estimating responses to uncorrelated dual and three-axis vibration;
- d) Investigate the absorbed power response of the body under multi-axis vibration and derive a frequency-weighting based on the power absorbed by the seated body; and
- e) Study the effects of important contributory factors such as back support, hands support and magnitude of vibration.

1.4 ORGANIZATION OF THE DISSERTATION

This “Manuscript-based” dissertation is organised in eight chapters. Chapter 2 presents the detailed analytical formulations and highlights of various phases of the dissertation research. Chapters 3 to 7 present five articles illustrating the results achieved in a sequential manner that address the objectives stated in section 1.3. Four of these articles have been published in peer-reviewed journals, while the last article has been submitted for review. Each of these articles present a portion of the dissertation research and contents of

the articles are interpreted as per the stated scope and rules and requirements defined in “Thesis Preparation and Thesis Examination Regulation” booklet of the school of graduate studies at Concordia University. The major conclusions drawn from the dissertation search are summarised in Chapter 8 together with a few recommendations and suggestions for further studies.

Chapter 2

CHARACTERIZATION OF SEATED BODY BIODYNAMIC RESPONSES TO MULTI-AXIS VIBRATION

2.1 GENERAL

The dissertation research was aimed at characterisation of ‘to-the-body’ and ‘through-the-body’ biodynamic responses of seated body exposed to single, dual and three-axis translational vibration. The vast majority of the experiments were conducted at the Japan National Institute of Occupational Safety and Health (JNIOSH) using their multi-axis whole-body vibration simulator. The results attained in the course of the dissertation research have been presented in a total of five articles published or submitted for publication in journals, and six articles in proceedings of different conferences. The five journal articles are reproduced in chapters 3 to 7 that illustrate the major findings in a sequential manner. The highlights of these articles are further summarised in the following sections that address the stated objectives of the dissertation. The underlying analytical formulations analyses methods are also described below, which could not be presented in the published articles.

2.2 RESPONSES OF SEATED OCCUPANTS UNDER SINGLE AND DUAL AXIS HORIZONTAL VIBRATION

“Apparent mass and seat-to-head transmissibility responses of seated occupants under single and dual axis horizontal vibration”, *Industrial Health* Vol. 48, (2010) 698-714.

The APMS responses for the back supported posture are characterised at both the driving-points formed by the buttock-seat pan and the upper-body-backrest interfaces under single (x , y) and dual (xy) axis horizontal vibration. This article presents a method to derive the total seated body responses from the driving-point responses measured at seat-pan and

the backrest interfaces. Further, the article also presents the dual-axis responses that are estimated from the direct and cross-axis responses obtained under single axis vibration. The measured and the computed dual-axis responses, however, did not present any coupling effects of dual-axis vibration even though the coupled x - y motions were strongly perceived by the subjects, and clearly observed by the experimenters. The lack of the coupling effect could be attributed to the negligible cross-axis components under horizontal axes, and the uncorrelated nature of the dual-axis vibration synthesised in the laboratory. However, this article presents important steps towards investigating the coupling in the dual-axis vibration.

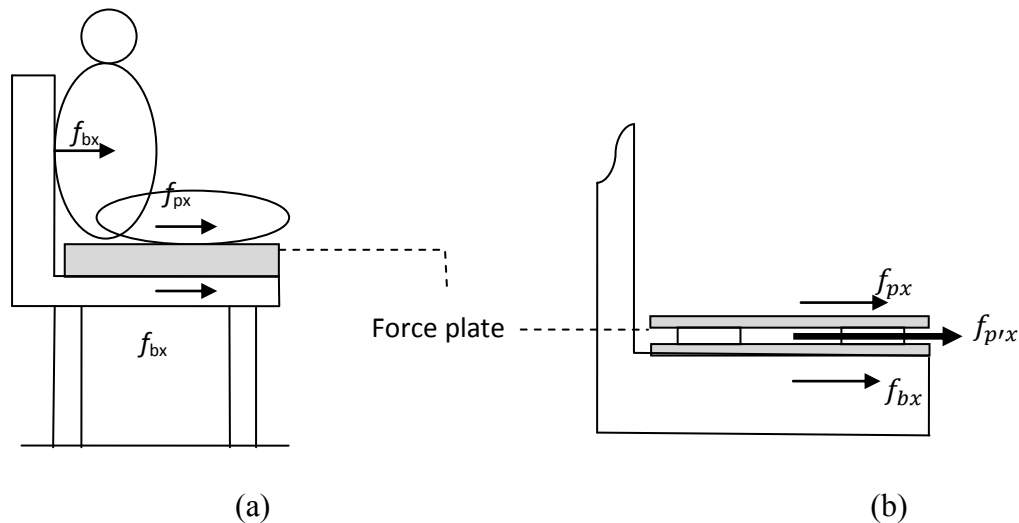


Figure 2.1: (a) Schematic of the test seat with force plate serving as the seat pan; and (b) reaction forces at the seat-pan result in the cancellation of force at the seat-pan: $f_{p'x}$ is the measured force at the seat-pan, f_{px} and f_{bx} are the actual forces at seat-pan and backrest interfaces, respectively.

The study concluded that the seat pan APMS is significantly lower when the seat pan driving-point force is measured directly at the seat pan as opposed to the seat base. The study subsequently proposed a method to determine the total APMS response from the forces measured at the two-driving points. Figure 2.1 illustrates the distribution of driving-point forces under fore-aft vibration. The upper body force imparted on the backrest opposes the force at the seat-pan, and thereby causes the seat pan APMS to be lower. Similar tendency

was also evident in the lateral and vertical APMS responses. The effect of such cancellation, however, was most significant in the fore-aft seat-pan APMS responses due to relatively stronger interactions of the upper body and the back support in the fore-aft axis.

Apart from the inertia correction of the measured response attributed to the inertia force of the seat structure, the direct and cross-axis *APMS* responses measured at the seat pan were derived upon considering of the force developed at the backrest driving-point. In case of fore-aft (x) axis vibration, the instantaneous force at the seat pan is obtained as:

$$f_{px}(t) = f_{p'x}(t) + f_{bx}(t) \quad (2.1)$$

The Fourier transform of Eq (2.1) yields:

$$F_{px}(f) = F_{p'x}(f) + F_{bx}(f) \quad (2.2)$$

Considering equal rms magnitudes of broadband vibration applied at the backrest and the seat pan, and multiplying by $a_x(f)$ on both the sides of Eq. (2.2) yields:

$$a_x(f)F_{px}(f) = a_x(f)F_{p'x}(f) + a_x(f)F_{bx}(f) \quad (2.3)$$

The cross-spectral density of the acceleration and the resulting driving-point forces, can be expressed as:

$S_{a_x F_{px}}(f) = \frac{1}{T} E[a_x(f)F_{px}(f)]$ Where $T=1/\Delta f$ is the time period or measurement duration. Eq. (2.3) can thus be expressed in terms of cross-spectral densities as:

$$S_{a_x F_{px}}(f) = S_{a_x F_{p'x}}(f) + S_{a_x F_{bx}}(f) \quad (2.4)$$

Using the definition of the apparent mass, as per the H_1 frequency response function estimator, eq (2.4) can be expressed in terms of *APMS*:

$$M_{px}(f) = M_{p'x}(f) + M_{bx}(f) \quad (2.5)$$

Where $M_{px}(f)$ is the total complex APMS at the seat pan driving-point, $M_{p'x}(f)$ is the complex APMS measured at the seat pan and $M_{bx}(f)$ is complex APMS measured at the seat back and given by:

$$M_{bx} = \frac{s_{ax}F_{bx}}{s_{ax}} \quad (2.6)$$

The corrected APMS at the seat pan is thus derived upon summation of those measured at the seat pan and the backrest.

$$|M_{px}(f)| = |\{ReM_{p'x}(f) + ReM_{bx}(f)\} + j\{ImM_{p'x}(f) + ImM_{bx}(f)\}| \quad (2.7)$$

Where *Re* and *Im* represent real and imaginary, respectively.

The study also presented the cross-axis responses to both *x*- and *y*-axis vibration, which were generally small. Assuming linearity of the responses, it was proposed that the total response to dual-axis vibration could be estimated from superposition of the direct and cross-axis responses to single axis vibration. This is illustrated in Figure 2.2 considering uncoupled vibration along the fore-aft and lateral axis, and the resulting force along the *x*-axis, $\bar{F}_x(t)$. The resulting force is superposition of direct force component F_{xx} due to a_x and cross-axis component F_{xy} due to a_y .

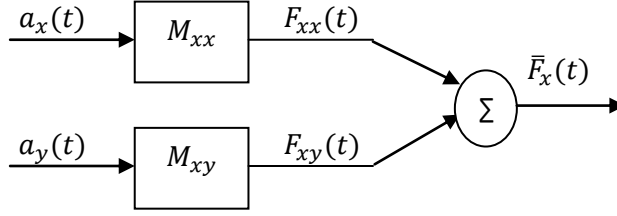


Figure 2.2: Schematic representation of the two-input-and-single-output model of the biodynamic functions under mutually uncorrelated fore-aft and lateral vibration.

Let $M_{xi}(f)$ represent the linear transfer function relating force along the x -axis acceleration $a_i(f)$ and the resulting force can be expressed as:

$$\bar{F}_x(f) = \sum_{i=x,y} M_{xi}(f) a_i(f) \quad (2.8)$$

The auto spectral density of the resultant force $S_{\bar{F}_x}$ can be obtained as:

$$S_{\bar{F}_x} = \bar{F}_x^*(f) \bar{F}_x(f) = [\sum_{j=x,y} M_{jx}^*(f) a_j^*(f)] [\sum_{i=x,y} M_{xi}(f) a_i(f)] \quad (2.9)$$

Where $\bar{F}_x^*(f)$, $M_{jx}^*(f)$ and $a_j^*(f)$ are complex conjugates of $\bar{F}_x(f)$, $M_{jx}(f)$ and $a_j(f)$, respectively.

$$S_{\bar{F}_x}(f) = \sum_{i=x,y} \sum_{j=x,y} M_{xj}^*(f) M_{xi}(f) a_j^*(f) a_i(f) \quad (2.10)$$

For uncorrelated vibration applied along the x - and y -axis, the above reduces to:

$$S_{\bar{F}_x}(f) = |M_{xx}(f)|^2 S_{a_x}(f) + |M_{xy}(f)|^2 S_{a_y}(f) \quad (2.11)$$

Where $S_{a_i}(f) = a_i^*(f) a_i(f)$ for $i=j$. The above equation yields the total apparent mass along the fore-aft axis, as:

$$\bar{M}_x(f) = \frac{S_{\bar{F}_x}(f)}{S_{a_x}(f)} = |M_{xx}(f)|^2 + |M_{xy}(f)|^2 \frac{S_{a_y}(f)}{S_{a_x}(f)} \quad (2.12)$$

Where $\bar{M}_x(f)$ is total fore-aft axis apparent mass under the dual-axis vibration. The above equation reveals that the extent of the coupling is dependent on the relative magnitudes of the vibration. Under special conditions based on equal magnitudes of broadband vibration, $\frac{s_{a_y}(f)}{s_{a_x}(f)} = 1$, the total seat-pan *APMS* responses along fore-aft axis, \bar{M}_x can be expressed as the sum of the direct and cross-axis seat-pan *APMS* responses obtained under single axis fore-aft and lateral vibration, respectively, such that:

$$\bar{M}_x(f) = \sqrt{|M_{xx}(f)|^2 + |M_{xy}(f)|^2} \quad (2.13)$$

The paper also presents the biodynamic response in terms of the STHT, which is also estimated in a similar manner:

$$\bar{T}_x(f) = \sqrt{|T_{xx}(f)|^2 + |T_{xy}(f)|^2} \quad (2.14)$$

Where \bar{T}_x , T_{xx} and T_{xy} are the total, direct and cross-axis, components respectively, of the seat-to-head vibration transmitted response along fore-aft axis. The results showed that the measured total responses were consistently lower than the estimated responses. This could be attributed to the fact that H_I response function estimator employed for analysis of total *APMS* and *STHT* responses suppressed the contributions due to cross-axis responses to uncorrelated dual-axis vibration.

Apart from the above, the paper also presented the coupled effects of hands and back support on the *APMS* and *STHT* responses, in addition to the effects of vibration magnitude.

2.3 BIODYNAMIC RESPONSES TO UNCORRELATED FORE-AFT AND VERTICAL WHOLE-BODY VIBRATION

“Analyses of biodynamic responses of seated occupants to uncorrelated fore-aft and vertical whole-body vibration”, Journal of Sound and Vibration 330 (16), (2011) 4064-4079.

This articles presents the STHT and APMS responses of the seated body exposed to single (x, z) and dual (xz) axis vibration, obtained using the two frequency response functions based on cross-spectral-densities and power-spectral-densities of the response and excitation. The method section illustrates that commonly used frequency response functions based on the cross-spectral-density are insufficient for analyses of seated occupants responses to uncorrelated multi-axis vibration, as it was evident in the previous article described in section 2.2. It is shown that the H_v frequency response function estimator can adequately account for contributions of the cross-axis components under uncorrelated multiple-axis vibration. The differences in the responses from the two methods are discussed in view of the coupled effects of dual-axis vibration.

The seated occupants responses to simultaneous dual or three-axis vibrations, reported in recent studies, have invariably employed, linear relationships (H_1 method) between the excitation and the measured responses. For dual-axis vibration along x and z axis, the biodynamic response functions along each axis are derived from:

$$H_k(f) = \frac{S_{a_k q_k}(f)}{S_{a_k}(f)}; k=x, z \quad (2.15)$$

Where $H_k(f)$ defines the complex biodynamic response function which relates the total measured response q_k to the excitation in the same axis k ($k = x, z$) corresponding to

excitation frequency f . $S_{a_k q_k}(f)$ is the cross-spectrum of the response q_k to the excitation a_k and $S_{a_k}(f)$ is the auto –spectrum of the excitation a_k .

For coupled motions of the seated body in the sagittal plane, the total response q_k would comprise of components due to excitations along both the axis. For instance, the response q_k would include the responses due to both the a_x and a_z excitations. Considering the uncorrelated nature of the excitations applied along the two axes, the response function, derived using Eq. (2.15), would ignore the contributions due to excitation along an axis other than the direct-axis. In particular, the total responses derived along x - and z - axis may suppress the contributions due to z - and x - axis vibration, respectively. This could be the reason for observing relatively similar APMS response magnitudes to single, dual or three-axis vibrations, reported in recent studies to single and dual or three-axis vibration [10,11]. Rocklin et al. [108], suggested that an alternate FRF estimator, H_v , for the modal extractions in multiple-input multiple-output (MIMO) systems. The biodynamic response function, derived from the H_v estimator, is expressed as:

$$H_k(f) = \frac{S_{a_k q_k}(f)}{|S_{q_k a_k}(f)|} \sqrt{\frac{S_{q_k}(f)}{S_{a_k}(f)}} \quad (k = x, z) \quad (2.16)$$

Where $S_{q_k}(f)$ is the auto-spectra of the total response measured along k under multi-axis vibration. It has been further suggested that the H_v method is better suited in the presence of noise in both the input and output signals. Under single-axis vibration, the magnitude of the FRF derived from the H_v method reduces to that obtained from PSD method. The PSD method, however, does not provide the phase information, which the H_v estimator yields the phase information identical to that obtained from the H_1 method. In this

study, the measured data were analysed to evaluate the APMS and STHT functions using three frequency response estimators, namely the H_1 , PSD and H_v methods.

The results obtained from the H_v method are used to illustrate the coupled effects of dual-axis vibration. The paper also illustrates the influences of vibration magnitude, and support conditions on both the APMS and STHT response functions.

2.4 BIODYNAMIC RESPONSES OF SEATED BODY TO THREE TRANSLATIONAL AXIS VIBRATION

“Apparent mass and head vibration transmission responses of seated body to three translational axis vibration”, International Journal of Industrial Ergonomics 42, (2012) 268-277.

This article presents the simultaneously measured STHT and APMS responses of the occupants seated under single (x , y and z) and combined three- (xyz) axis vibration, derived using both the H_1 and H_v frequency response function estimators. The differences observed in the responses obtained from the two methods are related to the contributions of the cross-axis response components. The responses to three-axis vibration derived using H_v method were further analysed to study the coupled effect of multi-axis vibration, and the back and hands supports.

Using the method described in the previous section, it is further proposed that the biodynamic response to three-axis vibration can be estimated from the direct- and cross-axis response to single-axis vibration, such that:

$$|\bar{H}_i(f)|^2 = |\bar{H}_{ii}(f)|^2 = \sum_{\substack{j=x,y,z \\ j \neq i}} |\bar{H}_{ij}(f)|^2 \frac{S_{a_j}}{S_{a_i}} \quad (2.17)$$

Where $\bar{H}_i(f)$ is the total biodynamic response, $\bar{M}_i(f)$ or $\bar{T}_i(f)$ along axis i ($i = x, y, z$) due to vibration applied along the three-axis simultaneously. $\bar{H}_{ii}(f)$ is the direct axis response to excitation along axis i only, and $\bar{H}_{ij}(f)$ is the cross-axis response along axis i due to excitation along j ($j \neq i$).

2.5 ABSORBED POWER ANALYSES TO MULTI-AXIS VIBRATION

“Energy absorption of seated body exposed to single and three-axis whole body vibration”, Journal of Low Frequency Noise, - submitted to Journal of Low Freq. Noise, Vibration and Active Control.

This article presents the vibration power absorbed (*VPA*) responses of the occupants seated with and without the back support, under single (x , y and z) and combined three- (xyz) axis vibration, which are derived, based on *APMS* responses. Thus derived responses are expected to contain the coupling due to the cross-axis components, as they are based on the H_v frequency response function estimators. This article also derives the total absorbed power of the seated occupant exposed to three-axis WBV, as the sum of absorbed power obtained along each individual axis. Further these *VPA* responses to combined three-axis vibration are applied to estimate the power absorbed responses of the drivers on the on-road (city bus) and off-road (forestry skidders and mining vehicles) vehicles based on reported vibration spectra. Frequency-weightings are suggested for the three-axis WBV exposures.

2.6 ABSORBED POWER BASED FREQUENCY WEIGHTINGS

“Energy absorption of seated occupants exposed to horizontal vibration and role of back support condition”, Journal of Industrial Health, vol. 46, 2008, pp 550-566.

This article presents a method to establish frequency-weightings on the basis of the absorbed power responses of the seated human subjects exposed to whole-body vibration. The proposed method, formulated jointly with researchers at National Institute of Occupational Safety and Health (NIOSH, USA), is applied to propose frequency-weightings corresponding to single axis fore-aft and lateral vibration. The absorbed power responses to horizontal vibration are formulated considering two driving-points formed by the seated body-seat pan and the upper body-seat backrest interfaces. The method section describes a different experimental set up used for this study as it was performed in CONCAVE laboratory. The study thus involved different human subjects and seat design with vertical as well as inclined backrest. The vibration power absorbed responses are suggested to develop improved frequency-weightings for risk assessments. The weightings derived suggests revision of the current international standard (ISO 2631-1) in order to consider seated postures involving backrest support.

Chapter 3

APPARENT MASS AND SEAT TO HEAD TRANSMISSIBILITY RESPONSES OF SEATED OCCUPANTS UNDER SINGLE AND DUAL AXIS HORIZONTAL VIBRATION

Summary: The apparent mass and seat-to-head-transmissibility response functions of the seated human body are investigated under exposures to fore-aft (x), lateral (y), and combined fore-aft and lateral (x and y) axis whole-body vibration. The experiments were performed to study the effects of hands support, back support and vibration magnitude on the body interactions with the seat pan and the backrest, characterised in terms of fore-aft and lateral apparent masses and the vibration transmitted to the head under single and dual-axis horizontal vibration. The data were acquired with 9 subjects exposed to two different magnitudes of vibration applied along the individual x- and y- axis (0.25 and 0.4 m/s² rms), and along both the-axis (0.28 and 0.4 m/s² rms) in the 0.5 to 20 Hz frequency range, and analyzed to derive the biodynamic responses. A method was further derived to obtain total seated body apparent mass response from those measured at the backrest and the seatpan. The results revealed coupled effects of hands and back support conditions on the responses, while the vibration magnitude effect was relatively small. For a given postural condition, the biodynamic responses to dual-axis vibration could be estimated from the direct- and cross-axis responses to single-axis vibration, suggesting weakly nonlinear behaviour.

3.1 INTRODUCTION

The biodynamic responses of the seated occupants exposed to whole body vibration (WBV) have been widely investigated in terms of apparent mass (APMS) or driving-point mechanical impedance, seat-to-head vibration transmissibility (STHT) and absorbed power, under broad ranges of vibration and postural conditions [2,3,51,52,73,116]. The majority of these studies focus on response analyses of seated body exposed to vertical vibration although a few have investigated the responses to fore-aft (x) and lateral (y) vibration [2,3]. Furthermore, most of the studies have been limited to single-axis vibration and response measurements in the direction of the applied vibration. Only a few recent studies have measured the seated occupants apparent mass responses to orthogonal dual and three-axis vibration [51,52,92] and only a single study has obtained cross axis responses of seated occupants exposed to dual-axis vibration [92]. Studies on horizontal biodynamics have

mostly considered a sitting posture without a back support with only few exceptions [51,92,117]. The vast majority of the studies reporting the biodynamic responses of subjects seated with back support have primarily focused on the body interactions with the seatpan alone, although the backrest is known to serve as an important secondary driving-point [3,21].

Although both the back and hands supports are representative of typical sitting postures for vehicle drivers, the effects of both the supports on the biodynamic responses to single and dual-axis horizontal vibration have not been quantified. A single study on horizontal biodynamics has shown considerable influence of hands support on the fore-aft apparent mass at the seatpan, while the body interactions with the back support were not considered [52]. The studies under single axis vibration have shown high magnitudes of biodynamic forces at the seatpan measured along the fore-aft direction under vertical vibration and vice versa, suggesting coupled movements of the human body in the sagittal (x - z) plane under either fore-aft or vertical vibration [21,92,118]. However, significantly smaller lateral forces at the seatpan were observed under the fore-aft or vertical vibration^{7,9,11)} suggesting weaker coupling between the x - and y -, and y - and z - axis responses. The vehicular vibration encompasses multi-axis whole-body vibration including translational and rotational components. The cross-axis biodynamic responses of the seated body observed under single-axis vibration would contribute to the total APMS and STHT responses to multi-axis vibration.

The international standard ISO 2631-1[6] defines identical weighting for assessing the exposure to both x - and y - axis vibration. It has been shown that the proposed W_d -weighting correlates reasonably well with the biodynamic responses of the body seated

without a back support [116]. The biodynamic responses of the occupants seated with a back support and exposed to fore-aft WBV, however, differed significantly from those corresponding to sitting with a back support and exposed to lateral vibration [2,3,51,116, 117]. The characterisation of biodynamic responses of the body seated assuming typical driving postures (back and hands supports) is thus essential for defining adequate frequency weightings for exposure assessments. Furthermore, the studies of upper body interactions with the back support together with the cross-axis biodynamic responses are vital for enhancing the seated body responses to single and dual-axis horizontal vibration. Only a few studies, however, have considered the backrest as the second important driving point and obtained the APMS responses at the backrest under fore-aft vibration [3,117]. A single study has reported the upper body interactions in terms of cross-axis APMS along all the three axes under fore-aft vibration [117].

Recent studies on seated occupants biodynamic to dual and three-orthogonal axis vibration have consistently reported similar seatpan APMS response trends, but slightly lower resonant frequencies and magnitudes compared to the single axis APMS responses [51,52,92]. These studies have considered either back supported or hands supported postures, although not both, and did not attempt measurements at the backrest and vibration transmitted to the head. The measurements of STHT responses have been limited to only single axis vibration where two studies have measured responses along 6-axes (3 translational and 3 rotational) of the occupants seated with unsupported and supported back postures [19,20]. These studies reported substantial head motions mainly in the mid-sagittal plane and have mostly shown increased head motions with the addition of the back support under individual fore-aft and vertical WBV. The lateral WBV mainly caused lateral head

motions and revealed minimal effect of the back support. On the basis of the ‘to-the-body’ and ‘through-the-body’ biodynamic responses to vertical vibration, it has been suggested that the two measures (APMS and STHT) tend to emphasize different modal responses of the seated body [47]. Both the measures are thus essential for describing the seated body responses to WBV. The STHT responses tend to emphasize the contribution to higher vibration modes compared to the APMS responses. This may partly be attributed to reduced contributions of the resonant oscillations of the low-inertia body substructures to the driving-point force. The transmissibility measures should thus be considered more appropriate for describing higher frequency vibration modes of the seated body and for developing higher order models.

Owing to the observed differences in the STHT and APMS responses measured in different laboratories under different test conditions with subjects of different anthropometry, simultaneous measurements of driving-point and vibration transmissibility responses have been suggested to yield more reliable biodynamic responses [47,59]. A few studies have measured both the biodynamic functions, either simultaneously or sequentially [4,46], while only one has explored the relationship between the two simultaneously measured responses to vertical vibration [47]. This study concluded that the STHT and APMS responses under vertical WBV correlate well in terms of peak magnitudes and corresponding frequencies. However, such comparisons have not been attempted under horizontal vibration.

The aim of this study is to characterise the seated body responses to single and dual-axis horizontal vibration in terms of the simultaneously measured fore-and-aft and lateral STHT and APMS responses, while the APMS responses for the back supported posture are characterised at both the driving-points formed by the buttock-seatpan and the upper-body-

backrest interfaces. The influences of the hands and back supports on the measured responses are investigated and relationships between the measured APMS and STHT responses are explored in terms of peak response magnitudes and corresponding frequencies.

3.2 METHODS

3.2.1 Exposure conditions and subjects

A rigid seat and a steering column were installed on a 6-DOF whole-body vibration simulator (IMV Corp.) for measurements of biodynamic responses to single and dual-axis horizontal vibration. A $600 \times 400 \text{ mm}^2$ force plate (Kistler 9281C) served as the seatpan at a height of 450 mm from the simulator platform. Another 450 mm high force plate served as the backrest, which was fabricated using three 3-axis force sensors (Kistler 9317B). The two force plates were used to acquire the forces developed at the two driving-points (seatpan and backrest) along the x , y and z directions. The platform vibration was measured by a three-axis accelerometer (Bruel & Kjaer 4506A) aligned with the translational axes of vibration. The head vibration was measured using a three-axis micro-accelerometer (Analog Devices ADXL-30) mounted on a light-weight helmet strap proposed by Wang et al. [37]. The frequency response characteristics of the helmet strap acceleration measurement system were measured by mounting the strap on the rigid seat subject to white-noise (flat power spectral density) two-axis horizontal vibration in the 0.5-20 Hz range. The results revealed nearly unity magnitude and negligible phase in the frequency range of interest (0.5-20 Hz).

A total of 9 healthy adult male subjects with average age 30.4 years (22-55 years), body mass 63.4 kg (57-69 kg) and height 173.4 cm (162-179 cm), participated in the experiments. The subjects had no prior history of back pain. Each subject was informed about the purpose of the study, experimental set up and usage of the emergency stop that

would suppress the simulator motion in a ramp-down manner, when activated. The experiment protocol had been approved by an ethics research committee prior to the study.

The measurements were performed for each subject assuming: (i) two different back support conditions (seated with no back support-NB; and with lower back against a vertical backrest-B0); (ii) two different hands positions (with lower arm horizontal to the platform and hands on steering wheel-HS; hands on lap- HL); and (iii) two different levels of un-weighted vibration applied along the individual x - and y - axis (0.25 and 0.4 m/s^2 rms acceleration), and along the dual-axis (0.28 and 0.4 m/s^2 rms acceleration) in the frequency range of 0.5-20 Hz. The broad-band random vibration along the single and dual-axis were synthesized to achieve nearly flat power acceleration power spectral density (PSD) in the 0.5-20 Hz range, and comparable magnitudes of single- and dual-axis vibration. The dual-axis vibration were synthesised to yield 0.28 and 0.4 m/s^2 along each axis, with overall rms accelerations of 0.4 and 0.57 m/s^2 , respectively. Each vibration exposure lasted for 60 seconds and each subject was asked to put on a cotton lab coat to ensure uniform friction between the back and the backrest across the subjects.

Each subject was asked to wear the head-accelerometer strap and adjust its tension to ensure a tight but comfortable fit, while the accelerometer orientation was appropriately adjusted by the experimenter to ensure its alignment with the basicentric axis system and was visually monitored before and during the vibration exposure. Furthermore, each subject was asked to maintain constant head posture by looking at a fixed visual marker in the line of sight during the vibration exposure. The subject was asked to sit comfortably with average thigh contact on the seatpan and lower legs oriented vertically with feet on the vibrating

platform. The feet support was adjusted to provide the desired sitting posture for each subject.

3.2.2 Data acquisition and analyses

The seatpan and backrest force, and platform and head acceleration data were acquired in the PulseLabShop™ (Bruel & Kjaer) and analysed to derive APMS and STHT biodynamic responses of seated body to single- and dual-axis horizontal vibration. The APMS response to single-axis vibration was computed from:

$$M_{kl}(j\omega) = \frac{S_{a_k F_l}}{S_{a_k}}; k=x, y \text{ and } l=x, y \quad (3.1)$$

Where $M_{kl}(j\omega)$ defines the complex APMS response corresponding to excitation frequency ω . $S_{a_k F_l}$ is the cross-spectral density of the force measured at the driving-point along direction l ($l=x, y$) and the acceleration a_k ($k = x, y$) at the platform and S_{a_k} is the auto spectral density of acceleration a_k . The above equation would yield direct-axis response for $k=l$ and the cross-axis APMS response for $k \neq l$. The direct and cross-axis components of the APMS at the seat back were also computed in a similar manner by considering the force measured at the backrest. For dual-axis vibration, the total APMS response at the seatpan and the backrest was computed from the total measured force along an axis due to excitation along both the axis and the acceleration along the axis of the measured force, such that:

$$M_k(j\omega) = \frac{S_{a_k F_k}}{S_{a_k}}; k=x, y \quad (3.2)$$

In the above equation, M_k is the complex APMS along axis k ($k=x,y$) due to vibration applied along both the axis, and $S_{a_k F_k}$ is the cross-spectral density of the force and acceleration measured along the same axis. The APMS of the rigid seat and the backrest

structures were initially computed through measurements of forces at the pan and backrest under single- and dual-axis vibration. The magnitudes of the APMS of both the structures were observed to be constant in the entire frequency range (0.5-20 Hz) with nearly zero phase between the measured force and acceleration signals. Furthermore, the magnitudes of cross-axis APMS of the seat structure under single axis vibration along the x - and y -axis were mostly negligible. The measured APMS responses of the seat and the backrest were subsequently applied to the data obtained for the seat-human subjects in order to perform inertial corrections to the responses measured at the pan and the backrest using the reported methodology [2,73].

The fore-and-aft and lateral STHT responses were computed in a similar manner from the measured head and seat accelerations, such that:

$$T_{kl}(j\omega) = \frac{S_{a_k a_l}}{S_{a_k}}, k=x, y \text{ and } l=x, y \quad (3.3)$$

Where $T_{kl}(j\omega)$ defines the complex direct ($k=l$) or cross-axis ($k \neq l$) vibration transmissibility corresponding to excitation frequency ω . $S_{a_k a_l}$ is the cross-spectral density of acceleration signal measured at the head along direction l ($l= x, y$), and the source vibration a_k along direction k ($k= x, y$).

The analyses were performed using a band width of 100 Hz with a resolution (Δf) of 0.125 Hz, accounting for 27 linear averages. The coherence between the response signals along the axis of applied vibration were continually monitored, which were generally close to 1.0 for the APMS measures but lower for the STHT measures at frequencies above 7 Hz.

3.2.3 Total Seatpan APMS response

The biodynamic force measured at the seatpan revealed strong coupling with the backrest force, when a back supported posture was considered. The majority of the studies reporting seatpan APMS response of the seated occupants employed the force plate at the seat base, where the measured force responses F_{px} and F_{py} would represent the total body interactions (seatpan and backrest) together with the inertia force due to the seat structure along the x - and y - axis, respectively [2,3]. In some studies, the force plate itself served as the seatpan to obtain the seatpan APMS responses, as in the present study. In this case the forces imparted on the backrest due to the upper body would not be reflected in the measured seatpan forces, as illustrated in Fig. 3.1. Let f_{px} be the total inertia-corrected force developed at the seatpan measured below the seat and f_{bx} be the inertia-corrected biodynamic force at the backrest under x -axis vibration. The total biodynamic force would be the sum of the forces developed at the pan f'_{px} and the backrest, as seen in Fig. 3.1, such that:

$$f_{px}(t) = f'_{px}(t) + f_{bx}(t) \quad (3.4)$$

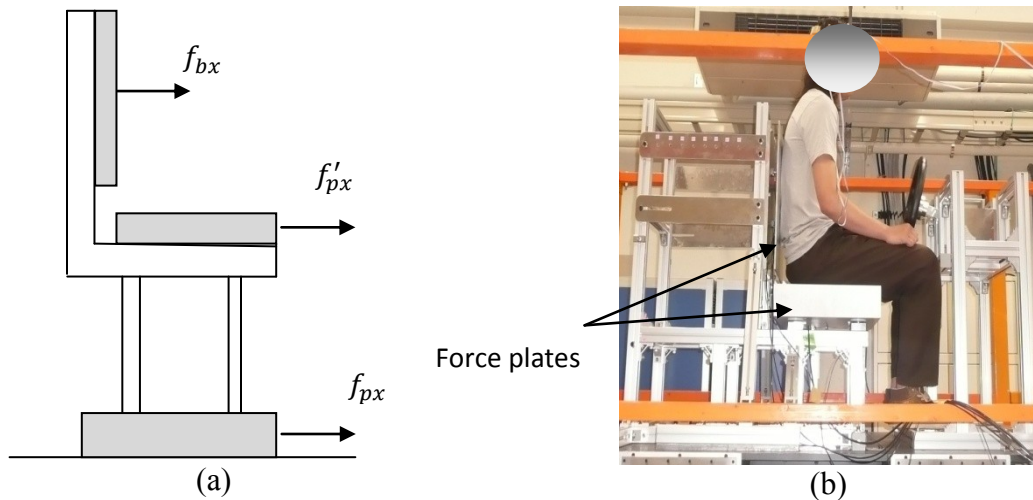


Figure 3.1: (a) Schematic of the test seat with force plate serving as the seatpan: f'_{px} and f_{bx} are forces measured at the seatpan and backrest, respectively, and f_{px} is the total force; (b) Experimental setup showing the subject seated with back supported posture and the locations of force-plates.

Greater upper body interaction with the back support would thus yield lower seatpan APMS response. Considering relatively larger magnitude of the fore-aft backrest APMS the effect of coupling on the seatpan APMS would be quite pronounced. It should be noted that the force measured at the backrest is not influenced by the location of the seatpan force measurement system. Considering equal magnitudes of broadband vibration applied at the backrest and seatpan along the fore-aft axis, and multiplying the terms in Eq. (3.4) by the complex conjugate of acceleration $a_x^*(f)$ yields:

$$a_x^*(f)F_{px}(f) = a_x^*(f)F'_{px}(f) + a_x^*(f)F_{bx}(f) \quad (3.5)$$

Where F_{px} , F_{bx} and F'_{px} are the Fourier transforms of f_{px} , f_{bx} and f'_{px} , respectively. Eq (3.5) can be expressed in terms of cross-spectral densities of the measured forces and accelerations, and auto-spectral density of the acceleration, as:

$$S_{a_x F_{px}}(f) = S_{a_x F'_{px}}(f) + S_{a_x F_{bx}}(f) \quad (3.6)$$

$$\frac{S_{a_x F_{px}}(f)}{S_{a_x}} = \frac{S_{a_x F'_{px}}(f)}{S_{a_x}} + \frac{S_{a_x F_{bx}}(f)}{S_{a_x}} \quad (3.7)$$

Where $S_{a_x F_{px}}(f) = \frac{1}{T} E[a_x^*(f)F_{px}(f)]$, $S_{a_x}(f) = \frac{1}{T} E[a_x^*(f)a_x(f)]$ and $T = 1/\Delta f$ is the duration of measurement. The above yields following relationship between the APMS of the seated body measured at the seatpan (M_{px}) and the backrest (M_{bx}):

$$M_{px}(f) = M'_{px}(f) + M_{bx}(f) \quad (3.8)$$

Where M'_{px} and M_{bx} are the apparent mass responses based on the forces measured at the seatpan and the backrest, respectively, such that:

$$M'_{px}(j\omega) = \frac{S_{ax}F'_{px}}{S_{ax}}; \text{ and } M_{px}(j\omega) = \frac{S_{ax}F_{bx}}{S_{ax}} \quad (3.9)$$

The total direct- and cross-axis seatpan APMS responses along the lateral (y -) axis were also derived using the same methodology, such that:

$$M_{pk,l}(f) = M'_{pk,l}(f) + M_{bk,l}(f); k=x, y \text{ and } l=x, y \quad (3.10)$$

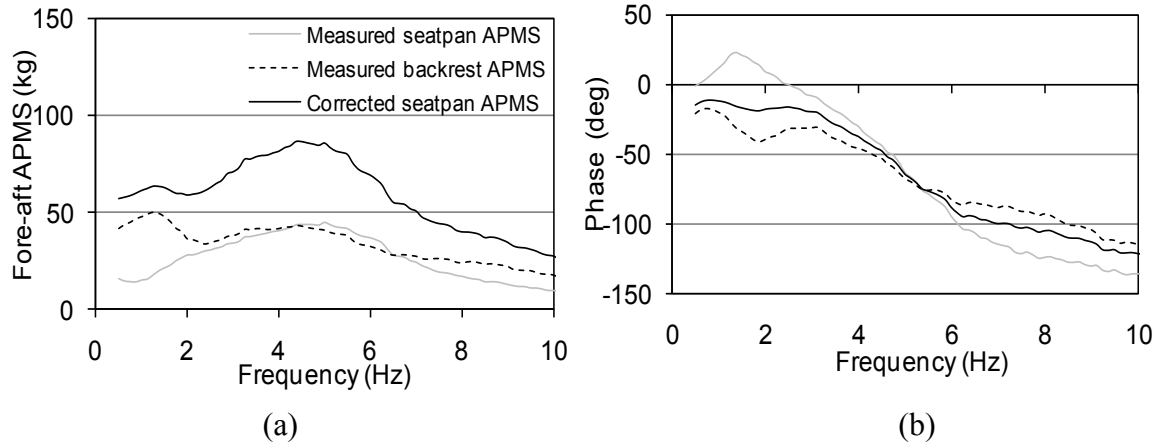


Figure 3.2: Mean measured fore-aft backrest and seatpan APMS, and corrected-seatpan APMS magnitude and phase responses of occupants seated with back support and exposed to fore-aft vibration of 0.25 m/s^2 rms acceleration magnitude.

As an example, Fig. 3.2 illustrates the mean fore-and-aft seatpan and backrest APMS magnitude and phase responses of the subjects seated with a back support and exposed to $a_x=0.25 \text{ m/s}^2$. The results derived from the inertia-corrected measured data show that the seatpan APMS magnitude is either lower or comparable to the backrest APMS magnitude. The magnitude of the total seatpan APMS, M_{px} , derived using Eq (3.10) is considerably higher than the measured APMS, M'_{px} , as shown in Fig. 3.2 (a). The phase response at the seatpan is also altered by the proposed method, as seen in Fig. 3.2(b). The studies employing force plate as the seatpan [51,117], generally, report lower magnitudes of the fore-and-aft APMS of the body seated with a back support, compared to those based on force measurement at the seat base [2,3], as illustrated in Fig. 3.3. This is directly attributable to

the coupled effects of the forces developed at the seatpan and the backrest. The total mean APMS magnitude response derived using Eq. (3.10) approached those reported in [2,3] (Fig. 3.3).

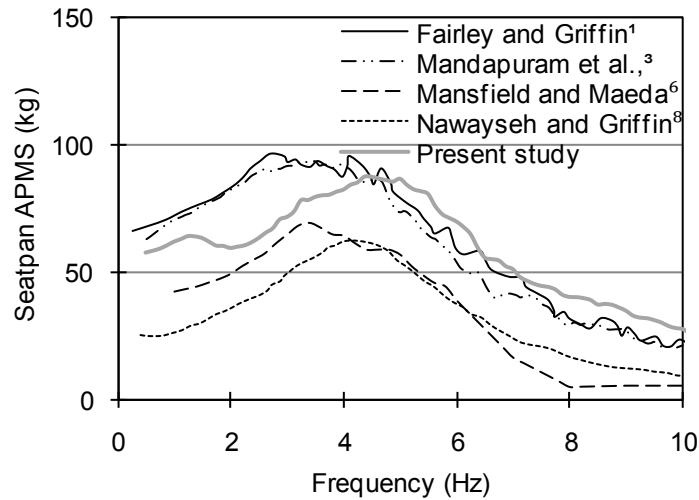


Figure 3.3: Comparison of reported APMS magnitude of subjects seated with a back support and exposed to fore-aft vibration, and the corrected APMS in the present study (0.25 m/s^2).

3.2.4 Normalisation factors

The APMS response characteristics of the seated human body exposed to WBV are known to be influenced by many anthropometric, excitation and seat related factors. A number of studies on vertical and horizontal APMS have mostly attributed the dispersion in the APMS data to variations in the body mass, particularly at low frequencies. The measured APMS is thus frequently normalized with respect to either the body mass supported by the seat, or by the APMS magnitude at a low frequency, e.g., 0.5 to 1 Hz [64,79] in order to study the effects of other contributing factors such as nature of WBV, sitting posture and seat geometry [47,92]. Such normalisation, however, cannot decouple the dynamic contributions due to body mass variations. While the APMS responses obtained under vertical WBV have been widely normalised using the low frequency magnitude, such normalisation has been

discouraged for horizontal APMS due to presence of a very low frequency resonance, near 0.7 Hz, particularly under the NB posture [2]. Furthermore, the effective body mass supported by the seat along a horizontal axis could not be quantified through static measures.

Furthermore, the body mass supported by the seatpan is affected by the human tendency to maintain the desired posture. It has been reported that subjects tend to stiffen their upper body and legs under fore-aft WBV exposures to maintain contact with the seat, which yields greater contact between the thighs and the seatpan [3]. Considering the participation of legs, particularly the thighs, under fore-aft WBV, the sum of masses due to the upper body and thighs is considered as the normalisation factor for the direct APMS responses under fore-aft WBV. The upper body comprising the head, neck, thorax and arms, and thighs contribute to the seatpan biodynamic response of the seated occupants with the hands in lap postures. The normalization factor of 87.8 % of the total body mass was estimated from the anthropometric data, which includes the proportions due to upper body (67.8%) and thighs (20%) [3,119]. The resulting fore-aft normalised APMS magnitudes were nearly unity at low frequencies. The same normalisation factor were also applied to the seatpan lateral APMS data, although the subjects maintained average thigh contact with the seat pan during exposure to lateral vibration. The normalised lateral APMS were thus generally lower. The occupants seated with the hands on steering wheel transfer a portion of the arms weight from the seatpan to the rigid steering wheel. The normalising factor for this posture was thus appropriately reduced to 77.8% of the total body mass by considering the arms mass as 10% of the total body mass.

The proportion of the upper body mass contributing to the APMS obtained at the backrest, however, differs with the axis of vibration. Under fore-aft vibration, the entire

upper body is considered to contribute; a normalisation factor of 67.8% of the total body mass is thus assumed. Under lateral vibration, a relatively smaller portion of the upper body, however, tends to slide along the backrest, which was evident from the relatively lower magnitudes of the lateral APMS measured at the backrest. Unlike under the fore-aft vibration, the backrest offers little resistance to the upper body lateral movement. It is thus assumed that the contribution of the pelvic mass to the low frequency lateral apparent mass would be very small. Considering the pelvic mass of 13.5% of the total body mass, the normalisation factor of 54.3% of the total body mass is assumed for the backrest APMS responses to lateral WBV. However, the defined normalisation factors based on the anthropometry alone may yield some error due to small changes in the sitting posture such as leaning forward. . The direct- and cross-axis APMS responses of each individual subject corresponding to each experimental condition were normalised using the normalisation factors summarised in Table 3.1, although a sound basis for normalisation of the cross-axis data is yet to be explored.

Table 3.1: Normalization factors (% of body mass), based on anthropometry [119].

Response		Sitting posture			
		NB-HL	NB-HS	B0-HL	B0-HS
<i>Seatpan APMS</i>	Fore-aft	87.8	77.8	87.8	77.8
	Lateral	87.8	77.8	87.8	77.8
<i>Back APMS</i>	Fore-aft	-	-	67.8	57.8
	Lateral	-	-	54.3	44.3

Multi-factorial analyses of variance (ANOVA) were performed on the corrected APMS and STHT data using SPSS to identify the statistical significance levels of the main factors such as the hands support, back support and the excitation magnitude.

3.2.5 Relationship between responses to single- and dual-axis vibration

The application of vibration along a single axis also yields biodynamic forces responses along the other axis. This is evident from the reported cross-axis APMS responses [87,92,117]. Assuming nearly linear response under a given excitation magnitude and posture, the APMS and STHT responses to multi-axis vibration may be evaluated from superposition of the direct- and cross-axis responses. Considering the seated body as a multiple input-multiple output system, the total APMS response can be evaluated from the resultant forces along x - and y - axis due to simultaneous x - and y - axis excitations, such that:

$$\bar{F}_x(f) = F_{xx}(f) + F_{xy}(f); \bar{F}_y(f) = F_{yy}(f) + F_{yx}(f) \quad (3.11)$$

Where \bar{F}_x and \bar{F}_y are the Fourier transforms of the total biodynamic forces along x - and y - axis respectively. F_{ij} are the Fourier transforms of the biodynamic forces developed along axis i ($i=x,y$) due to single-axis vibration applied along j ($j=x,y$). F_{ij} represents the direct component of the biodynamic force for $i=j$ and cross-axis component for $i \neq j$. For the seated body exposed to single axis vibration along the x - and y - axis, let $M_{xi}(f)$ represent the linear transfer function between the force F_{xi} and the acceleration $a_i(f)$ along axis i ($i=x,y$), such that:

$$F_{xi}(f) = M_{xi}(f)a_i(f) \quad (3.12)$$

Where M_{xi} represents the direct-axis APMS due to single axis excitation along x -axis ($i=x$), and the cross-axis APMS under single axis excitation along y -axis ($i=y$). The resultant

force \bar{F}_x under simultaneous dual axis vibration (x and y) can be derived using Eqs (3.11) and (3.12), as:

$$\bar{F}_x(f) = \sum_{i=x,y} M_{xi}(f) a_i(f) \quad (3.13)$$

Let \bar{F}_x^* , M_{xi}^* and a_i^* be the complex conjugates of $\bar{F}_x(f)$, $M_{xi}(f)$ and $a_i(f)$, respectively. The square of the modulus of the resultant force can be written as:

$$\bar{F}_x^*(f) \bar{F}_x(f) = \left[\sum_{i=x,y} M_{xi}^*(f) a_i^*(f) \right] \left[\sum_{i=x,y} M_{xi}(f) a_i(f) \right] \quad (3.14)$$

For uncoupled excitations along the x - and y - inputs, the above can be expressed as:

$$S_{\bar{F}_x}(f) = \sum_{i=x,y} |M_{xi}(f)|^2 S_{a_i}(f) \quad (3.15)$$

Where $S_{\bar{F}_x}$ and S_{a_i} are the auto spectral densities of the total force along the x -axis, and acceleration along axis i ($i=x,y$). Eq (3.15) yields the resultant APMS \bar{M}_x along the x - axis under simultaneous dual-axis vibration, as:

$$|\bar{M}_x(f)|^2 = |M_{xx}(f)|^2 + |M_{xy}(f)|^2 \frac{S_{a_y}(f)}{S_{a_x}(f)} \quad (3.16)$$

In similar manner, the resultant APMS \bar{M}_y along y -axis under simultaneous dual axis vibration can be obtained as:

$$|\bar{M}_y(f)|^2 = |M_{yy}(f)|^2 + |M_{yx}(f)|^2 \frac{S_{a_x}(f)}{S_{a_y}(f)} \quad (3.17)$$

The resultant APMS under identical magnitudes of x - and y -axis vibration could be simply derived as the sum of direct and cross-axis APMS under single axis vibration. The magnitudes of x - and y -axis WBV in most work vehicles, however, differ considerably. For

instance, the frequency-weighted x - and y - axis vibration of an off-road tractor during ploughing have been reported to vary in the 0.3 to 1.3 m/s^2 and 0.2 to 0.6 m/s^2 ranges, respectively, while those of a forklift truck lie in the 0.1 to 0.9 and 0.1 to 2.5 m/s^2 ranges, respectively [18,120]. Relatively higher magnitudes of lateral vibration would yield greater contribution of the cross-axis APMS to the resultant APMS along the x -axis but smaller to the APMS along the y -axis.

The seat-to-head transmissibility responses to dual-axis horizontal vibration may also be related to the responses to single-axis vibration in a similar manner, such that:

$$|\bar{T}_x(f)|^2 = |T_{xx}(f)|^2 + |T_{xy}(f)|^2 \frac{S_{a_y}(f)}{S_{a_x}(f)} \quad (3.18)$$

$$|\bar{T}_y(f)|^2 = |T_{yy}(f)|^2 + |T_{yx}(f)|^2 \frac{S_{a_x}(f)}{S_{a_y}(f)} \quad (3.19)$$

Where \bar{T}_x and \bar{T}_y represent the resultant STHT responses along x - and y - axis to dual-axis horizontal vibration, and T_{ij} defines STHT response along axis i ($i=x,y$) to single-axis excitation along axis j ($j=x,y$).

Owing to the equal magnitudes of the uncorrelated broad-band random vibration inputs considered in this study the ratios $\frac{S_{a_x}(f)}{S_{a_y}(f)}$ and $\frac{S_{a_y}(f)}{S_{a_x}(f)}$ are considered equal to unity.

3.3 RESULTS

The APMS and STHT magnitude responses of individual subjects to single and dual-axis horizontal vibration revealed strong dependence upon the back support, hands position, direction of excitation and vibration magnitude. Considerable scatter among the individual data acquired for each test condition was observed, and it was particularly significant in the

cross-axis components. The peak APMS and STHT magnitudes, however, occurred within narrow frequency ranges for all subjects for both single and dual-axis vibration responses. The coefficient of variation (CoV) obtained for the APMS magnitude responses along the axis of applied vibration were generally lower in the vicinity of the resonant frequency, while the peak values of CoV in seatpan APMS magnitudes over the experimental conditions considered were in the of 21-40% range. The CoV of the seatpan APMS data obtained under dual axis vibration were consistently lower compared to those under single axis vibration. The observed ranges of CoV of the seatpan APMS magnitudes, however, were considerably lower than those reported³⁾. The peak values of CoV of the backrest APMS data were in the range of 22-75% and significantly higher compared to those observed in the seatpan APMS data. This is attributable to variations in the upper body contact with the vertical backrest. Owing to the high variability and lower mean magnitudes, the CoV of the cross axis APMS magnitude responses were higher. The STHT responses revealed far greater variability in the data with peak values of CoV approaching 30% near resonances and even larger at higher frequencies, where the magnitudes are considerably small.

The coherence values for the direct APMS responses over the 0.5-20 Hz frequency range were generally about 1 and below 0.5 in case of the cross-axis fore-aft and lateral responses. Furthermore, the coherence values of the responses under single and dual axis

Table 3.2: Statistical significance (p -values) of hands support attained from ANOVA performed on the seatpan APMS and STHT magnitude responses to single-axis fore-aft and lateral vibration under different conditions (back support: NB and B0; vibration magnitude: 0.25 and 0.4 m/s²)

Factor	Hands support (HL vs HS)															
	Fore-aft								Lateral							
	NB				B0				NB				B0			
	0.25 m/s ²		0.4 m/s ²		0.25 m/s ²		0.4 m/s ²		0.25 m/s ²		0.4 m/s ²		0.25 m/s ²		0.4 m/s ²	
APMS	STHT	APMS	STHT	APMS	STHT	APMS	STHT	APMS	STHT	APMS	STHT	APMS	STHT	APMS	STHT	
0.75	0.01	0.19	0.11	0.18	0.06	0.76	0.11	0.44	0.00	0.05	0.00	0.10	0.00	0.97	0.00	0.04
1	0.01	0.36	0.26	0.15	0.06	0.75	0.05	0.24	0.00	0.01	0.00	0.04	0.00	0.47	0.00	0.32
2	0.33	0.03	0.11	0.27	0.12	0.04	0.01	0.01	0.00	0.08	0.00	0.00	0.00	0.09	0.00	0.01
3	0.00	0.19	0.00	0.41	0.23	0.18	0.79	0.00	0.00	0.01	0.00	0.01	0.00	0.00	0.00	0.00
4.5	0.00	0.02	0.00	0.01	0.04	0.01	0.02	0.00	0.01	0.82	0.04	0.96	0.02	0.66	0.01	0.05
6	0.03	0.00	0.04	0.40	0.00	0.01	0.00	0.01	0.01	0.67	0.00	0.67	0.01	0.49	0.00	0.16
8	0.01	0.00	0.02	0.00	0.03	0.59	0.09	0.79	0.13	0.07	0.02	0.19	0.05	0.53	0.00	0.28
10	0.03	0.00	0.05	0.01	0.19	0.24	0.02	0.25	0.03	0.34	0.00	0.12	0.06	0.36	0.00	0.22
12	0.01	0.00	0.02	0.00	0.28	0.73	0.26	0.90	0.00	0.83	0.00	0.13	0.03	0.63	0.00	0.36
14	0.91	0.18	0.91	0.00	0.57	0.44	0.75	0.58	0.00	0.02	0.00	0.08	0.03	0.66	0.00	0.32
16	0.09	0.41	0.31	0.06	0.72	0.71	0.81	0.63	0.00	0.20	0.00	0.33	0.02	0.19	0.00	0.06
18	0.09	0.09	0.36	0.10	0.70	0.51	0.55	0.46	0.00	0.36	0.00	0.44	0.01	0.21	0.00	0.05
20	0.08	0.83	0.44	0.35	0.66	0.48	0.51	0.31	0.00	0.21	0.00	0.51	0.01	0.06	0.00	0.20

Table 3.3: Statistical significance (p -values) of back support attained from ANOVA performed on the seatpan APMS and STHT magnitude data under different conditions (back support: NB and B0; hands support: HL and HS; vibration magnitude: 0.25 and 0.4 m/s^2 ; vibration direction: fore-aft and lateral; number of vibration axis: single and dual-axis)

Factor	Back support (NB vs B0)															
	Single axis								Dual axis							
	Fore-aft				Lateral				Fore-aft				Lateral			
	0.25 m/s^2		0.4 m/s^2		0.25 m/s^2		0.4 m/s^2		0.25 m/s^2		0.4 m/s^2		0.25 m/s^2		0.4 m/s^2	
APMS	STHT	APMS	STHT	APMS	STHT	APMS	STHT	APMS	STHT	APMS	STHT	APMS	STHT	APMS	STHT	
0.75	0.80	0.18	0.01	0.31	0.09	0.00	0.01	0.00	0.03	0.03	0.01	0.11	0.01	0.11	0.00	0.01
1	0.08	0.01	0.00	0.68	0.24	0.01	0.01	0.00	0.00	0.03	0.00	0.48	0.00	0.12	0.00	0.02
2	0.00	0.93	0.00	0.93	0.07	0.83	0.16	0.16	0.00	0.10	0.00	0.07	0.03	0.68	0.03	0.41
3	0.00	0.00	0.00	0.00	0.00	0.02	0.00	0.08	0.00	0.00	0.00	0.00	0.00	0.92	0.00	0.77
4.5	0.00	0.38	0.00	0.27	0.00	0.88	0.00	0.12	0.00	0.02	0.00	0.15	0.00	0.93	0.00	0.60
6	0.00	0.80	0.00	0.76	0.00	0.09	0.00	0.02	0.00	0.48	0.00	0.00	0.00	0.02	0.00	0.02
8	0.00	0.28	0.00	0.18	0.00	0.00	0.00	0.00	0.00	0.37	0.00	0.06	0.00	0.00	0.00	0.01
10	0.00	0.00	0.00	0.00	0.00	0.00	0.00	0.00	0.00	0.00	0.00	0.00	0.00	0.00	0.00	0.32
12	0.00	0.00	0.00	0.00	0.00	0.07	0.00	0.56	0.00	0.00	0.00	0.00	0.00	0.27	0.00	0.78
14	0.00	0.00	0.00	0.00	0.00	0.32	0.00	0.62	0.00	0.00	0.00	0.00	0.00	0.82	0.00	0.10
16	0.00	0.00	0.00	0.00	0.00	0.43	0.00	0.71	0.00	0.00	0.00	0.00	0.00	0.00	0.00	0.00
18	0.00	0.00	0.00	0.00	0.00	0.65	0.00	0.43	0.00	0.00	0.00	0.00	0.00	0.84	0.00	0.14
20	0.00	0.00	0.00	0.00	0.00	0.56	0.00	0.10	0.00	0.00	0.00	0.00	0.01	0.03	0.00	0.06

vibration were observed to be similar. The fore-aft and lateral STHT responses of the subjects seated with NB and B0 posture revealed coherence in the order of 0.8 up to 5 Hz, while that of the cross-axis responses were 0.5 or below.

Owing to the relatively higher values of the coefficients of variation of the data, the mean data of the 9 subjects were considered to provide trend information on the effects of single- and dual-axis vibration, and hands and back supports. The mean magnitude and phase responses of direct and cross-axis components of the seatpan APMS and STHT under single-axis vibration, and total responses under dual-axis vibration were evaluated for each experimental condition. Although considerable magnitudes of cross-axis APMS and STHT were observed along the vertical axis under fore-aft vibration, the results are limited only to responses along the fore-aft and lateral axis. Both the APMS and STHT magnitudes were generally observed to be very small at frequencies above 10 Hz; the results are thus presented in the 0.5-10 Hz range with only a few exceptions. Furthermore, the results are presented for identical overall rms accelerations due to single and dual-axis vibration, namely 0.28 m/s^2 along each of the dual-axis vibration (overall magnitude = 0.4 m/s^2). The results attained from multi-factor ANOVA are presented in Tables 3.2 and 3.3 at selected frequencies in the 0.75-20 Hz range. The tables show the pair-wise comparisons of effects of hands support (HL vs HS) and the back support (NB vs B0), respectively, on both the APMS and STHT responses, while the interactions between the two were observed to be insignificant.

3.3.1 Apparent mass responses

Figure 3.4 illustrates comparisons of mean total fore-aft and lateral APMS magnitude and phase responses of subjects, seated with NB-HL posture, to single and dual-axis horizontal vibration. The APMS magnitudes along the axis of applied vibration are nearly 1.0 at low

frequencies along the fore-aft axis but lower under lateral vibration. The lower values of lateral APMS are attributed to the selected normalization factor (Table 3.1). The direct fore-aft seatpan APMS magnitudes of occupants seated with NB-HL posture revealed peaks near 0.75, 2.5 and 4.13 Hz, which are similar to those reported [2,3,87]. The frequencies corresponding to the peak values of mean APMS obtained under different vibration and support conditions are summarised in Table 3.4, which may also referred to as the resonant frequencies. The direct lateral seatpan APMS responses reveal two distinct peaks near 0.88 and 1.88 Hz, which are also comparable to those reported [2,3].

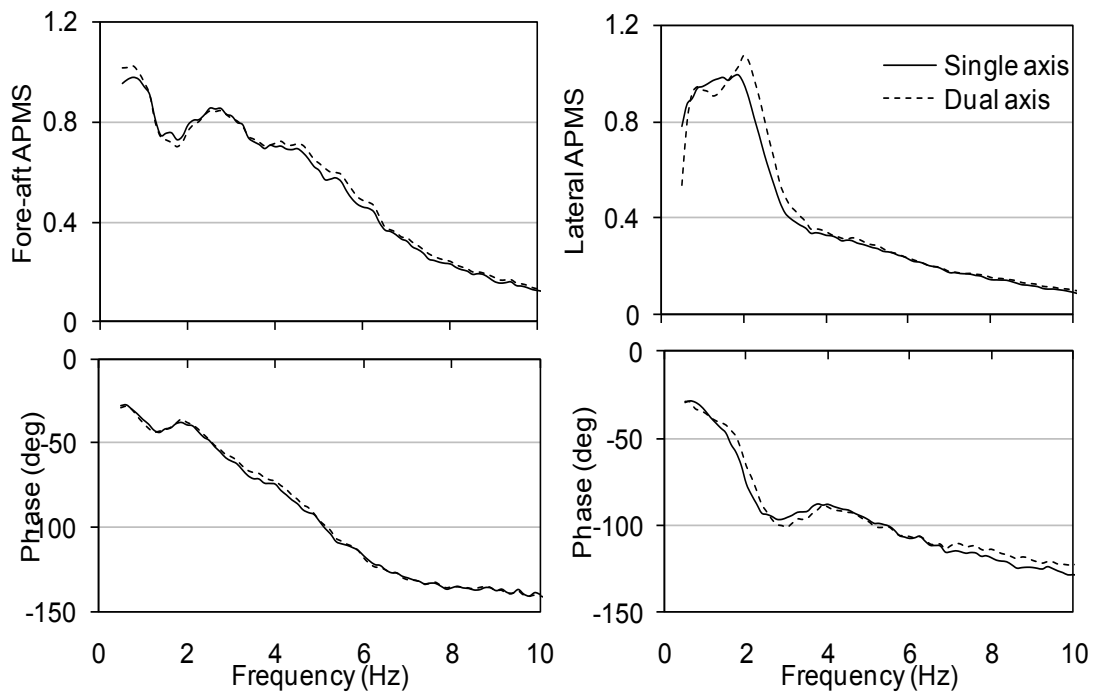


Figure 3.4: Comparisons of mean APMS magnitude and phase responses to single- and dual-axis fore-aft and lateral vibration (No back support; hands in lap; single axis: $a_x=a_y=0.4 \text{ m/s}^2$; dual-axis: $a_x=a_y=0.28 \text{ m/s}^2$).

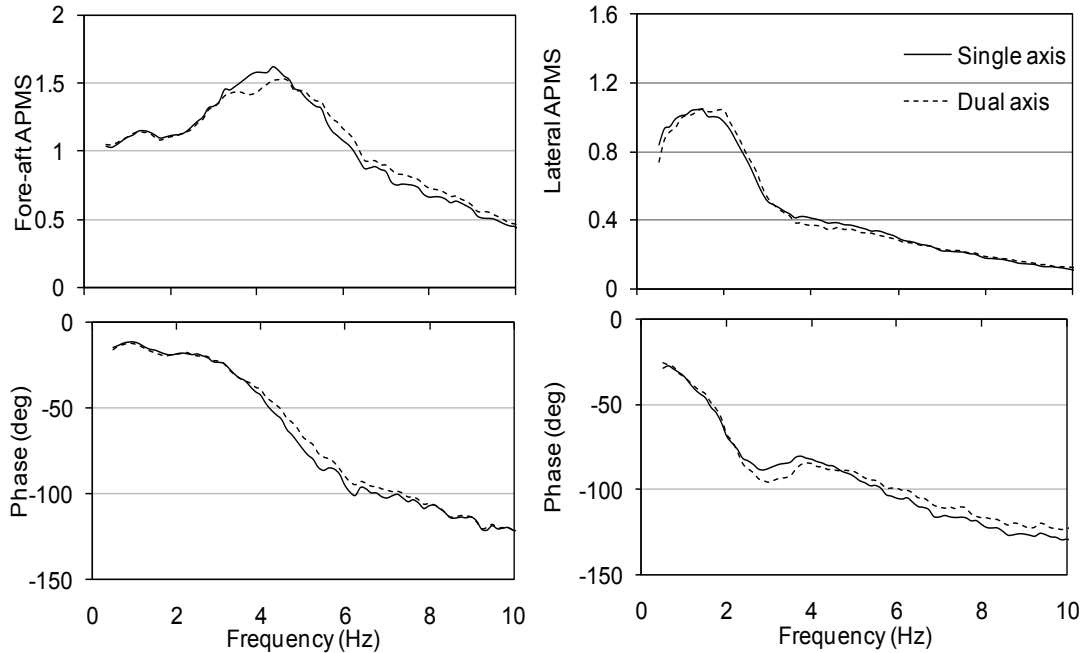


Figure 3.5: Comparisons of mean APMS magnitude and phase responses to single- and dual-axis fore-aft and lateral vibrations (Back support; hands in lap; single axis: $a_x=a_y=0.4 \text{ m/s}^2$; dual-axis: $a_x=a_y=0.28 \text{ m/s}^2$).

Figure 3.5 illustrates comparisons of the mean total fore-aft and lateral APMS magnitude and phase responses of subjects seated with B0-HL posture to single and dual-axis horizontal vibration. The fore-aft APMS responses of the occupants seated with back supported and hands in lap posture revealed peaks near 1.38 and 5 Hz. The observed low frequency peak was more distinct compared to that reported in the previous study [3]. The direct lateral seatpan APMS responses under single and dual axis vibration mostly revealed a single broad peak centred near 1.38 Hz. The lower magnitude vibration (0.25 m/s^2), however, revealed two peaks near 1 and 2 Hz (Table 3.4).

Figure 3.6 illustrates comparisons of the mean total fore-aft and lateral APMS magnitude and phase responses of the subjects seated with back support measured at the backrest to single and dual-axis horizontal vibration. The backrest APMS exhibits two peaks near 1.25 and around 4.5 Hz under fore-aft, and 0.88 and 2.25 Hz under lateral vibration, respectively. The mean

cross-axis APMS magnitude responses, M_{xy} and M_{yx} , of subjects seated with NB-HL and B0-HL, and exposed to single axis horizontal vibration of magnitude of 0.4 m/s^2 are compared in Figs. 3.7(a) and 3.7(b), respectively. The cross-axis APMS magnitudes under single-axis vibration were significantly lower and the phase responses revealed excessive scatter in the data. Considering the wide scatter and relatively low coherence of the cross-axis data, the phase responses could not be considered reliable.

Table 3.4: Frequencies (Hz) corresponding to important peak magnitudes observed in the mean APMS and STHT responses of seated occupants exposed to single axis horizontal vibration.

Vibration & measurement axis	Posture	Magnitude	Seatpan				Back rest	
			HL		HS		HL	HS
			APMS	STHT	APMS	STHT	APMS	APMS
Fore-aft	NB	0.25 m/s^2	0.88	1.38				
			2.75	2.8	3.13	1.38	-	-
			4.5		4.5			
		0.40 m/s^2	0.75	1.38				
			2.5	2.8	2.75	1.38	-	-
			4.13		4.5			
	B0	0.25 m/s^2	1.25	1.8	1.38	1.8	1.25	1.38
4.5			3.13	5	3.75	4.3	4.38	
				9.88		9.5		
		0.40 m/s^2	1.38	1.38	1.38	1.38	1.25	1.25
			5	3	4.34	3.25	4-5	4-5
				9.88		10.38		
Lateral	NB	0.25 m/s^2	0.88	1.25	0.88	1.25	-	-
			2	2.13	2.13	2		
						5.63		
		0.40 m/s^2	0.88	1.5	1	1.25	-	-
			1.88	1.88	1.88	1.88		
	B0	0.25 m/s^2	1	1.25	1	1.25	0.88	0.75
2			1.88	2.38	2	2.25	2.38	
		0.40 m/s^2	1.38	1.13	1.5	1.5	1	<0.5 [†]
					1.88		2	2.38

[†] peak occurring at a frequency below 0.5 Hz

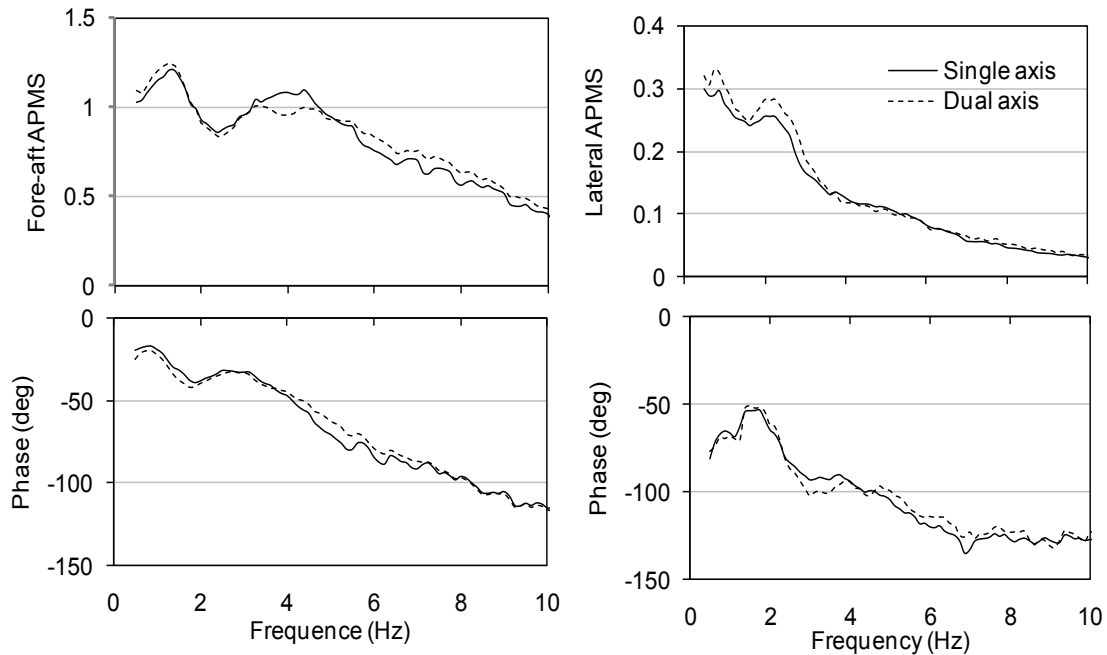


Figure 3.6: Comparisons of mean backrest APMS magnitude and phase responses to single- and dual-axis fore-aft and lateral vibrations (hands in lap; single axis: $a_x=a_y=0.4 \text{ m/s}^2$; dual-axis: $a_x=a_y=0.28 \text{ m/s}^2$).

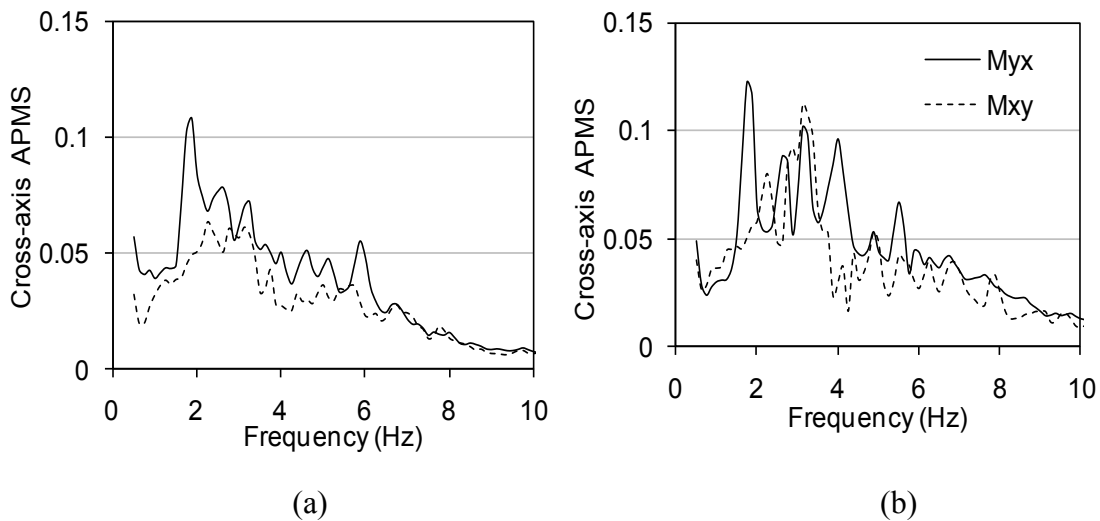


Figure 3.7: Comparisons of mean cross-axis APMS responses obtained at the seatpan along fore-aft (M_{yx}) and lateral (M_{xy}) axis (single axis vibration: $a_x=a_y=0.4 \text{ m/s}^2$): (a) No back support; (b) Back support.

3.3.2 Seat-to-head-transmissibility responses

The mean fore-aft and lateral STHT magnitude and phase responses of subjects seated with NB-HL posture and exposed to identical overall magnitudes of single and dual-axis

horizontal vibration are compared in Fig. 8. The fore-aft STHT magnitude responses revealed values nearly 1.5 to 2 at 0.5 Hz suggesting higher head motions of the seated body due to horizontal vibration. The mean fore-aft STHT responses revealed peak magnitudes near 1.38 and 2.8 Hz with peak magnitude approaching 2.7. The lateral STHT responses revealed peaks near 1.5 and 1.88 Hz with peak magnitude in the order of 2. The magnitude of the principle peak was slightly higher under dual axis vibration. These frequencies differ from those observed in the APMS responses (Table 3.4). The fore-aft and lateral STHT phase responses decrease with frequency and approach nearly 600° at 10Hz. The phase responses under single and dual-axis vibration, however, are nearly identical.

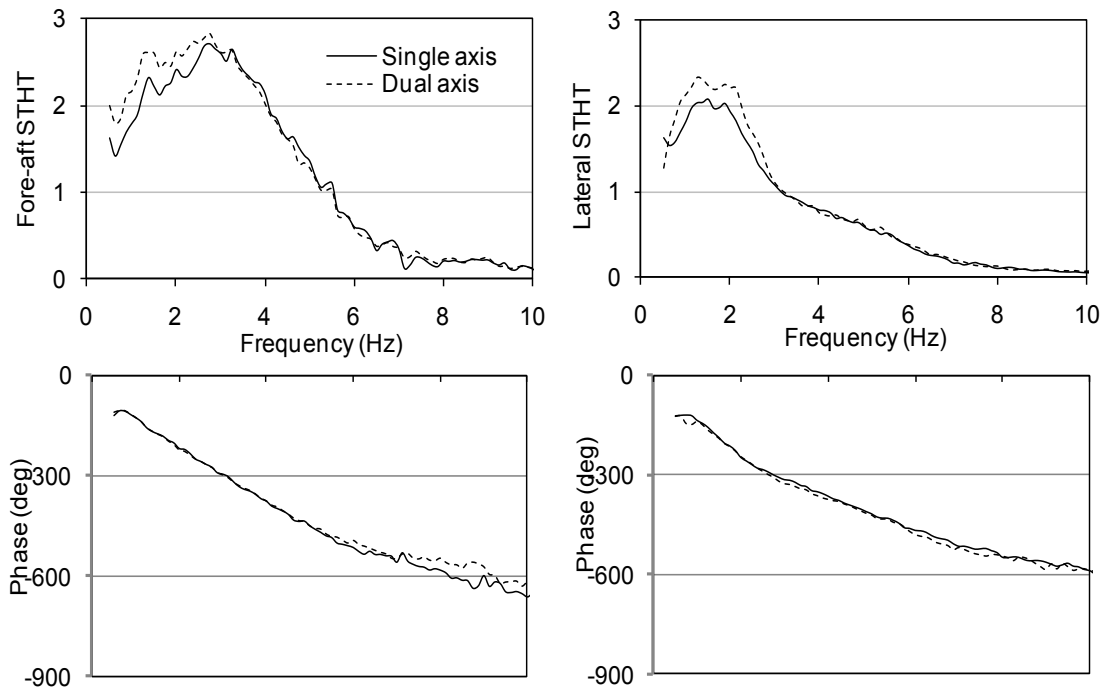


Figure 3.8: Comparisons of mean STHT magnitude and phase responses to single and dual-axis fore-aft and lateral vibrations (No back support; hands in lap; single axis: $a_x=a_y=0.4 \text{ m/s}^2$; dual-axis: $a_x=a_y=0.28 \text{ m/s}^2$).

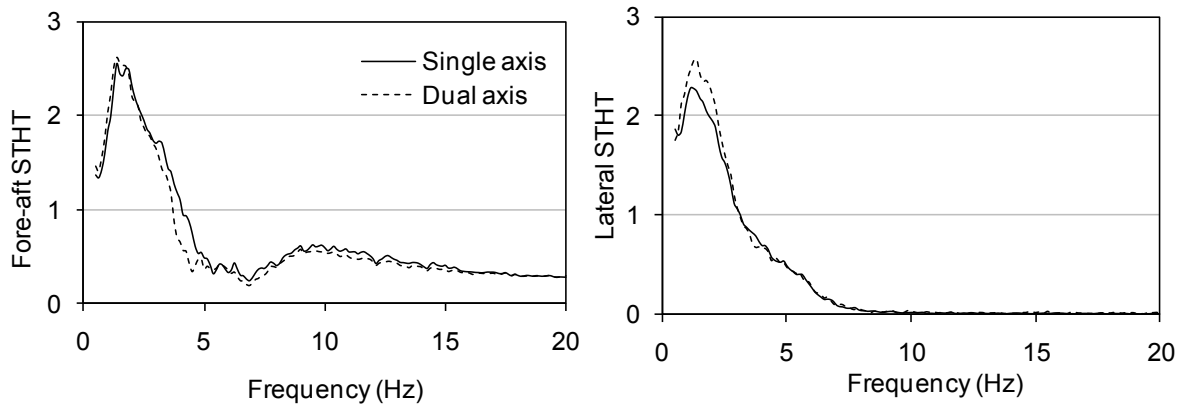


Figure 3.9: Comparisons of mean STHT magnitude responses to single and dual-axis fore-aft and lateral vibrations (Back support; hands in lap; single axis: $a_x=a_y=0.4 \text{ m/s}^2$; dual-axis: $a_x=a_y=0.28 \text{ m/s}^2$).

Figure 3.9 illustrates comparisons of mean fore-aft and lateral STHT magnitude responses of subjects seated with B0-HL posture and exposed to single and dual-axis horizontal vibration. The fore-aft responses revealed peaks near 1.38, 3 and 10Hz (Table 3.4), with a high magnitude narrow band peak near 1.38 Hz with magnitude in the order of 2.5, which is significantly different from the broad peak observed near 3Hz with NB posture (Fig. 3.8). Furthermore, the fore-aft STHT responses exhibit patterns that are considerably different from the APMS. The lateral STHT response revealed higher resonant magnitudes under dual axis vibration, where the peaks occur near 1.13 Hz and 1.2 Hz under single and dual axis vibration, respectively. The lateral STHT response to lower lateral vibration (0.25 m/s^2), however, revealed two peaks near 1.25 and 1.88 Hz (results not shown), which were comparable under those observed under dual axis vibration, as seen in Fig. 3.9. These two peaks converged to a single peak near 1.13 Hz under the higher magnitude lateral vibration. The cross-axis fore-aft and lateral STHT magnitude responses were observed to be insignificant, generally below 0.2, irrespective of the experimental conditions. These results are thus not presented.

3.3.3 Effect of hands position

Figure 3.10 illustrates comparisons of mean fore-aft and lateral APMS responses of the subjects seated with HL and HS condition under dual-axis vibration and NB posture. The results show that the HS condition yields higher fore-aft and lateral APMS magnitudes compared with those attained with HL condition in the 1-8 Hz range. The results also show comparable responses at low frequencies confirming the validity of the normalisation factors (87.8% and 77.8% of body mass for HL and HS conditions, as seen in Table 3.1). The primary peak observed in the fore-aft APMS responses with the HL condition was not observed in the response with HS condition. This was more distinctly observed from the single-axis responses (results not shown). The second and third peaks in the fore-aft APMS, however, occurred in comparable frequency bands for both hands positions (Table 3.4).

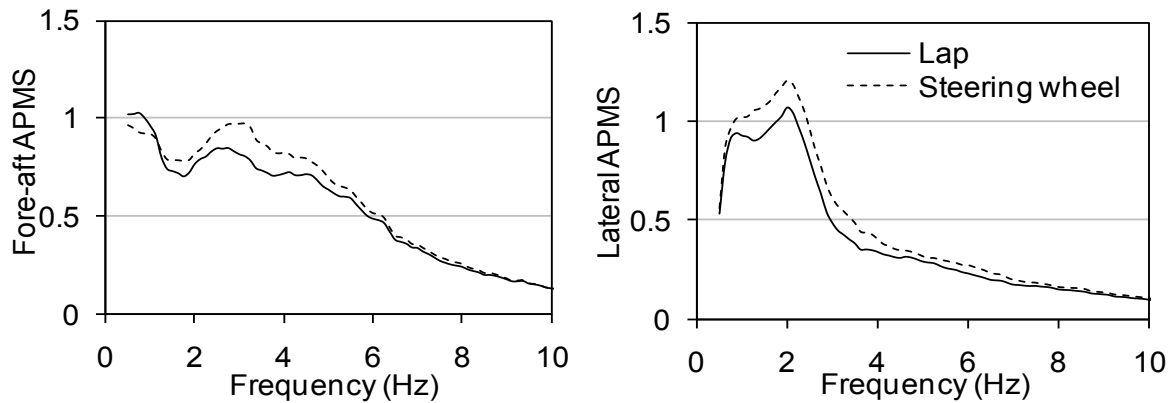


Figure 3.10: Comparisons of mean seatpan APMS responses of occupants seated with hands in lap and hands on steering wheel (No back support; dual-axis: $a_x=a_y=0.28 \text{ m/s}^2$).

Figure 3.11 illustrates comparisons of mean total and backrest APMS responses obtained with HL and HS conditions under dual-axis vibration with B0 posture. The responses with B0 posture reveal considerably higher magnitudes with hands on steering wheel compared to those with HL condition under both fore-aft and lateral vibration, particularly in the vicinity of the

resonance. The total APMS responses under fore-aft vibration revealed slightly lower magnitudes at low frequencies up to 1.6 Hz, while no effect of the hands support was observed in 1.8-2.4 Hz frequency range. The HS condition, however, yields higher magnitudes at frequencies above 2.4 Hz. The backrest APMS responses under fore-aft vibration also revealed strong effects of hands support at frequencies about 1.8 Hz, as illustrated Fig. 3.11(a). The peaks observed in the fore-aft backrest responses with hands in lap and on steering wheel occurred at nearly identical frequencies (Table 3.4). The total and backrest APMS responses under lateral vibration with HS are also considerably higher compared to the HL position.

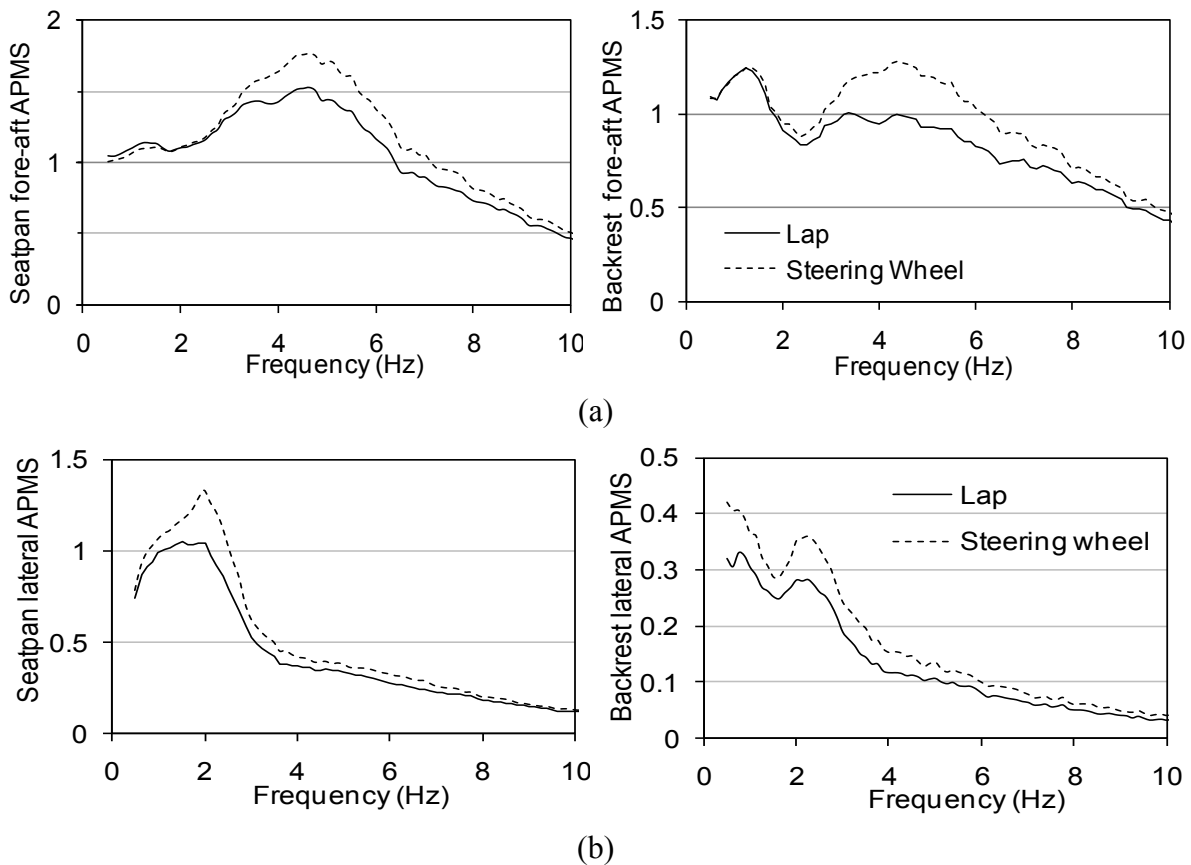


Figure 3.11: Comparisons of mean total and backrest APMS responses of occupants seated with hands in lap and hands on steering wheel to: (a) fore-aft; and (b) lateral vibration (Back support; dual-axis vibration: $a_x=a_y=0.28 \text{ m/s}^2$).

Figure 3.12 illustrates comparisons of mean STHT responses of the subjects seated with HL and HS conditions, with NB and B0 postures under dual axis vibration. The fore-aft STHT responses revealed only minimal effect of the hands support with NB posture, while a considerable effect was observed in the lateral STHT responses, particularly in the vicinity of the resonance. Although the upper body motion is known to be restrained by the hands support, particularly under fore-aft vibration, only a small effect was observed on the vibration transmitted to the head. The results attained from ANOVA also revealed insignificant effect ($p>0.05$) of the hands support on the fore-aft STHT response, while a significant effect ($p<0.05$) on the lateral STHT data was evident in the vicinity of the resonance (Table 3.2). The fore-aft and lateral STHT responses revealed considerable effect of the hands support with B0 posture, as seen in Fig. 3.12(b). The fore-aft STHT responses with hands and back supported posture revealed higher magnitudes in the 1.5 to 6.5 Hz range but minimal effect at frequencies below 1.5 Hz and relatively lower magnitudes in the 6.7 to 10.3 Hz range. The fore-aft STHT response with B0 posture showed trends that are quite different from the corresponding APMS; while the peak STHT occurred near 1.38 Hz, the peak APMS is observed near 4.3 Hz. The lateral APMS and STHT, however, show comparable trends in frequencies corresponding to peak responses and the hands support effect. Furthermore, statistically significant effect ($p<0.05$) of the hands support was observed on both the fore-aft and lateral STHT responses (Table 3.2). The higher magnitudes of lateral STHT responses were observed in 1.2 to 5.2 Hz frequency range with hands and back supported posture. The significant hands support effect was observed particularly in the vicinity of the resonance, in both the mean data ($p<0.05$), as shown in Table 3.2.

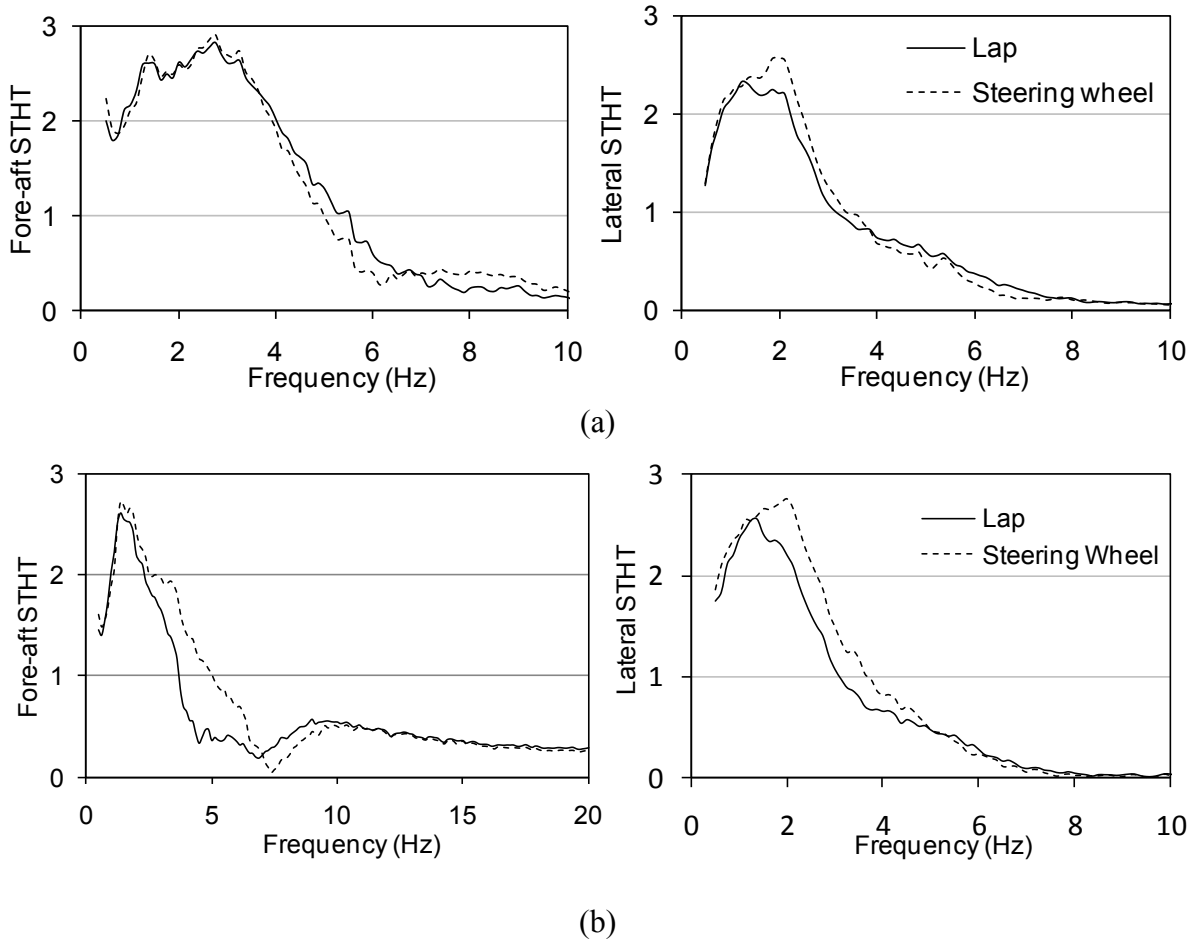


Figure 3.12: Comparisons of mean STHT responses of the occupants seated with hands in lap and hands on steering wheel (dual-axis: $a_x=a_y=0.28 \text{ m/s}^2$): (a) No back support and (b) Back support.

3.3.4 Effect of back support

Figure 3.13 illustrates comparisons of mean responses obtained with NB and B0 postures under dual-axis vibration. The APMS and STHT responses are presented for both HL and HS conditions, along fore-aft and lateral axis. The fore-aft APMS magnitudes near 0.5 Hz frequency were nearly unity, validating the considered normalisation factors (Table 3.1). The addition of the vertical back support resulted in the shift in the primary resonance to a higher frequency, while the dominant magnitude peak occurred in the 4-5 Hz range (Table 3.4) with normalised magnitude peak approaching 1.7 under HS condition. Although a back support is believed to

suppress the pitch motion of the upper body to an extent, the back support resulted in higher magnitudes of vibration transmissibility and fore-aft APMS responses, which could be attributed to additional vibration from the backrest and greater contact with the back support. The statistical significance ($p < 0.05$) of the back support under fore-aft vibration was observed in the entire frequency range (Table 3.3). However, relatively smaller but significant effect of the back support was also observed in the lateral APMS responses, which can be attributed to the tendency of the upper body to slide against the backrest surface and therefore offer less resistance to the upper body sway motion. Furthermore, the statistical significance ($p < 0.05$) of the back support in view of the APMS is also evident from the ANOVA results attained considering two hands support conditions for each back support under single- as well as dual-axis vibration (Table 3.3).

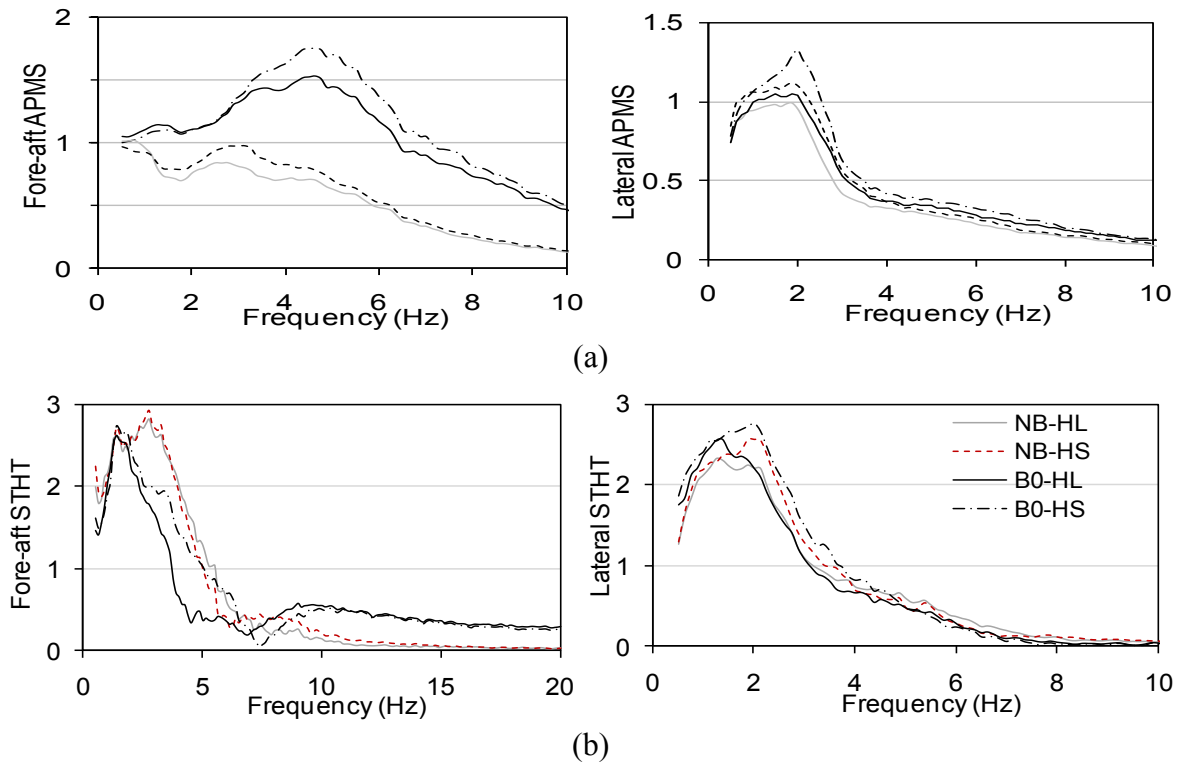


Figure 3.13: Comparisons of mean (a) total APMS and (b) STHT responses of occupants seated with back unsupported (NB) and supported (B0), and hands in lap (HL) and hands on steering wheel (HS) under dual axis vibration ($a_x = a_y = 0.28 \text{ m/s}^2$).

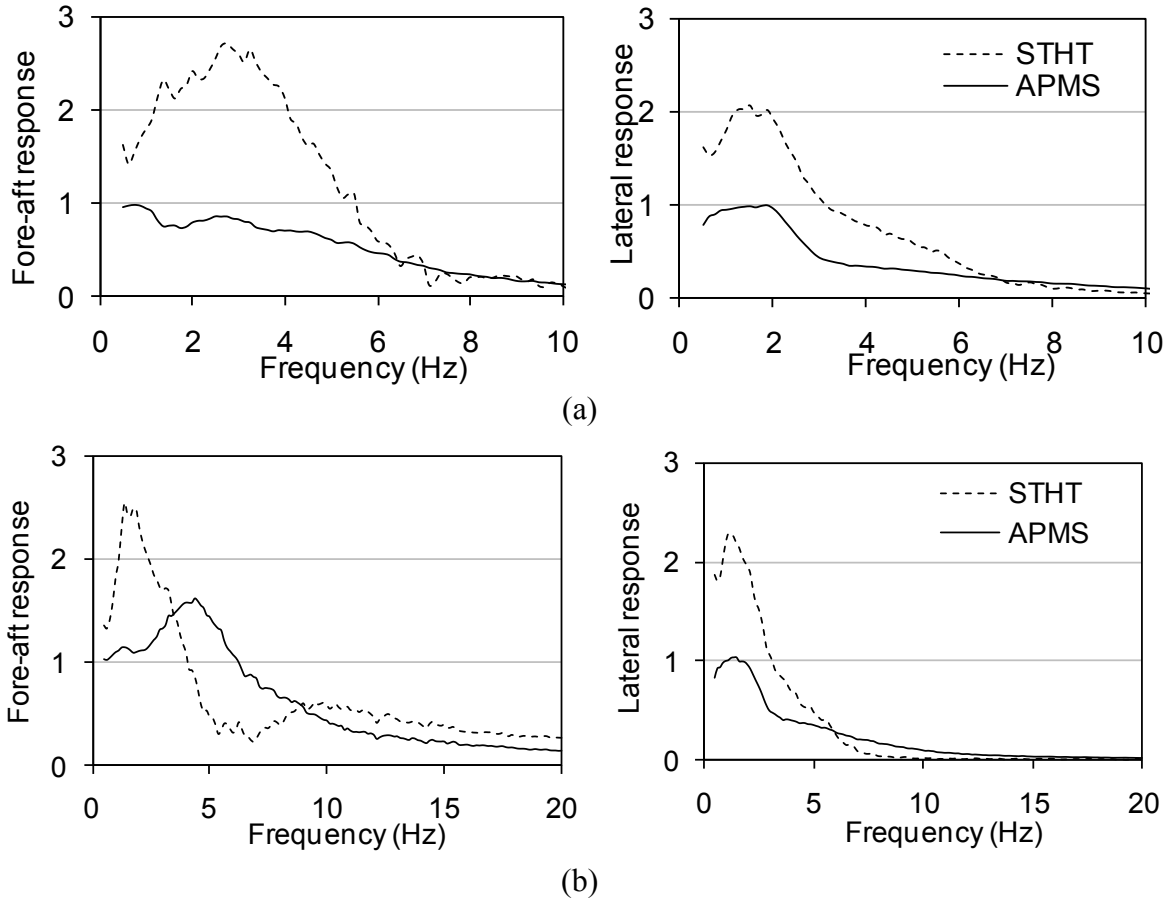


Figure 3.14: Comparison of normalized total APMS and STHT measures of occupants seated with hands in lap and exposed to dual-axis vibration ($a_x=a_y=0.28 \text{ m/s}^2$): (a) No back support and (b) Back support.

The fore-aft APMS responses obtained at the backrest revealed significant dynamic interactions of the upper body with the back support, as evident in Fig. 3.6. Unlike the trends observed in APMS responses with the B0 posture, the STHT responses along fore-aft show significantly lower magnitudes in 1.5 to 6.5 Hz frequency range, and a secondary peak near 9.88 Hz, as illustrated in Fig 3.13(b). The higher fore-aft STHT response observed with NB posture in the 1.5 to 6.5 Hz range could be attributed to the pitch motion of the upper body which is partly restrained with the back support. The significant effects of the back support on the STHT responses are also evident in terms of the resonant frequencies (Table 3.4) and results attained from ANOVA (Table 3.3). However, the effect of back support was small on the lateral STHT

responses. Mean APMS and STHT responses of occupants seated with NB-HL and B0-HL postures under dual-axis horizontal vibration are further compared in Fig 3.14, which show significantly different trends in the two measures in terms of magnitudes and the corresponding frequencies, particularly along the fore-aft axis. The lateral-axis responses, however, exhibit comparable frequencies but differ considerably in peak magnitudes.

3.3.5 Effect of excitation magnitude

The mean APMS responses generally revealed slightly lower peak magnitudes and corresponding frequencies with increase in the vibration magnitude from 0.25 to 0.4 m/s² (Table 3.4). The lower frequencies under higher magnitude of vibration were attributed to the softening effect of the human body [1]. The STHT responses revealed relatively lower magnitudes but comparable resonant frequencies with increase in the magnitude of vibration (Table 3.4). The results attained from ANOVA with vibration magnitude as the independent variable and considering both hands and back support conditions showed that the effect of vibration magnitude is significant ($p < 0.05$) on both the APMS and STHT responses, particularly in the vicinity of the resonance frequencies.

3.4 DISCUSSIONS

The fore-aft APMS measures of the seated body with a back support necessitate careful consideration of the location of the force measurement. The measurement of biodynamic force directly at the buttock-seat interface does not account for the upper body interactions with the backrest and thus yields considerably lower magnitude. The total seat APMS, however, can be estimated from the sum of seatpan and backrest responses, using Eq. (3.9), when the seatpan AMPS is derived from the force measured directly at the seatpan. The results show that the biodynamic responses of the seated body exposed to single and dual-axis horizontal vibration are

strongly influenced by the motion constraints caused by the hands and back support conditions. Sitting with partial back support and hands on a steering wheel, representative of a typical vehicle driving posture, yields considerably higher peak magnitudes of APMS responses and corresponding frequencies compared to those attained with a posture involving no back and hands supports (Figs. 3.11 and 3.13). The hands support help maintain a stable sitting posture under horizontal vibration, although it may serve as an additional source of vibration. Sitting with hands support yields higher magnitude of fore-aft APMS at frequencies above 2.4 Hz for the back supported posture, while the effect on fore-aft STHT was insignificant ($p>0.05$). The lateral APMS response with hands supports tends to be higher at frequencies above 2 Hz compared to that with hands in lap for the back supported posture.

The hands support also affects the lateral STHT significantly ($p<0.05$), particularly with the back supported condition. The effect of hands support appeared to be relatively smaller when sitting with a back support, which suggests coupled effects of both the supports. The use of a back support significantly alters the biodynamic responses of the seated body, particularly along the fore-aft axis. This is attributable to the constraint due to the backrest support. The effect of back support on the fore-aft responses was observed to most significant in the entire frequency range ($p<0.05$). The effect was also significant on lateral APMS response, although relatively small, which is again attributable to the motion resistance offered by the back support. The use of a hands support also helps maintain greater and uniform contact of the upper body with the backrest. Relatively higher magnitudes of the lateral seatpan and backrest APMS with the hands support can be attributed to greater contact of the upper body with the backrest and thereby larger friction force. The higher magnitudes of the STHT responses observed with HS posture

can be attributed to the greater contact with the backrest and thus increase in the vibration transmitted from the backrest.

Sitting with the B0 posture yields greater interactions of the upper body with the back support, while the back support serves as an additional source of vibration. Such interactions were observed to be greatly significant under single-axis fore-aft vibration, however, minimal under lateral vibration [2,3,117]. These interactions are also known to effect the vibration transmitted to the head particularly under fore-aft vibration [106]. Furthermore, the fore-aft seatpan APMS responses of seated occupants with B0 posture are strongly coupled with those at the back support [3,117]. The lateral backrest APMS responses exhibit significantly lower values in the 0.3 to 0.4 range suggesting relatively smaller dynamic interactions of the upper body with the backrest, which is limited to sliding only. The lower magnitude at low frequencies could also be attributed to the selected normalisation factors, and suggests the need for identification of appropriate normalisation factors based on human anthropometry.

It has been shown that the STHT and APMS responses to vertical vibration exhibit comparable trends in terms of the resonant frequencies and peak magnitudes [48]. The fore-aft and lateral STHT responses, however, exhibit patterns that are considerably different from the APMS (Fig. 3.14), irrespective of the back support condition. This suggests that the upper body modes contributing to the STHT response differ from the modes contributing to the body-seatpan interactions under horizontal vibration. The STHT magnitude responses obtained in this study were significantly greater compared to those reported [20], which is partly due to differences in the measurement location and method. The STHT response in the reported study was measured at the mouth level using a bite-bar, while the present study measured the STHT at the skull near

the coronel suture. It is believed that the pitch and roll rotations of the head and neck contributed to greater fore-aft and lateral responses at the head.

The APMS and STHT magnitude as well as phase responses to simultaneously applied dual-axis horizontal vibration were generally very close to those attained under singleaxis vibration, suggesting a weaker coupling between the fore-aft and lateral axis responses. These observations are consistent with those reported in terms of APMS [51,52]. These studies, however, presented comparisons of single and dual-axis responses under different magnitudes of vibration. Mansfield and Maeda [51] and Hinz et al. [52] compared the APMS responses to single- and multiple-axis vibration under identical magnitudes of vibration along each axis, which would result in higher effective vibration magnitude of the multi-axis vibration. The dual and three-axis responses suggested lower peak APMS magnitudes and the corresponding frequencies compared to the single-axis responses, which could in-part be attributed to higher effective magnitude of multi-axis vibration. However, the magnitudes of the direct-axis lateral and fore-aft STHT responses to single axis vibration were lower than those to the dual axis vibration magnitudes at frequencies below 3 Hz (Fig. 3.8).

Experimental studies involving biodynamic responses of the seated human exposed to vertical vibration have reported considerable saggital plane motion of the upper body suggesting the coupled vertical and fore-aft motions [19,20,87,92,117]. This is also evident from the magnitudes of the cross-axis APMS and STHT responses under either vertical or fore-aft vibration. The APMS and STHT responses measured under the considered experimental conditions, however, revealed only minimal effect of dual axis vibration, suggesting negligible or weak coupling between the fore-aft and lateral axis responses. This is further supported by the results attained from ANOVA, which revealed insignificant differences in the single- and dual-

axis responses ($p>0.05$) in most of the frequency range, for all the test conditions considered. Significant differences, however, were obtained between the lateral STHT responses to single and dual-axis vibration ($p<0.01$) in the vicinity of the resonance frequencies, which are also evident in Figs. 3.8 and 3.9.

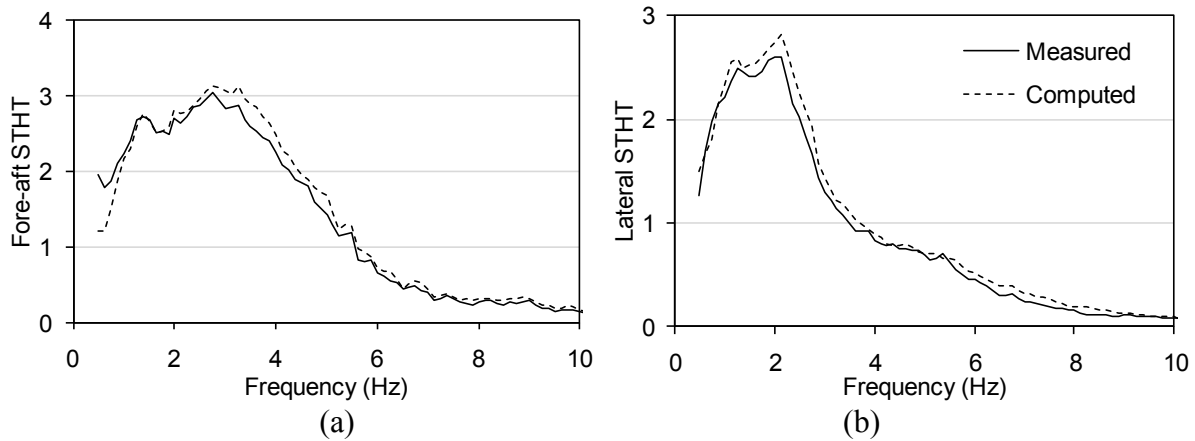


Figure 3.15: Comparisons of estimated and measured fore-aft and lateral STHT responses to dual-axis vibration: (a) fore-aft; and (b) lateral (No back support; $a_x=a_y=0.28 \text{ m/s}^2$).

The small magnitudes of the cross-axis APMS and STHT responses under all conditions of the experiments further indicate weak coupling in the responses to dual-axis horizontal vibration (Fig. 3.7). The total APMS and STHT responses to dual-axis WBV were further estimated considering the single-axis direct and cross-axis responses based on the principle of superposition described in Eqs (3.16) to (3.19), for each experimental condition. The analyses were performed on the single axis data acquired with each subject. The mean of the estimated total responses were then compared with the mean measured data under dual-axis vibration to illustrate the validity of the superposition. The comparisons generally revealed either comparable or slightly higher estimated responses compared to the measured dual-axis responses. As an example, Fig. 3.15 illustrates a comparison of the estimated and measured fore-aft and lateral STHT responses of the occupants seated with NB and HL condition to dual axis WBV. The

results show only small differences between the estimated and measured responses. The validity of the linear superposition theory, however, could not be concluded considering very small magnitudes of the cross-axis components under horizontal vibration, small differences in the single and dual-axis responses and consideration of identical magnitudes of x - and y - axis excitation in the present study.

Unlike the biodynamic responses to vertical vibration, the APMS and vibration transmissibility measures under fore-aft vibration show considerably different trends in terms of magnitudes and resonance frequencies. The differences observed in the fore-aft and lateral responses may in-part be attributed to greater flexibility of the upper body in the sagittal-plane (x - z) compared to the coronal plane (y - z). Moreover, the seat-to-head vibration transmissibility responses encompass the translational and rotational motions of the head and upper body compared to the APMS responses, which reflect the dynamic interaction of the seated occupant with the seat at the driving-points: seatpan and the backrest. It has been suggested that the vibration modes associated with the upper body and head-neck, and other low-inertia body segments may not be adequately reflected in the driving-point measures [47]. This could be observed from the higher frequency peak in the fore-aft STHT response near 9.88 Hz, which is not evident in the APMS in Fig. 3.14(b). Both the biodynamic measures are thus suggested to fully characterise the seated occupants responses to horizontal vibration and to identify reliable target functions for defining the biodynamic models and frequency weightings.

Chapter 4
**ANALYSES OF BIODYNAMIC RESPONSES OF SEATED OCCUPANTS
TO UNCORRELATED FORE-AFT AND VERTICAL WHOLE-BODY
VIBRATION**

Summary: The apparent mass and seat-to-head-transmissibility response functions of the seated human body were investigated under exposures to fore-aft (x), vertical (z), and combined fore-aft and vertical (x and z) axis whole-body vibration. The coupling effects of dual-axis vibration were investigated using two different frequency response function estimators based upon the cross- and auto-spectral densities of the response and excitation signals, denoted as H_1 and H_v estimators, respectively. The experiments were performed to measure the biodynamic responses to single and uncorrelated dual-axis vibration, and to study the effects of hands support, back support and vibration magnitude on the body interactions with the seatpan and the backrest, characterised in terms of apparent masses and the vibration transmitted to the head. The data were acquired with 9 subjects exposed to two different magnitudes of vibration applied along the individual x - and z - axis (0.25 and $0.4 \text{ m/s}^2 \text{ rms}$), and along both the-axis (0.28 and $0.4 \text{ m/s}^2 \text{ rms}$ along each axis) in the 0.5 to 20 Hz frequency range. The two methods resulted in identical single-axis responses but considerably different dual-axis responses. The dual-axis responses derived from the H_v estimator revealed notable effects of dual-axis vibration, as they comprised both the direct and cross-axis responses observed under single axis vibration. Such effect, termed as the coupling effect, was not evident in the dual-axis responses derived using the commonly used H_1 estimator. The results also revealed significant effects of hands and back support conditions on the coupling effects and the measured responses. The back support constrained the upper body movements and thus showed relatively weaker coupling compared to that observed in the responses without the back support. The effect of hand support was also pronounced under the fore-aft vibration. The results suggest that a better understanding of the seated human body responses to uncorrelated multi-axis whole-body vibration could be developed using the power-spectral-density based H_v estimator.

4.1 INTRODUCTION

The biodynamic responses of the seated occupants exposed to whole body vibration have been widely investigated in terms of apparent mass (APMS) or seat-to-head vibration transmissibility (STHT) under broad ranges of vibration and postural conditions [2,3,19,20,33,64,77]. The majority of these studies have focused on response analyses of seated body exposed to vertical (z) vibration, and relatively a few have investigated the responses to fore-aft (x) or lateral (y) vibration [2,3,20]. Furthermore, the reported studies, with the exception of a few recent studies, have been limited to single-axis vibration, where the response

measurements are generally attained only in the direction of the applied vibration. A few studies have also investigated cross-axis STHT and APMS responses, and reported notable upper body movements along fore-aft axis under vertical vibration excitation and vice versa, suggesting coupled movements of the human body in the sagittal (x - z) plane [19-21,37,44,87,92,118]. The vibration environments of work vehicles comprise vibration along all the translational and rotational axes, while the applicability of reported single axis biodynamic responses to such vehicular environment has not yet been established. The characterization of biodynamic responses of seated human body to multi-axis vibration could yield better understanding of the human responses to more realistic vehicular vibration and contribute towards developments in multi-dimensional biodynamic models.

Only a few recent studies have measured the APMS responses of the seated occupants exposed to broad-band random translational vibration along the two- or three-axis [51,52,92,107,112]. The reported APMS responses to dual and three-axis vibration were generally quite comparable with those obtained under single-axis vibration. The peak APMS magnitudes and the corresponding frequencies measured under multi-axis vibration, however, were slightly lower than those observed in the single-axis responses. Mansfield and Maeda [92] further showed that the peak magnitudes of vertical APMS response to dual-axis vibration along y - and z - axis (yz) were lower than those under the z -axis vibration alone at frequencies below 6 Hz, although negligible coupling is observed in the responses in the y - z plane under individual axis vibration. This effect was also evident from the three-axis vibration (xyz) responses [51]. The observed differences could in-part be attributed to higher effective magnitudes of dual and three-axis vibration used in these studies compared to that of the single-axis vibration, which would lead to softening effect in the response [2,64,121]. Similar effect was also observed in the

responses to combined x - and z - axes (xz) vibration reported by Qui and Griffin [107], which showed decreasing peak vertical APMS magnitude and the corresponding frequency under increasing x -axis vibration, and vice-versa. The lower resonant frequency under dual-axis vibration was clearly shown statistically which was also reported by Mansfield et al. [51] under three-axis vibration. A definite trend in the primary peak frequencies, however, was not evident from the reported data, which may in part be attributed to relatively poor frequency resolution used in the above studies, 0.25 Hz and 0.39 Hz [51,107]. The APMS responses to comparable effective magnitudes of single (x and y) and dual (xy) axis vibration revealed considerably smaller differences in the peak magnitude and the corresponding frequencies [121]. The data reported by Hinz et al. [52], however, suggested a few anomalies with regard to the number of vibration axis and the excitation magnitudes. The peak fore-aft APMS response magnitude to three-axis (xyz) vibration was observed to be higher than that due to the x -axis vibration alone under low excitation magnitudes. The peak magnitudes, however, were comparable under higher excitation magnitudes.

The APMS responses to dual and three-axis vibration have been mostly characterized for body seated without a back support and hands in lap. The effect of a vertical back support on the APMS responses have been reported by Mansfield and Maeda [37,92] under combined dual and three-axis vibration, and by Mandapuram et al. [121] under dual-axis (xy) vibration. The effects of a back support on the measured responses were significant and similar to those observed under single axis vibration, while the peak APMS magnitudes were slightly lower under dual-axis vibration. The effects of hands support (hands in lap vs hands on steering wheel) have been reported in a single study under dual (xy) axis vibration, which suggested that hands support affects fore-aft APMS as well STHT responses considerably [121]. It has been suggested that

STHT measure may exhibit greater emphasis of higher body modes associated with the lower inertia components of the seated body compared to the driving-point measure (APMS) [47]. The STHT responses to dual and three-axis translational vibration, however, have been reported in only two studies. Hinz et al. [53] performed comprehensive measurements of the translational and rotational STHT responses of the occupants seated without a back support and hands supported on a handle bar under single (x, y, z) and three (xyz) axis vibration. Another study reported the translational STHT responses of subjects seated with and without back and hands support under dual-axis (xy) vibration [121]. Both the studies showed definite differences between the single and multi-axis responses compared to those observed in the APMS responses, irrespective of the back and hands supports. This would suggest greater coupling effects of multi-axis vibration on the upper-body movements, which may not be entirely captured by the driving-point measures.

The observed differences between the responses to single and dual/three-axis vibration, however, were small compared to the magnitudes of the reported cross-axis STHT responses under single-axis vibration [19,20,53]. The comprehensive magnitudes of cross-axis STHT and APMS responses reported under single axis vibration suggest coupled motions of the seated body in the saggital plane, which would be expected to influence the responses to combined dual/ three-axis vibrations considerably [19-21,37,44,87,92,118]. Furthermore, the coupled motions of the upper body were clearly perceived by the subjects exposed to dual-axis vibration, and observed by the experimenter [121]. The reported small differences in the single and multi-axis responses thus raise an important concern on the method of characterization of the biodynamic responses to multi-axis vibration. The studies reporting the biodynamic responses to multi-axis vibration have invariably employed linear frequency response function (FRF), also

known as the H_1 estimator, based on the cross-spectral density (CSD) of the response and the excitation variables. The CSD-based FRF considers correlated excitation and response data, and would not account for the contributions due to cross-axis responses under uncorrelated dual or three-axis orthogonal vibration [110] used in the reported studies [92,51,52,107,121].

The biodynamic responses to single-axis vibration have also been derived from the ratio of the power-spectral density (PSD) of the response and excitation, referred to as the PSD method [122]. It has been shown that both PSD and CSD methods yield very similar single-axis responses, while the PSD method does not provide the coherence and the phase relation, which is vital for deriving biodynamic models. Alternatively, Rocklin et al. [108] suggested an H_v estimator, which is similar to the PSD method but yields the necessary phase information. Under uncorrelated multi-axis vibration, the PSD method would consider the auto-spectra of the biodynamic response, including the contributions due to cross-axis responses to uncorrelated inputs. This method could thus help identify the possible coupling effects in the biodynamic responses to multi-axis vibration. Furthermore, the coupling effects of simultaneously applied multi-axis vibration may also depend on various factors such as the sitting posture including the hands and back support apart from the excitation magnitude. The sitting postures in vehicular environments generally involve both the hands as well as the back supports, which tend to alter the fore-aft, vertical and pitch motions of the upper body and may thus influence the biodynamic behaviour of the seated body, although only minimal efforts have been made to study their effects under multi-axis vibration. The influences of back and hands supports on both the STHT and APMS responses to coupled vertical and horizontal vibration have not yet been reported.

In this study, the STHT and APMS responses of the seated body exposed to single (x and z) and dual (xz) axis vibration are obtained using the H_1 and H_v , frequency response estimators

based on CSD and PSD of the measured response and excitation, respectively. The PSD method is expected to reveal contributions due to cross-axis responses and thus the coupling effects in the biodynamic responses under dual-axis vibration, which would be suppressed by the CSD method considering the uncorrelated nature of the dual-axis vibration. Furthermore, for the back supported posture, the APMS responses are characterized at the two driving-points formed by the buttock-pan and the upper-body-backrest interfaces together with the STHT responses.

4.2 METHOD

A rigid seat and a steering column were installed on a 6-DOF whole-body vibration simulator (IMV Corporation). A $600 \times 400 \text{ mm}^2$ tri-axial force plate (Kistler 9281C) served as the pan of the seat at a height of 450 mm from the simulator platform. Another 450 mm force plate served as the vertical backrest, which was fabricated using three 3-axis force sensors (Kistler 9317B). The two force plates were used to acquire the forces developed at the two driving-points formed at the seatpan and the backrest, along the x -, y - and z - axis. The platform vibration was measured by a three-axis accelerometer (Brüel and Kjaer 4506A) aligned with the translational axes of vibration.

The body segment vibration transmissibility is generally measured through accelerometers attached to body surface at the measurement location [44,48]. It has been shown that vibration measured at the body surface differs from the vibration of the underlying bones due to visco-elastic properties of the tissue and the skin [27]. Kitazaki and Griffin [126], proposed a skin-effect correction method based on inverse transfer function assuming single degree-of-freedom behaviour of the skin and tissue at the measurement location.

The measurements of head vibration have been mostly conducted using bite-bar in order to reduce tissue contributions [19,20,44,53]. A bite bar offers good coupling to the skull but generally poses greater degree of discomfort among the subjects. Furthermore, it has been suggested that variations in the bite strength may alter the measured vibration [37] and that a biting action could lead to muscles stiffening and thus dynamic behaviour [127]. Alternatively, a few studies have employed helmet-mounted accelerometers to measure STHT. The relative movement of the helmet with respect to the head and relatively high helmet mass tends to alter the nature of vibration [123,124].

Wang et al. [37], developed a light-weight head strap acceleration measurement system with adjustable tension around the skull in order to reduce the potential measurement errors attributed to mass and tissue effects. Furthermore, it has been shown that contributions of the skin and tissue to the potential error are relatively low when skin- tissue volume is low near the measurement location [48,126], as in the case of the skull. In this study, the head vibration was measured using a three-axis micro accelerometer mounted on a light-weight helmet strap [37]. Owing to the different measurement location (skull), the measurements are expected to differ from those measured at the mouth level using the bite bar, particularly in the fore-aft axis due to pitch rotation of the head.

Both the STHT and APMS responses were measured under individual fore-aft (x) and vertical (z) axis vibration, and combined vertical and fore-aft (xz) vibration. The experiment design included: (i) two different back support conditions (seated without a back support- NB; and with lower back against a vertical backrest- B0); (ii) two different hands positions (hands on steering wheel- HS; and hands on lap- HL); and (iii) two different levels of broad-band vibration with constant PSD in the 0.5-20 Hz frequency range applied along the individual x - and z - axis

(0.25 and 0.4 m/s² rms un-weighted acceleration), and dual-axis (0.28 and 0.4 m/s² rms, un-weighted acceleration along each axis). The lower magnitude dual-axis vibration was synthesised to achieve overall rms acceleration of 0.4 m/s² (0.28 m/s² along each axis), comparable to that of the single axis vibration. This facilitated the study of the effects of dual-axis vibration under identical effective magnitudes of single and dual-axis vibration. The measurements performed with the seat loaded with a rigid mass of 60 kg revealed some degree of cross-talk in the simulator. A 0.4 m/s² vertical excitation revealed peak fore-aft vibration in the order of only 5% over the concerned frequency range (0.5-20 Hz). Figure 1 schematically illustrates the four sitting postures realised with two back (NB and B0) and two hands (HL and HS) positions. Each subject was advised to maintain a consistent backrest contact during vibration exposure, which was further monitored by examining the backrest force plate signal and magnitude of the low frequency backrest APMS (near 0.5 Hz).

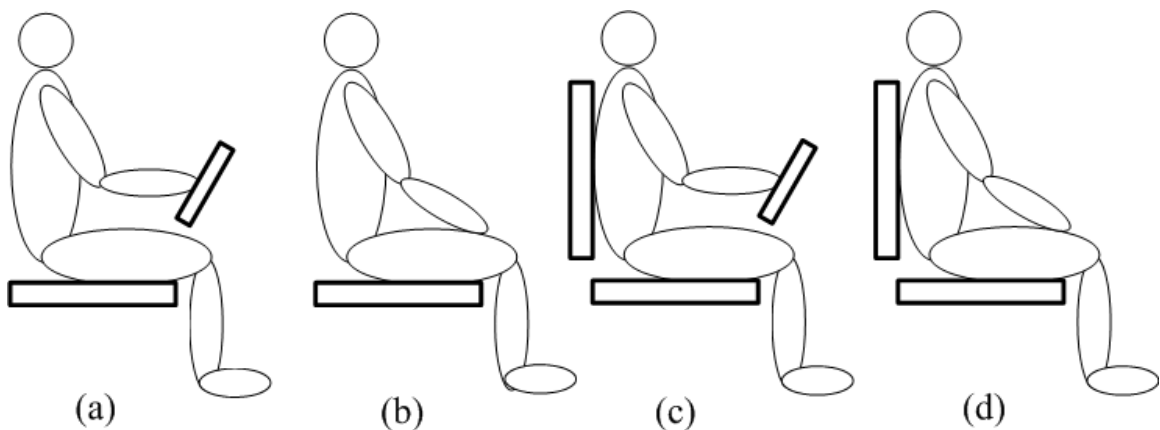


Figure 4.1: Schematic illustration of the sitting postures realised by the subjects during the vibration exposure; (a) No back support but hands supported, NB-HS; (b) No back support and hands in lap, NB-HL; (c) Back supported and hands on steering wheel, B0-HS; and (d) Back supported but hands in lap, B0-HL.

The experiments employed a total of 9 healthy adult male subjects with average age 30.4 years (22-55), body mass 63.4 kg (57-69) and height 173.4 cm (162-179). The subjects had no prior history of back pain. Each subject was informed about the purpose of the study,

experimental setup and usage of an emergency stop that would suppress the stimulator motion in a ramp-down manner, when activated. The experiment protocol had been approved by an ethics research committee prior to the study. Each vibration exposure lasted for nearly 60 s and each subject was asked to put on a cotton lab coat to ensure uniform friction between the upper-body and the vertical back support. Each subject was asked to wear the head-accelerometer strap weighing around 220 grams and adjust its tension using the ratchet mechanism to ensure a tight but comfortable fit. The subject was asked to sit assuming the selected posture, as determined by the back and hands support conditions, comfortably with average thigh contact on the pan and lower legs oriented vertically with feet on the vibrating platform, as illustrated in Fig. 4.1. The feet support was adjusted vertically to provide the desired sitting posture for each subject. Prior to application of vibration, the head-band accelerometer orientation was visually monitored and appropriately adjusted by the experimenter to align the accelerometer with the chosen axis system. For this purpose, each seated subject was advised to aim at a fixed marker in the line of sight, while maintaining the desired posture. Experimenter ensured the tight fit of the head band so as to minimize the effects of hair and skin tissue. Wang et al [37] showed flat frequency response characteristics of the band, in the 0.5-20 Hz range measured on a skull-shaped rigid body when the band was sufficiently tight. The subject was subsequently advised to maintain the same head and neck posture by continually aiming at the fixed marker while being exposed to vibration. The order of the experiments was randomised and each experiment was repeated twice.

4.3 DATA ANALYSIS

The seatpan and backrest forces, and the head and platform acceleration data were acquired in the PulseLabShop™ and analysed to derive the STHT and APMS responses of

occupants seated with different back and hands support conditions, while exposed to single and dual-axis whole-body vibration (WBV). The analyses were performed using a band width of 100 Hz with a resolution (Δf) of 0.125 Hz. Inertial corrections of the measured APMS data were performed using the method described in [64]. The APMS response measured at the seatpan was considered as the total seated body APMS in the absence of a back support. In the presence of the upper-body contact with the back support, the total APMS was estimated from the sum of APMS responses measured at the seatpan and the backrest, such that [121]:

$$M_{sk,l}(f) = M_{pk,l}(f) \quad (\text{without back support posture, NB})$$

$$M_{sk,l}(f) = M_{pk,l}(f) + M_{bk,l}(f) \quad (\text{with back support posture-B0}) \quad (4.1)$$

Where $M_{sk,l}(f)$ represents the total seated body APMS response, $M_{pk,l}(f)$ and $M_{bk,l}(f)$ represent the seat pan and backrest APMS responses, respectively, derived from the force response along axis k ($k=x, z$) due to acceleration input along axis l ($l=x, z$).

4.3.1 Analyses of biodynamic responses to multi-axis vibration

The biodynamic responses to single axis vibration have been derived using linear relationships between the excitation and the measured responses along the direct (axis of applied vibration) and the cross-axis. The seated occupant exposed to single axis vibration (x or z) can be considered as a single-input and multiple-output system as illustrated in Fig. 4.2, where q_{xx} and q_{zx} represent the direct and cross-axis forces or acceleration responses due to fore-aft vibration (a_x). Similarly, q_{zz} and q_{xz} represent the direct and cross-axis responses due to vertical axis (a_z) vibration. The direct and cross-axis biodynamic responses have been mostly derived from the linear frequency response function (FRF), also denoted as H_1 estimator, which involves the complex ratio of cross-spectral density (CSD) of the input and the measured response, and the

auto-spectral density of the input. Under the single axis excitation along x or z -axis, the direct and cross-axis response functions are derived from [2,92,87]:

$$H_{kl}(f) = \frac{S_{a_l q_k}(f)}{S_{a_l}(f)}; k=x, z \text{ and } l=x, z \quad (4.2)$$

Where $H_{kl}(f)$ defines the direct ($k=l$) or cross-axis ($k \neq l$) complex biodynamic function under excitation along axis l ($l = x, z$) corresponding to excitation frequency f . $S_{a_l q_k}$ is the CSD of the response (q_k) measured along k ($k=x, z$) and input acceleration a_l ($l = x, z$), and S_{a_l} is the auto spectral density of the input acceleration.

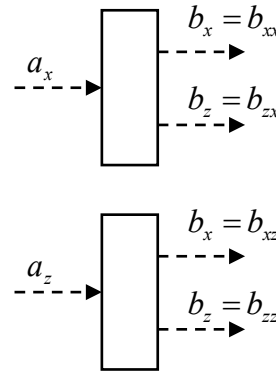


Figure 4.2: Schematic illustration of the direct and cross-axis responses developed during single-input and multiple-output (SIMO) system under single vibration.

The seated occupants' responses to simultaneous dual or three-axis vibrations, reported in recent studies, have invariably employed H_1 estimator. For dual-axis vibration along x and z axis, the biodynamic response functions along each axis are derived from:

$$H_k(f) = \frac{S_{a_k q_k}(f)}{S_{a_k}(f)}; k=x, z \quad (4.3)$$

Where $H_k(f)$ defines the complex biodynamic function which relates the total measured response q_k along axis k ($k = x, z$) corresponding to excitation frequency f .

For coupled motions of the seated body in the sagittal plane, the total response q_k would comprise of components due to excitations along both the axes, a_x and a_z . Considering the uncorrelated nature of the excitations applied along the two axes, the biodynamic response function, derived using Eq (4.3), would ignore the contributions due to excitation along an axis other than the direct-axis. In particular, the total responses derived along x - and z - axis may suppress the contributions due to z - and x - axis vibration, respectively. This could be the reason for observing comparable APMS response magnitudes to single, dual or three-axis vibrations, reported in the recent studies [92,51]. These studies have shown that the APMS responses to dual and three-axis vibration exhibit slightly lower peak magnitude and the corresponding frequency compared to the single-axis responses. This in-part may be attributed to relatively higher effective magnitude of the multi-axis vibration compared to that of the single-axis vibration used in the studies.

The above is also evident from the cross-axis responses to dual and three-axis vibration that have been presented in two studies [53,107]. The cross-axis responses to dual (xz) axis vibration are derived from

$$H_{xz}(f) = \frac{S_{azq_x}(f)}{S_{a_z}(f)}; \text{ and } H_{zx}(f) = \frac{S_{a_xq_z}(f)}{S_{a_x}(f)} \quad (4.4)$$

Where $H_{xz}(f)$ is the cross axis response relating the total measured response q_x under dual axis vibration to excitation a_z alone, while H_{zx} relates the total response q_z under both axis of vibration to excitation a_x alone. The total responses q_x and q_z comprise the responses to direct (a_x and a_z , respectively) and the cross-axis (a_z and a_x , respectively) excitations, where the components due to the direct axis excitations are predominant. The reported cross axis responses evaluated using CSD (H_1) approach did not reveal significant magnitudes of APMS

and STHT, which would be attributed to the uncorrelated nature of the dual and three-axis vibration employed in these studies.

Similarly, the reported coherence functions (γ^2) of the responses to dual or three-axis vibrations are derived as a function of the CSD, $S_{a_k q_k}(f)$:

$$\gamma^2 = \frac{|S_{a_k q_k}(f)|^2}{S_{a_k}(f) S_{q_k}(f)}, k = x, z \quad (4.5)$$

Where $S_{a_k q_k}(f)$ considers the correlated input (a_k)–output (q_k) component only of the actual total response to dual-axis vibration. $S_{q_k}(f)$, however, is auto-spectral density of the total response measured along axis k to dual axis vibration. The presence of coupling in the x - z plane would lead to relatively larger values of $S_{q_k}(f)$ and thus lower coherence values of the response. This is also evident in the reported coherence values under dual and three-axis vibration [53,107]. It has been suggested that the coherencies of the responses along the axis of vibration can be derived from the sum of the coherencies of the direct and cross-axis responses [107].

The studies reporting either APMS or STHT responses to dual or three-axis vibrations have therefore not revealed substantial effects of dual or three axis vibrations. The expected coupling in the fore-aft and vertical responses to simultaneous dual or three-axis vibration could not be clearly observed in the reported responses [92,21,53,87,117,118], although many studies reporting biodynamic responses to vertical vibration have clearly illustrated coupled sagittal plane motions of the body [87,118].

4.3.2 PSD method of analysis

The modulus of the biodynamic response to single-axis vibration can also be derived by relating the PSD values of response and excitation variables assuming that the output response is due to input alone, such that [122]:

$$H_k(f) = \sqrt{\frac{S_{q_k}(f)}{S_{a_k}(f)}} \quad (k = x, z) \quad (4.6)$$

Where $H_k(f)$ is the response function, and $S_{q_k}(f)$ and $S_{a_k}(f)$ are the PSDs of the biodynamic response and excitation along axis k , respectively. The output, however, may include the contributions due to noise present in both the input and output signals [110]. A few reported studies have shown that the APMS responses derived using the PSD method is similar to that obtained from the CSD-based H_1 estimator, suggesting that the contributions of the signal noise are relatively small [21,87,117,118]. Under uncorrelated multi-axis vibration, $S_{q_k}(f)$ would represent the PSD of the total response to multi-axis excitations. The PSD method may thus be considered better suited for the analysis of biodynamic responses to uncorrelated multi-axis vibration. This approach, however, does not yield the phase information, which is vital for deriving biodynamic models of the seated body exposed to vibration.

4.3.3 H_v Estimator

Rocklin et al. [108] suggested an alternate FRF estimator for the modal extractions of responses of the multiple-input multiple-output (MIMO) systems. The estimator, denoted as H_v , is derived from:

$$H_k(f) = \frac{S_{a_k q_k}(f)}{|S_{q_k a_k}(f)|} \sqrt{\frac{S_{q_k}(f)}{S_{a_k}(f)}} \quad (k = x, z) \quad (4.7)$$

In the above equation, H_k defines the frequency response along axis k ($k=x, z$), while $S_{q_k}(f)$ is the auto-spectra of the total response measured along k under multi-axis vibration. It has also been suggested that this estimator is better suited in the presence of input and output noises. Under single-axis vibration, the magnitude of the FRF derived from the H_v method reduces to that obtained from the PSD method, as seen in Eq (4.6). Unlike the PSD method, the H_v estimator also yields the phase information of the signals, which would be identical to that obtained from the H_1 method. In this study, the measured data were analysed to evaluate the APMS and STHT functions using the two frequency response estimators, namely the H_1 and H_v methods. The resulting responses are compared to illustrate the validity of the H_v method for analyses of biodynamic responses to uncorrelated dual-axis excitations.

4.4 NORMALISATION FACTORS

Owing to the significant effect of the seated body mass on the measured APMS responses, the single-axis responses have been generally normalized with respect to the static seated body mass or the APMS magnitude at a very low frequency such as 0.5 Hz [64,77]. Hinz et al. [14] applied the static seated mass as a normalization factor for the APMS responses measured along x -, y - and z -axis to three-axis vibration. The static seated mass, however, tends to differ with the sitting posture, particularly when a back support is used [77]. Alternatively, the available anthropometric data have been applied to determine the seated body mass supported by both the seatpan and the back support [121].

In this study, the normalisation factors for the direct and cross-axis vertical seatpan APMS responses have been obtained from the static body mass measured below the entire seat reported in [4]. The fore-aft APMS data were normalized by considering the proportions of the body mass supported by the seatpan and the backrest along each axis, which were determined

from the human anthropometric data [3,119]. Table 4.1 summarizes the proportions of body weights supported by the seatpan and the back support corresponding to each axis for the 4 postural conditions considered in the study, namely NB-HL, NB-HS, B0-HL and B0-HS.

Table 4.1: Normalization factors (% of body mass supported by the seatpan and back support derived from the anthropometric data [3,47]). No back support but hands supported, NB-HS; no back support and hands in lap, NB-HL; back supported and hands on steering wheel, B0-HS and back supported but hands in lap, B0-HL.

Measurement		Posture			
location	axis	NB-HL	NB-HS	B0-HL	B0-HS
<i>Seat APMS</i>	Fore-aft	87.8	77.8	87.8	77.8
	Vertical	77.8	76.4	79.8	77.6
<i>Back APMS</i>	Fore-aft	-	-	67.8	57.8
	Vertical	-	-	67.8	57.8

4.5 RESULTS

The measured data were analyzed to determine the STHT and APMS responses of each subject to single and dual-axis vibration using the H_l and H_v FRF estimators. The direct and cross-axis STHT and APMS magnitude responses to single axis vibration derived using both the estimators were observed to be nearly identical for all the subjects considered in the study. As an example, Fig. 4.3 illustrates comparisons of the direct and cross-axis STHT magnitude responses of one subject to individual x - and z -axis vibration, derived from the H_l and H_v methods. The results are presented for the back unsupported and hands in lap (NB-HL) posture and 0.4 m/s^2 excitation along each axis. Both the methods also resulted in nearly identical phase response (results not shown). In order to avoid the effects of averaging and the inter-subject variability, the results attained from H_l and H_v estimators for single as well as dual-axis vibration were compared using the individual subjects' responses. As examples, Figs. 4.4 and 4.5 compare the fore-aft and vertical STHT and APMS responses to dual-axis vibration of two different subjects (denoted as S1 and S2), seated with back support and hands in lap posture (B0-HL). The figures

also illustrate the direct and cross-axis responses of the same subjects to single axis vibration derived using the H_l estimator. The responses under identical effective magnitudes of single (0.4 m/s^2) and dual (0.28 m/s^2 along each axis) are considered to study the effects of dual-axis vibration. Similar trends were observed in the results attained with all the subjects, although considerable inter-subject variability was evident.

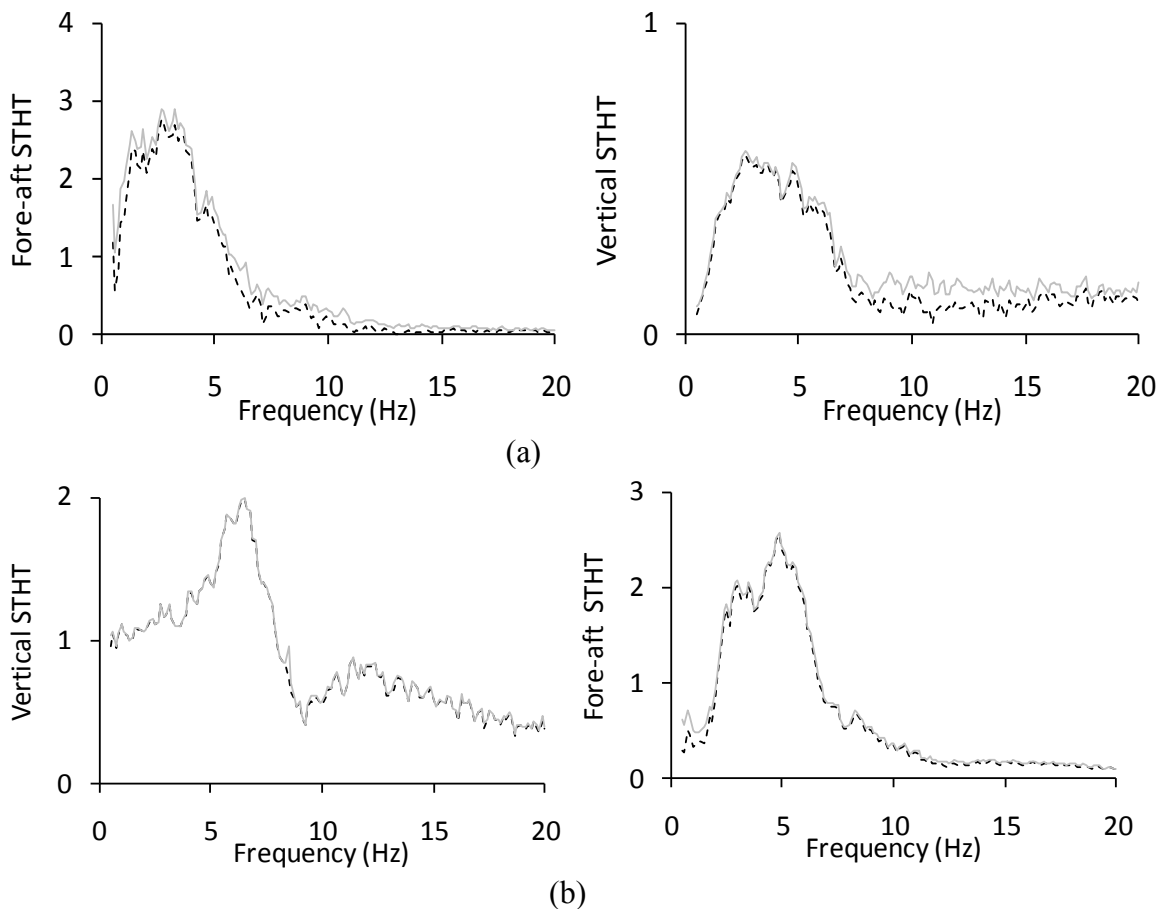


Figure 4.3: Comparisons of the direct and cross-axis seat-to-head-transmissibility (STHT) magnitude responses of a subject (S1) seated with no back support and hands in lap posture (NB-HL) derived using H_l and H_v methods under single axis vibration: (a) fore-aft vibration; and (b) vertical vibration.

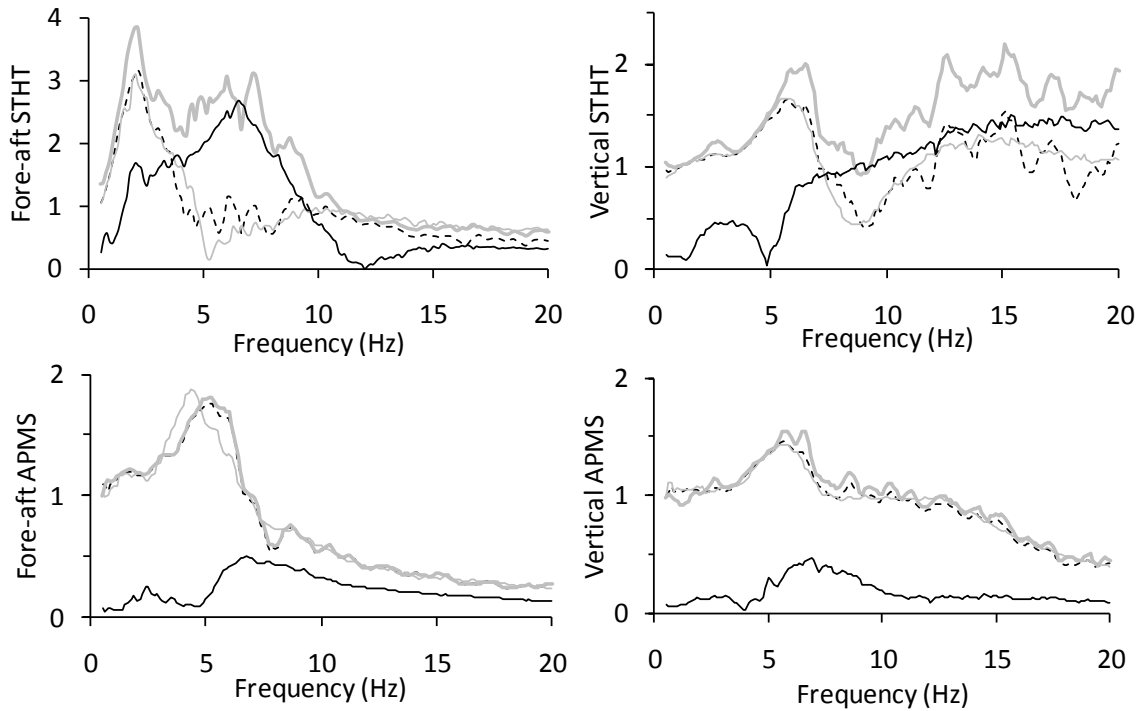


Figure 4.4: Comparisons of the single subject's (S1) APMS and STHT magnitude responses to single and dual (xz) axis vibrations. (seated with back support and hands in lap posture, B0-HL) ——— dual-axis (H_v); - - - - dual-axis (H_1); ——— direct, and ——— cross axis single axis vibration (H_1).

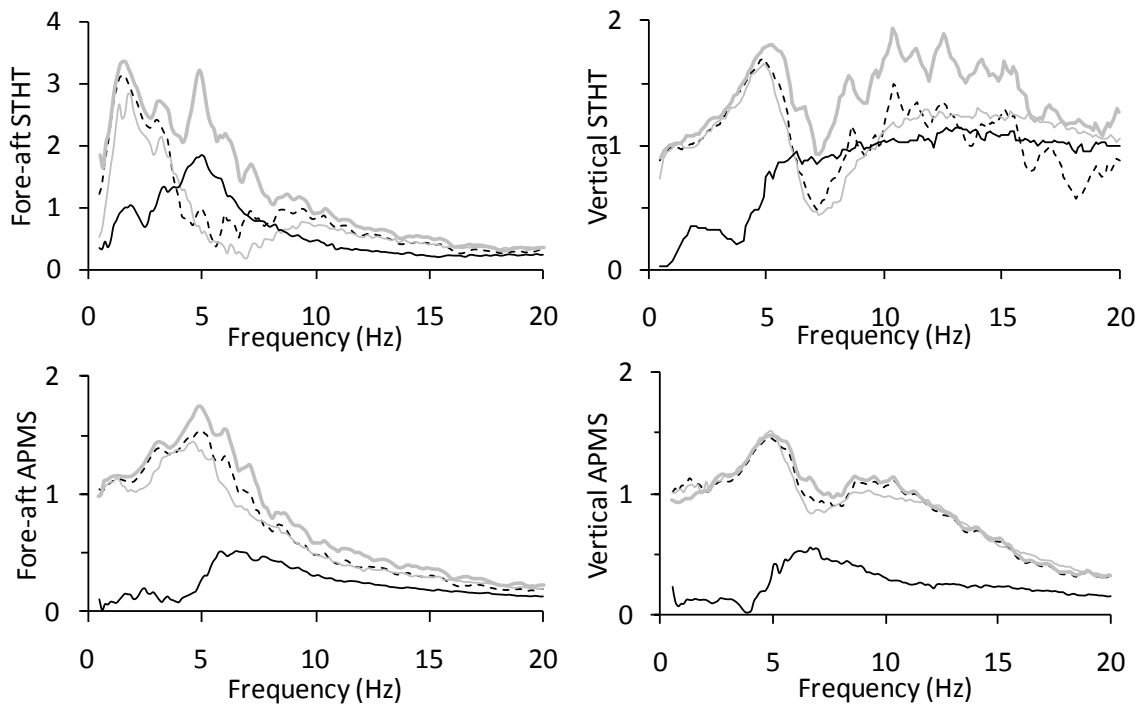


Figure 4.5: Comparisons of the single subject's (S2) APMS and STHT magnitude responses to single and dual (xz) axis vibrations. (seated with back support and hands in lap).

Owing to the considerable scatter among the individual data acquired for each test condition, the mean data of the 9 subjects were obtained to study the differences due to the method of analysis (H_I vs H_v), dual-axis vibration, contributory factors such as hands and back support, and the vibration magnitude. The results are limited to magnitude responses only while both the H_I and H_v estimators resulted in very similar STHT and APMS phase responses. Figures 4.6 and 4.7 illustrate the mean STHT and APMS magnitude responses of the subjects seated without and with the vertical back support, respectively, and hands in lap posture to dual (xz) axis vibration derived using the H_I and H_v estimators. Figures also show the mean direct and cross-axis responses obtained under single (x or z) axis vibration derived using the H_I estimator.

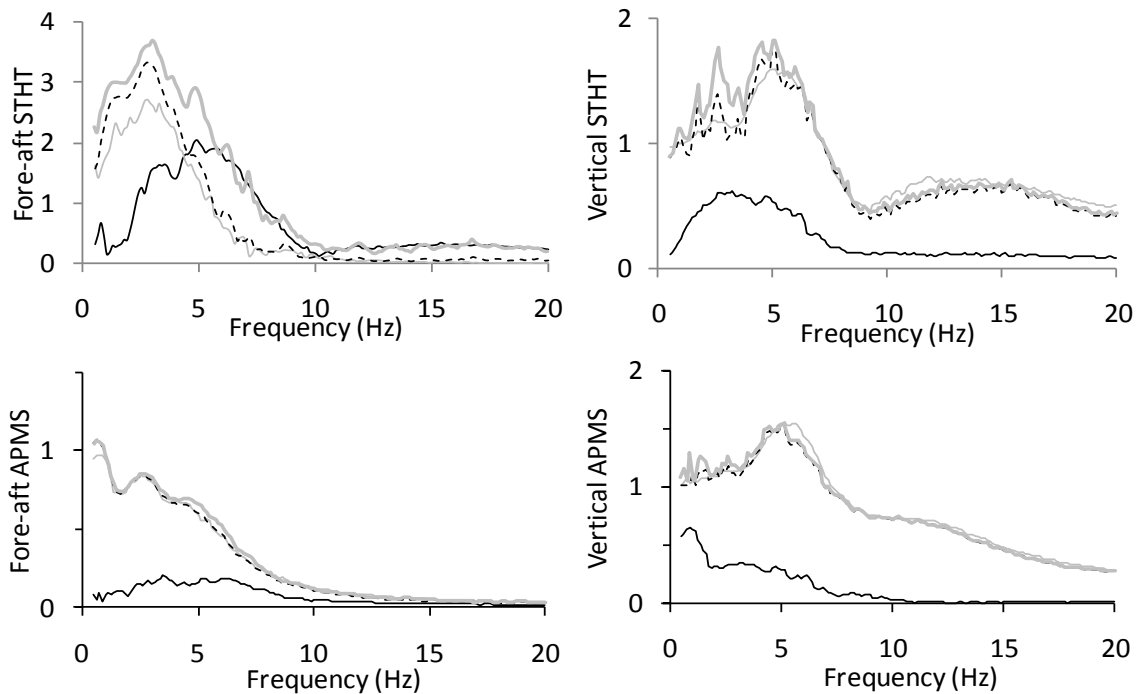


Figure 4.6: Comparisons of the mean fore-aft and vertical APMS and STHT magnitude responses under single and dual axis vibrations. (seated without back support and hands in lap posture, NB-HL) ——— dual-axis (H_v); ——— dual-axis (H_I); - - - - direct and cross axis single axis vibration.

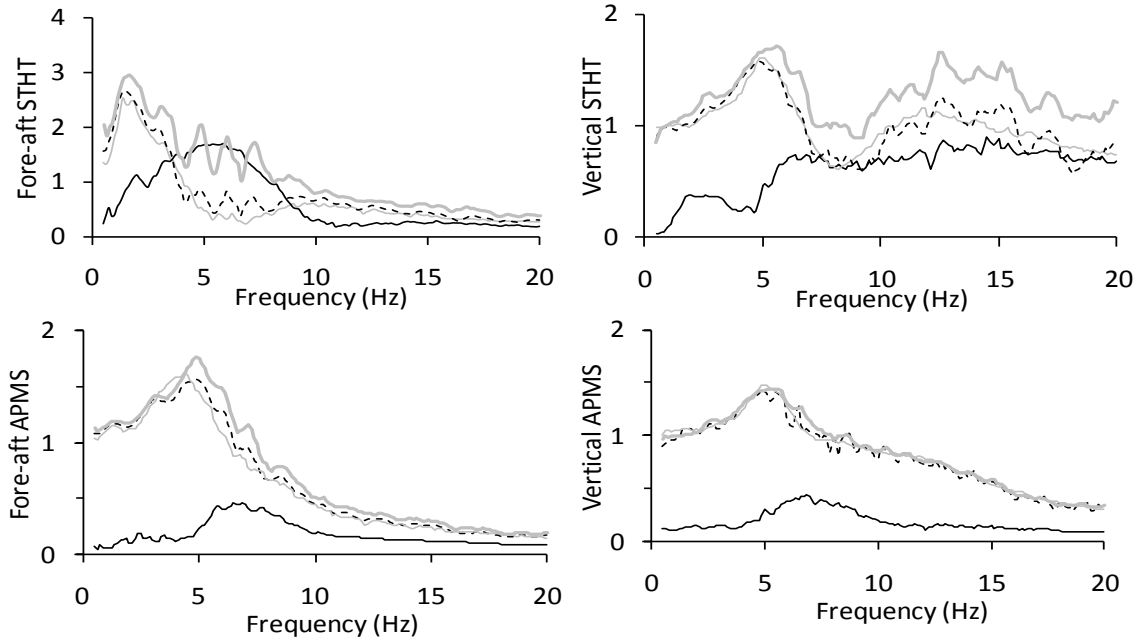


Figure 4.7: Comparisons of the mean fore-aft and vertical APMS and STHT magnitude responses under single and dual axis vibrations. (seated with back support and hands in lap posture, B0-HL) ——— dual-axis (H_v); - - - - dual-axis (H_l); direct and - - - - cross axis single axis vibration.

The pair-wise comparison was performed to determine the statistical significance of the method of analysis at some of the excitation frequencies (Table 4.2), using the data corresponding to two levels each of the hands supports and the excitation magnitudes. The effect of method of analyses (H_l and H_v) was observed to be significant ($p < 0.01$) in the fore-aft STHT responses in the 4-10 Hz frequency range, irrespective of the back support condition. The effect on the vertical STHT, however, was significant at frequencies below 4 Hz for both with and without back supported postures, and additionally at frequencies above 5 Hz with the back supported posture. The fore-aft APMS responses of subjects seated without a back support posture derived using both the estimators were observed to be nearly identical ($p > 0.2$) in the entire frequency range, while the difference in the vertical APMS response was significant at frequencies below 4 Hz ($p < 0.01$). Addition of a vertical back yields higher magnitudes of fore-aft APMS in most of the frequency range above 4-5 Hz and vertical APMS at frequencies below

Table 4.2: p -values illustrating the effect of the method of analysis (H_1 vs H_0) on the seat-to-head-transmissibility (STHT) and apparent mass (APMS) magnitudes under dual-axis vibration. (NB - no back support; B0- with back support)

Posture	Axis	Frequency (Hz)											
		1	2.5	4	4.5	5	5.5	6	7.5	9	10	12.5	15
STHT													
NB	Fore-aft	0.33	0.32	0.01	0.00	0.00	0.00	0.00	0.00	0.00	0.00	0.00	0.00
	Vertical	0.00	0.00	0.17	0.28	0.48	0.16	0.27	0.71	0.45	0.64	0.57	0.78
B0	Fore-aft	0.18	0.07	0.00	0.00	0.00	0.00	0.00	0.00	0.00	0.04	0.13	0.03
	Vertical	0.01	0.00	0.71	0.51	0.25	0.01	0.00	0.00	0.00	0.00	0.00	0.00
APMS													
NB	Fore-aft	0.93	0.98	0.48	0.73	0.39	0.47	0.61	0.40	0.73	0.85	0.23	0.24
	Vertical	0.00	0.00	0.59	0.58	0.59	0.68	0.66	0.86	0.90	0.96	0.93	0.92
B0	Fore-aft	0.60	0.86	0.26	0.33	0.00	0.01	0.16	0.00	0.01	0.07	0.34	0.21
	Vertical	0.00	0.00	0.40	0.31	0.22	0.02	0.00	0.05	0.19	0.57	0.60	0.59

Table 4.3: Frequencies corresponding to peak magnitudes in the seat-to-head-transmissibility (STHT) and apparent mass (APMS) responses of seated occupants to single (H_1) and dual-axis (H_0) vibrations. (No back support but hands supported, NB-HS; no back support and hands in lap, NB-HL; Back supported and hands on steering wheel, B0-HS and Back supported but hands in lap, B0-HL).

STHT	Posture	Single-axis vibration	Dual-axis vibration
Fore-aft	NB-HL	1.38, ≈ 3	1.38, 3, 4.88, 6.25
	NB-HS	1.38, 2.75	1.25, 2.88, 4.75, 6.25
	B0-HL	1.38, 3.13, 8-11Hz	1.63, 3, 4.88, 6, 7.25
	B0-HS	1.38, 3.25, 8-11Hz	1.75, 3, 4.75, 6, 7.25
Vertical	NB-HL	$\approx 2.38, 5.1, \approx 11.75$	0.88, 1.75, 2.63, $\approx 5, 12-16$
	NB-HS	$\approx 2.38, 5, \approx 11.75$	0.88, 1.75, 2.63, $\approx 5, 12-16$
	B0-HL	5, 11.75	2.63, 5.5, 6.5, ≈ 12.5
	B0-HS	$\approx 2.38, 5.1, \approx 11.75$	2.63, 5.5, 6.5, 8.1, 2.5 15.13
Seatpan APMS			
Fore-aft	NB-HL	0.75, 2.63, 4.63	0.63, 2.63, 4.63
	NB-HS	< 0.5, 2.88, 4.5	< 0.5, 2.88
	B0-HL	1.38, 4.38	1.38, 3, 4.88, 7.1
	B0-HS	1.38, 4.34	3.25, 4.88, 6.25, 7
Vertical	NB-HL	5, ≈ 11.75	0.63, 0.88, 1.38, 2.63, ≈ 5
	NB-HS	5, ≈ 11.75	0.63, 0.88, 1.38, 2.63, ≈ 5
	B0-HL	5	2.63, $\approx 5.5, 6.63$
	B0-HS	5	2.5, $\approx 5.5, 6.5,$
Backrest APMS			
Fore-aft	HL	1.25, 4-5	1.25, 3.13, 4.25-6, 8.6
Fore-aft	HS	1.25, 4-5	1.25, 3.13, 4-6.25, 8.6

4 Hz and in the 5.5-7.5 Hz range (Fig. 4.6) compared to those observed with the unsupported back posture. The frequencies corresponding to peak STHT and APMS magnitude responses to single and dual-axis vibration are shown in Table 4.3.

The coupling effects in the responses evaluated from H_l and H_v estimators are further studied through pair-wise comparisons of the STHT and APMS responses to single and dual-axis vibration for each back support condition (Table 4.4). The results suggest that the differences between the STHT responses to single and dual-axis vibration are generally more significant in a wider frequency range when H_v estimator is used, compared to the H_l estimator.

Table 4.4: p -values illustrating the effect of dual-axis vibration (single vs dual-axis vibration) in the seat-to-head-transmissibility (STHT) and apparent mass (APMS) magnitudes derived using H_l and H_v methods. NB- no back support and B0- with back support.

Posture	Axis	Frequency (Hz)												
		1	2.5	4	4.5	5	5.5	6	7.5	9	10	12.5	15	
STHT														
NB	Fore-aft	H_l	0.01	0.00	0.00	0.80	0.04	0.84	0.33	0.27	0.00	0.00	0.10	0.01
		H_v	0.00	0.00	0.00	0.00	0.00	0.00	0.00	0.00	0.00	0.00	0.00	0.00
	Vertical	H_l	0.00	0.00	0.08	0.04	0.05	0.08	0.81	0.95	0.16	0.07	0.09	0.21
		H_v	0.00	0.00	0.00	0.00	0.01	0.76	0.30	0.65	0.50	0.16	0.25	0.00
B0	Fore-aft	H_l	0.53	0.67	0.00	0.77	0.00	0.30	0.02	0.48	0.71	0.80	0.24	0.61
		H_v	0.07	0.03	0.00	0.00	0.00	0.00	0.00	0.00	0.00	0.07	0.01	0.16
	Vertical	H_l	0.17	0.00	0.06	0.66	0.37	0.93	0.07	0.22	0.05	0.00	0.04	0.63
		H_v	0.00	0.00	0.03	0.30	0.89	0.00	0.00	0.00	0.01	0.47	0.00	0.00
APMS														
NB	Fore-aft	H_l	0.32	0.35	0.05	0.96	0.99	0.86	0.86	0.97	0.47	0.58	0.71	0.16
		H_v	0.25	0.34	0.15	0.79	0.39	0.56	0.48	0.37	0.74	0.45	0.08	0.68
	Vertical	H_l	0.00	0.79	0.39	0.06	0.57	0.04	0.19	0.53	0.42	0.66	0.47	0.34
		H_v	0.01	0.00	0.17	0.02	0.28	0.09	0.38	0.65	0.50	0.70	0.52	0.39
B0	Fore-aft	H_l	0.07	0.04	0.02	0.75	0.00	0.44	0.00	0.82	0.14	0.57	0.19	0.56
		H_v	0.01	0.02	0.16	0.50	0.00	0.00	0.00	0.00	0.28	0.25	0.03	0.07
	Vertical	H_l	0.00	0.00	0.03	0.79	0.01	0.67	0.15	0.46	0.04	0.13	0.88	0.58
		H_v	0.79	0.00	0.01	0.26	0.15	0.01	0.12	0.09	0.49	0.36	0.48	0.27

The mean biodynamic responses, derived using H_v estimator are subsequently considered to further analyse the effects the posture and magnitudes of dual-axis vibration. Figure 8

compares the mean fore-aft STHT and APMS responses obtained with hands in lap (HL) and on the steering wheel (HS) for both the unsupported and supported back conditions (NB and B0). The figure shows the total fore-aft APMS measured at the seatpan, while those measured at the backrest for hands in lap and on the support (HL and HS) conditions are compared in Fig. 4.9 for effective vibration magnitude of 0.4 m/s^2 . The hands support yields higher APMS magnitude in the 1.5-4.0 Hz frequency range for the unsupported back (NB) posture ($p < 0.01$) but considerably lower magnitude near the primary resonance of 0.7 Hz, compared to the hands in lap condition.

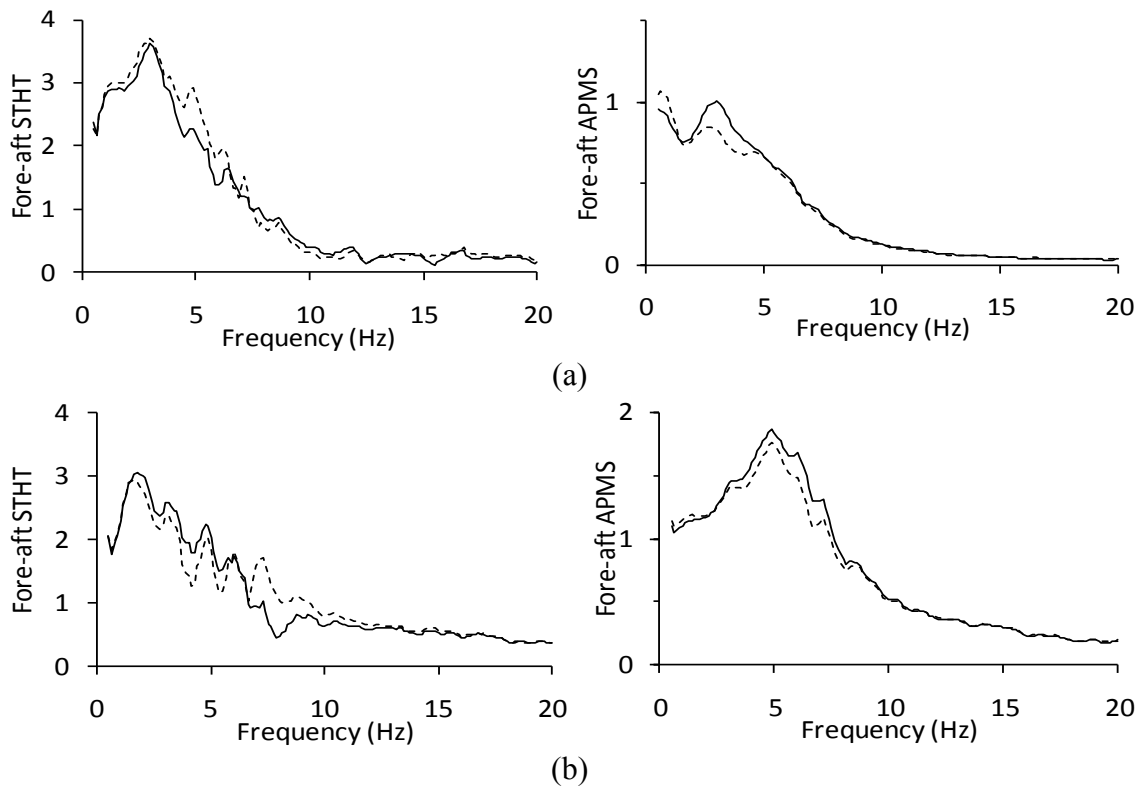


Figure 4.8: The effect of hands support on the fore-aft seat-to-head-transmissibility (STHT) and apparent mass (APMS) responses under dual-axis vibration derived using H_v estimator. (a) without back support, NB and (b) with back supported posture, B0; Vibration magnitude 0.28 m/s^2 along each axis) - - - - Hands in lap, HL; and _____ Hands on steering wheel, HS.

For the supported back (B0) posture, higher APMS magnitude is obtained in the 4-7.5 Hz range when the hands are supported ($p < 0.01$). Similar differences are also evident from the upper-body APMS measured at the back support (Fig. 4.9), which clearly show the significant

effect of the hands support ($p < 0.01$, as seen in Table 4.5). The results in Fig. 4.9 also show near unity low frequency APMS magnitude that corresponds to 67.8% of total body mass as evident from the normalization factors presented in Table 4.1. The low frequency back APMS magnitudes for individual subjects also revealed similar values, which further confirmed the consistency of the backrest contact during vibration exposure. The pair-wise comparisons of the measured dual-axis responses revealed insignificant effect of the hands support on the vertical STHT and the APMS measured at the seatpan ($p > 0.05$), in majority of the frequency range, irrespective of the back support condition (Table 4.5). The vertical APMS measured at the backrest, however, revealed significant effect of hands support in the 4-5.5 and 7.5-10 Hz frequency ranges ($p < 0.01$), although the APMS magnitudes were very small.

Table 4.5: p -values illustrating the effect of hands support (HL vs HS) in the seat-to-head-transmissibility (STHT) and apparent mass (APMS) magnitudes derived using H_v estimator under dual-axis vibration. NB- no back support and B0- with back support.

Posture	Axis	Frequency (Hz)											
		1	2.5	4	4.5	5	5.5	6	7.5	9	10	12.5	15
		STHT											
NB	Fore-aft	0.89	0.12	0.04	0.00	0.01	0.42	0.06	0.44	0.17	0.15	0.80	0.31
	Vertical	0.26	0.58	0.98	0.66	0.75	0.38	0.69	0.43	0.73	0.18	0.56	0.18
B0	Fore-aft	0.95	0.13	0.00	0.00	0.51	0.04	0.23	0.85	0.07	0.03	0.23	0.41
	Vertical	0.56	0.10	0.61	0.20	0.14	0.50	0.75	0.93	0.15	0.61	0.32	0.05
		APMS											
NB	Fore-aft	0.00	0.00	0.00	0.12	0.80	0.51	0.35	0.53	0.75	0.48	0.24	1.00
	Vertical	0.00	0.00	0.54	0.91	0.52	0.32	0.34	0.74	0.94	0.52	0.94	0.44
		Seatpan											
B0	Fore-aft	0.01	0.83	0.00	0.00	0.00	0.00	0.00	0.01	0.45	0.38	0.82	0.90
	Vertical	0.61	0.10	0.74	0.17	0.33	0.76	0.19	0.38	0.26	0.11	0.45	0.52
	Backrest												
	Fore-aft	0.92	0.24	0.00	0.00	0.00	0.00	0.00	0.01	0.20	0.21	0.56	0.69
Vertical	0.43	0.10	0.01	0.01	0.01	0.01	0.06	0.01	0.00	0.01	0.09	0.34	

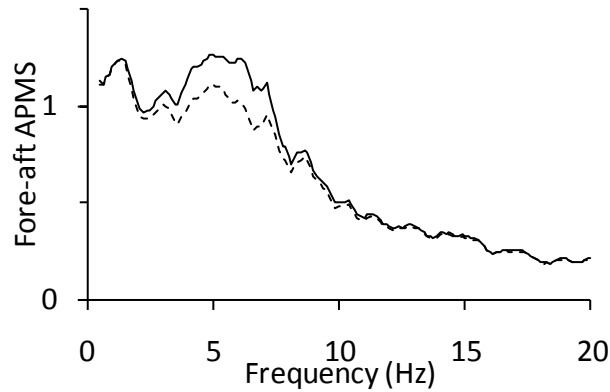


Figure 4.9: The effect of hands support on the fore-aft backrest apparent mass (APMS) responses of the seated occupant seated with back supported (B0) posture derived using H_v estimator. (Vibration magnitude 0.28 m/s^2 along each axis) — Hands in lap, HL and - - - Hands on steering wheel, HS.

Figure 4.10 illustrates comparisons of mean STHT and APMS responses obtained with unsupported and supported back (NB and B0) conditions, with hands in lap under single and dual (xz) axis vibration. The dual-axis response magnitudes, evaluated from the H_v estimator, are in general are higher than those due to single axis vibration. The mean fore-aft STHT response with the back supported (B0) posture is considerably lower than that with the unsupported back (NB) posture at frequencies up to 6.5 Hz. The same trend is also evident in the fore-aft STHT response. At frequencies above 6.5 Hz, the back supported (B0) posture yields higher fore-aft STHT magnitude, compared to the unsupported back (NB) posture. This could be attributed to contributions of pitch motion of the upper body, which is constrained by the backrest. The back supported (B0) posture, however, yields substantially higher magnitudes of fore-aft APMS responses in nearly entire frequency range.

An increase in the single axis vibration magnitude from 0.25 to 0.4 m/s^2 yields lower direct-axis fore-aft STHT response at frequencies below 5 Hz but lower cross-axis STHT response in the 5-10 Hz range, as seen in Fig 4.11. The similar trends are also observed in the direct and cross-axis vertical STHT responses in the 5-10 Hz and 3-10 Hz ranges, respectively.

The effect of magnitude of dual-axis vibration is more significant on the STHT responses (Fig. 4.12) compared to the APMS for the back unsupported and supported (NB and B0) postures.

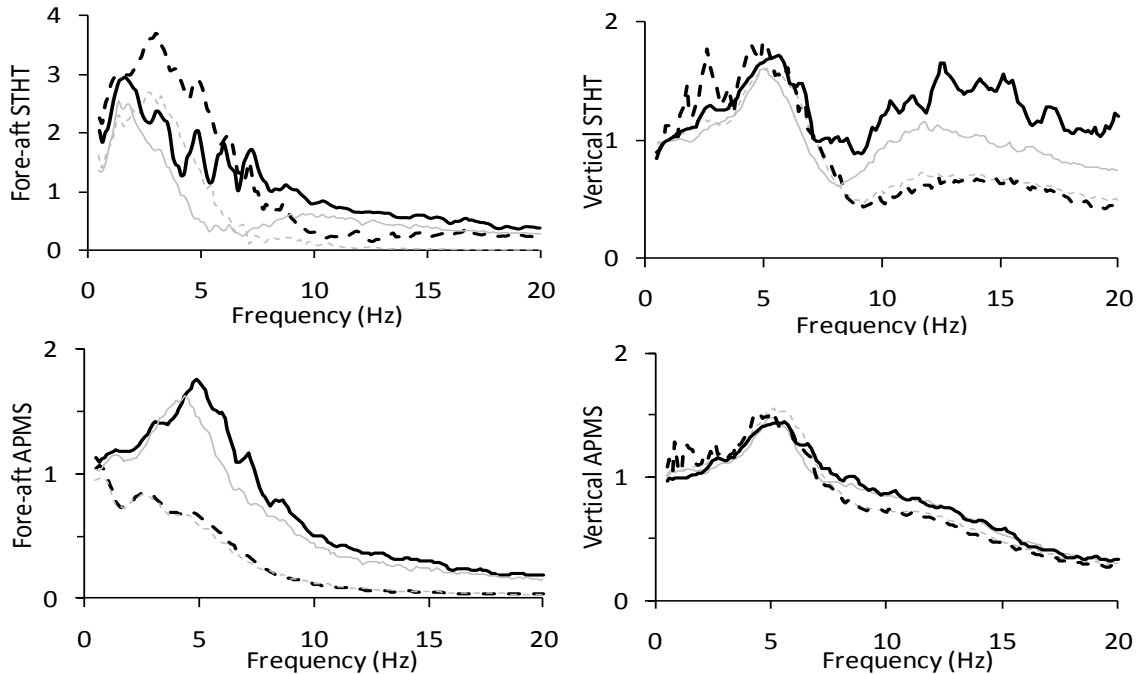


Figure 4.10: The effect of back support in terms of mean seat-to-head-transmissibility (STHT) and apparent mass (APMS) responses of the seated occupants derived using H_v estimators under single and dual-axis vibration with hands in lap posture. - - - - NB, single axis (H_1); - - - - NB, dual axis (H_v); ——— B0, single axis (H_1); ——— B0, dual axis (H_v).

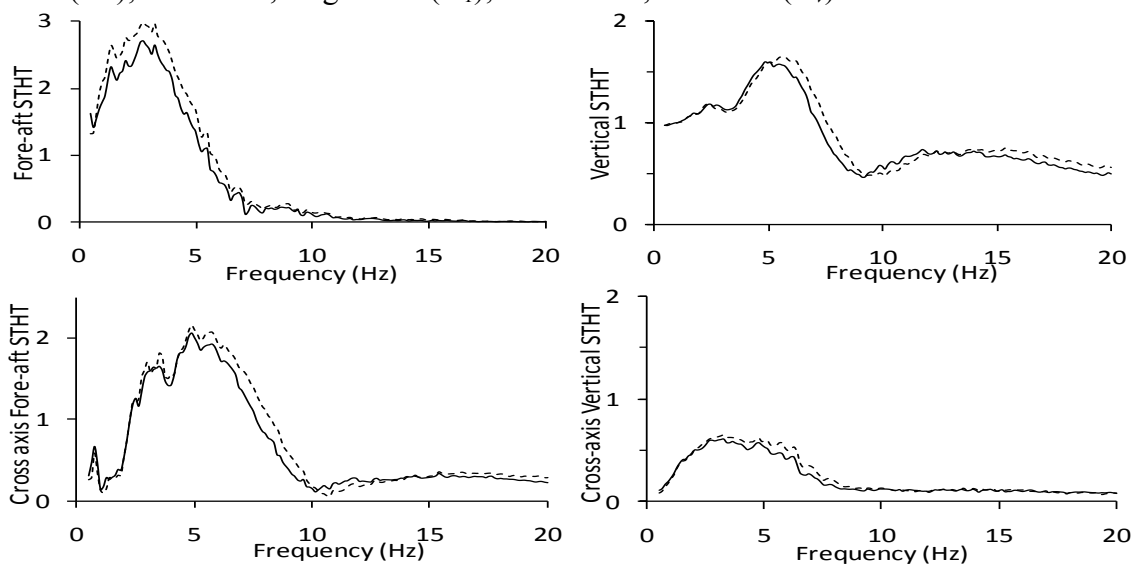


Figure 4.11: Effect of vibration magnitude on the direct and cross-axis seat-to-head-transmissibility (STHT) responses of seated occupants without back support (NB) and exposed to single axis fore-aft and vertical vibration derived using H_1 estimator. - - - - 0.25 m/s^2 ; ——— 0.40 m/s^2 .

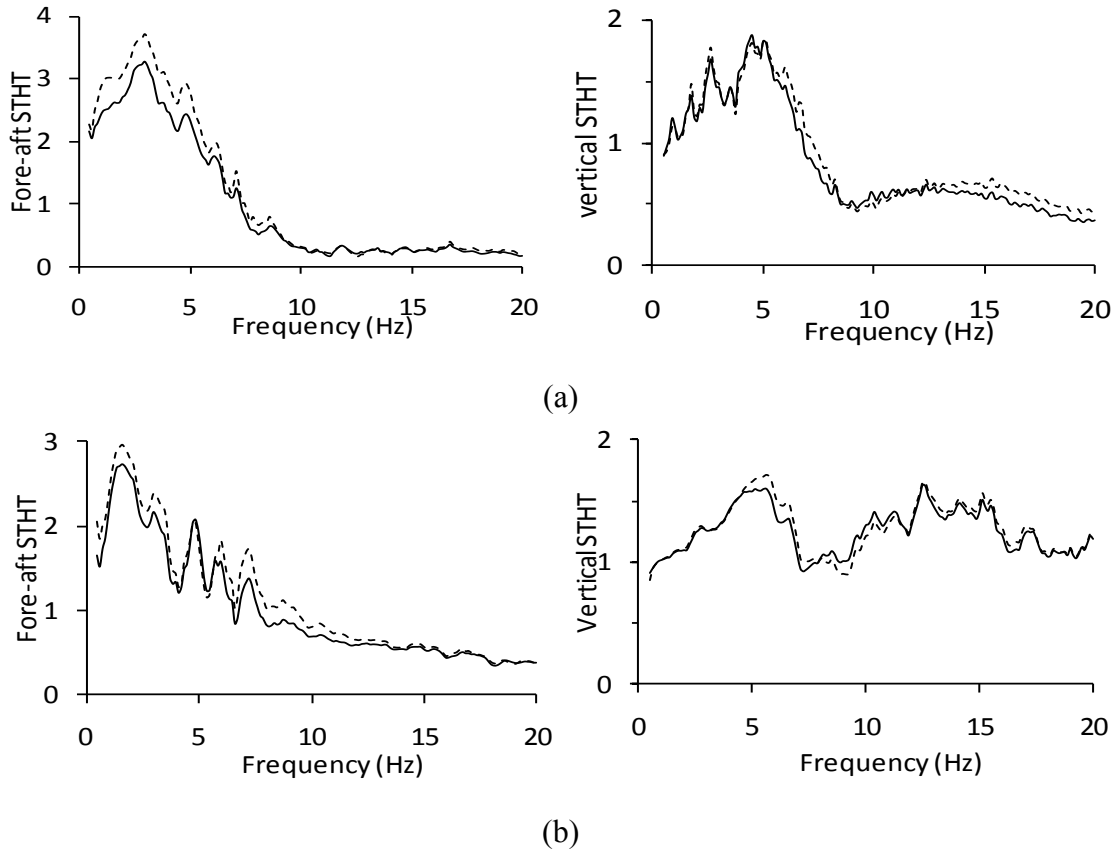


Figure 4.12: The effect of vibration magnitude on the fore-aft and vertical seat-to-head-transmissibility (STHT) responses of the seated occupants with hands in lap (HL) derived using H_v estimator. (a) without back support, NB; (b) with back support, B0. ----- dual-axis (0.4 m/s^2); ——— dual-axis (0.58 m/s^2).

4.6 DISCUSSIONS

The STHT and APMS responses to single axis vibration derived from both H_l and H_v estimators were observed to be similar while those under dual-axis vibration differed. The comparisons of results obtained from the H_l and H_v estimators (Figure 4.4 and 4.5) show that the dual-axis STHT and APMS responses derived using H_l estimator are comparable to those obtained under single axis vibration, as observed in the reported studies [92,51,52,107,121]. This is attributed to the uncorrelated nature of the dual-axis excitations, as described in section 4.1. Small differences observed in the single and dual-axis responses are most likely due to small

correlation between the fore-aft and vertical vibration (dual-axis) caused by the cross-talk among the different actuators in the multi-axis vibration generator.

The results clearly show that the H_v estimator accounts for the contributions due to the cross-axis responses, while the H_l estimator does not clearly show such contributions under uncorrelated dual-axis vibration. The magnitudes of STHT and APMS dual-axis responses determined from the H_v estimator are thus generally higher than the responses to single axis vibration. The fore-aft STHT responses of all the subjects under dual-axis vibration, estimated using H_v , exhibit an additional peak in the 5-6 Hz range associated with the vertical mode resonance that is clearly evident from the cross-axis fore-aft response (H_{xz}) under single axis vertical vibration, as seen in Figs. 4.4 and 4.5. This suggests the notable contribution of the cross-axis response and thus the coupling effects of dual-axis vibration, which is not evident from the fore-aft STHT response evaluated using the H_l estimator. Similarly, the magnitude of dual-axis vertical STHT response derived using the H_v estimator revealed additional peak near 2 Hz, which is also evident from the cross-axis vertical response (H_{zx}) under single axis fore-aft vibration. Furthermore, the peak magnitudes estimated from H_v in the 5-6 Hz range are substantially higher than those estimated from the H_l estimator, which is also attributed to contributions due to the cross-axis responses shown in Figs. 4.4 and 4.5. These results further confirm the coupling effects of dual-axis vibration that are evident only in the responses derived from the H_v estimator.

The APMS responses to dual-axis vibration derived from H_v , tend to differ from those obtained from H_l . The differences were, however, smaller compared to those observed in the STHT responses. These small differences can partly be attributed to relatively lower magnitudes of the cross-axis APMS responses to individual axis vibration compared to those in STHT

responses, as seen in Figs. 4.6 and 4.7. Owing to its definition, the APMS predominantly relies on the dynamic interactions of the lower body (buttocks, thighs, pelvis) with the seatpan, where the cross-axis motion would be considerably small. Thus the dual-axis coupling effects in the seatpan APMS responses are expected to be relatively small.

4.6.1 Effects of supports

The seated body supports (back and hands supports) tend to alter the upper body movements and thus the biodynamic responses. In particular, sitting with a back support yields greater interactions of the upper body and the backrest along the fore-aft direction, and thereby affects both the fore-aft STHT and APMS responses substantially [1,3,16]. A back support also tends to limit the coupling in the sagittal plane motions of the seated body, which yields relatively lower magnitudes of cross-axis vertical STHT and APMS responses to fore-aft vibration at frequencies below 5 Hz, as seen in Figs. 4.6 and 4.7. The magnitudes of these cross-axis responses, however, tend to be considerably higher at frequencies above 5.5 Hz, which can be attributed to the fact that backrest serves as an additional source of fore-aft vibration to the upper body. The cross-axis vertical responses contribute to the coupling effect of dual-axis vibration and yield higher magnitudes of the vertical biodynamic responses in the presence of a back support compared to those with the unsupported back, particularly at frequencies above 5.5 Hz (Fig. 4.10).

While the important effects of a back support on the biodynamic responses are evident under both single and dual-axis vibration ($p < 0.05$), the contributions due to the cross-axis responses and thus the coupling effect is more clearly evident from the dual-axis responses obtained using H_v . The dual-axis vertical STHT responses revealed additional peak near 2 Hz, which is evident in the cross-axis responses (Figs. 4.6 and 4.7). This response peak is not clearly

evident in the dual axis vertical responses obtained from the H_v estimator. The effect of the back support is also evident in the cross-axis fore-aft APMS and STHT responses to vertical vibration, which yields relatively higher magnitudes at frequencies above 4.37 Hz and 7 Hz, respectively, which is due to contributions of the cross-axis response component and additional vibration through the back support. The fore-aft seatpan APMS is substantially greater in the entire frequency range, as it has been reported under single-axis fore-aft vibration [2,3]. The pair-wise comparisons of the measured dual-axis responses also revealed significant ($p<0.01$) effect of the back support on the fore-aft APMS in the entire frequency range, while the effect on the STHT responses is significant at frequencies below 5 and above 9 Hz (Table 4.6). The effect of back support on the vertical STHT and APMS responses are also significant below 5 Hz and at frequencies above 9 Hz, with only a few exceptions.

Table 4.6: p -values illustrating the effect of back support (NB vs B0 posture) in the seat-to-head-transmissibility (STHT) and apparent mass (APMS) magnitudes derived using H_v estimator under dual-axis vibration. NB- no back support and B0- with back support.

Posture	Axis	Frequency (Hz)											
		1	2.5	4	4.5	5	5.5	6	7.5	9	10	12.5	15
STHT	Fore-aft	0.01	0.00	0.00	0.00	0.05	0.05	0.47	0.11	0.00	0.00	0.00	0.00
	Vertical	0.00	0.00	0.14	0.01	0.00	0.55	0.08	0.99	0.00	0.01	0.00	0.00
APMS	Fore-aft	0.00	0.00	0.00	0.00	0.00	0.00	0.00	0.00	0.00	0.00	0.00	0.00
	Vertical	0.00	0.47	0.22	0.00	0.00	0.74	0.15	0.29	0.00	0.10	0.00	0.00

Apart from the back support, the hands support could also serve as an important constraint that may enhance the upper-body-backrest interactions while limiting the upper body pitch. The results show higher magnitudes of the backrest APMS with hands on steering wheel (HS) compared to that with hands in lap (HL) condition, in the 2-8 Hz frequency range (Fig. 4.9). Similar trend was also observed in the fore-aft seatpan APMS; the hands support yielded higher magnitudes in the 2.3-8 Hz frequency range for the supported back posture, while the magnitudes are lower near 1 Hz and higher in the 1.25-4.3 Hz frequency range for the

unsupported back posture. The significant effect of the hands support on the backrest and seatpan fore-aft APMS responses ($p < 0.01$) is also evident at different frequencies in Table 4.5.

Unlike the seatpan fore-aft APMS response, the fore-aft STHT magnitudes for the unsupported back (NB) posture in the 4.5-5 Hz range tend to be only slightly lower with the hands support (Fig. 4.8). This may be attributed to two factors: (i) a hands supported posture tends to limit upper-body pitch motion; and (ii) the presence of a back support could serve as an additional source of vibration to the upper body. However, the vertical biodynamic responses show relatively small effects of the hands support as reported in [77].

4.6.2 Vibration magnitude effect

An increase in the single axis vibration magnitude from 0.25 to 0.4 m/s^2 has shown nonlinear effects of vibration magnitude on the direct and cross-axis fore-aft and vertical STHT responses (Fig. 4.11), similar to those reported in the single and dual-axis fore-aft and vertical APMS responses to dual-axis vibration [2,3,37,53,64,107]. The studies reporting the biodynamic responses to single-axis vibration have shown notable effects of vibration magnitude on the APMS and STHT responses, which is substantial under the fore-aft vibration but relatively small under vertical vibration. Such effect was attributed to the subjects tendencies to stiffen under greater upper body motion caused by higher fore-aft vibration magnitudes, and to shift greater portion of the weight towards the legs to realize a more stable sitting posture [2,3,37,64,87].

The effect of magnitude of dual-axis vibration, however, is far more significant on the STHT responses (Fig. 4.12) compared to the APMS for both the back unsupported and supported (NB and B0) postures. This is attributable to greater contributions of the upper body movement to the STHT response, particularly in the fore-aft axis, as seen in Fig 4.12 (a), for the unsupported back condition. The effect on vertical STHT, however, is relatively small as

observed in the single axis response but statistically significant near 2.5 Hz and in the 6-7.5 Hz range. Further, the magnitude effect on the fore-aft response is relatively smaller for the supported back condition, as seen in Fig 4.12 (b), due to partly constrained upper body movements. The higher vibration magnitude yields considerably lower peak magnitude of the fore-aft STHT, while the widely reported softening effect is not clearly evident. The relatively smaller effects of vibration magnitude are most likely attributed to small difference in the selected vibration magnitudes in the study (0.4 and 0.58 m/s²).

4.7 CONCLUSIONS

The dual-axis responses derived using H_v estimator differ considerably from those derived using the commonly used H_l frequency response function estimator. The differences were related to the contributions of the corresponding cross-axis responses, which were observed under single-axis vibration. Such contributions of the cross-axis responses were not evident in the dual-axis responses derived from the H_l estimator, which was attributed to uncorrelated nature of the dual-axis excitation. It is thus suggested that H_v estimator be employed for characterization of biodynamic responses of the seated body to uncorrelated dual- or multi-axis vibration. Evidence of the contributions of the cross-axis responses in the fore-aft and vertical biodynamic responses derived using H_v estimator illustrated greater coupling in the responses to uncorrelated dual-axis vibration, compared to the H_l estimator. The results also revealed that addition of the back and hands supports results in higher fore-aft APMS responses compared to unsupported hands and back postures, which can be attributed to the constrained upper body movements and imposed backrest vibration to the seated body. However, the supported postures resulted in restrained upper-body movements and thus revealed lower coupling, compared to those with back unsupported posture under dual-axis vibration.

Chapter 5
**APPARENT MASS AND HEAD VIBRATION TRANSMISSION
RESPONSES OF SEATED BODY TO THREE TRANSLATIONAL AXIS
VIBRATION**

Summary: The apparent mass and seat-to-head vibration transmissibility response functions of the seated human body were investigated under whole-body vibration exposures to fore-aft (x), lateral (y), and vertical (z) applied individually and simultaneously. The experiments were performed with 9 adult male subjects to measure the biodynamic responses to single and uncorrelated three-axis vibration with and without hands and back supports under different magnitudes of random vibration in the 0.5 to 20 Hz frequency range. The apparent mass and the head vibration transmission responses were derived using two different frequency response function estimators based upon the cross and auto-spectral densities of the response and excitation signals, denoted as H_1 and H_v estimators, respectively. The two methods resulted in identical single axis responses but considerably different responses under multi-axis vibration. The responses derived from the H_v estimator revealed significant coupling effects of three-axis vibration, which could be directly related to contributions of cross-axis responses observed under single axis vibration, particularly those attributed to sagittal plane motion of the upper body. Such coupling effect, however, was not evident in the three-axis responses derived using the commonly used H_1 estimator. The results also revealed significant effects of hands and back support conditions on the coupling effects of multiple axis vibration and the measured responses. The results suggest that biodynamic responses of the seated body exposed to simultaneous three-axis vibration, commonly encountered in work vehicles, differ considerably from the widely reported responses to individual axis vibration. A better understanding of the seated human body responses to uncorrelated three-axis whole-body vibration could be developed using the power-spectral-density based H_v estimator.

5.1 INTRODUCTION

The seated body responses to whole-body vibration (WBV) have been widely characterized in terms of apparent mass (APMS) and seat-to-head-vibration transmissibility (STHT) under single axis fore-aft (x), lateral (y) or vertical (z) vibration [e.g., 2,19,20,37,47,64,131]. Such studies have provided considerable insights into vibration modes and resonances of the seated body, and effects of body supports and intensity of vibration, in addition to the guidance on modelling of the seated body for application to seating design and dynamics [42,114] and frequency-weightings [13,116]. Compared to the vertical vibration, relatively fewer studies have investigated the horizontal vibration biodynamics, even though a

large number of work vehicles transmit substantial magnitudes of fore-aft and lateral vibration in addition to the vertical vibration [128,129]. The seated body responses to simultaneous multi-axis vibration, representative of the vehicular vibration environment, however, have been investigated in even fewer recent studies. These have mostly focused on driving-point apparent mass response of the seated body to dual- or three-axis translational whole-body vibration [51-53,92,107,121], and generally suggest small effects of multi-axis vibration. The apparent mass responses under dual- and three-axis vibration were comparable to those obtained under single axis vibration, even though notable cross-axis responses and coupled body motions, particularly in the sagittal ($x-z$) plane have been reported under single axis fore-aft or vertical vibration [21,8792, 117,118]. Lack of notable coupling in the measured responses could be partly attributed to method of analysis used and relatively lower contributions of coupled upper body motions to the driving-point measures. The reported studies have invariably derived APMS responses using H_I frequency response function involving cross-spectrum of the response and excitation along each axis, which tends to suppress the contributions of the cross-axis response components under uncorrelated multi-axis vibration [110,121]. These studies have further reported lower peak APMS magnitudes under three-axis vibration compared to those observed under single axis vibration, which may be attributed to the effect of higher overall magnitudes of multi-axis vibration.

Furthermore, the APMS measured at the driving-point may not entirely reflect the contributions of coupled upper-body motions that have been more clearly visually observed under multi-axis vibration [121,130]. The biodynamic measures involving segmental or head vibration transmissibility would thus be expected to exhibit greater coupled effects of multi-axis vibration. It has been shown that STHT biodynamic responses to vertical vibration alone exhibit

greater contributions of the cross-axis motions of the low inertia upper body segments [19]. Hinz et al. [53], measured the STHT responses of the seated body exposed to three-axis vibration, while Mandapuram et al. [121] reported the responses to dual-axis horizontal (xy) vibration. Unlike the APMS responses, the STHT responses to dual- and three-axis vibration differed notably from the respective single axis responses, suggesting relatively greater coupled effects of multi-axis vibration. The differences, however, were relatively small in relation to the reported cross-axis response magnitudes under single axis vibration, particularly in the sagittal plane [19,20,53]. This again could be partly attributed to the method of analysis employed under uncorrelated multi-axis vibration.

Alternatively, H_v frequency response function (FRF) estimator was suggested to analyse the responses to uncorrelated multi-axis vibration [108]. The magnitude responses obtained by the H_v FRF estimator, were identical to those obtained by the power-spectral-densities (PSD) of the response and excitation variables, commonly noted as the PSD method in the literature [21,87,117,118]. Furthermore, unlike the PSD method, the H_v FRF estimator also yields the phase data, which is identical to those derived by the commonly used H_l estimator. A very recent study under dual (xz)-axis vibration has explored the methods of the analysis and suggested that responses to multi-axis vibration derived using H_l function estimator would suppress the contributions of the uncorrelated multi-axis excitations [130]. The STHT and APMS responses to dual (xz)-axis vibration derived using H_v function estimator revealed considerable effect of dual (xz)-axis vibration that could be related to the cross-axis components reported under single axis vibration. Another recent study under dual (xy) axis vibration has suggested that the total response along an axis can be obtained by the sum of direct and cross-axis components to single axis vibration obtained in the same direction [121].

The coupling in the responses to multi-axis vibration may be further influenced by the body supports such as back and hands supports, which tend to alter the fore-aft, vertical and pitch motions of the upper body. Only minimal efforts, however, have been made to study their effects under multi-axis vibration. The influence of a back support on the APMS responses to dual- and three-axis vibration has been reported in two studies [51,121], while the effect on STHT responses to dual-axis horizontal (xy) vibration has been reported only in a single study [121]. The combined effect of the back and hands supports have not been considered in studies reporting the STHT and APMS responses of the seated occupants to three-axis vibration. Considering that the STHT emphasizes the vibration modes associated with low inertia upper body segments and the APMS relates to global seated body response, it is desirable to characterize seated body biodynamics in terms of both the measures to facilitate biodynamic model development and enhance understanding of the seated body response to multi-axis vibration [47].

In this study, the STHT and APMS responses of the seated body exposed to single (x , y and z) and combined three- (xyz) axis vibration are measured simultaneously. The responses are analyzed using both H_l and H_v frequency response function (FRF) estimators. The results are discussed to illustrate the effect of methods of analysis under uncorrelated multi-axis vibration, and coupled effects of multi-axis vibration. The measurements of APMS were performed at the two driving-points formed by the buttock-pan and upper body-backrest interfaces. The responses to three-axis vibration derived using H_v estimator are further analyzed to study the effect of the back and hands supports.

5.2 METHOD

The experiment set up and subjects used in this study are identical to those reported [121,130]. Briefly, a rigid seat and a steering column were installed on a 6-DOF whole-body vibration simulator (IMV). A tri-axial force plate (Kistler 9281C) served as the seat pan at a height of 450 mm from the simulator platform and another 450 mm high force plate, fabricated using three 3-axis force sensors (Kistler 9317B), served as the backrest. These force plates were used to acquire the forces developed along the x -, y - and z - axis, at the two driving-points formed at the seatpan and the backrest. The simulator and the seat used in the study have been described [51,92]. The platform vibration was measured using a three-axis accelerometer (Brüel and Kjaer 4506A) aligned with the translational axes of vibration. A three-axis micro-machined accelerometer mounted on a light-weight helmet strap was used to measure the head vibration, as reported by Wang et al. (2006).

The experiments were conducted with a total of 9 healthy adult male subjects with average age of 30.4 years (22-55), body mass of 63.4 kg (57-69) and height of 173.4 cm (162-179). The subjects had no prior history of back pain and were informed about the experimental set up and usage of the emergency procedures. The experiment protocol had been approved by an ethics research committee prior to the study.

The experiment matrix included: (i) two levels of back support conditions (seated with no back support-NB; and with lower back against the vertical backrest-B0); (ii) two levels of hands positions (hands on steering wheel-HS; hands on lap- HL); and (iii) two levels of broad-band vibration with constant PSD in the 0.5-20 Hz frequency range applied along the individual x -, y - and z - axis (0.25 and 0.4 m/s^2 rms acceleration), and along the three-axis (0.23 and 0.4 m/s^2 rms acceleration along each axis). The lower magnitude three-axis vibration was synthesised to

achieve overall rms acceleration of 0.4 m/s^2 (0.23 m/s^2 along each axis), comparable to that of the single axis vibration, as illustrated in Table 5.1. This facilitated the study of the effect of single and three-axis vibration under identical effective magnitudes. Each vibration exposure lasted for 60 seconds and the subjects were asked to put on a cotton lab coat to ensure uniform friction between the upper-body and the back support. The order of the experiments was randomized and each experiment was repeated twice.

Table 5.1: Summary of the broadband vibration magnitudes employed in this study.

<i>Vibration magnitudes(rms, m/s²)</i>			Overall rms
<i>x-axis</i>	<i>y-axis</i>	<i>z-axis</i>	
0.25	-	-	- 0.25 m/s^2 single axis
-	0.25	-	
-	-	0.25	
0.4	-	-	- 0.4 m/s^2 single axis
-	0.4	-	
-	-	0.4	
0.23	0.23	0.23	- 0.4 m/s^2 three-axis
0.4	0.4	0.4	- 0.7 m/s^2 three-axis

Each subject was asked to sit comfortably with average thigh contact on the seatpan, lower legs oriented vertically and feet supported on the vibrating platform, as shown in Fig. 5.1. The feet support was adjusted vertically to provide the desired sitting posture. The subjects were asked to wear the head-accelerometer strap and adjust its tension to ensure a tight but comfortable fit, and orientation was visually monitored and appropriately adjusted by the experimenter to align the accelerometer with the chosen axis system. During the vibration exposure, the subject was advised to aim at a fixed marker in the line of sight, while maintaining the desired posture.

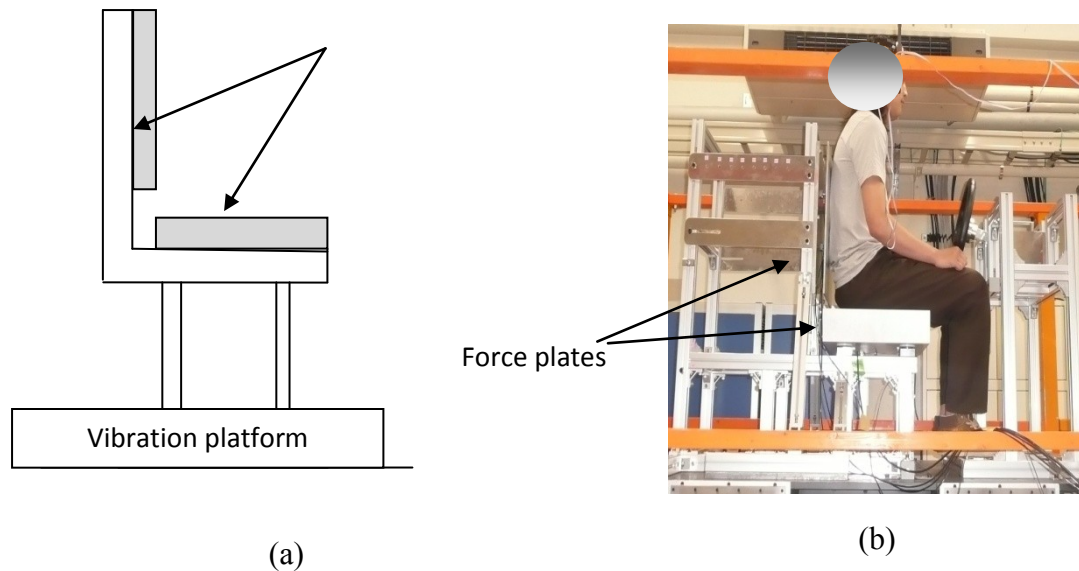


Figure 5.1: (a) Schematic of the test seat with force plate serving as the seatpan and backrest; (b) Experimental setup showing the subject seated with back supported posture and the locations of force-plates.

5.3 DATA ANALYSIS

The seatpan and backrest forces, and the head and platform acceleration data were acquired in the PulseLabShop™ and analyzed to derive the APMS and STHT responses of occupants seated with different back and hands support conditions, while exposed to single and three-axis whole-body vibration (WBV). The analyses were performed using a bandwidth of 100 Hz with a resolution of 0.125 Hz. Inertial corrections of the measured APMS data were performed using the method described [2,64]. The APMS response measured at the seatpan was considered as the total seated body APMS in the absence of a back support. In the presence of the upper-body contact with the back support, the total seat APMS was estimated from the sum of APMS responses measured at the pan and the backrest, as suggested [121,130]:

5.3.1 Analyses of biodynamic responses to three-axis vibration

Majority of the studies reporting the biodynamic responses to single axis vibration have employed linear frequency response function (FRF), also denoted as H_l estimator, which

involves the complex ratio of cross-spectral density (CSD) of the input and the measured response, and auto-spectral density of the input [19-21,87,117,118].

The direct and cross-axis components of the biodynamic responses to single (x, y, z) axis vibration relate the response and excitation vectors in the following manner:

$$\begin{Bmatrix} q_x \\ q_y \\ q_z \end{Bmatrix} = \begin{bmatrix} H_{xx} & H_{xy} & H_{xz} \\ H_{yx} & H_{yy} & H_{yz} \\ H_{zx} & H_{xy} & H_{zz} \end{bmatrix} \begin{Bmatrix} a_x \\ a_y \\ a_z \end{Bmatrix} \quad (5.1)$$

In the above relation, H_{ij} represents the direct biodynamic response quantity for $i=j$ and the cross-axis response for $i \neq j$.

The seated occupants' responses to simultaneous three-axis vibrations, reported in recent studies, have invariably employed H_I FRF estimator.

Considering the uncorrelated nature of excitations applied along the three-axis, the biodynamic response function along an axis, derived using H_I FRF estimator would suppress the contributions due to cross-axis components [110]. For example, the total biodynamic response measured along x - axis would primarily consist of the direct-axis component H_{xx} since the cross-axis components due to y - and z - axis vibration, H_{xy} and H_{xz} , would be suppressed [130]. The studies reporting either APMS or STHT responses to three-axis vibrations have therefore not revealed substantial effects of three-axis vibrations compared to responses to single-axis vibration.

In this study, the measured data were analysed to evaluate the APMS and STHT functions using the two H_I and H_v FRF estimators. The resulting biodynamic responses are

analysed to study the effects of the method of analysis, uncorrelated three-axis vibration, and postural and vibration conditions.

5.4 APMS NORMALISATION FACTORS

Owing to the significant effect of the seated body mass on the measured APMS responses, the single-axis responses have been generally normalized with respect to the static seated body mass or the APMS magnitude at a very low frequency such as 0.5 Hz [64,77]. Hinz et al. [52] applied the static seated mass as a normalization factor for the APMS responses measured along the x -, y -and z -axis to single and three-axis vibration. The static seated mass, however, tends to differ with the back support conditions [77]. The static seated mass along the vertical axis can be conveniently measured, and it corresponds well with the APMS magnitude at a low frequency of 0.5 Hz [64]. The body mass supported in the fore-aft and lateral axis, however, differs considerably from the respective low frequency APMS magnitudes, which has been attributed to relatively greater participation of the thighs and legs, and resonance at the low frequency below 1 Hz [3]. In this study, the direct and cross-axis vertical seatpan APMS responses are normalized with respect to static body mass supported by the seat as reported [77]. The normalization factors for the fore-aft and lateral APMS data are estimated from reported proportions of the body mass supported by the seatpan and the backrest along each axis, which were determined from the human anthropometric data [119] as reported [3,121].

Analyses of variance (ANOVA) was performed on the APMS and STHT data using SPSS to identify the statistical significance of the effect of three-axis vibration, hands support, back support and the excitation magnitude.

5.5 RESULTS

The measured data were analysed to determine STHT and APMS responses of each subject to single and three-axis vibration using both H_I and H_V FRF estimators. The direct and cross-axis STHT and APMS responses of each subject to single axis vibration derived using both the FRF estimators were observed to be nearly identical. Similar to the reported studies, the data acquired for each test condition, however, revealed scatter among the individual subjects datasets, mostly attributed to inter-subject variability. The results show greater variability in the STHT responses compared to the APMS data, although consistent trends are also evident in view of the dominant frequencies, which are also considered as the resonant frequencies. The maximum coefficient of variation (CoV) of the APMS and STHT data ranged from 15-30% and 25-45%, respectively, in the vicinity of the resonant frequencies (results not presented). The CoV of the data obtained under other test conditions were also observed to be in the similar range. The mean responses were subsequently evaluated to study the effects of method of analysis (H_I vs H_V), simultaneous three-axis vibration, hands and back supports, and the vibration magnitude. The results are limited to magnitude responses only, while both the H_I and H_V estimators resulted in nearly identical STHT and APMS phase responses, as reported [130].

Figure 5.2, as an example, illustrates the mean direct- and cross-axis STHT responses of subjects seated without back and hands supports (NB-HL), and exposed to single axis vibration (0.4 m/s^2), which describe the (3×3) transfer function matrix in Eq (5.3). The notation H_{ij} in the figure represents the direct-axis STHT response for $i=j$ and cross-axis STHT for $i \neq j$. The observed magnitudes of the cross-axis H_{xz} and H_{zx} , suggest coupled body motions in the saggital plane under individual x - and z -axis vibration. H_{xz} in particular were in the order of 2 for the STHT magnitudes suggest major coupling.

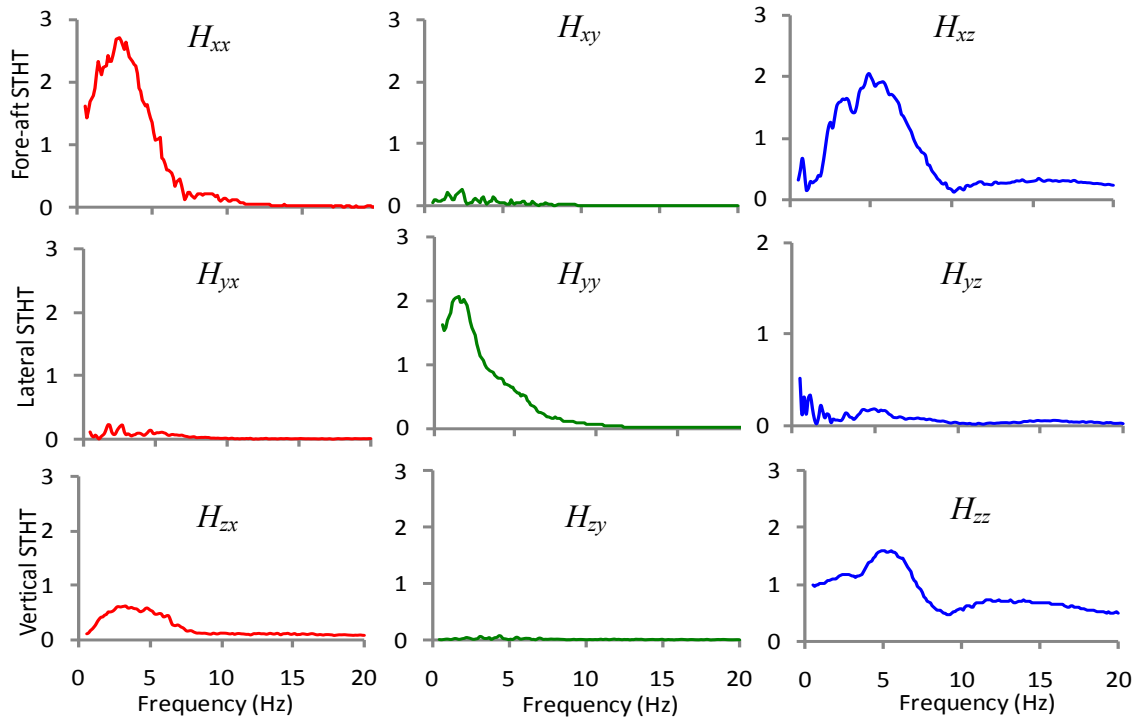


Fig. 5.2. The mean direct and cross-axis seat-to-head-transmissibility (STHT) magnitude responses of the occupants seated without back support and hands in lap posture under single axis fore-aft, lateral and vertical axis of 0.4 m/s^2 rms vibration magnitude.

Unlike the responses to single-axis vibration, the mean STHT responses to three-axis vibration derived using H_l and H_v FRF estimators differed considerably, irrespective of the sitting condition and vibration magnitude. Figure 5.3 compares mean STHT responses obtained from the H_l and H_v FRF estimators for the two back support conditions and 0.23 m/s^2 excitation magnitude along each axis (overall $=0.4 \text{ m/s}^2$). The results are also compared with those obtained under single axis vibration of identical magnitude (0.4 m/s^2). The STHT responses of the seated occupants to three-axis vibration obtained from H_v estimator are generally higher than those obtained from the H_l estimator. In particular, the fore-aft STHT responses derived using H_v estimator revealed greater magnitudes in the entire frequency range. The mean vertical STHT responses to three-axis vibration derived from both the estimators were nearly identical in the higher frequency range for without back support (NB) condition. The vertical STHT response for

the back supported (B0) posture obtained from the H_v estimator, however, is greater than that from the H_l estimator in the entire frequency range, which is attributable to relatively higher magnitude of H_{zx} for the back supported posture. The mean APMS responses derived using H_l and H_v estimators, however, revealed relatively smaller differences compared to those observed in STHT responses (results not presented). These differences were particularly evident near 5 Hz, 0.75 Hz and 2.5 Hz in the fore-aft, lateral and vertical APMS responses, respectively.

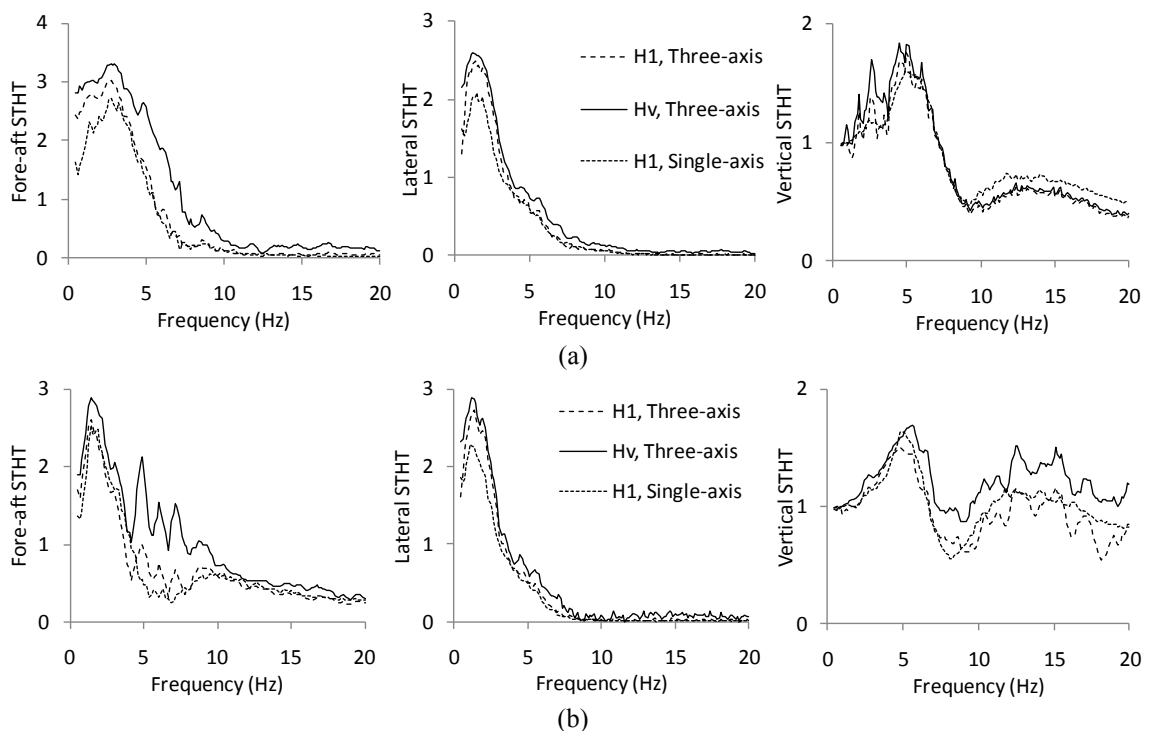


Fig. 5.3. Comparison of the mean seat-to-head-transmissibility (STHT) magnitudes obtained with the H_l and H_v methods of the seated occupants seated with the hands in lap and exposed to single ($a_x=a_y=a_z=0.4 \text{ m/s}^2$) and three-axis ($a_x=a_y=a_z=0.23 \text{ m/s}^2$); (a) No back support and (b) Vertical back support.

The mean APMS and STHT responses of the seated occupants derived using H_v FRF estimator under identical effective magnitudes of single (0.4 m/s^2) and three-axis (0.23 m/s^2 along each axis) vibration are compared to study the effects of uncorrelated multi-axis vibration. The mean STHT responses of occupants seated without and with back support, and exposed to three-axis vibration generally revealed higher magnitudes compared to those under single axis

vibration, as illustrated in Fig. 5.4. Relatively smaller differences, however, were observed in the APMS responses to single and three-axis vibration, as illustrated in Fig. 5.4. The APMS responses of human body seated without back support (NB) and exposed to individual fore-aft, lateral and vertical vibration, revealed primary resonance frequencies near 0.75 Hz, 1 Hz and near 5 Hz, respectively. The mean vertical APMS responses of occupants seated without a back support (NB) under three-axis vibration exhibit additional peaks in the 0.5-2.5 Hz, which are not evident in the response to purely vertical vibration. These peaks could be directly related to those observed under x - and y -axis vibrations, and notable magnitude of cross-axis response observed under fore-aft vibration, suggesting couplings between the multi-axis motions of the body. Similarly, the fore-aft APMS responses of occupants seated without a back support under three-axis vibration showed slightly higher magnitudes around the vertical mode resonant frequency (near 5 Hz) which can be related to the cross-axis fore-aft response observed under vertical vibration alone.

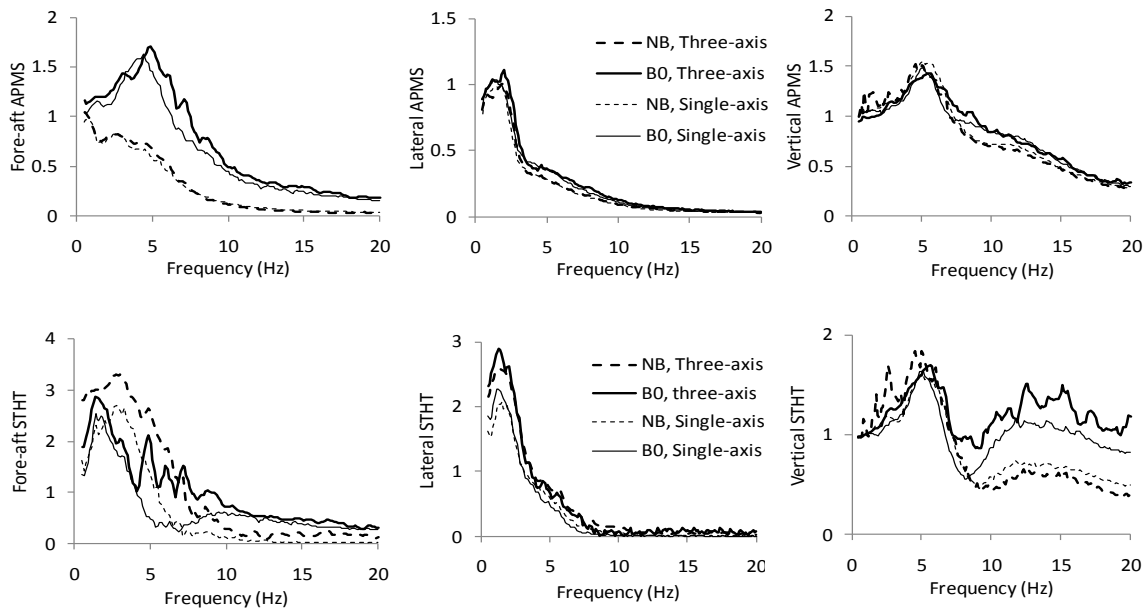


Fig. 5.4. Comparisons of mean apparent mass (APMS) and seat-to-head-transmissibility (STHT) magnitude responses to single and three-axis fore-aft, lateral and vertical vibration of the occupants seated without and with back support and hands in lap; three-axis vibration ($a_x=a_y=a_z=0.23 \text{ m/s}^2$).

The comparison of the responses to single and three-axis vibration of the seated body with the back support (B0) generally revealed higher APMS magnitudes under three-axis vibration at frequencies above the primary resonance along each axis. The higher magnitudes of the mean fore-aft APMS response of the subjects seated with a back support were observed under three-axis vibration at frequencies above 5 Hz. Furthermore, the frequency corresponding to the peak magnitude is also higher. The lateral APMS response to three-axis vibration is also slightly higher in the 2-4 Hz range, while the frequency of peak magnitude is higher than that observed under single axis vibration.

The pair-wise comparisons of the data attained for both the back supported conditions suggest significant effect of three-axis vibration on the APMS magnitudes ($p < 0.05$) in the fore-aft, lateral and vertical axis in the 0.75-2 Hz range (around the fore-aft and lateral mode resonant frequencies). Furthermore, the effect in the fore-aft APMS is significant in the 5-7.5 Hz frequency range, and in the vertical APMS near 7.5 Hz. The significant effect of multi-axis vibration on the STHT response, on the other hand, is evident in a wider frequency range. The effect on fore-aft and lateral STHT is more significant in most of the frequency range up to 9 Hz, while the effect on vertical STHT is evident in the 1-4.5 and 6-7.5 Hz ranges.

The effects of the back support on the mean fore-aft, lateral and vertical STHT and APMS responses under three-axis vibration were observed to be very similar for both the hands support conditions (HL and HS). The results attained with HL condition alone are thus presented to show the effect of the back support on the responses to three-axis vibration. The greater effect of the back support compared to the hands support was observed in both the APMS and STHT responses of the seated occupants, particularly along the fore-aft and vertical axis, as illustrated in Fig. 5.4.

The APMS and STHT responses to both the single and three-axis vibration are compared to illustrate effect of the back support in addition to the coupling effects of three-axis vibration. The mean fore-aft STHT magnitudes under three-axis vibration with back support posture (B0) are considerably lower compared to those without the back support (NB) posture at frequencies up to 6.5 Hz but higher at frequencies above 6.5 Hz. The back supported posture (B0), however, caused substantially higher magnitudes of fore-aft APMS responses in the entire frequency range, under both single and multi-axis vibration. The addition of back support also resulted in slightly higher resonant magnitudes of lateral APMS and STHT responses compared to the NB posture under both (single and three-axis) excitations. The vertical STHT magnitudes are also substantially higher for the B0 posture compared to NB posture at frequencies above 7 Hz.

The pair-wise comparisons of the data acquired under three-axis vibration revealed most significant effect ($p < 0.01$) of the back support on the fore-aft APMS response in the entire frequency range, while this effect on vertical APMS is also observed in most of the frequency range except for 4, and 5.5 to 7.5 Hz range. Very similar significance on the vertical STHT is also evident. The back support effects on the fore-aft STHT are observed to be significant at fewer frequencies (below 1, 2.5-4, and 9-12 Hz), while the effect on lateral STHT is nearly insignificant.

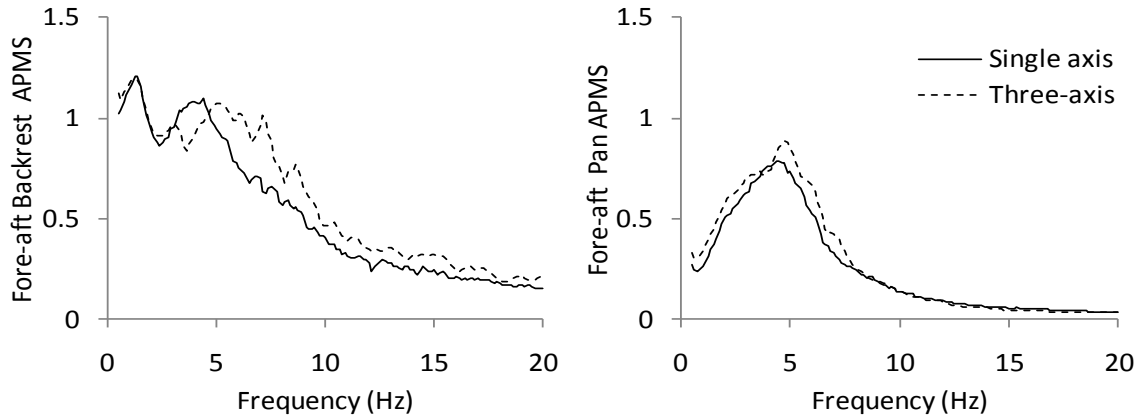
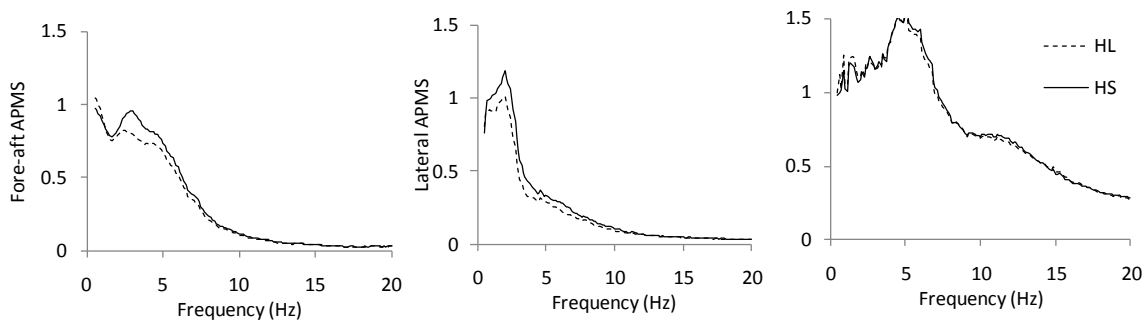


Fig. 5.5: Comparisons of mean backrest and pan apparent mass (APMS) magnitude responses to single and three-axis fore-aft, lateral and vertical vibration with hands in lap; single axis: $a_x=0.4 \text{ m/s}^2$; three-axis ($a_x=a_y=a_z=0.23 \text{ m/s}^2$).

The upper body interactions with the back support yields considerable magnitude of force along the fore-aft axis but negligible forces along the lateral and vertical axis at the backrest. The fore-aft APMS responses, measured at the backrest and the pan to vibration applied along the three-axis and along the fore-aft axis alone are compared in Fig. 5.5, which clearly show considerable effects of three-axis vibration on both the APMS responses. Greater magnitudes of backrest fore-aft APMS are observed under three-axis vibration at frequencies above 4.1 Hz, while effect on the pan APMS is evident at frequencies up to 8 Hz.



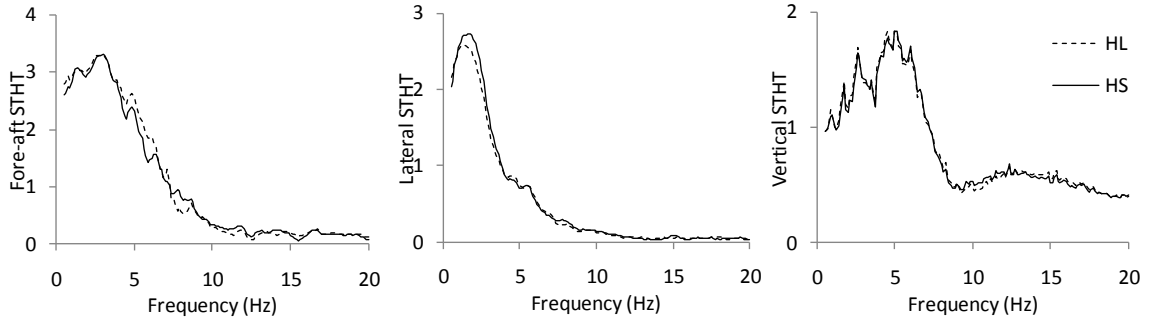


Fig. 5.6: Comparisons of mean apparent mass (APMS) and seat-to-head-transmissibility (STHT) magnitude responses to three-axis fore-aft, lateral and vertical vibration of the occupants seated with hands in lap and on steering wheel and no back support; three-axis vibration ($a_x=a_y=a_z=0.23 \text{ m/s}^2$).

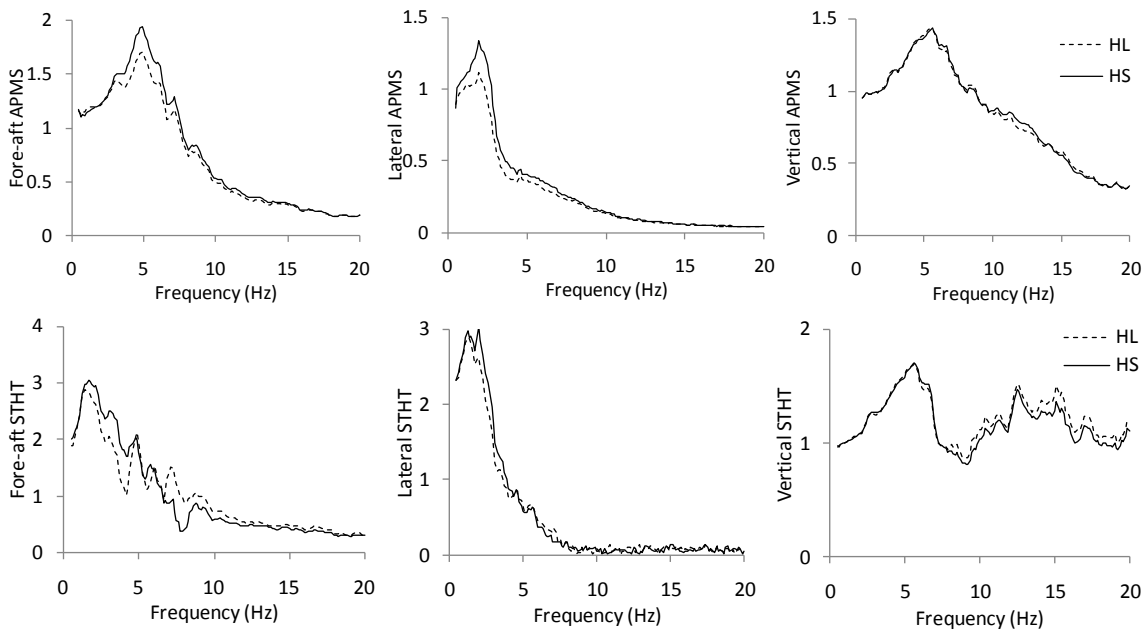


Fig. 5.7. Comparisons of mean apparent mass (APMS) and seat-to-head-transmissibility (STHT) magnitude responses to three-axis fore-aft, lateral and vertical vibration of the occupants seated with hands in lap and on steering wheel and vertical back support; three-axis vibration ($a_x=a_y=a_z=0.23 \text{ m/s}^2$).

The mean APMS and STHT responses to three-axis vibration derived using H_v FRF estimator are further considered to illustrate the effect of the hands and back supports. The effects of hands support on the APMS and STHT responses of the occupants seated without and with a back support, and exposed to three-axis vibration are illustrated in Figs. 5.5 and 5.6, respectively. The fore-aft APMS response without and with back support postures show higher

magnitudes with the hands support in the 1-3 Hz and 2.5-7 Hz frequency ranges, respectively, enveloping the primary resonant frequencies in the fore-aft mode. Both the back and hands support also yield higher fore-aft STHT magnitudes in the 1-4 Hz frequency range, as seen in Fig. 5.6. The lateral APMS and STHT responses of the occupants seated with and without back support were also observed to be greater with the hands support in the vicinity of the primary resonance compared to those with hands in lap posture. Both the vertical APMS and STHT responses, however, revealed relatively smaller effects of the hands support, irrespective of the back support condition.

The effect of magnitude of excitations (0.23 and 0.4 m/s² rms acceleration along each axis of the three-axis) on the APMS and STHT responses of the occupants seated without and with back support were observed to be very small, on the APMS but the STHT responses exhibit notable effect.

5.6 DISCUSSIONS

The seated human body biodynamic responses to single axis vibration derived using H_l and H_v methods were found to be identical. The responses to simultaneous three-axis vibration, obtained from the H_l and H_v methods, however, differed considerably for all the test conditions considered. The observed differences could be directly related to the notable contributions of the cross-axis responses to single axis vibration. The H_l method, owing to its definition, would be applicable for analysis of biodynamic responses only if the response and the excitation were correlated. This method, however, tends to suppress the cross-axis response components under uncorrelated multi-axis excitations employed in the present as well as recent reported studies [110,130]. The H_v method, on the other hand, considers the power-spectrum of the response along an axis that also includes the contributions due to response components under uncorrelated

vibration applied along the other axis. The whole-body vibration environment of work vehicles may exhibit strong correlations between vibration along some of the axis, which is attributable to strong couplings between the vertical, fore-aft, roll and pitch modes, and the lateral and yaw modes of vehicle vibration [105]. The H_v method would thus be essential for the study biodynamic responses of the seated body under realistic multi-axis vehicular vibration.

5.6.1 Effect of three-axis vibration

Both, the H_l and H_v methods yield identical APMS and STHT responses to single axis vibration, which were also identical to those derived from the PSD method [117,118]. The APMS responses to three-axis vibration, derived using H_l method, were observed to be quite similar to those under single axis vibration, as it has been reported by Hinz et al. [52] and Mansfield and Maeda [51]. In a similar manner, the STHT responses to three-axis vibration, derived from the most commonly used H_l method, were also comparable to those obtained under single-axis vibration with a few exceptions (Fig. 5.2), as reported in [53,121]. These suggest negligible effects of three-axis vibration on the biodynamic responses of the seated body, even though substantial coupled motions of the body have been observed in the saggital plane under single-axis vibration along the fore-aft and vertical axis [53,87] and also evident in Fig.5.1. The lack of coupled effects of three-axis vibration could be attributed to two primary factors. Firstly, the APMS measured at the driving-point does not reflect the contributions due to observed coupled motions of the upper body. It has been shown that the contributions due to multi-axis upper body motions, widely observed under single-axis vibration, and the motions associated with vibration modes of low inertia organs, could be identified from vibration responses of individual body segments or the head [19,20,53].

Secondly, the widely used H_I method of analysis tends to suppress the contributions of cross-axis response components that directly relate to the coupled-axis body motions, which are known to be of substantial magnitude in the saggital plane (Fig.5.1). The multi-axis vibration applied in the current and reported laboratory studies [51-53] are uncorrelated, and thereby show negligible coupling effects of multi-axis vibration (Fig. 5.2). Mansfield and Maeda [51], however, showed that the peak AMPS magnitudes and the corresponding frequencies under three-axis vibration were slightly lower than those under single-axis vibration. Similar effects were also reported in the STHT responses to dual and three-axis vibration [53,121]. Such differences are attributable to two factors: (i) the effective magnitude of three-axis vibration was higher than those applied along the single-axis, which is known cause softening of the body [2,64]; and (ii) small degree of correlation among the fore-aft, lateral and vertical vibration caused by minor cross-talk between the servo-actuators employed in multi-axis vibration platforms.

The STHT and APMS responses to three-axis vibration derived using H_v method, however, differed considerably from those obtained from the H_I method (Figs. 5.2 and 5.3). The H_v method, which is based upon PSD of the response and excitation variables effectively accounts for the contributions of the cross-axis components and thus exhibits coupled effects of three-axis vibration in both the APMS and STHT responses. The responses to three-axis vibration derived using H_v method suggest coupled seated body motions. The observed differences in the responses obtained from the two methods can be directly related to the contributions of the cross-axis responses. For example, the cross-axis STHT responses (H_{xz} and H_{zx}) observed in the saggital ($x-z$) plane (Fig. 5.1), also reported by Hinz et al. [53], indicate notable fore-aft and vertical movements of the upper body under single axis vibration along

vertical and fore-aft axis. However, such cross-axis movements of the upper-body are not completely captured by the driving-point measure APMS compared to the STHT measure. This is evident from the relatively smaller magnitudes of cross-axis APMS components measured under single axis vibration compared to those in STHT responses.

The magnitudes of lateral cross-axis responses under fore-aft and vertical axis vibration, were observed to be nearly negligible (Fig. 5.1), suggesting smaller or negligible coupling between the lateral and fore-aft (H_{xy} and H_{yx}), and lateral and vertical motions of the seated body. The lateral STHT response to three-axis vibration, however, showed relatively higher magnitude ($p < 0.001$) in the vicinity of the primary resonance (near 1 Hz) compared to that under single axis lateral vibration. This may in part be attributed to the subjects tendency to stiffen the upper body under three-axis vibration. Comparable magnitudes of the lateral STHT responses to three-axis vibration derived using both the H_l and H_v FRF estimators further confirmed the lack of coupling in the lateral responses and that the higher magnitudes are most likely due to stiffening tendency of the subjects. Such increase in the lateral vibration transmitted to head was also reported under dual (xy)-axis vibration [121]. However, the lateral APMS responses to single and three-axis vibrations were observed to be comparable which can be attributed to negligible contribution of the smaller cross-axis body movements to the lateral biodynamic force developed at the driving-point.

The fore-aft and vertical APMS and STHT responses to three-axis vibration suggest greater coupled effects, which can be mostly attributed to greater upper body movements of the seated body. The responses (Figs. 5.3) comparable to those reported under the dual (xz) axis vibration. This further shows negligible contributions of lateral excitation to the seated body movements along fore-aft and vertical axis, as illustrated in Fig. 5.1.

5.6.2 Effects of supports

The effects of the back support on the vertical and fore-aft responses to three-axis vibration in general were observed to be greater compared to those reported under single-axis vibration reported [2,319,20,37]. The seated body supports serve as important restraints, which tend to alter the upper body movements and thus the biodynamic responses. The back supported posture resulted in considerably higher magnitudes of the mean fore-aft APMS responses under both single and three-axis vibration, although the magnitudes were generally higher under the single axis fore-aft vibration, as seen in Fig. 5.3. The frequency corresponding to the dominant peak also increased to nearly 5 Hz for the back support, compared to only 0.75 Hz for the back supported posture. The unsupported upper body undergoes considerable pitch motion about the pelvis at very low frequency, while the back support contributes to higher stiffness in the pitch mode and greater coupling with the vertical motion of the upper body. This is mainly attributed to greater interactions of the upper body with the back support, and application of vibration directly to the upper-body through the back support, which is also evident from the higher magnitudes of the fore-aft APMS responses measured at the backrest (Fig. 5.4). The magnitudes of APMS measured at backrest under multi-axis vibration are considerably higher those under single axis fore-aft vibration, which is attributable to greater coupling between the vertical and fore-aft modes of vibration.

The lateral APMS response, however, revealed only slightly higher magnitudes with the back supported posture (B0) compared to the unsupported back posture (NB), which suggest that a vertical backrest offers only minimal restraints to the upper-body in the lateral direction. An inclined backrest however, would be expected to yield higher magnitudes of fore-aft and lateral forces at the backrest due to greater adhesion of the upper-body with the back support. The fore-

aft and lateral APMS and STHT responses with the back support were observed to be relatively higher under three-axis vibration compared to those obtained under single axis vibrations. Sitting with a back support tends to reduce the vertical vibration transmitted to the head at lower frequencies up to 2.5 Hz but greatly amplifies the vibration at frequencies above 7 Hz (Fig. 5.3). This could be attributed to cross-axis vertical movements of the restrained upper body due to the fore-aft vibration in the low frequencies. The higher magnitudes of vibration transmitted in frequencies above 8 Hz, can be attributed to additional vibration imposed by the backrest and the corresponding cross-axis components. The greater effect of back support ($p < 0.001$) was also evident at most of the frequencies in the APMS responses compared to those in the STHT.

Apart from the back support, the hands support could also serve as an important constraint that may enhance the upper-body and backrest interactions. The vertical STHT and APMS responses to three-axis vibration obtained for both the hands on lap and support revealed nearly identical magnitudes suggesting negligible effect of the hands support, similar to those reported under single (z) and dual (xz) axis vibration [77,131]. The hands support, however, resulted in higher magnitudes of lateral STHT and APMS responses, in the vicinity of the resonance, which can be attributed to two factors: stiffening of the upper body due to hands support, and additional vibration transmitted through the hands support. The fore-aft APMS response obtained without (NB) and with back support (B0) also show higher peak magnitudes with the hands support (Figs. 5.5 and 5.6). Such trends have also been reported under single (x) and dual (xy and xz) axis vibration [121,130]. The mean fore-aft STHT magnitudes in the 1.25-4.6 Hz frequency range, are also tends to be higher when seated with both the back and hands supports, (Fig. 5.7), while the effect of hands support is negligible with back unsupported posture (Fig. 5.6). This is most likely caused by greater adhesion of the upper-body with the back

support when hands are supported and additional vibration transmitted to the upper body through the back support.

5.7 CONCLUSIONS

The seated body biodynamic responses to simultaneous three-axis vibration derived using H_v frequency response function estimator revealed considerable contributions of the cross-axis responses which were observed under single axis vibration. Such contributions of the cross-axis responses were not evident in the responses derived from the most commonly used H_l estimator, which was attributed to uncorrelated nature of the three-axis excitations employed in such studies. It is thus suggested that H_v estimator be employed for characterization of biodynamic responses to uncorrelated multi-axis vibration, and under vehicular vibration that may comprise both uncorrelated and correlated multi-axis vibration. The responses to uncorrelated three-axis vibration derived using the H_v estimator further illustrate greater coupling in the sagittal plane and relatively smaller contributions due to lateral vibration. The results also revealed the backrest acts as additional source of vibration to the seated body and further suggest the coupled effects of back and hands supports.

Chapter 6

ENERGY ABSORPTION OF SEATED BODY EXPOSED TO SINGLE AND THREE-AXIS WHOLE BODY VIBRATION

Summary: The absorbed power characteristics of seated body exposed to whole-body vibration along individual and combined, fore-aft (x), lateral (y) and vertical (z) axis are investigated through measurements of body-seat interactions at the two driving-points formed by the body and the seat-pan, and upper body and the seat backrest. The experiments involved two levels of back support conditions (no back support and vertical backrest) and two levels of broad-band vibration with constant PSD in the 0.5-20 Hz frequency range applied along the individual x-, y- and z- axis (0.25 and 0.4 m/s² rms acceleration), and along the three-axis (0.23 and 0.4 m/s² rms acceleration along each axis). The biodynamic responses, measured at the seat-pan and the backrest are applied to characterize the total seated body's energy transfer under each individual axis of vibration. Furthermore, an alternative frequency response function method H_v is employed to capture the coupling in the seated body responses to uncorrelated multi-axis vibration. The total vibration absorbed power responses to simultaneous fore-aft, lateral and vertical vibration are subsequently derived as the summation of vibration absorbed power along the individual axis within each one-third frequency band. The mean responses measured at the seat-pan suggest strong effects of the back support, and the direction and magnitude of vibration. The results revealed most significant interactions of the upper body against the back support under fore-aft vibration. The total vibration power absorbed by the seated body is further estimated under multi-axis vibration environment of four different work vehicles. The results show trends that are quite different from those observed under broad band vibration.

6.1 INTRODUCTION

Occupational off-road vehicle drivers are exposed to comprehensive magnitudes of whole body vibration (*WBV*) which has been strongly associated with discomfort, an array of health disorders and reduced occupational functioning [18,22]. The biodynamic responses of the seated body exposed to *WBV* form an essential basis for an understanding of the mechanical-equivalent properties and thereby the body responses to vibration. Such responses have been widely studied in terms of driving-point measures: apparent mass (*APMS*) or mechanical impedance (*MI*) [2,64,84]. These studies have provided important insights into vibration modes and resonances of the seated body, and the effects of the body supports and intensity of vibration. The biodynamic responses to *WBV* have also contributed to the development of seated body models for seating

design and frequency-weightings for evaluations of the health risks associated with WBV exposure [6,42,114]. The biodynamic responses have also been characterized by an alternate driving-point measure, the vibration power absorbed (*VPA*) by the seated body exposed to *WBV*, which is considered meritorious compared to the *APMS* or *MI* [9,16]. The vibration power absorbed or the dissipated energy, attributed to relative motions of the visco-elastic tissues, muscles and skeletal systems, is believed to be better associated with potential physical damages due to *WBV* exposure [9,16]. Unlike the *APMS* or *MI*, the *VPA* response combines both the acceleration due to source vibration, considered to represent the vibration hazard, and the biodynamic response of the seated body. Furthermore, it permits consideration of exposure duration. The absorbed power may be derived from integration of power absorption density, related to product of stress due to vibration and the strain rate, over the tissue volume associated with the biodynamic response. This includes the mechanical stimuli leading to biological response and adaptation [26]. Further, *VPA* measures have been employed to characterize the energy absorption in human hand-arm system to study the impact of the vibration tools [13,132].

A few studies have reported absorbed power response characteristics of the seated body under single axis vertical, fore-aft and lateral vibration. These revealed that the *VPA* increased quadratically with the rms acceleration magnitude of vibration [11,12]. The advantage with the *VPA* measure compared to other driving-point measures is that the overall *VPA* can be obtained from scalar summation of the absorbed power: (i) within each frequency band; (ii) at each interface (e.g., backrest, footrest, hands support) and (iii) in each direction of the excitation [11,16]. Furthermore, *VPA* can also account for duration of vibration exposure in addition to magnitude, frequency and direction of vibration, which are related by the other driving-point measures [16].

The reported studies have related *VPA* to the driving-point measured such as *APMS* [116]. The seated body *VPA* has been linearly related with the body mass, consequently a few studies have normalised the absorbed power responses using the sitting body mass [13,104]. The seated body biodynamic studies have employed normalisation factors based on the seated body mass to minimise the scatter in the measured *APMS* or *MI* responses of the subjects, particularly at low frequencies, so as to facilitate the study of the effects of various contributory factors [e.g., 64,71,84]. However, such normalisations had smaller effect on the scatter in the *VPA* responses, suggesting that directly measured *VPA* data could be used to study the effect of the contributory factors [92]. The *VPA* responses have also shown substantial effects of body support conditions (e.g., backrest, footrest, hands support), similar to those observed in the *APMS* responses [11,12,116]. The upper body interactions with the back support alone contribute to about 60% of the total *VPA* of the seated body when exposed to fore-aft vibration [92]. Owing to the frequency-dependency of the absorbed power responses, a few studies have derived frequency-weightings [6,11]. Different frequency-weightings were suggested for the back supported posture particularly along the fore-aft axis [92]. These weightings were however, based only on the single axis vibration.

The reported studies have invariably considered either harmonic or white-noise random vibration in the frequency ranges up to 20 Hz. Considering that the *VPA* is strongly dependent upon the magnitude and frequency contents of vehicle vibration, the reported *VPA* data cannot be directly applied for assessing the potential hazards of a particular vehicle vibration. The *VPA* of the seated body exposed to a particular vehicle vibration, however, could be estimated from the reported *VPA* characteristics and the known vehicle vibration spectra, as reported for the power hand tools [52].

Although, the ride vibration environments of heavy road and off-road vehicles exhibit substantial vibration along the three translational axis [e.g., 51], the studies on VPA of the seated body have been invariably limited to single axis vibration exposure. A few recent studies have investigated driving-point (*APMS*) and transmissibility measures (*STHT*) of the seated body under more representative dual- and three-axis vibration [53,121,130,133,108,109,105]. Some of these studies revealed negligible coupling effects of multi-axis vibration. The *APMS* responses to multi-axis vibration were thus quite similar to those under single axis vibration, even though the subjects experienced substantial coupled motions [130,133,108]. The lack of the coupling effects in the data was attributed to the use of H_1 frequency response function estimator based on cross-spectral density (CSD) of the response and excitation that suppressed the contribution of cross-axis responses under uncorrelated multi-axis vibration [118]. A recent study has suggested an alternative frequency response function (H_v) method to analyse seated body responses to uncorrelated multi-axis vibration and revealed notable coupling effects of multi-axis vibration in the driving-point and transmissibility responses, particularly in the sagittal plane [109,105]. The total VPA of the body exposed to multi-axis vibration is thus expected to differ from the reported characteristics under single-axis vibration, which have not been investigated thus far.

This study investigated the absorbed power responses of the seated occupants exposed to single and combined fore-aft, lateral and vertical axis vibration, on the basis of measured APMS responses. The effects of three-axis vibration along with those of the back support and vibration magnitude on the total VPA are presented. Consequently, the total VPA is derived that may be applied in assessing relative exposure risks of different vehicles. The laboratory measured characteristics are applied to derive total VPA of the seated body exposed to WBV due to total four different road and off-road vehicles.

6.2 METHOD

An experiment was designed to evaluate the power absorbed by the seated body exposed to single and multi-axis vibration. The forces along the three translational axes at the two body-seat interfaces (buttocks-seat pan and the upper body-backrest) were measured when exposed to single as well as three-axis whole-body vibration. The experimental setup used in this study is identical to that used for characterization of apparent mass reported in [121, 130]. Briefly, a rigid seat and a steering column were installed on a 6-DOF whole-body vibration simulator (IMV Corp.) at the National Institute of Occupational Safety and Health, Japan. Two force plates were used to acquire the forces developed along the x -, y - and z - axis, at the two driving-points formed at the seat pan and the backrest: (i) a tri-axial force plate (Kistler 9281C), which also served as the seat pan at a height of 450 mm from the simulator platform; and (ii) a 450 mm high force plate, fabricated using three 3-axis force sensors (Kistler 9317B), served as the backrest. The platform vibration was measured using a three-axis accelerometer (Brüel and Kjaer 4506A) aligned with the translational axes of vibration. The setup with the seat and the measurement systems is schematically illustrated in Fig. 6.1.

The experiments were conducted with a total of 9 healthy adult male subjects with average age of 30.4 years (22-55 yrs), body mass of 63.4 kg (57-69 kg) and height of 173.4 cm (162-179 cm). Each subject was asked to sit comfortably with average thigh contact on the seatpan, lower legs oriented vertically and feet supported on the vibrating platform. The height of the feet support was adjusted vertically to provide the desired sitting posture. Each subject was advised to sit upright without a back support (*NB*) and with lower back against the vertical backrest (*B0*), while the hands rested on the thighs. The measurements were performed under two levels of broad-band vibration with constant power-spectral-density in the 0.5-20 Hz

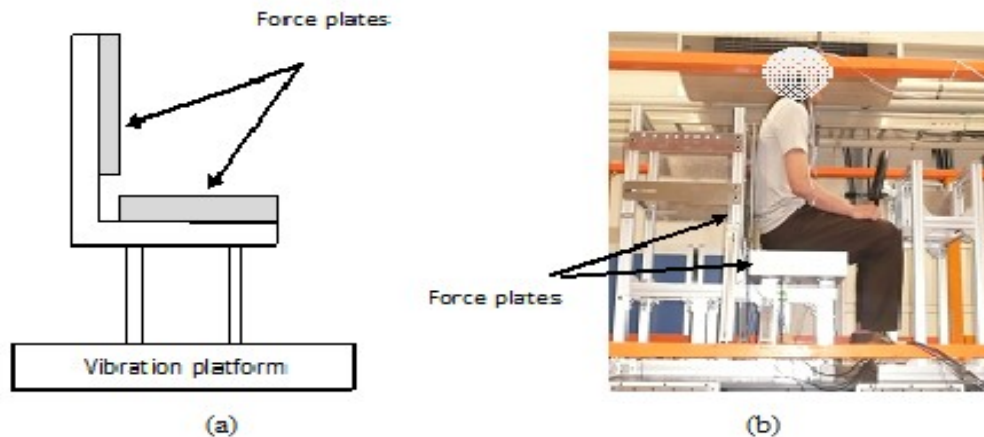


Figure 6.1: (a) Schematic of the test seat with force plate serving as the seatpan and backrest; (b) Experimental setup showing the subject seated with back supported posture and the locations of force-plates.

frequency range applied along the individual x -, y - and z - axis (0.25 and 0.4 m/s^2 rms acceleration), and along the three-axis (0.23 and 0.4 m/s^2 rms acceleration along each axis). The lower magnitude three-axis vibration was synthesized to achieve overall rms acceleration of 0.4 m/s^2 (0.23 m/s^2 along each axis), which is comparable to one of the chosen single axis vibration magnitude. This facilitated the study of the effect of single and three-axis vibration under identical effective magnitudes. Each vibration exposure lasted for 60 seconds and the order of the experiments was randomized, while each measurement was repeated twice. Prior to the test, each subject was given written information about the experiment and was requested to sign a consent form previously approved by a Human Research Ethics Committee of Concordia University in Montreal.

6.3 DATA ANALYSIS

The seat pan and backrest forces, and platform acceleration data were acquired in the Pulse LabShop™. The analyses were performed using a bandwidth of 100 Hz with a resolution

of 0.125 Hz. The *VPA* characteristics of the seated body were evaluated using two approaches: a direct method and an indirect method. In the direct method, the *VPA* was obtained from the cross spectrum of the measured force and the velocity [11,104,92]: for exposure to single-axis vibration, the *VPA* is given by:

$$P(f) = Re[S_{vF}(f)] \quad (6.1)$$

where *Re* indicates the real part of the absorbed power spectrum and *P* is the *VPA*. Alternatively, the derived the absorbed power response can be obtained indirectly from the apparent mass response [12], such that:

$$P(f) = \frac{Im[M^*(f)]S_a(f)}{2\pi f} \quad (6.2)$$

where M^* is the complex conjugate of the apparent mass response of the seated body, ‘*Im*’ designates the imaginary part and S_a is the power spectrum of the acceleration excitation.

The total absorbed power response of the human body can be computed from summation of the absorbed power over the frequency range of interest. The total *VPA* is generally evaluated upon summation of the power over third-octave frequency bands, such that:

$$\bar{P} = \sum_{i=1}^N P(f_i) \quad (6.3)$$

where \bar{P} denotes the average absorbed power response measured under single-axis vibration, *P* denoted the power in the *i* th third-octave frequency band, and *N* is the number of frequency bands considered. The total absorbed power may be derived upon summation of absorbed power responses corresponding to each third-octave frequency band.

The average absorbed power under individual axis of vibration is strongly dependent upon the magnitude of vibration, and may be expressed as:

$$\bar{P} = \alpha a^\beta \quad (6.4)$$

Where β is the exponent of the overall rms acceleration (a) of the excitation and α is the proportionality constant. It has been shown that the exponent is nearly 2 and 1.8-2.8 under vertical and horizontal vibration, respectively [12,116].

6.3.1 Analyses of absorbed power responses to three-axis vibration

In this study, the indirect approach based on the *APMS* responses, Eq (6.2), is applied to derive the *VPA* responses to single as well as multi-axis vibration. The *APMS* responses to single-axis vibration also exhibit considerable cross-axis response [118,119]. The cross-axis responses under single axis vibration do not contribute to the *VPA*, since the cross-axis force component and the applied excitation are in the orthogonal directions. Under three-axis vibration, however, the total apparent mass measured along a given axis incorporates the cross-axis components [133].

$$\bar{F}_i(f) = \sum_j F_{ij}(f) \quad (6.5)$$

Where \bar{F}_i is the force measured along axis i ($i=x, y, z$) and F_{ij} describes the direct ($i=j$) and cross-axis ($i \neq j$) force response components along axis i under vibration applied along j ($j= x, y, z$). Under three-axis vibration, the *VPA* measured along each vibration axis is thus expected to differ from that measured under the individual axis vibration. Owing to the uncorrelated nature of the three-axis vibration employed in the study, the *APMS* responses of the body exposed to three-axis vibration were derived using the H_v frequency response function estimator [133]:

$$M_k(f) = \frac{S_{a_k q_k}(f)}{|S_{q_k a_k}(f)|} \sqrt{\frac{S_{q_k}(f)}{S_{a_k}(f)}} \quad (k = x, y, z) \quad (6.6)$$

In the above equation, M_k defines the *APMS* response along axis k ($k = x, y, z$), $S_{a_k q_k}(f)$ is the cross spectrum of force q_k and excitation a_k and $S_{q_k}(f)$ is the auto-spectra of the total force response measured along k under multi-axis vibration. The M_k estimator yields the real and imaginary components of the response. The *APMS* responses of seated body were derived from the forces measured at both the seat pan and the backrest (when used). The measured *APMS* responses were inertia corrected to account for the masses of the force plates used in the seat pan and the backrest using the method described in [64]. In the absence of the backrest, the force measured at the seat pan alone was used to compute the *APMS*. In case of the back support, the total *APMS* was derived upon summation of these computed from the forces at the seat pan and the backrest, such that:

$$M_i(f) = M_{pi}(f) + M_{bi}(f); \quad i = x, y, z \quad (6.7)$$

Where M_{pi} and M_{bi} are the complex *APMS* responses measured at the seat pan and the backrest, respectively, along axis i .

The average power absorbed along each axis is subsequently evaluated from:

$$P_i(f) = \frac{Im[M_i^*(f)]S_a(f)}{2\pi f} \quad (6.8)$$

The total *VPA* under exposure to three-axis vibration can be obtained as the scalar summation of the powers along each individual axis:

$$\bar{P}(f) = \sum_{i=x,y,z} P_i(f) \quad (6.9)$$

Figure 6.2, illustrates procedure involved in computing the *VPA* response of the seated body exposed to three-axis whole-body vibration, using the biodynamic forces measured at the seat-body interfaces and the acceleration excitation. The *VPA* of the body is subsequently expressed in the third-octave frequency bands, and the total power absorbed is computed using Eq (6.3).

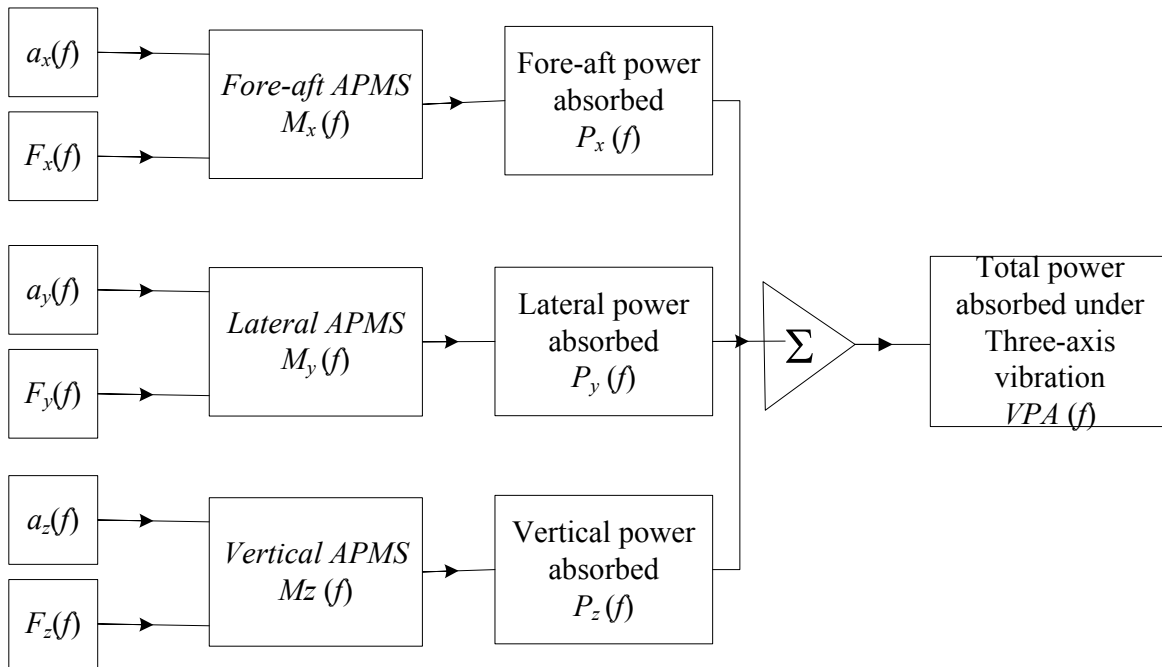


Figure 6.2: Computation of power absorbed by the seated body under three-axis vibration.

6.3.2 Estimation of power absorbed under vehicular vibration

The *VPA* and total average power derived from the mean *APMS* responses, can be considered valid under the idealised broad-band vibration employed for characterisation of the *APMS*. This cannot be directly applied to assess the relative *WBV* exposure risk in typical vehicles since the *VPA* is strongly dependent upon the intensity of vibration, as seen in Eq. (6.4), and nature of vibration (intensity and spectral characteristics) of vehicles differ from the idealised vibration spectrum. The *VPA* of operators of different vehicles, however, could be

estimated from the known vibration spectrum and the seated body *APMS*, as seen in Eqs. (6.2) and (6.8). This could provide the relative WBV exposure risks of different vehicles. Considering that *APMS* of the seated body varies with the body mass, back support condition and magnitude of vibration excitation [2,64,71,84], the estimated *VPA* would be limited to the conditions used to define mean *APMS*. It has been shown that variations in vibration magnitude cause only slight changes in the frequency corresponding to primary *APMS* peak, while the effect on *APMS* magnitude is very small [2,64,71,84].

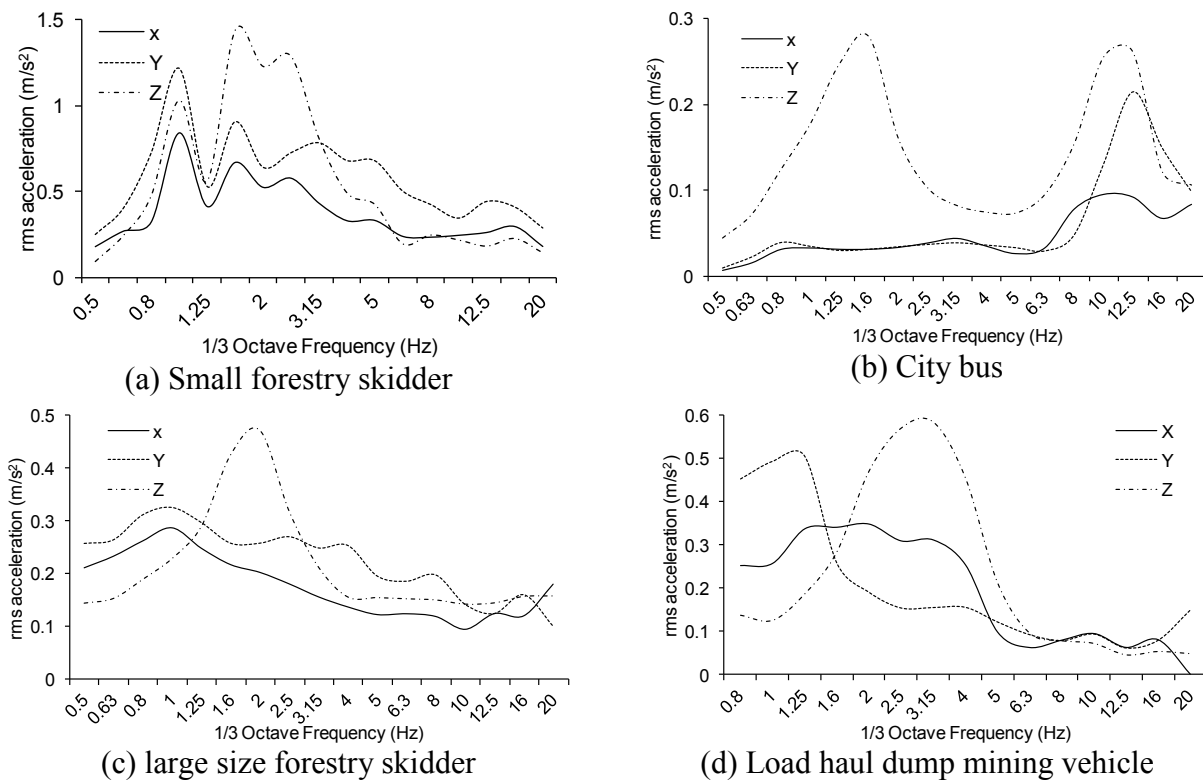


Figure 6.3: The rms acceleration spectra of selected vehicles [120,128,129,134].

The mean *APMS* response and the *VPA*, obtained in this study, would be considered valid for the mean body mass of 63.4 kg and chosen back support condition. The *VPA* characteristics of the seated body exposed to three-axis vibration spectra of four different vehicles are estimated on the basis of reported vibration spectra. These include the reported vibration spectra of a small size

forestry skidder [129], a load haul dump (mining) vehicle [128], a large size forestry skidder [134] and a city bus [120]. The rms acceleration spectra of the vibration measured at the seat of these vehicles along the x -, y - and z - axis are presented in Fig. 3. The overall rms accelerations of the reported spectra were obtained as 2.87, 0.95, 1.58 and 1.75 m/s^2 , respectively, for the small skidder, city bus, large forestry skidder and load haul (mining) vehicle.

6.4 RESULTS

The absorbed power responses of the seated body to single and three-axis whole body vibration were evaluated for the 9 subjects, at each of the third-octave band centre frequency in the 0.5-20 Hz frequency range. The results revealed considerable scatter in the *VPA*, particularly in the vicinity of the primary resonance frequency. The peak coefficients of variations of the *VPA* for the back supported (*B0*) and unsupported (*NB*) conditions, were identical to those reported under single axis vibration [116,92]. The *VPA* responses were subsequently considered to study the effect of three-axis vibration, the support conditions and the excitation magnitude. Figures 6.4 and 6.5 illustrate the mean *VPA* responses of the subjects seated without and with the back support, respectively, and exposed to single axis fore-aft, lateral and vertical vibration, of magnitudes 0.25 and 0.40 m/s^2 . The results, presented in the third-octave frequency bands, clearly show significantly higher *VPA* with the increase in vibration magnitude, in the entire frequency range. Figure 6.6 further compares the mean *VPA* responses of the subjects seated with and without the back support and exposed to single axis fore-aft, lateral and vertical vibration of magnitude 0.40 m/s^2 . The results clearly show substantial effect of the back support on the fore-aft *VPA*, while the effect of back support on the lateral and vertical *VPA* is considerably small. The *VPA* responses exhibit peaks in the 1, 1.6 and 3.2 Hz bands under fore-aft and lateral vibration and in the 5-8 Hz bands under vertical vibration, when seated without a

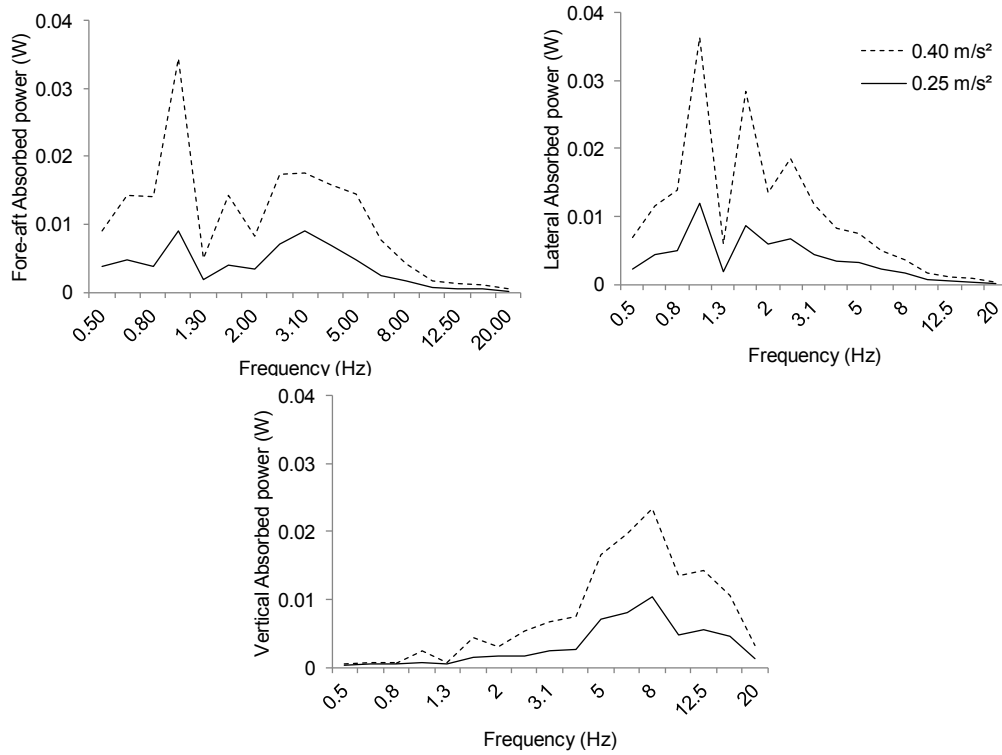


Figure 6.4: Comparisons of the mean absorbed power responses of 9 subjects seated without the back support (*NB*) and exposed to single axis fore-aft, lateral and vertical vibration of rms acceleration magnitudes 0.25 and 0.40 m/s^2 .

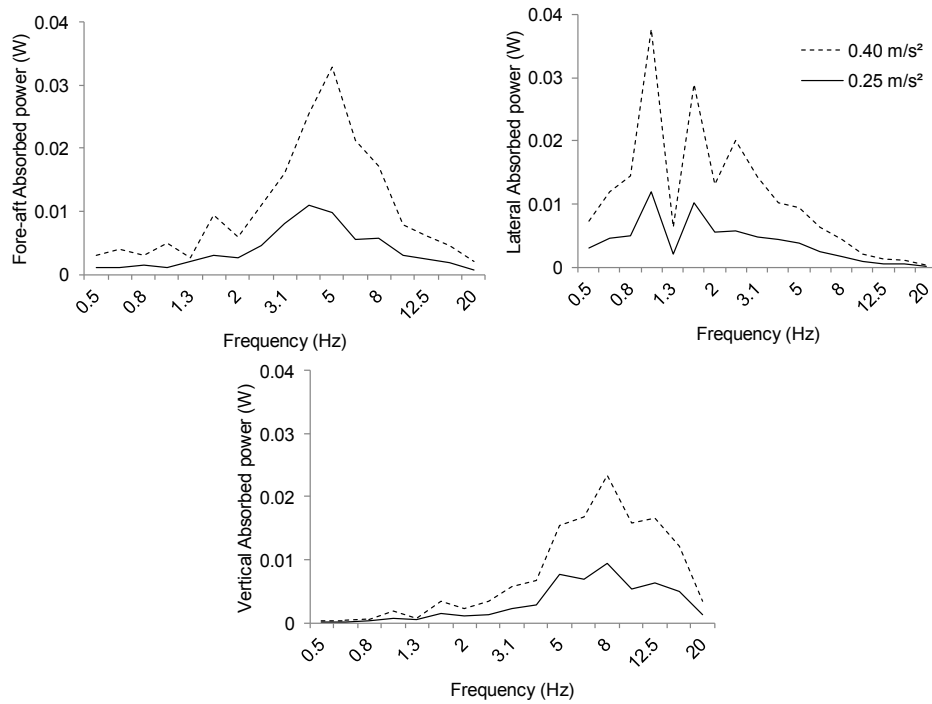


Figure 6.5: Comparisons of the mean absorbed power responses of occupants seated with back support (*B0*) and exposed to single axis fore-aft, lateral and vertical vibration of rms acceleration magnitudes 0.25 and 0.40 m/s^2 .

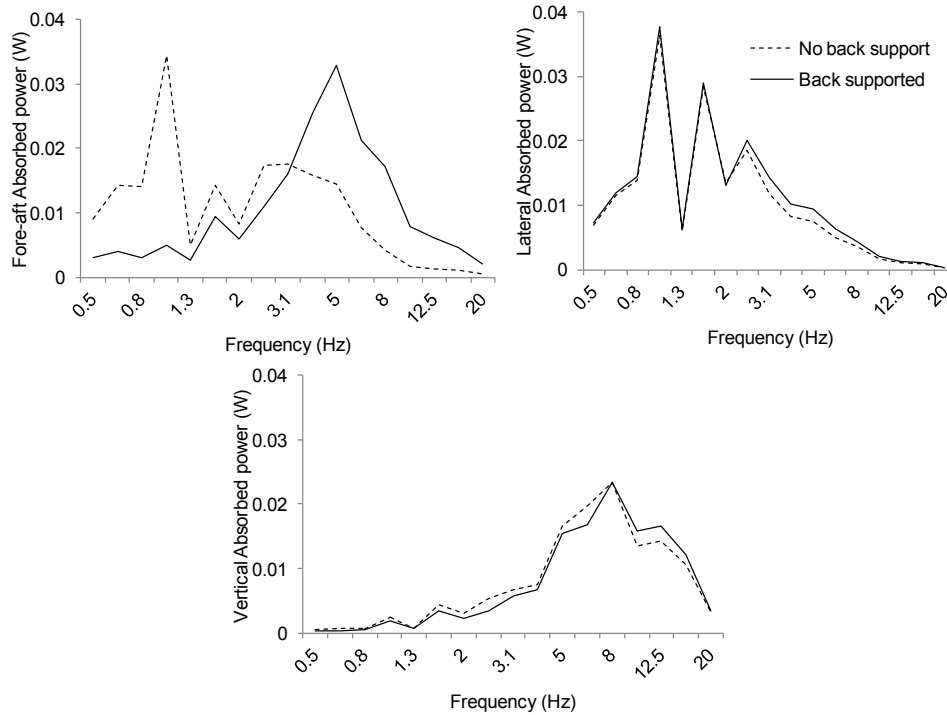


Figure 6.6: Comparisons of the mean absorbed power responses of occupants seated with and without back support and exposed to single axis fore-aft, lateral and vertical vibration of rms acceleration magnitude 0.40 m/s^2 .

back support. The *VPA* peaks under fore-aft vibration shift to the 6 Hz band, when the back support is used. The results further show that the peak *VPA* under vertical vibration is considerably lower than those under horizontal vibration, irrespective of the back support and excitation condition.

The mean *VPA* responses of the seated body along the fore-aft, lateral and vertical axis, and the total *VPA* responses, when exposed to vibration along the three-axis, are presented in Figure 6.7. The results are presented for 0.23 m/s^2 rms acceleration excitation along each axis (effective magnitude = 0.4 m/s^2). The results clearly show that the total *VPA* under three-axis is substantially higher compared to those obtained along the individual axis. This is partly attributable to higher effective magnitude of the three-axis vibration (0.4 m/s^2), compared to that along the individual axis (0.23 m/s^2).

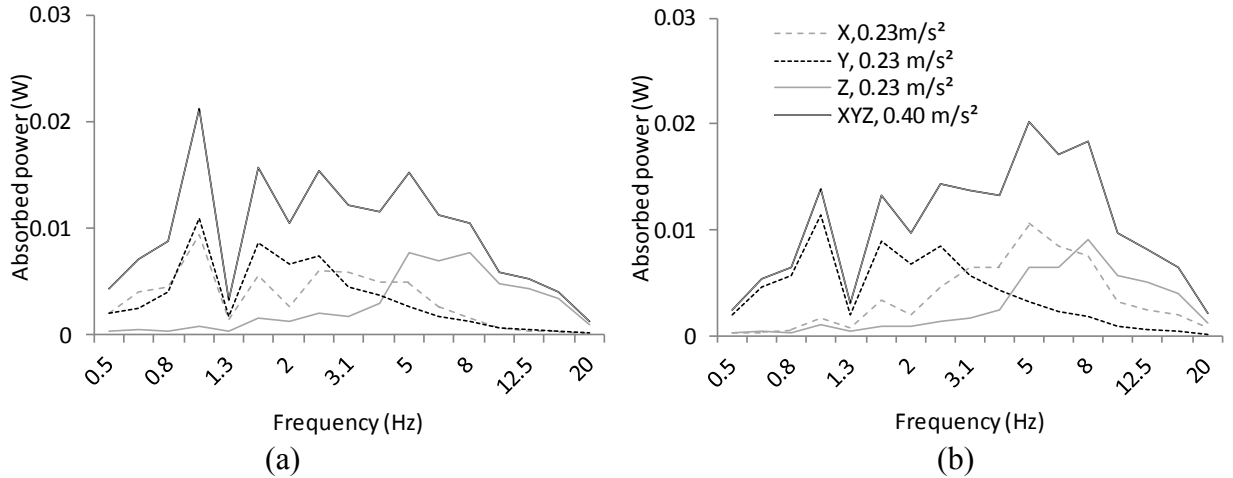


Figure 6.7: The mean absorbed power responses of the subjects along the fore-aft (x), lateral (y) and vertical (z) axis, and the total absorbed power when exposed to three-axis whole-body vibration (a) No back support- NB ; (b) Vertical back support- $B0$.

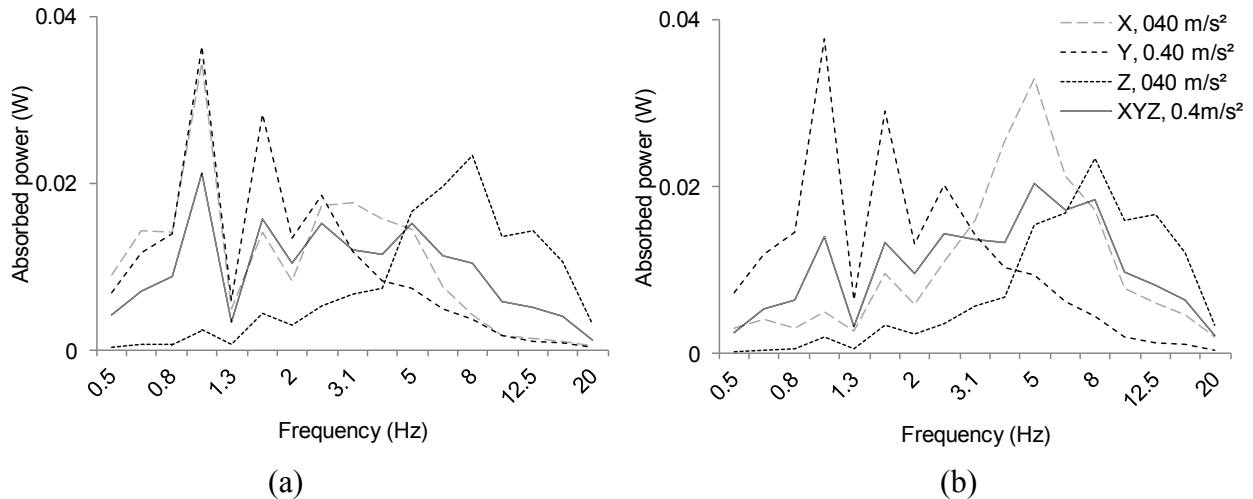


Figure 6.8: Comparisons of the absorbed power responses of the seated occupants exposed to single- and three-axis whole-body vibration of identical effective magnitude of 0.4 m/s^2 : (a) No back support- NB ; and (b) Vertical back support- $B0$.

The mean VPA responses along the individual axis and the total VPA of the seated body with and without back supported posture are further compared under single and multi-axis vibration of identical effective magnitude of 0.4 m/s^2 , in Fig. 6.8. The results show that the VPA peaks under single axis vibration are considerably higher than those under three-axis vibration of identical effective magnitude, irrespective of the back support condition. The mean total power \overline{P} , obtained using Eq. (6.3) over 0.5 to 20 Hz range, however, are comparable for the single and

three-axis vibration of overall effective rms acceleration of 0.4 m/s^2 , as seen in Table 6.1. The table summarises the mean total power absorbed by the seated body with and without back support and exposed to different magnitudes of single and three-axis vibration. The mean total power under three-axis vibration is 0.16 W compared to 0.18 W and 0.13 W under individual axis horizontal (x , y) and vertical vibration, respectively, of 0.4 m/s^2 magnitude. Figure 6.9 illustrates the total *VPA* of the seated occupants with and without the back support and exposed to three-axis vibration of effective magnitudes 0.4 and 0.7 m/s^2 .

Table 6.1: The total average power absorption of the seated occupant exposed to single and combined fore-aft, lateral and vertical-axis whole-body vibration of different magnitudes.

Posture	Vibration magnitude (m/s^2)			Overall rms Vibration magnitude (m/s^2)	Total absorbed power (W)
	x	y	z		
NB	0.25	-	-	0.25	0.06
	-	0.25	-	0.25	0.06
	-	-	0.25	0.25	0.05
	0.40	-	-	0.40	0.18
	-	0.40	-	0.40	0.18
	-	-	0.40	0.40	0.13
	0.23	0.23	0.23	0.40	0.16
	0.40	0.40	0.40	0.70	0.54
B0	0.25	-	-	0.25	0.06
	-	0.25	-	0.25	0.07
	-	-	0.25	0.25	0.05
	0.40	-	-	0.40	0.18
	-	0.40	-	0.40	0.19
	-	-	0.40	0.40	0.13
	0.23	0.23	0.23	0.40	0.18
	0.40	0.40	0.40	0.70	0.57

Table 6.2: The total *VPA* of the seated body exposed to combined fore-aft, lateral and vertical axis vibration along with the % of *VPA* along each axis of excitation.

Posture	Overall rms Vibration magnitude (m/s^2)	Total <i>VPA</i> (W)	Percent of Total <i>VPA</i> (%)		
			x	y	z
NB	0.40	0.16	34.6	36.4	29.0
	0.70	0.54	32.7	37.9	29.4
B0	0.40	0.18	34.5	38.7	26.8
	0.70	0.57	36.1	36.8	27.0

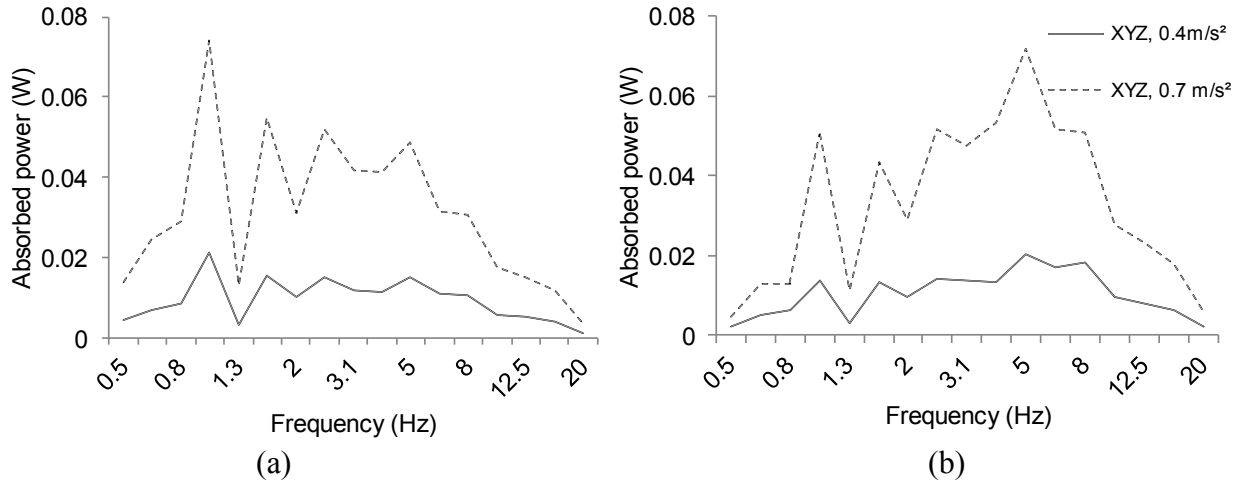


Figure 6.9: Comparisons of the total absorbed power responses of the seated occupant exposed to three-axis whole-body vibration of rms acceleration of 0.4 and 0.7 m/s^2 : (a) No back support-NB; (b) Vertical back support-B0.

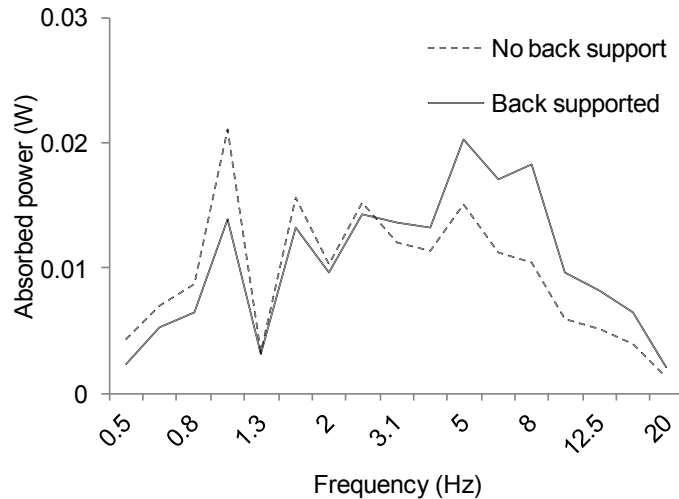


Figure 6.10: Comparison of the total *VPA* responses of occupants seated without and with back support and exposed to three-axis vibration of magnitude 0.4 m/s^2 .

The total average power under combined three-axis vibration of two different effective magnitudes are summarised in Table 6.2. The table also presents the mean power along each axis as percent of the total mean power. The results suggest relatively greater absorbed power absorbed along the horizontal axis compared to the vertical axis, irrespective of the back support condition, even though identical magnitudes of vibration were applied along each axis. The total *VPA* is strongly influenced by the back support condition, as seen in Fig. 6.10. Sitting without a back support yields higher peak *VPA* in the 1 and 1.8 Hz bands attributed to fore-aft and lateral

modes of the seated body resonances. The presence of a back support causes higher *VPA* peaks in the 5 Hz band, this corresponds to vertical and fore-aft resonances of the seated body. The body seated with a back support tends to absorb greater vibration power at frequencies above 3 Hz compared to the back unsupported condition. An opposite trend, however, is evident at frequencies below 3 Hz.

The mean total power values under different magnitudes of single and three-axis vibration in the 0.5-20 Hz frequency range revealed nearly quadratic relation with the overall rms acceleration of excitation the exponent β value ranged from 1.9 to 2.2 under single axis of vibration. Under three axis vibration, the exponent values were obtained as 2.14 and 2.19 for the *NB* and *B0* back conditions, respectively as illustrated in Table 6.3.

Table 6.3: Constant α and exponent β values derived for the average total power relationship between average total power of the body seated with and without a back support and the rms acceleration of the single and combined fore-aft, lateral and vertical axis vibration: NB-No back support; B0: Vertical back support.

<i>Back support</i>	<i>NB</i>		<i>B0</i>	
	α	β	α	β
<i>Axis of vibration</i>				
<i>x</i>	1.4	2.2	1.3	2.2
<i>y</i>	1.3	2.2	1.4	2.2
<i>z</i>	0.8	1.9	0.8	1.9
<i>xyz</i>	1.2	2.2	1.3	2.1

6.5 RELATIVE *VPA* CHARACTERISTICS UNDER VEHICULAR VIBRATION

The relative characteristics of the seated body exposed to multi-axis vibration of the selected vehicles are estimated using the mean *APMS* responses corresponding to *B0* sitting condition. Figure 6.11 illustrates the *VPA* responses for four selected vehicle vibration spectra. The results suggest higher peak *VPA* for the load haul dump and lowest for the city bus. This trend is identical to that observed in the vibration spectra of the vehicles in Fig. 6.3. The results

in Fig. 6.11 reveal trends that are widely different from the *VPA* responses to multi-axis broad band vibration (Fig. 6.9). All the vehicles, with the exception of the city bus, exhibit highest peak power along the lateral axis near 1 Hz band. This can be attributed to two factors: (i) the forestry skidders and the mining vehicles show greater lateral vibration in the 1 and 1.25 Hz bands (Fig. 6.3); and (ii) the *y*-axis *APMS* magnitude dominates in these frequency bands, which are close to the primary resonance frequency of the seated body. The fore-aft *APMS* magnitude peak, on the other hand, occurs around 4-4.5 Hz, where the vibration magnitudes are very small as seen in Fig. 6.3. The resulting *VPA* along the fore-aft axis is thus considerably small compared to the lateral axis in the skidder and the load-haul dump mining vehicles.

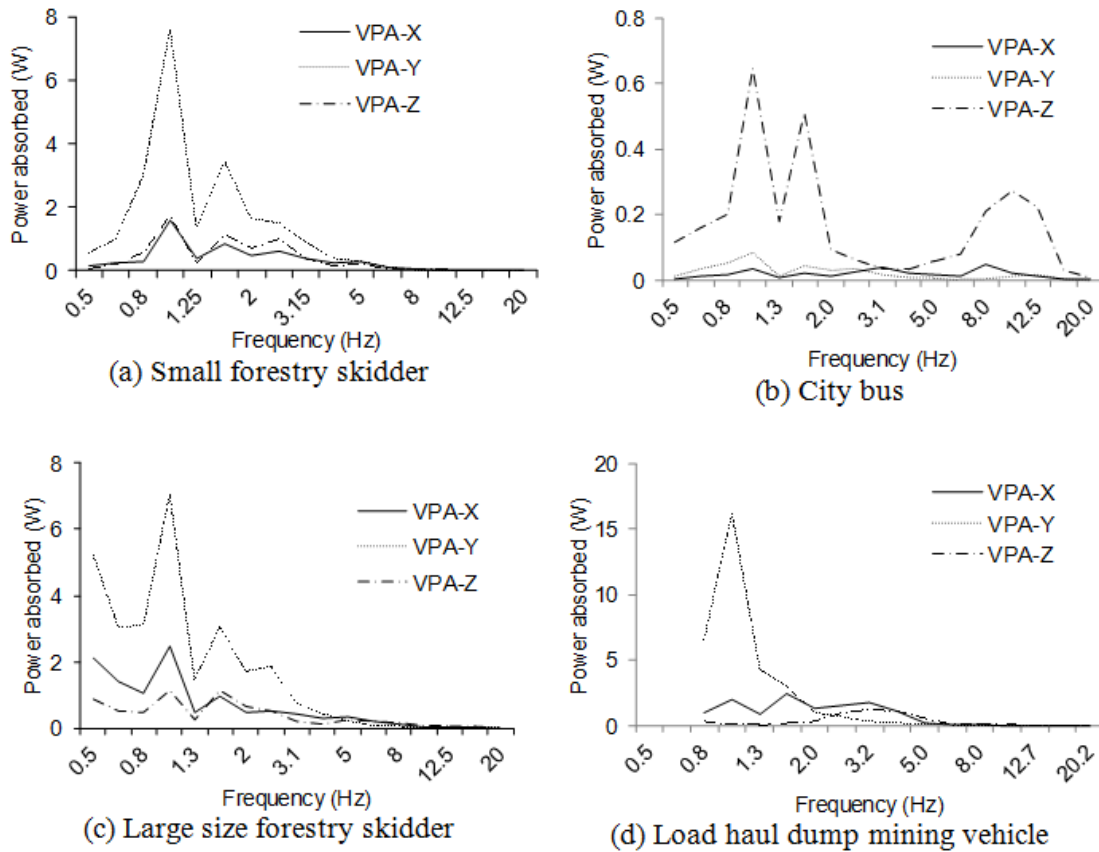


Figure 6.11: Estimated *VPA* values along fore-aft, lateral and vertical axis in the vehicles based on the measured vibration at the seat location.

All the off-road vehicles spectra also exhibit highest vertical acceleration peaks that occur in 1.25 to 3.15 Hz, around 2 Hz and around 3.15 Hz bands, respectively, for the small size skidder, large size skidder and the load-haul-dump mining vehicles. The *VPA* along the vertical axis, however, is considerably lower than those along the *y*-axis. This is attributed to the fact that the frequencies corresponding to peak accelerations are considerably lower than the primary vertical mode resonance of the seated body, as observed from the *APMS* response [84]. The city bus, on the other hand, exhibits peak *VPA* along the vertical axis, while the peak power (≈ 0.6 W) is substantially lower than those observed for the other vehicles. This is directly related to considerably higher vertical acceleration peaks in the 1.6 and 12.5 Hz bands, attributed to resonance frequencies of the sprung and unsprung masses of the vehicle, as seen in Fig. 6.3 (b).

The average total absorbed power are further derived and shown in Fig. 6.12 as function of the overall effective rms acceleration due to three-axis vibration of the selected vehicles. The results suggest that the total average absorbed power is directly related to overall rms acceleration due to vehicle vibration, and follows nearly quadratic relation with exponent $\beta = 2.03$ and constant $\alpha = 4.7$.

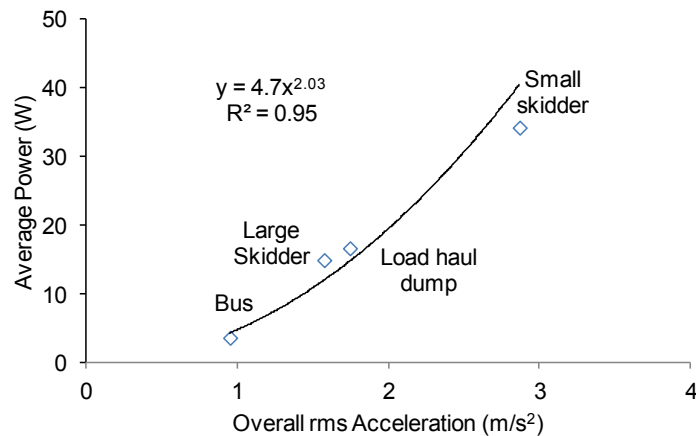


Figure 6.12: Relationship between the total average vibration power absorption and the overall rms acceleration due to vibration spectra of selected vehicles.

6.6 DISCUSSION

The *VPA* responses of the seated occupants exposed to single and three-axis vibration revealed very low values in the 0.5 Hz frequency band suggesting rigid system like behaviour of the seated human body, which is consistent with the reported studies [11,12,92,104,116]. The total *VPA* values of the seated occupant exposed to single axis fore-aft, lateral and vertical vibration, increased with the rms acceleration magnitudes of vibration (Table 6.3), in a nearly quadratic manner which is again consistent with the reported studies [11,12,92,104,116].

The higher *VPA* values of the occupant seated without back support and exposed to fore-aft or lateral vibration were observed at frequencies below 2 Hz, while that under vertical vibration was observed at frequencies above 5 Hz (Fig. 6.4). However, higher *VPA* values were observed in the frequencies above 4 Hz under fore-aft vibration when the back support was used, while those under lateral and vertical vibration remained nearly the same. This suggest that the back support has most important effect on the *VPA* along the fore-aft axis, since the back support serves as an important constraint to the upper body motion along the fore-aft axis. The effect of the back support on the *VPA* responses of the seated occupants exposed to single axis fore-aft, lateral and vertical vibration (Fig. 6.6) are consistent with the reported studies [116,92]. The total *VPA* values along each axis, however, were not greatly affected by the addition of backrest (Tables 6.1 and 6.2) under both single and three-axis vibration. The total power absorbed by the seated body exposed to three-axis vibration is merely the summation of the power absorbed under individual axis of vibration. The power along individual axis, however, is similar to that obtained under single-axis of vibration. This is caused by relatively small coupling effect of multi-axis vibration, as reported in the APMS responses [109,105]. The total average power under simultaneous three-axis vibration of effective magnitude 0.4 m/s^2 revealed relatively

higher power absorption along x - and y -axis, compared to the vertical axis, even though identical magnitudes of broad band vibration were applied along each axis. The results revealed that the total average absorbed power along the x , y and z -axis are nearly 35, 36 and 29% respectively for the *NB* support. An increase in the effective magnitude of the three-axis vibration to 0.7 m/s^2 also revealed similar trends. Similar proportions of mean total power were also observed with the back support condition. The results suggest that the mean total power absorbed by the seated body is not greatly affected by the back support condition, even though the use of a back support tends to shift the peak fore-aft power to a considerably higher frequency of nearly 5 Hz. The total *VPA* was higher for the *NB* condition compared to the *B0* condition up to 3 Hz. An opposite trend, however, was evident at frequencies above 3 Hz (Fig. 6.10).

The *VPA* response and the mean total power of the seated occupants exposed increased considerably with the increase in the vibration magnitude in the entire frequency range under both single and three-axis vibration. The total average power increased nearly quadratically with the overall rms acceleration magnitude of vibration (Table 6.3), irrespective of the back support condition.

The *VPA* properties of seated body exposed to idealised broad-band vibration along a single axis have been reported in many studies. These cannot be directly used to assess the exposure risk and relative ride ranking of different work vehicles. The nature of vibration (intensity and frequency components) of vehicles are not represented by broad-band vibration and strongly depend on the size and design features of the vehicles, the tasks being performed and the terrain roughness. The vibration power absorption of the vehicle operators thus strongly relies on the type of vehicle and its ride vibration spectra. The *VPA* responses to typical vehicle vibration spectra show widely different trends compared to those obtained under broad-band

vibration (Fig. 6.11). The *VPA* responses of the selected vehicles are substantially higher along the *y*-axis compared to the other axis, except for the city bus. The higher power along the *y*-axis is attributable to relatively higher magnitudes of lateral vibration in the vicinity of the lateral mode resonance frequency of the seated body. The primary lateral mode resonance frequency of the seated body lies in the vicinity of 1 Hz [2]. The closeness of the lateral mode resonance of the seated body and the lateral vehicle vibration leads to very large *VPA* peaks along the lateral axis compared to the other axis. The city bus vibration, on the other hand, exhibits considerably higher magnitudes of vertical vibration around the 1.6 and 12.5 Hz bands related to vertical mode resonance frequencies of the sprung masses of the bus [120]. The magnitudes of lateral and fore-aft vibration encountered at the bus seat are relatively very small. The *VPA* due to bus vibration, therefore, exhibits considerably higher magnitudes along *z*-axis with peaks near 1, 1.6 and 12.5 Hz bands. The magnitudes of *VPA* along the *x*- and *y*-axis are substantially lower. Furthermore, the vertical *VPA* in the vicinity of the vertical mode resonance of the seated body ($\approx 5\text{Hz}$) is very small, since the vibration intensity near 5Hz is very low. The results show that total average power absorbed under reported vehicular vibration is directly related to vibration intensity, expressed in terms of effective rms acceleration. The average power varies with the effective acceleration in nearly quadratic manner, as observed under broad-band vibration excitation.

The results show that the absorbed power integrates both the nature of vehicle vibration and biodynamic response of the seated body. This is similar to the vibration exposure assessment derived upon the application of frequency weighting defined in ISO 2631-1 [6]. However, it has been shown that the W_d frequency-weighting defined for the fore-aft vibration exposure may not be valid when a back support is used [92].

The application of the *VPA* method however, necessitates a thorough characterisation of the *APMS* properties of the seated body. The *APMS* of the seated body is strongly dependent upon the body mass and the back support [2,64]. Furthermore, variations in the vibration magnitude yield slight shifts in the frequency corresponding to the magnitude peaks, while the effect on peak magnitude is very small [2,64]. The effect of vibration excitation magnitude on the *APMS* responses may thus be considered negligible compared to the body mass and the back support. The body mass effect is most substantial on the *APMS* magnitude along all the three axis of vibration, while the effect of a backrest is most important on the fore-aft *APMS*. The *VPA* and average power responses obtained in this study, however, was be considered valid for mean body mass of 63.4 kg, and sitting without a back support and with a vertical back support.

6.7 CONCLUSIONS

The results show higher *VPA* values under single axis *WBV* along horizontal axis compared to those along vertical axis. The total P_{ABS} by the seated body exposed to three-axis vibration is calculated as the summation of the power absorbed under individual axis of vibration. The total *VPA* of the seated body exposed to *WBV* along simultaneous three-axis is substantially higher compared to those obtained along the individual axis. These responses show higher *VPA* with the increase in vibration magnitude, in the entire frequency range and the total *VPA* values show nearly quadratic relationship to the rms magnitudes of the excitation. The *VPA* responses also show substantial effect of the back support integrating the effect observed along the fore-aft, lateral and vertical axis. The *VPA* integrates both the nature of vehicle vibration and biodynamic response of the seated body. The *VPA* responses with the back supported condition, can be further applied to derive a weighting similar to the existing ISO 2631-1: W_d , W_k for individual axis of vibration. Thus derived weighting can be applied to better estimate the vibration risk and safety.

Chapter 7

ENERGY ABSORPTION OF SEATED OCCUPANTS EXPOSED TO HORIZONTAL VIBRATION AND ROLE OF BACK SUPPORT

Summary: The absorbed power characteristics of seated human subjects exposed to fore-aft (x-axis) and lateral (y-axis) vibration are investigated through measurements of dynamic interactions at the two driving-points formed by the body and the seat pan, and upper body and the seat backrest. The experiments involved: (i) three different back support conditions (no back support, and upper body supported against a vertical and an inclined backrest); (ii) three different seat pan heights (425, 390 and 350 mm); and three different magnitudes (0.25, 0.5 and 1.0 m/s² rms acceleration) of band limited white-noise random excitations in the 0.5-10 Hz frequency range, applied independently along the x- and y- axes in an uncoupled manner. The body force responses, measured at the seat pan and the backrest along the direction of motion, are applied to characterize the total energy transfer reflected on the seat pan, and that of the upper body reflected on the backrest for the back supported conditions. The mean responses measured at the seat pan and the backrest suggest strong contributions due to the back support condition, and the direction and magnitude of horizontal vibration, while the influence of seat height was observed to be very small. In the absence of a back support, the seat pan responses dominated in the lower frequency bands centred around 0.63 and 1.25 Hz under both directions of motion, although an additional peak also occurred at relatively higher frequencies. The results revealed most significant interactions of the upper body against the back support under fore-aft vibration. The addition of back support caused the seat pan response to converge mostly to a single primary peak near a considerably higher frequency of 4 Hz under x- axis, with only little effect on the responses under y-axis motions. A relaxed posture with an inclined backrest, however, revealed a slight softening effect under fore-aft motion, when compared to support against the vertical backrest. The back support serves as an additional source of vibration to the seated occupant and an important constraint to limit the fore-aft movement of the upper body and thus relatively higher energy transfer under fore-aft vibration. The mean absorbed power data were further explored to examine the W_d frequency-weighting used for assessing exposure to horizontal vibration. The results show that the current weighting is suited for assessing the vibration exposure of human subjects seated only without a back support.

7.1 INTRODUCTION

Occupational off road vehicle drivers are exposed to considerable magnitudes of whole-body vibration (WBV), which is known to cause discomfort, annoyance, and several health and safety risks. Many studies have suggested strong association between the exposure to WBV and low back pain [18,22]. The vast majority of the studies on human responses to vibration have emphasized the exposure to vertical WBV, since heavy on-road and off-road vehicles are believed to transmit relatively higher magnitudes of vertical vibration than those along the other

axes. Such vehicles, however, also transmit substantial magnitudes of horizontal vibration (HV) along the fore-aft and side-to-side axes [31,135-138]. Table 7.1 lists examples of the frequency-weighted rms accelerations (a_{wx} , a_{wy} and a_{wz}) due to vibration transmitted along the fore-aft (x -), side-to-side or lateral (y -) and vertical (z -) axes of various industrial and heavy road vehicles, derived on the basis of W_d - and W_k - weighting filters defined in ISO 2631-1[6]. These data suggest that drivers of such vehicles are also exposed to considerable magnitudes of weighted HV, which may even approach or exceed the magnitudes of vertical vibration in some of the vehicles.

Table 7.1: Magnitudes of frequency weighted rms accelerations due to vibration measured along the x -, y - and z - axis on the seats of the heavy vehicles [31,135-138].

<i>Vehicle</i>	a_{wx} (m/s^2)	a_{wy} (m/s^2)	a_{wz} (m/s^2)
Tracked forestry vehicle	≈ 0.25	≈ 0.12	≈ 0.39
Cargo trucks (1-2 Tons)	0.36-0.70	0.39-0.75	0.65-1.29
Cargo trucks (> 10 Tons)	0.20-0.42	0.20-0.24	0.42-0.70
All terrain vehicles (cargo)	0.30-1.0	0.50-1.10	1.0-1.80
On-road passenger vehicle (rough surface)	0.17-0.23	0.38-0.54	0.59-0.62
Mini city bus	0.10-0.60	0.00-0.90	0.20-0.60
Fork lift (off-road)	0.10-0.90	0.10-2.50	0.50-1.60
Port Crane	0.80-1.30	≈ 0.10	≈ 0.10
Dump truck 2 Ton	0.29-1.31	0.23-1.72	0.30-1.64
Garbage 4 Ton	0.50-0.94	0.56-1.98	0.37-2.45

Despite the substantial magnitudes of HV, relatively fewer studies have investigated the seated body response to HV. Furthermore, the majority of the reported studies on HV have focused on the motion sickness (kinetosis) response under extremely low frequency vibration (≤ 1 Hz). The motion sickness caused by low frequency HV is known to impede an operator's ability to handle the vehicle and perform desired tasks, while the symptoms have been characterised as temporary minor annoyances in most of the cases [139]. Considerable efforts have been made to characterise seated human biodynamical response to vibration and

contributing factors, in terms of force-motion relationships, such as apparent mass (APMS) and driving-point mechanical impedance (DPMI) [64,84,85]. These studies have provided the resonance frequencies and guidance to the sensitivity of seated human body to WBV. The vast majority of the reported studies have concentrated on vertical vibration; only a few have investigated the biodynamic response to HV [2,3,85,87,107,117].

The acceleration due to source vibration measured at either the seat or the floor, on the other hand, is considered to represent the vibration hazard [6]. The vibration hazard takes effect through the biodynamic response of the human body [109]. The vibration power absorbed (P_{Abs}) by the exposed body is a measure that combines both the vibration hazard and the biodynamic response of the body. Physically, the absorbed power relates to dissipation of energy attributed to relative motions of the visco-elastic tissues, muscles and skeletal system, which under prolonged exposures could lead to physical damages in the musculoskeletal system [9,16]. Mathematically, the absorbed power can be computed from the integration of the power absorption density, which is equivalent of the product of vibration-induced stress and the strain rate, over the volume of tissues involved in the biodynamic response, which includes the essential mechanical stimuli that cause the biological responses and adaptation [109]. It is thus reasonable to hypothesize that the power absorption is associated with the vibration-induced discomfort and some health effects. However, their exact relationship has not been sufficiently studied.

The concept of energy absorbed by the seated human body exposed to seat-transmitted vibration, first evolved in the mid-60's as a measure for evaluating the safety and comfort of occupants of military vehicles [16]. The absorbed power responses of the seated human body exposed to vertical WBV, have been investigated under continuous sinusoidal and random vibration considering both supported and unsupported back postures [10-13,104,140]. The P_{Abs}

has been related to APMS and DPMI²⁶, and the reported P_{Abs} spectra generally exhibit peaks at frequencies that are comparable to those corresponding to APMS/DPMI magnitude peaks. The P_{Abs} response of the body increases nearly quadratically with the acceleration magnitude. The studies have also shown important influences of variations in the sitting posture and seat geometry factors (seat height, footrest position, hands position, backrest and seat pan angle) on the P_{Abs} response of human occupants exposed to vertical WBV [11,12]. Relatively larger magnitudes of absorbed power have been associated with mechanical shock stimuli compared to the continuous vibration, suggesting greater sensitivity of the human body response to shocks [10].

Unlike the vertical WBV, the P_{Abs} responses of seated subjects under HV have been reported only from one study. Lundstrom, et al. [13] reported the P_{Abs} characteristics of seated male and female subjects, exposed to x - and y - axis sinusoidal vibration at various discrete frequencies in the 1.13 to 80 Hz range. The experiments were performed with subjects seated without a back support with feet on a stationary support and exposed to different magnitudes of vibration (rms acceleration ranging from 0.25 to 1.4 m/s²). The measured data under x - and y - axes vibration revealed dominant energy dissipation at frequencies below 3 Hz, while considerably large inter-subject variability was observed at frequencies up to 10 Hz. The study also reported that the W_d - frequency weighting, defined in ISO 2631-1[6], underestimates the exposure risk in the 1.5-3 Hz frequency range, and overestimates the risk at frequencies above 5 Hz. The study also suggested need for differential guidelines assessing HV exposures risks for females and males.

The biodynamic responses of the seated body exposed to WBV are known to depend upon back support condition and posture in a highly complex manner. Moreover, the body-seat

system represents multiple driving-points formed by the lower body-seat pan, upper body-backrest, hands-steering wheel and feet-footrest interfaces. A single driving-point formed by the lower body and seat pan, however, has been mostly considered in the reported biodynamic studies, irrespective of the axis of WBV. Nawayseh and Griffin [21] and Rakheja et al.[96] performed measurements of biodynamic responses of the seated body at the seat pan and back support interfaces under vertical vibration using a vertical and an inclined backrest, respectively; which were reported in terms of forces at the backrest and cross-axes APMS. These studies considered negligible contributions due to driving-points formed by the feet and the hands. These studies revealed significant dynamic interactions of the upper body with the backrest; the magnitude of the biodynamic force measured at the inclined backrest along a direction normal to the back support was substantial even though the vibration was applied along the vertical axis.

The seated body is expected to exhibit greater interactions with the backrest under fore-aft HV, which have not been adequately quantified. The characterisation of biodynamic responses to HV thus necessitates consideration of at least two important driving-points formed by the lower body-pan and upper body-backrest interfaces. The biodynamic responses in terms of APMS/DPMI of the seated body to HV have been mostly measured at the body-seat pan interface with either no back support[2, 3, 85,101] or a vertical back support [2,3]. The forces developed at a vertical back support and the APMS under HV have been reported in a recent study by Nawayseh and Griffin [85]. Mandapuram et al.[3] reported the APMS responses for both vertical and an inclined backrest under fore-aft and side-to-side vibration. These studies revealed significant magnitudes of APMS response measured at the backrest, when compared to that measured at the seat pan.

The influence of back support condition on the dissipated energy under HV has not yet been reported. Moreover, a study of seated body interactions with the backrest, which also serves as a source of vibration excitation under HV, has not been attempted. In this study, the absorbed power characteristics of seated human subjects are investigated under fore-aft and side-to-side vibration at two driving-points formed by seated body-seat pan and the upper body-seat backrest interfaces. The experiments involved three different back support conditions, three different seat pan heights and three different magnitudes of band limited random excitations in the 0.5-10 Hz frequency range, applied independently along the x - and y - axes. The biodynamic force responses, measured at the seat pan and the backrest along the direction of motion, are applied to characterize the total body P_{Abs} reflected on the seat pan, and that of the upper body reflected on the backrest.

7.2 METHOD

A rigid seat with adjustable backrest and height was designed for the experiments. The seat consisted of a 500x400 mm flat seat pan and a 470 mm high backrest installed on a truss structure. The seat was installed on a HV simulator through two three-axis force plates (Kistler 9257AB each 170x140 mm) capable of measuring forces at the seat base along the three translational axes. A summing junction was used to sum the force signals from the two force plates along the respective axes to compute the resultant dynamic force due to the rigid seat and the occupant at the seat pan interface, as illustrated in the x - z plane of the seat in Fig. 7.1, for the x - axis motion. An additional three-axis force plate (Kistler 9257A, 170x140 mm) was also installed between the backrest support plate and the seat back truss structure to capture the dynamic forces arising at the occupant's upper body and the backrest interface. Under x -axis motion, the force acting along an axis normal to the backrest alone, however, was acquired, since

the forces along the side-to-side (lateral) and vertical directions of the backrest were expected to be significantly small in magnitude [117]. Under y -axis excitations, the measurement of backrest force was limited to y -axis alone. A pictorial view of the test seat installed on the vibration platform for measurement of responses under y -axis excitation is illustrated in Fig. 7.2. Single-axis accelerometers (Analog Devices, ADXL) were further installed on the seat back and the platform, oriented along the axis of the motion, to capture the acceleration due to excitations at the two driving-points. The seat was designed such that it could be easily oriented along the x - or y -axis of motion of the vibration platform, which consisted of a magnesium slip table sliding on an oil film over a granite slab. The slip table was driven by a 48 cm stroke servo-controlled hydraulic actuator.

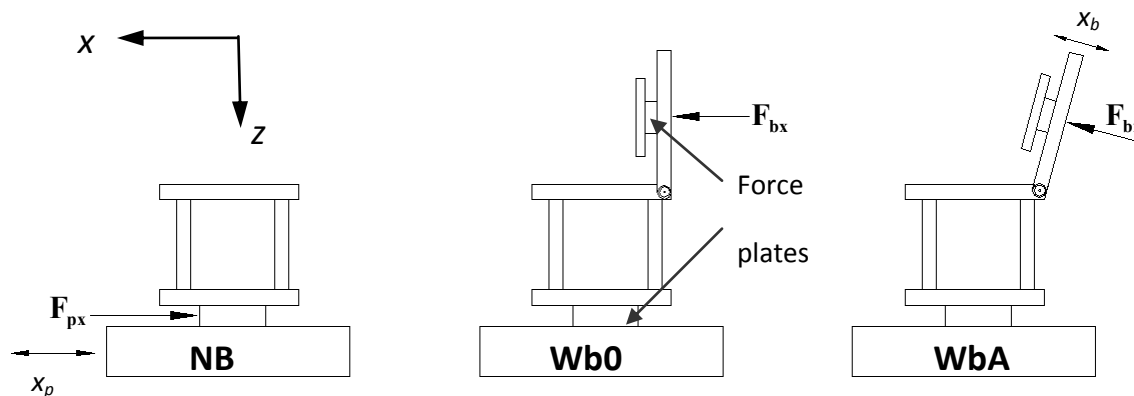


Fig. 7.1: Schematic illustrations of the three different sitting postures used in the study under fore-aft (x -axis) vibration. (NB - No back support; Wb0 - Vertical back support; WbA - Inclined back support).

The experiments were performed under excitations along the x - and y - axes, applied in an uncoupled manner. A total of 8 healthy male volunteers, aged between 21-51 years, took part in the experiment. The subjects had no prior known history of musculo-skeletal system disorders. The subjects' mass ranged from 59.4 kg to 92 kg, with mean mass of 71.2 kg and standard deviation of the mean of 10.6 kg. The standing height of the subjects varied from 1.70 m to 1.78 m (mean = 1.73 m; standard deviation = 0.025 m). Prior to the test, each subject was informed

about the purpose of the study, experimental set up and usage of the hand-held emergency stop. Subjects were given written information about the experiment and were requested to sign a consent form that was previously approved by a Human Research Ethics Committee.

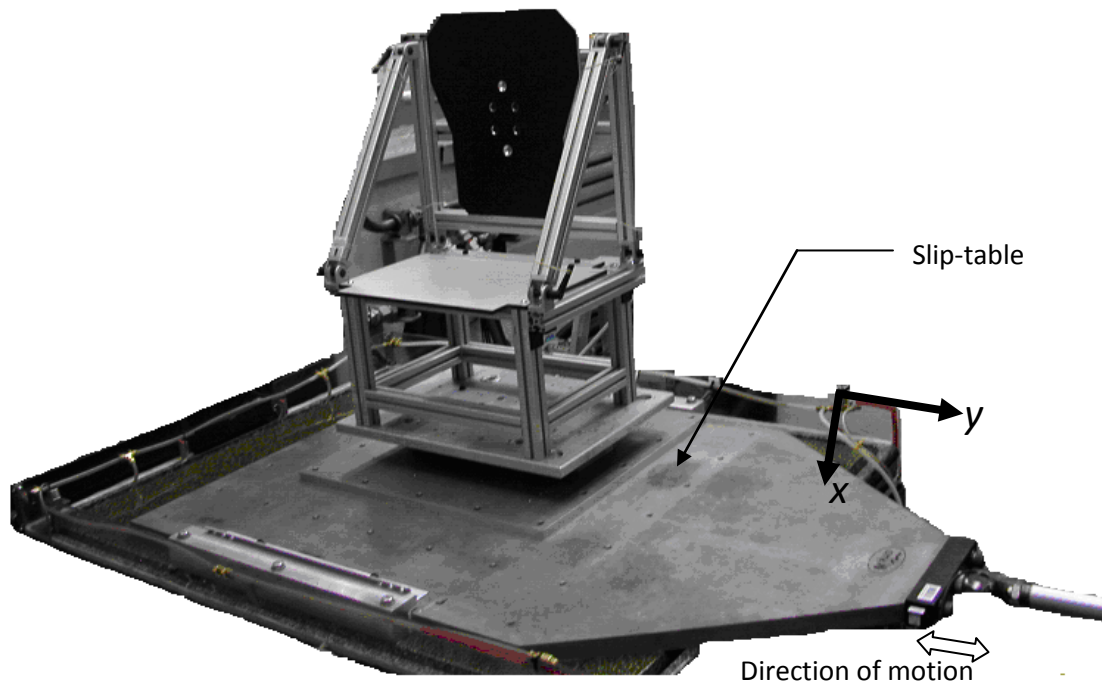


Fig. 7.2: Arrangement of the test seat on the horizontal vibration platform for measurement of the responses under y -axis excitation.

The measurements were performed for each subject assuming different sitting postures realized by three different back support conditions and three different seat heights (referred to as H_1 , H_2 and H_3). The back support conditions included: (i) sitting erect with no back support, NB; (ii) Sitting erect with upper body supported against a vertical backrest, Wb0; and (iii) seated relaxed with upper body supported against backrest inclined at an angle of 12.5° with respect to the vertical axis WbA (Fig. 7.1). The measurements of energy absorption were performed under three different levels of constant acceleration spectral density random excitations in the 0.5-10 Hz frequency range applied independently along the x - and y - axes. The overall rms

accelerations of the selected excitations for the two directions were 0.25, 0.5 and 1.0 m/s². The subjects were seated with their hands in the lap and feet supported on the moving platform for each posture. The vibration transmitted from the feet to the upper body is assumed to be small relative to the source vibration at the pan and the back support. Each subject wore a cotton lab coat to ensure uniform friction between the back and the backrest, which was judged to be an important factor under lateral excitation. Each test was performed two times and the data were examined for repeatability. The resulting test matrix involved a total of 54 trials for each axis of vibration, comprising three types of back support conditions, three seat heights, three excitation levels and two repeats. Table 7.2 summarizes the test matrix. The duration of each measurement was 128 s, while the subject's posture during a trial was visually checked by the experimenter to ensure consistency. The experiments were randomized, and each participant was asked to dismount the seat and vibration platform after each trial to relax for at least 2 minutes.

Table 7.2: Test matrix

Posture	No-back support, NB	Vertical back support, Wb0	Inclined back support, WbA
Excitation Magnitude (rms)	0.25 m/s ²	0.5 m/s ²	1.0 m/s ²
Seat height	H ₁ (425 mm)	H ₂ (390 mm)	H ₃ (350 mm)
Direction of motion	Fore-aft (<i>x</i>)	Lateral (<i>y</i>)	

7.3 ANALYSIS OF ABSORBED POWER

The instantaneous power $P(t)$ absorbed by the human body can be computed from the force exerted on the body $F(t)$ at the body-seat interface and the velocity $v(t)$ due to vibration excitation:

$$P(t) = F(t) \cdot v(t) \quad (7.1)$$

The average vibration energy transferred to the body during a period T can be expressed as:

$$P_{(avg)} = \int_{t_0}^{t_0+T} F(t)v(t)dt \quad (7.2)$$

The absorbed power in the frequency domain can be obtained from the cross-spectrum of the force and velocity, such that [16]:

$$P(j\omega) = S_{Fv}(j\omega) = C(\omega) - jQ(\omega) \quad (7.3)$$

Where $S_{Fv}(j\omega)$ is the complex co-spectrum of measured force and velocity, $C(\omega)$ is the coincident spectral density function (co-spectrum) and imaginary component $Q(\omega)$ is referred to as quadrature spectral density function (quad-spectrum). In the context of the vibration energy transferred to a seated human body, the real component reflects the energy dissipated in the biological structure per unit time and the imaginary component reflects the energy stored/released by the system [13]. The biological system with finite damping consumes the vibratory energy by means of relative motions between the tissues, muscles and skeletal systems, which is transformed into heat. It has been speculated that this dissipative component could be related to musculoskeletal disorders, while the restoring part relates to vibration comfort and perception.

The vibration power absorbed by the vibration-exposed seated body $P_a(\omega)$ is thus expressed as the real part of the cross-spectrum between the force and velocity signals, such that:

$$P_a(\omega) = Re[S_{Fv}(j\omega)] \quad (7.4)$$

Where Re designates the real component. The absorbed power can also be evaluated from the apparent mass using an indirect approach [12, 141]:

$$P_a(\omega) = \int_0^\infty \frac{\text{Im}[(M^*(\omega))] S_{aa}(\omega)}{\omega} d\omega \quad (7.5)$$

Where M^* is the complex conjugate of the apparent mass, ' Im ' designates the imaginary part and S_{aa} is the spectral density of the acceleration excitation.

In this study, instantaneous forces developed at the base and the backrest were acquired together with the acceleration signals in the multi-channel Pulse Labshop™. The data were analyzed to compute the absorbed power responses at the seat base and the backrest attributed to the forces measured at the two driving-points, respectively. Under the x -axis vibration, the absorbed power responses were computed from the forces measured at the two driving-points, such that:

$$P_{px}(\omega) = Re[S_{F_{px}v_{px}}]; \text{ and } P_{bx}(\omega) = Re[S_{F_{bx}v_{bx}}] \quad (7.6)$$

Where P_{px} and P_{bx} are the absorbed power responses measured at the seat pan and the backrest, respectively, under x - axis vibration. F_{px} and F_{bx} are the respective forces measured at the seat pan and the backrest. v_{px} and v_{bx} are velocities measured at the seat pan and the backrest, respectively, due to x - axis vibration. Owing to the rigid nature of the seat structure the two velocities were found to be identical ($v_{px} = v_{bx}$) for the vertical backrest. $S_{F_{px}v_{px}}$ and $S_{F_{bx}v_{bx}}$ are the cross-spectra of the forces and velocities, at the pan and the backrest respectively. The absorbed power responses measured at the seat pan (P_{py}) and the backrest (P_{by}) under y -axis excitations were also evaluated in the similar manner.

Each subject was seated assuming the desired posture with hands on the lap and feet on the vibrating slip table. The selected excitation signal was then applied and the total forces measured at the seat pan and backrest were acquired to compute the P_{Abs} responses of the seated occupant using Eq. (7.6) for the respective axis of vibration. The cross-spectra were obtained in the Pulse Labshop™ using a band width of 50Hz with frequency resolution of 0.0625 Hz and 75% overlap. The measurements were initially performed with the rigid seat alone. The data analysis resulted in negligible magnitude of absorbed power in the entire frequency range.

The coherence of the measured forces and accelerations were also evaluated and monitored during each trial. The measurements at the seat base invariably revealed high coherency of the force and acceleration signals under both axes of motion (≥ 0.95) in the 0.5-10 Hz frequency range, irrespective of the sitting posture and the excitation level considered. The measurements at the backrest along x - and y - axes also revealed coherence values greater than 0.95 under lower magnitude (0.25 m/s^2) of vibration for both back supported conditions (Wb0 and WbA). The coherence value decreased to 0.9 in the 0.5-4.5 Hz frequency range under higher magnitude of vibration (1 m/s^2) for both axes of motion. The coherency of the y -axis measurements increased with frequency in the higher frequency range for the Wb0 posture but decreased slightly for the x -axis measurements. This was most likely attributed to the pitching and rocking motions of the upper body, and intermittent loss of contact with the vertical backrest under fore-aft vibration. The measurements with the inclined backrest, however, revealed good coherency of the force and acceleration signals measured at the backrest under both axes of motion in the entire frequency range. The coherence values for the back supported conditions generally improved with the decrease in seat height suggesting increased stability and greater adhesion of the body with the supports.

The total absorbed power response of the human body subjected to either x - or y - axis vibration can be computed from integration of the real component of the cross-spectrum density over the frequency range of interest. For x - axis excitation, the total power may be derived from:

$$\overline{P}_{px} = \int_{\omega_1}^{\omega_2} \text{Re}[S_{F_{px}v_{px}}(j\omega)]d\omega; \quad \text{and} \quad \overline{P}_{bx} = \int_{\omega_1}^{\omega_2} \text{Re}[S_{F_{bx}v_{bx}}(j\omega)]d\omega \quad (7.7)$$

Where \overline{P}_{px} and \overline{P}_{bx} are the total absorbed power responses measured at the seat pan and the backrest interfaces, respectively, under x -axis vibration. The limiting frequencies ω_1 and ω_2 define the frequency range of interest.

Alternatively, the total power may be derived upon summation of absorbed power responses corresponding to each one third-octave frequency band, such that:

$$\overline{P}_{px} = \sum_{i=1}^N P_{px}(f_i); \quad \text{and} \quad \overline{P}_{bx} = \sum_{i=1}^N P_{bx}(f_i) \quad (7.8)$$

Where $P_{px}(f_i)$ and $P_{bx}(f_i)$ are the absorbed power responses at the centre frequency f_i of the i^{th} 1/3-octave frequency band and N is the total number of frequency bands in the frequency range of interest.

The measured absorbed power responses of the seated subjects exposed to vibration generally show considerable variations. A number of studies on vertical biodynamic responses in terms of APMS of seated individuals and a few on HV biodynamics have mostly attributed the dispersion in the measured data to variations in the body mass. The APMS magnitude normalization with respect to the magnitude near 0.5 Hz or static seated mass have been widely employed to reduce the variability in vertical APMS data [12,13,104]. The normalization factors

for the seat pan and backrest APMS magnitudes under HV, were suggested as 87.8% and 67.8%, respectively, of the total body mass [3], which represented portions of the body mass reflected at the seat pan and the backrest [119]. In a similar manner, different forms of normalized power have also been reported, such as power normalized by the body mass (W/kg), power density normalized by acceleration spectral density (Ns^3/m) and that by the product of acceleration spectral density and the body mass ($\text{Ns}^3/\text{m}/\text{kg}$). It has been suggested that the normalization with respect to acceleration spectrum helps to smoothen the small magnitude oscillations in the power response [104]. Lundström and Holmlund [13] normalized the measured absorbed power spectra under HV with respect to the body mass supported by the seat pan in order to reduce the degree of dispersion in the data.

7.4 RESULTS AND DISCUSSIONS

The averages of the measured absorbed power at the seat pan and the backrest of an individual in two trials were taken to derive the mean responses of each participant, as different trials revealed high degree of consistency. The mean P_{Abs} responses obtained for the 8 subjects were evaluated at each of the one third-octave band centre frequency in the 0.5-10 Hz frequency range. Figure 7.3 illustrates the mean responses of 8 individuals measured at the seat pan under 1 m/s^2 excitation along the x - and y - axes (P_{px} and P_{py}). The figure shows responses measured with all three sitting conditions (NB, Wb0 and WbA), while the seat height was 425 mm (H_1). The results clearly show considerable variability in the measured absorbed power, although consistent trends with respect to spectral components could be observed for the three postures and two excitation directions considered. The results particularly show the concentration of magnitude peaks around the comparable frequency bands for most of the subjects. The NB posture generally caused a sensation of instability among the subjects, particularly under x -axis

vibration, and encouraged the subjects to shift more weight to and from their feet, specifically when the displacement was perceived to be high. A considerably larger variability of the measured data is thus observed for the NB posture. The variability among the individual data set is greatly reduced with back supported postures, particularly under x -axis vibration. This may be attributed to more controlled sitting against the back support. The P_{Abs} responses of seated occupants with the NB posture under x - and y - axis vibration reveal comparable frequencies corresponding to the peaks. The frequencies corresponding to peak magnitude responses under x - and y - axis vibration, however, differ considerably for the back supported postures.

The absorbed power responses clearly demonstrate important effects of the back support condition and direction of vibration, which are also evident from the reported APMS responses to HV [3]. The effect of the back support condition appears to be far more important under x -axis vibration. This effect, however, is quite small under y - axis vibration, since the magnitudes of corresponding y -axis forces developed at the back support are relatively small. An inclined back support generally yields lower peak magnitudes under fore-aft vibration for the majority of participants compared to that obtained with the vertical back support.

The variability in the measured responses may be attributed to a number of factors, namely the body mass, body build and upper body adhesion with the back support [11,12]. The responses measured at the back support also show a similar degree of variability, as shown in Fig. 7.4, for the Wb0 and WbA postures. Owing to considerably lower dynamic interactions of the upper body with the backrest under y -axis vibration, the absorbed power responses tend to be substantially small compared to those obtained under x -axis vibration. Furthermore, the measured data reveals far greater variability under y -axis vibration. The low frequency y -axis vibration caused excessive side-to-side sliding of the upper body with respect to the back

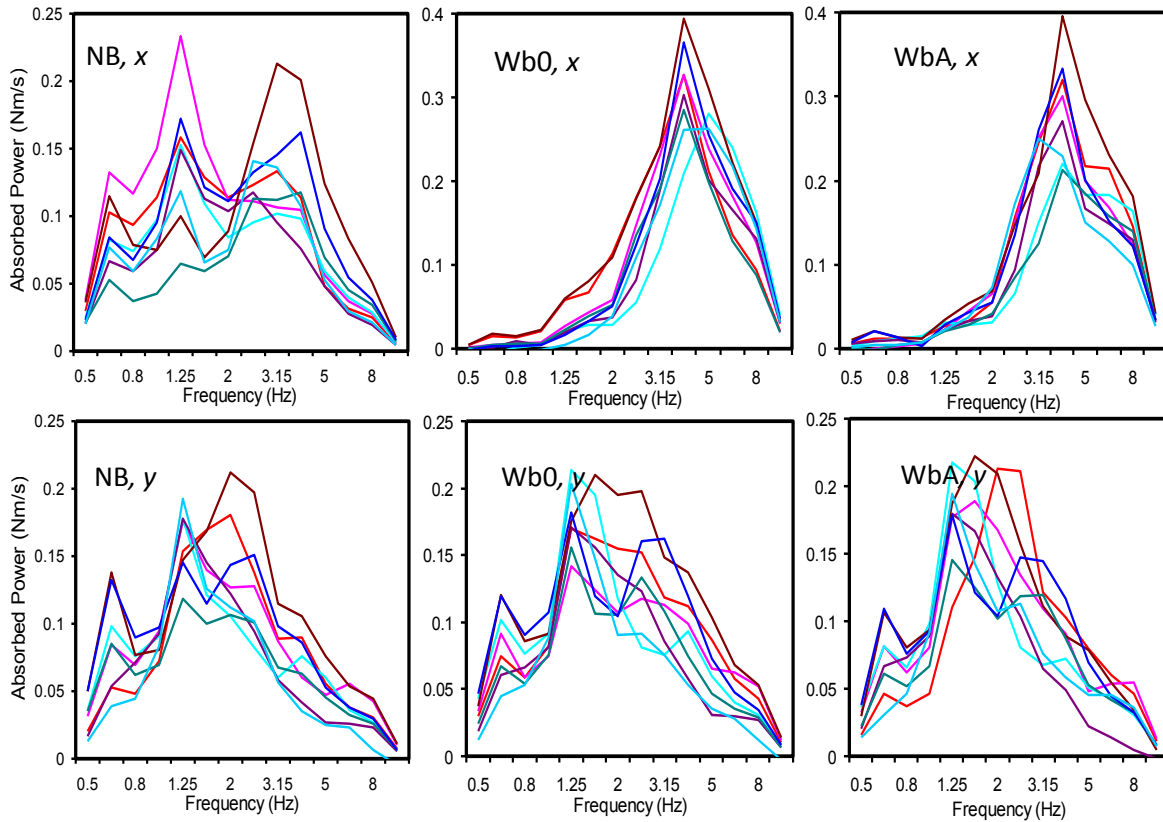


Fig. 7.3: Comparison of absorbed power magnitude responses measured at the seat pan of eight subjects seated with NB (no back support), Wb0 (vertical back support) and WbA: (inclined back support) postures, and exposed to 1 m/s^2 rms acceleration along the fore-aft (x) and lateral (y) directions (seat height H_1).

support. Subjects generally showed stiffening tendency to resist this motion. The greater variability in the measured data at lower frequencies was thus attributed to this body stiffening behaviour. The relatively lower magnitudes of absorbed power at some of the frequencies cause considerably higher values of the coefficient of variation (CoV), even though the standard deviation of the mean could be small. Relatively higher values of CoV, exceeding 100%, were observed for measured responses along both directions in a few of the frequency bands, where the magnitudes were very small. Otherwise, the observed CoV values under NB sitting condition were found to be comparable with those reported for measured APMS responses under HV [3,85,117].

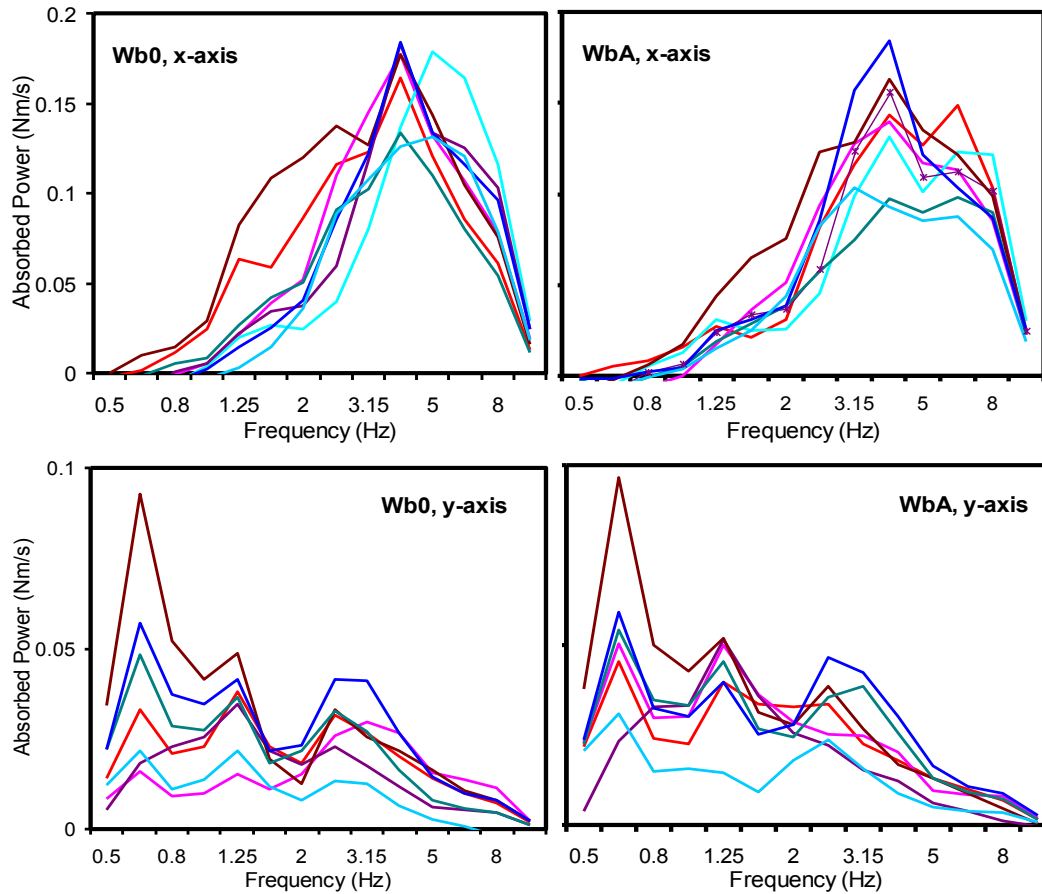


Fig. 7.4: Comparison of absorbed power magnitude responses measured at the backrest of eight subjects seated with Wb0 (vertical back support) and WbA (inclined back support) postures, and exposed to 1 m/s^2 rms acceleration along the fore-aft (x) and lateral (y) directions (seat height H_1).

The results show that the peak magnitude responses of the subjects occur within narrow frequency ranges, and are strongly dependent upon sitting posture and direction of excitation. Thus the mean magnitudes in 1/3-octave frequency bands are evaluated to study the important trends related to the effect of sitting posture, seat height and magnitude of vibration in view of both the seat pan and the backrest responses. Furthermore, the mean responses are considered to evaluate the effects of various factors.

Single-factor ANOVA, ‘with-in subjects’ were performed to identify the most significant factors affecting the absorbed power responses measured at the seat pan and the backrest. The

analysis involved excitation magnitude, seat height and back support conditions as the main factors. Two-factor ANOVA were also performed to analyse the significance of interactions between the two contributing factors on the absorbed power response obtained at the seat pan and the backrest. Tables 7.3 and 7.4 summarize the results attained for the responses measured at the seat pan under *x*- and *y*-axis excitations, respectively, corresponding to selected frequencies, considering the three levels each of the excitation magnitude and seat height, and their interactions, for each sitting posture. Owing to important observed effects of back support conditions, the significant differences in the measured absorbed power response at the seat pan are also evaluated for the two back-supported postures (Wb0 vs WbA) and all the three postures (NB vs Wb0 vs WbA). The results are summarized in Table 7.5 for both axes of vibration. Owing to relatively small magnitudes of measured power and greater CoV of the measured data, a few studies have employed either peak magnitudes or total absorbed power to study the effects of contributing factors [12,13]. In this study, the total absorbed power responses of 8 subjects were also evaluated from the one third-octave bands spectra, using Eq. (7.8).

Table 7.3: *p*-values attained from single and two-factor ANOVA performed on the seat pan absorbed power magnitude under fore-aft vibration.

Factor Frequency(Hz)	Excitation (.25, .5, 1.0 m/s ²)			Height (H ₁ , H ₂ , H ₃)			Excitation*Height		
	NB [†]	Wb0 [‡]	WbA [§]	NB	Wb0	WbA	NB	Wb0	WbA
0.63	0.000	0.000	0.000	0.054	0.294	0.005	0.031	0.319	0.006
0.75	0.000	0.000	0.000	0.223	0.508	0.017	0.005	0.365	0.011
1	0.000	0.000	0.000	0.142	0.569	0.101	0.898	0.318	0.153
1.13	0.000	0.000	0.000	0.386	.557	0.335	0.532	0.756	0.546
2	0.000	0.000	0.000	0.235	0.806	0.628	0.605	0.54	0.495
3	0.000	0.000	0.000	0.597	0.176	0.392	0.929	0.371	0.372
4	0.000	0.000	0.000	0.716	0.008	0.064	0.905	0.004	0.007
5	0.000	0.000	0.000	0.401	0.054	0.070	0.792	0.076	0.053
6	0.000	0.000	0.000	0.299	0.513	0.016	0.69	0.68	0.039
8	0.000	0.000	0.000	0.899	0.504	0.007	0.915	0.782	0.000

NB[†] – No back support; Wb0[‡] – Vertical back support; WbA[§] – Inclined back support

Table 7.4: p-values attained from single and two-factor ANOVA performed on the seat pan absorbed power magnitude under lateral vibration.

Factor Frequency(Hz)	Excitation (.25, .5, 1.0 m/s ²)			Height (H ₁ , H ₂ , H ₃)			Excitation*Height		
	NB [†]	Wb0 [‡]	WbA [§]	NB	Wb0	WbA	NB	Wb0	WbA
0.63	0.000	0.253	0.008	0.322	0.785	0.965	0.437	0.657	0.879
0.75	0.000	0.000	0.000	0.382	0.178	0.747	0.811	0.25	0.568
1	0.000	0.000	0.000	0.756	0.811	0.698	0.392	0.992	0.838
1.13	0.000	0.000	0.000	0.081	0.927	0.861	0.051	0.962	0.976
2	0.000	0.000	0.000	0.013	0.581	0.378	0.96	0.532	0.277
3	0.000	0.000	0.000	0.381	0.215	0.302	0.616	0.035	0.216
4	0.000	0.000	0.000	0.024	0.028	0.798	0.340	0.001	0.938
5	0.000	0.000	0.000	0.001	0.226	0.669	0.009	0.153	0.931
6	0.000	0.000	0.000	0.000	0.757	0.377	0.000	0.714	0.682
8	0.000	0.000	0.000	0.000	0.036	0.313	0.000	0.088	0.746

NB[†] – No back support; Wb0[‡] – Vertical back support; WbA[§] – Inclined back support

Table 7.5: Effect of posture shown by the p-values derived from single-factor ANOVA performed on the seat pan absorbed power magnitude data under Fore-and-aft and lateral excitations.

Axis	Frequency (Hz)	0.63	0.75	1	1.13	2	2.75	4	5	6	8
x-	Wb0 [‡] vsWbA [§]	0.003	0.121	0.388	0.830	0.054	0.495	0.000	0.000	0.027	0.038
	NB [†] vsWb0 [‡] vsWbA [§]	0.000	0.000	0.702	0.036	0.157	0.004	0.000	0.000	0.000	0.000
y-	Wb0 [‡] vsWbA [§]	0.064	0.001	0.278	0.094	0.004	0.009	0.906	0.000	0.000	0.250
	NB [†] vsWb0 [‡] vsWbA [§]	0.000	0.000	0.000	0.000	0.000	0.125	0.000	0.000	0.000	0.000

NB[†] – No back support; Wb0[‡] – Vertical back support; WbA[§] – Inclined back support

The CoV values of the total P_{Abs} data were computed to analyze the inter-subject variability. The CoV values up to 20% were obtained over the experimental conditions considered. Moreover, no particular trends in the values of CoV could be observed with respect to the magnitude of excitation, sitting posture, seat height or direction of excitation.

The absorbed power derived on the basis of dynamic interactions at the seat pan driving-point can be considered to represent the total energy transferred to the body, while that resulting from backrest driving-point may be interpreted as energy transferred to the upper body from the seat pan and the back support. In order to quantify the effect of the back support, the ratio of the total power absorbed at the backrest to that at the seat pan is computed, such that:

$$P_{yx} = \frac{\overline{P_{bx}}}{\overline{P_{px}}} \quad \text{and} \quad P_{yy} = \frac{\overline{P_{by}}}{\overline{P_{py}}} \quad (7.9)$$

Where $P_{\gamma k}$ ($k=x, y$) is the ratio of total power derived from the seat back response to that from the seat pan response under excitations along axis k . The total power measured at the seat pan and the backrest, together with absorbed power ratio (APR, $P_{\gamma k}$) are summarized in Table 7.6 for both axes of vibration, under the influence of unsupported and supported back postures and magnitudes of vibration. Considering the relatively small effect of seat height in most of the frequency range (Tables 7.3 and 7.4), the results are presented for the seat height of 425 mm (H_1). Further analyses of the absorbed power spectra revealed that the energy transfer in frequency bands corresponding to the principal resonances account for nearly 70% and 90% of the total absorbed power in the 0.5-10 Hz frequency range, under the x - and y - axis vibration, respectively. This suggests relatively larger deformations of musculoskeletal structure around the principle resonances, and thus the greater energy dissipation.

Table 7.6: The total absorbed power measured at the seat pan and the backrest, under the influence of various unsupported and supported back postures, and magnitudes of vibration at seat height 425mm.

Axis	Vibration Level	Total absorbed power (Nm/s)					APR P_{γ} %	
		Seat Pan			Backrest		Wb0	WbA
		NB [†]	Wb0 [‡]	WbA [§]	Wb0	WbA		
x	0.25m/s ²	0.09	0.08	0.07	0.05	0.04	59.93	58.08
	0.5m/s ²	0.32	0.34	0.32	0.21	0.19	60.64	57.95
	1.0 m/s ²	1.14	1.38	1.32	0.85	0.78	61.83	59.27
y	0.25m/s ²	0.09	0.09	0.09	0.04	0.04	38.49	40.56
	0.5m/s ²	0.31	0.34	0.34	0.11	0.12	31.31	36.04
	1.0 m/s ²	1.09	1.20	1.18	0.31	0.36	25.85	30.14

NB[†] – No back support; Wb0[‡] – Vertical back support; WbA[§] – Inclined back support

7.4.1 Normalization of the measured absorbed power response

The magnitudes of the total absorbed power obtained at the seat pan ($\overline{P_{px}}$) and backrest ($\overline{P_{bx}}$) revealed superior correlation ($r^2 > 0.8$) with the body mass for both the back-supported

postures and all three levels of fore-aft vibration. Similar degree of correlation of \overline{P}_{py} with the body mass was also observed under y -axis vibration ($r^2 > 0.9$), while extremely poor correlation was obtained for \overline{P}_{by} ($r^2 < 0.2$). This could be attributed to relatively small magnitudes of lateral forces developed at the upper body-seat back interface and sliding of the upper body against the backrest under y -axis vibration.

The normalizations of absorbed power spectra with respect to the seated mass resulted in nearly 10% reduction in CoV values at frequencies above 2.5 Hz for the NB posture, while only negligible effects were observed in the 1-2.5 Hz frequency range. The effect of normalization on the CoV of the absorbed power spectra with back supported postures was noticed only near frequencies corresponding to the peaks. Consequently, the subsequent analyses of the measured data were performed without the normalization, which allows for interpretations of the contributing factors on the basis of the unbiased frequency responses.

7.4.2 Effect of vibration magnitude

The reported studies [10-13,104] both under vertical and HV have consistently concluded that the total absorbed power increases approximately in proportion to the square of the excitation magnitude. The strong effects of the vibration magnitude are most likely attributed to many factors, such as, the nonlinear behaviour of the seated body, excessive upper body movements under higher excitations, increase in shifting tendencies of the occupants to realize more stable posture under higher vibration magnitudes, and contributions due to the legs. The across subjects mean responses attained with NB and WbA postures (n=8), under different magnitudes x - and y -axis excitations, obtained at the seat pan and the backrest, respectively, are illustrated in Figs. 7.5 and 7.6. The figures show mean responses to 0.5 and 1.0 m/s^2 excitations,

while those to 0.25 m/s^2 rms acceleration excitation are omitted due to very small power values. Furthermore, the mean responses attained with Wb0 posture are also omitted, since these were quite similar to those obtained with WbA posture. The results clearly show strong and nonlinear effects of vibration magnitude on both the seat pan and backrest responses, irrespective of the direction of excitation. The strong influence of the vibration magnitude is also evident from the results attained from ANOVA, presented in Tables 7.3 and 7.4 for the x - and y -axes, respectively, where $p < 0.005$ in most of the frequency range. The effect of vibration magnitude on the power derived from seat pan interactions is highly significant ($p < 0.001$) in the entire frequency range under both axes of vibration and all the three sitting postures.

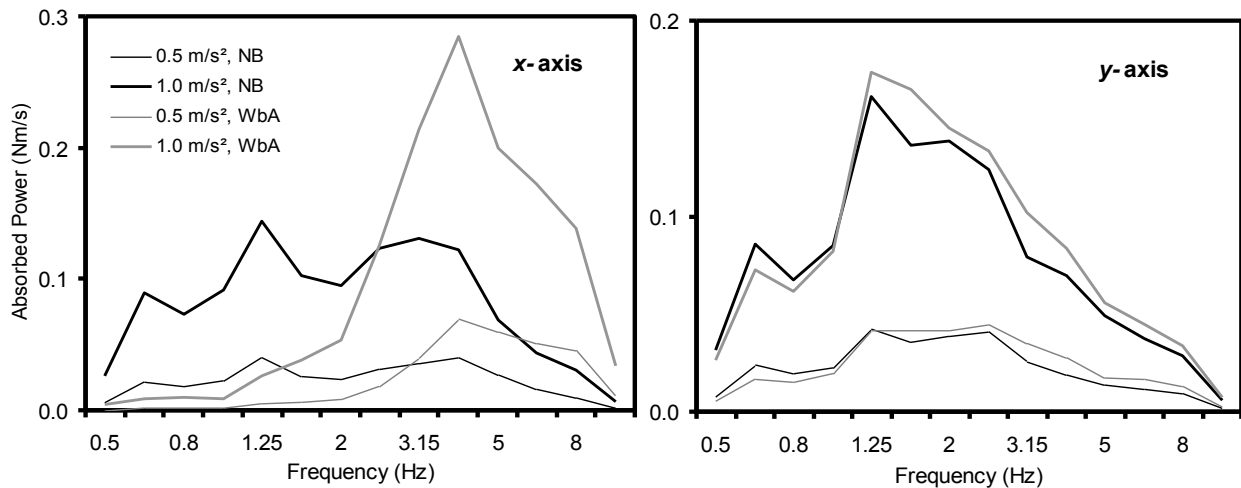


Fig 7.5. Mean across subjects ($n=8$) absorbed power characteristics measured at the seat pan under different magnitudes of excitation 0.5 and 1.0 m/s^2 rms, and, NB (no back support) and WbA (inclined back support) postures, along fore-aft (x) and lateral (y) vibration.

The total absorbed power responses derived from the two driving-points under both axes of vibration suggest a nearly quadratic relation with the magnitude of vibration, which may be expressed in the form:

$$\bar{P} = \alpha a^\beta \quad (7.10)$$

Where β is the exponent of the overall rms acceleration a due to excitation and α is the proportionality constant. The regression analysis of the measured total power data resulted in a correlation coefficient (r^2) in excess of 0.9 for all the experimental conditions considered. Table 7.7 summarizes the constant and the exponent values obtained for different excitation and postural conditions. The exponent values for the pan measured power range from 1.84-2.07 and 1.81-1.86 under x - and y -axis vibration, respectively. The corresponding values of the constants range from 1.15-1.39 and 1.09-1.21, respectively. Both the constant and exponent values tend to be higher for the back supported postures compared to those for the NB posture under fore-aft vibration, suggesting greater dependence of the total energy transfer on the vibration magnitude when the upper body is supported against a backrest. Under y -axis vibration, the exponent value for the NB posture tends to be only slightly smaller compared to those for the Wb0 and WbA postures, while the difference in the proportionality constant is considerable. These suggest that energy transfer to the body increases at a greater rate of excitation acceleration, when the upper body is supported under both axes of HV. This may be partly attributed to the fact that contact with the back serves as an additional driving-point or source of vibration.

Table 7.7: Constant and exponent values for different excitation and postural conditions.

Location	Axis of vibration	exponent β			constant α		
		NB [†]	Wb0 [‡]	WbA [§]	NB	Wb0	WbA
Seat pan	x	1.84	2.05	2.07	1.15	1.39	1.33
	y	1.81	1.85	1.86	1.09	1.21	1.19
Backrest	x	-	2.07	2.08	-	0.86	0.79
	y	-	1.56	1.64	-	0.31	0.36

NB[†] – No back support; Wb0[‡] – Vertical back support; WbA[§] – Inclined back support

The results further show relatively lower values of the exponent and the constant under lateral axis excitation, compared to the fore-aft vibration. These suggest that relatively smaller amount of energy is dissipated within the body exposed to lateral vibration, compared to that under identical magnitude of fore-aft vibration, which encourages greater interactions of the

upper body with the back support. This is also evident from the total power derived from back support interactions, which tends to be considerably higher under x -axis vibration. The exponent values for the \overline{P}_{bx} range from 2.07 to 2.08 under x -axis vibration, which are considerably larger than those for the \overline{P}_{by} (1.56-1.64) under y -axis vibration. Even larger difference is evident from the constant values, which range from 0.79 to 0.86 and 0.31 to 0.36 under x - and y -axes vibration, respectively, which further attest to enhanced interactions of the upper body with the back support under fore-aft motions. This is further evident from the absorbed power ratio (APR), which lies in the 58-62% range for the fore-aft vibration but is only 25-40% under lateral vibration of different magnitudes considered in the study. Reduced power measured at the back support under lateral vibration can be attributed to relatively smaller magnitude of force developed along the y -axis, and lower resistance provided by the backrest to limit the upper body motion. It is essential to note that variations in seat height revealed only minimal effect of the total power, irrespective of the excitation magnitude and back support condition.

7.4.3 Effect of posture

The results show most important effect of back support on the absorbed power responses measured at the seat base under x - axis vibration, while the effect under y -axis is very small, as seen in Fig. 7.5 and Table 7.5. The results show significant effects of posture on the seat pan-measured power ($p < 0.001$), when the variations are considered for all three postures, except in a few frequency bands in the x -axis response. The variations in the back support (Wb0 vs WbA) also show effect on the x -axis response at frequencies above 2.75 Hz ($p < 0.05$), while the effect is more evident above 4 Hz under the y -axis motion. Owing to the very low power magnitudes under 0.25 m/s^2 excitation and relatively smaller effects of the two back supported postures, the figure illustrates comparisons of the results attained with NB and WbA conditions, and two

magnitudes of vibration. Figure 7.6 further shows the comparisons of spectra of absorbed power for the two back support conditions, derived from the back support driving-point.

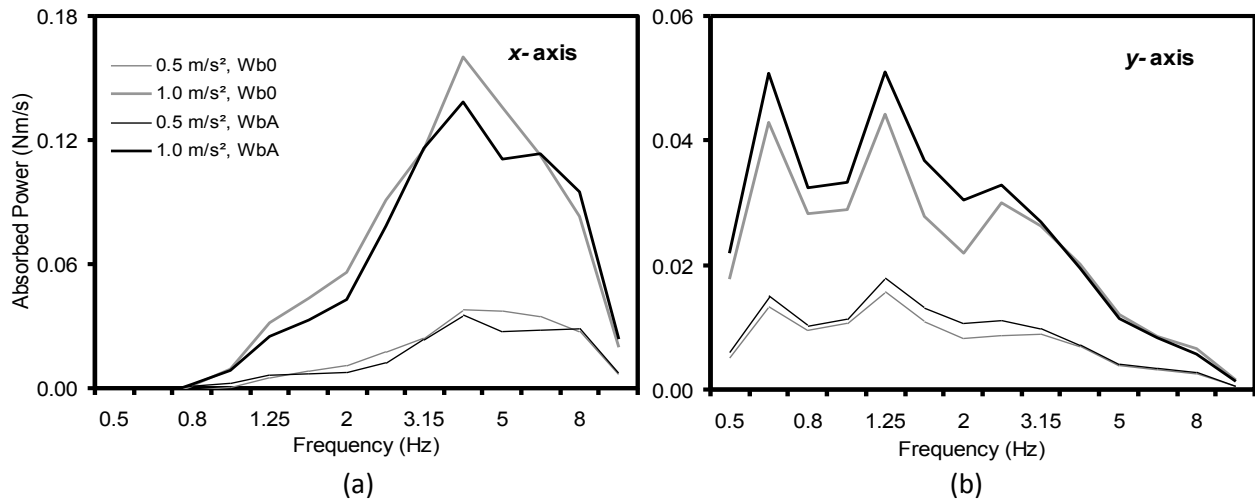


Fig 7.6. Mean across subjects (n=8) absorbed power characteristics measured at the backrest under different magnitudes of excitation 0.5 and 1.0 m/s² rms, and Wb0: (vertical back support) and WbA (inclined back support) postures: a) fore-aft (x) vibration; b) lateral (y) vibration.

The influences of the back support conditions, considered in this study, on the mean absorbed power spectra in the 0.5-10 Hz frequency range under *x*- and *y*-axis vibration of magnitude of 1.0 m/s² are further illustrated in Fig. 7.7. For the NB condition, the absorbed power response under *x*- axis vibration reveals peaks in the frequency bands centered around 0.63, 1.25 and 3.15 Hz, while the response under *y*-axis vibration reveal peaks near 0.63, 1.25 and 2 Hz. These frequencies corresponding to the peaks are comparable to those observed in the APMS responses of seated occupants exposed to HV [3]. It has been reported that the primary resonance occurring at lower frequencies is due to pitch motion of the upper body¹⁵. An analysis of total power absorbed further showed that nearly 50% of the total power under an NB posture is absorbed in the lower frequency range of 0.5-2.19 Hz, and can be attributed to the upper body motion. The upper body restrained against a vertical or inclined backrest reveals peak magnitude at a considerably higher frequency under the fore-aft motion, as seen in Fig. 7.7. The dominant

peak response shifts to centre frequency of 4 Hz, when the back is supported, while the peak magnitude tends to be considerably larger. A slight secondary peak is also observed in the band centered around 6.3 Hz for the WbA posture. This suggests that the use of a back support helps to stiffen the upper body under fore-aft motion. This tendency, however, is not evident under lateral vibration. The total power attained from the pan measurements suggest comparable total power of the 3 sitting conditions under both axes of vibration of smaller magnitudes (0.25 and 0.5 m/s²). An increase in the excitation magnitude, however, seems to cause greater energy transfer for the back supported postures. Under the 1 m/s² fore-aft excitation, nearly 16-20% larger energy is transferred to the body with the back support than the NB sitting condition (Table 7.6). This increase reduces to approximately 10% for the lateral acceleration excitation of the same magnitude.

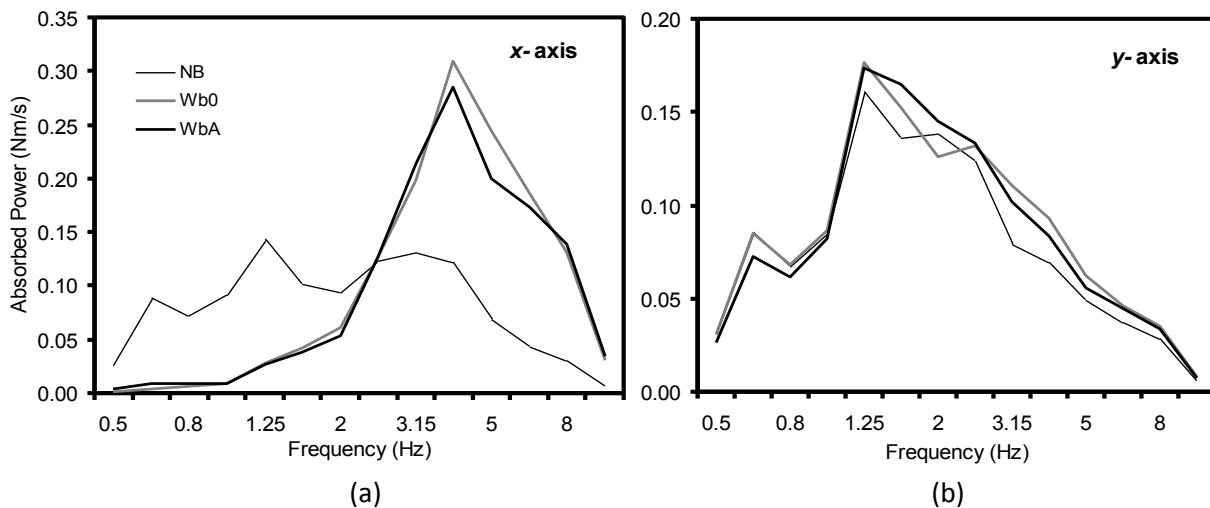


Fig 7.7. Mean absorbed power characteristics (n=8) measured at the seat pan under NB (no back support) Wb0 (vertical back support) and WbA (inclined back support) postures (excitation magnitude – 1.0 m/s² rms): a) fore-aft (*x*) vibration; b) lateral (*y*) vibration.

Figure 7.8 illustrates a comparison of the 1/3-octave band spectra of powers measured at the seat pan and the back support (WbA) under fore-aft motion. The two responses show peaks in the identical frequency bands centered around 4 and 6.3 Hz. An inclined back support would

impose relatively less vibration to the upper body along a direction normal to the contact surface, and could thus yield slightly lower absorbed power. The response measured at the backrest along the fore-aft direction show that a WbA posture yields slightly lower values of total power measured at the back support and APR than the Wb0 posture (Table 7.6). This may be attributed to more stable upper body support in the WbA condition. An inclined back support tends to limit the backward upper body motion, while the forward motion is limited by the weight of the subject resting against the back support. The measured power responses under the lateral motion, however, show an opposite trends, where the APR values for the WbA posture tend to be slightly higher than the Wb0 posture, irrespective of the excitation magnitude. This may be attributed to relatively less sliding of the upper body against the inclined back support.

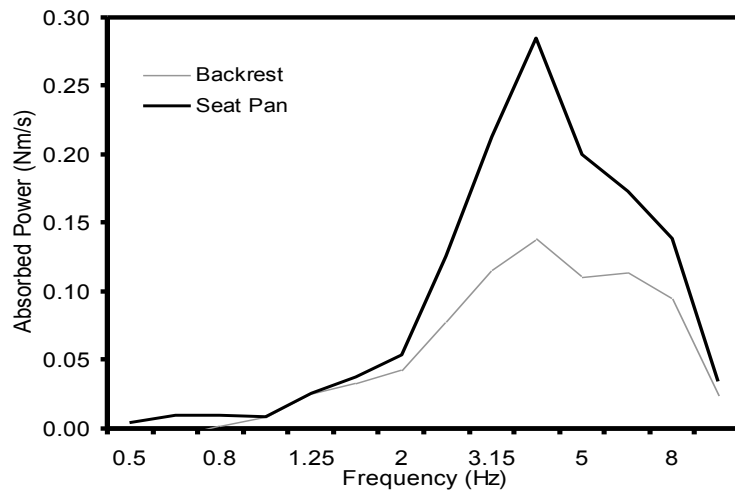


Fig. 7.8: Comparison of mean absorbed power response (n=8) measured at the seat pan and the backrest under fore-and-aft (x) vibration (WbA - inclined back supported posture, Seat height-H1).

7.4.4 Effect of seat height

The absorbed responses revealed very small effect of the seat height, irrespective of the back support condition and excitation magnitude. The effect was particularly negligible for the NB and Wb0 sitting conditions ($p>0.05$) when exposed to fore-aft vibration, and for WbA

posture under lateral vibration. The NB posture showed only small influence of the seat height under lateral vibration at frequencies above 4 Hz ($p < 0.05$), as seen in Table 7.4.

7.5 DISCUSSIONS IN VIEW OF THE REPORTED RESULTS

The absorbed power characteristics of the seated human exposed to HV have been reported in a single study [13]. This study considered only NB posture with feet resting on a stationary support and thus not vibrated. The study considered different magnitudes of sinusoidal fore-aft and lateral vibration ($0.25\text{-}1.4\text{ m/s}^2$ rms) at discrete frequencies in the 1.13-20 Hz range with steps of 1/6 octaves and reported that peak responses occur below 3 Hz. The present study considered sitting with back supported and unsupported conditions on a rigid seat with three different heights, while exposed to three levels of white noise random vibration in the 0.5-10 Hz range. The mean responses of the seated body with NB posture revealed primary resonant peaks near 0.63 and 1.25 Hz under each axis of vibration. An additional peak in the 3.15 Hz band was also observed under fore-aft vibration. The lower frequency peaks could not be observed in the reported study, since it considered vibration at 1.13 Hz and above, while a peak in the fore-aft response near 2.5 Hz was evident. Moreover, the reported study was conducted under sinusoidal vibration, which could yield different magnitudes of absorbed power than those observed under random vibration. The differences in the responses are also partly attributable to the stationary legs support used in the reported study. Under exposure to HV, the occupants' legs are expected to undergo relative movements and thus contribute to energy transfer. Similar to another reported study under vertical vibration [12], the total power obtained in this study at both the seat pan and backrest revealed good correlation with the body mass under the experimental conditions considered, irrespective of the axis of vibration. The mean total power measured under 1.0 m/s^2 rms vertical vibration (0.5-15 Hz) with NB posture and hands in lap was reported as 0.2 W [12],

the present study revealed total power under the same posture and HV magnitude (0.5-10 Hz) in the order of 1.1 W. Considering the differences in the frequency bands used in the two studies and thus the magnitude, these results suggest that the energy transfer to the body under HV could be equally important when compared to that under vertical vibration.

7.5.1 A Discussion on Frequency-Weighting of Vibration Power Absorption (VPA)

According to ISO 2631-1 [6], the frequency-weighted acceleration (a_w) at a frequency (ω) for a given vibration acceleration (a) is calculated from

$$a_w(\omega) = W_d(\omega) \cdot a(\omega), \quad (7.11)$$

where W_d is the frequency weighting function defined in ISO 2631-1 [6].

In order to make a direct comparison of the VPA and the ISO-weighted acceleration, the VPA must be transferred to a function with the same form as that shown in Eq. (7.11) [142]. As it is evident in Eq. (7.10), the absorbed power is statistically proportional to a^β , therefore, the required proportional function is obtained by taking β -root of the P_{Abs} . The resulting function is further normalized to a reference value using the methodology proposed by Dong et al. [142], so that the VPA-based vibration measure has the same form as that shown in Eq.(7.11) and the VPA-based frequency weighting is directly comparable with the ISO W_d -weighting. The resulting VPA-based weighting is expressed as follows:

$$W_{pj}(\omega) = \sqrt[\beta]{\frac{P_{pj}(\omega) / a_{pj}^\beta(\omega)}{(P_{pj} / a_{pj}^\beta)_{Ref}}}; \quad j = x, y \quad (7.12)$$

where W_{pj} is the magnitude of the weighting filter derived from spectra of power measured at the pan under vibration along direction j ($j = x, y$), a_{pj} is the root-mean-square value of the

acceleration input to the body in the VPA measurement, and $\sqrt[\beta]{(P_{pj} / a_{pj}^\beta)_{Ref}}$ is the reference value of the non-normalized VPA weighting, which can be selected based on the purpose of the weighting application.

With the VPA-based frequency weighting, the VPA-based vibration measure (a_{VPA}) is expressed as follows [142]:

$$a_{VPA}(\omega) = W_{pj}(\omega) \cdot a(\omega), \quad (7.13)$$

This equation clearly demonstrates that the VPA-based vibration measure is indeed composed of two components: (i) the vibration hazard represented by the input acceleration; and (ii) the biodynamic response represented by the VPA-based frequency weighting. An earlier study by Dong et al. [142] has shown that the VPA-based frequency weighting may also be derived from the driving-point mechanical impedance or apparent mass.

Since the VPA-based weighted acceleration in Eq. (7.13) and the ISO-weighted acceleration in Eq. (7.11) have the same form and the same vibration hazard or acceleration, the comparison of the two weightings can be used to identify the difference or similarity between the two measures. For the purpose of comparison, the VPA-based frequency weighting was computed using the β values defined in Table 7.7 and the mean power spectra corresponding to 0.5 and 1.0 m/s² excitations along each axis. Each of the VPA-based frequency weightings is normalized to its peak value, while the maximum weighting is taken as unity. Figure 7.9 illustrates comparisons of magnitudes of W_{pj} attained for the three sitting conditions and 1 m/s² excitation along each direction of vibration with the current W_d -weighting defined in ISO-2631-

1[6]. The magnitudes of W_{pj} and W_d -weightings are further compared and summarized in Table 7.8 in the 0.5-10 Hz frequency range.

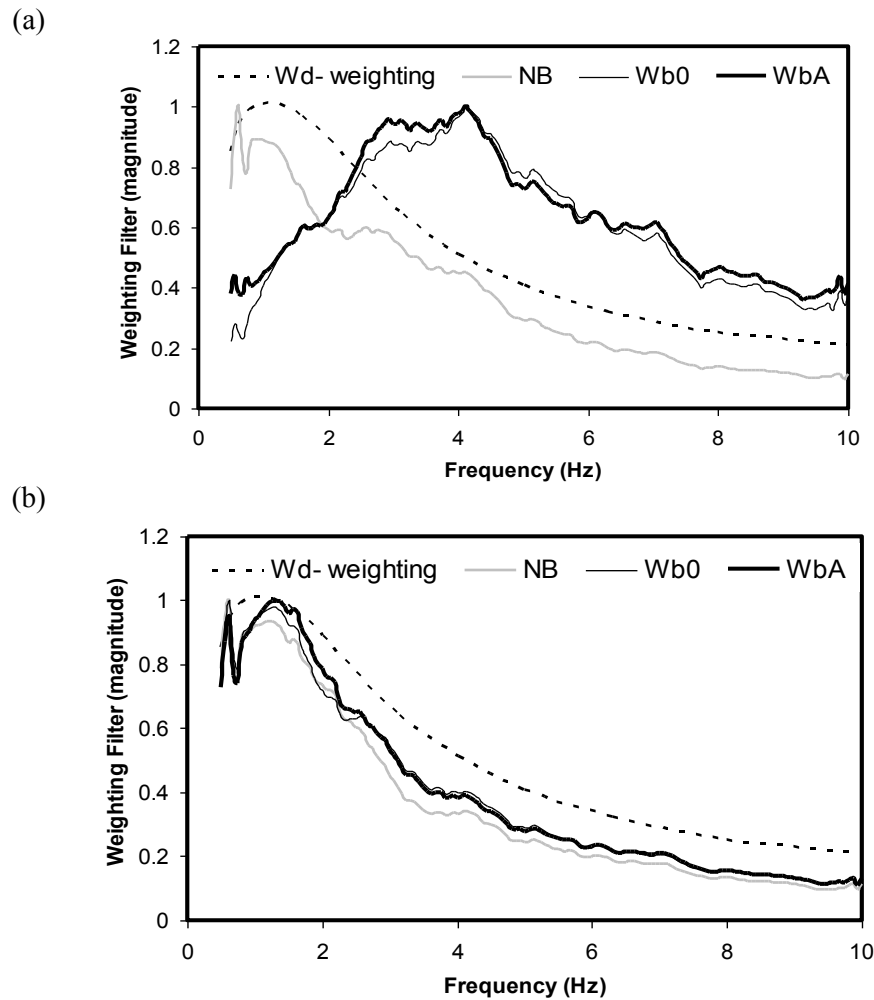


Fig. 7.9: Comparisons of weighting filter magnitudes derived from mean absorbed power responses corresponding to NB (no back support), Wb0 (vertical back support) and WbA: (inclined back support) postures (a) Fore-aft (x) vibration; and (b) Lateral vibration.

As shown in Fig. 7.9, the two vibration magnitudes resulted in very similar values of the VPA-based frequency weighting function. This suggests that the VPA-based frequency weighting is not very sensitive to the variation of the vibration magnitude. The results also show that the general trend of the weighting function derived from the absorbed power responses to side-to-side vibration, W_{py} , is generally consistent with that of W_d -weighting function, as seen in

Fig. 7.9(b). The W_d -weighting also corresponds reasonably well with the W_{px} derived from the fore-aft VPA corresponding to the sitting condition without using the back support, as seen in Fig. 7.9(a). Since W_d is derived primarily based on the subjective comfort data [92] measured for a sitting posture comparable to the NB posture used in the VPA measurement, the reasonably good agreement between the VPA-based and the ISO weightings suggests that the vibration power absorption in the horizontal vibration could be associated with the vibration sensation or perception for the NB posture. This reveals that the VPA could serve as an important measure of the vibration perception, which has also been observed in the hand-transmitted vibration exposure along the forearm direction [142]. Considering that the ISO-weighted acceleration is an acceptable measure for assessing a health effect, the VPA may also be associated with the same health effect. These observations support the general hypothesis presented in the introduction section of this chapter.

Table 7.8: Comparisons of the weighting values obtained in this study with the W_d -weighting defined in ISO-2631-1[6].

Frequency(Hz)	W_d -weighting	<i>Fore-aft</i>			<i>Lateral</i>		
		NB [†]	Wb0 [‡]	WbA [§]	NB [†]	Wb0 [‡]	WbA [§]
0.5	0.853	0.746	0.214	0.373	0.651	0.635	0.556
.63	0.944	1	0.243	0.375	1	1	0.901
0.8	0.992	0.89	0.319	0.4	0.806	0.814	0.769
1	1.011	0.899	0.4	0.438	0.854	0.895	0.880
1.25	1.008	0.871	0.498	0.500	0.886	0.962	0.994
1.6	0.968	0.741	0.604	0.596	0.775	0.836	0.932
2	0.89	0.619	0.632	0.63	0.573	0.544	0.638
2.5	0.776	0.614	0.788	0.871	0.402	0.428	0.450
3.15	0.642	0.606	0.885	0.941	0.187	0.267	0.253
4	0.512	0.482	1	1	0.143	0.188	0.174
5	0.409	0.32	0.761	0.723	0.078	0.1	0.093
6.3	0.323	0.225	0.588	0.596	0.047	0.058	0.057
8	0.253	0.161	0.42	0.459	0.026	0.033	0.032
10	0.212	0.138	0.366	0.374	0.019	0.024	0.017

NB[†] – No back support; Wb0[‡] – Vertical back support; WbA[§] – Inclined back support

In the current ISO standard, the same W_d -weighting function is recommended for assessing the discomfort and health effects in the horizontal vibration exposure without differentiating the sitting postures with or without the back support. The results of this study suggest that this may not be a good practice. As shown in Fig. 7.9(a), the VPA-based fore-aft weightings (W_{px}) with back support differ greatly from that without the back support, as well as the W_d -weighting. This is attributed to greater interactions of the upper body with the back support under fore-aft motion. The biodynamic responses under these two sitting postures have been shown to be significantly different [2,3]. Consequently, the resulting vibration perception or health effect should be different for the two postures. The frequency weightings used for assessing the vibration exposure for different back support conditions should also differ. Considering that the VPA measured under the sitting posture with the back support is likely to have some association with the discomfort or a health effect under such a sitting posture, the VPA-based frequency weighting for this posture may be used as one of the references for the development of an improved weighting for the risk assessment of the exposure under this posture. However, further studies of the comfort and health effects under this posture are required to test this VPA-based frequency weighting.

7.6 CONCLUSIONS

The absorbed power response characteristics of seated human subjects exposed to fore-aft and lateral vibration reveal considerable dynamic interactions between the upper body and the seat backrest, apart from those of the body and the seat pan. The results show that the vibration energy transferred and dissipated within the exposed body is strongly influenced by the back support condition, excitation magnitude and individual body mass, while the effect of seat height is nearly negligible. The responses measured at the seat pan and the backrest clearly show most

important influences of the back support, particularly under fore-aft vibration. The absorbed power responses of the body seated without a back support dominate in the low frequency bands of 0.63 and 1.25 Hz under both axes of vibration, associated with the rocking and swaying motions of the upper body. An additional peak is also observed in the vicinity of 3.15 and 2 Hz under *x*- and *y*-axis motion, respectively. These frequencies are similar to those observed from the reported apparent mass responses to HV. The presence of a backrest helps to stabilize the sitting posture by limiting the motions of the upper body, particularly under fore-aft excitations, and thereby stiffening of the body. The dominant responses of the body seated with a back support and exposed to fore-aft vibration shift to a considerably higher frequency band of 4 Hz, irrespective of the excitation magnitude considered. Such interaction under the side-to-side motion is considerably small due to relatively small biodynamic force developed at the back support driving-point, which is partly caused by lateral sliding of the upper body.

The sitting posture yields small influence on the total power dissipated within the body, derived from the seat pan driving-point measurements, under both axes of vibration of smaller magnitudes (0.25 and 0.5 m/s²). An increase in the excitation magnitude to 1 m/s², however, caused greater energy transfer for the back supported postures under both axes of vibration. An inclined back support would impose relatively less fore-aft vibration to the upper body compared to vertical support, and help to limit the upper body motion, and thereby result in slightly lower energy transfer. The absorbed power responses under the lateral motion revealed an opposite trend, where the inclined support causes slightly larger power at the back support, which may be attributed to relatively less sliding of the upper body against the inclined back support.

The large variation of the vibration power absorption in different vibration directions and postures suggest that a single frequency weighting is not sufficient for the risk assessment of the

horizontal vibration exposure. More specifically, the VPA-based frequency weightings derived in this study suggest that the W_d -weighting defined in the current ISO-2631-1[6] is acceptable for assessing the horizontal vibration exposure of human subject seated without a back support but it is not appropriate for the sitting posture with the body firmly in contact with the back support. The VPA-based frequency weightings may be used to help develop better frequency weighting for the discomfort and risk assessment.

Chapter 8

CONCLUSIONS AND RECOMMENDATIONS FOR FUTURE WORK

8.1 MAJOR CONTRIBUTIONS OF THE DISSERTATION RESEARCH

This dissertation is mainly concerned with the characterisation of seated human body biodynamic responses to uncorrelated multi-axis whole-body vibration (WBV). The major contributions of the dissertation research are summarised below:

- a) Simultaneous measurements of the driving-point biodynamic responses (APMS) and seat-to-head vibration transmissibility (STHT) under individual single axis (fore-aft- x , lateral- y and vertical- z axis); dual axis (xy -, yz - xz -) and three axis (xyz) uncorrelated vibrations;
- b) A methodology for deriving total seated body apparent mass (APMS) on the basis of measures obtained from the two driving-points, namely the seat-pan and the backrest;
- c) Identification of limitations of the currently used frequency response function method (H_1), and application and verification of an alternate frequency response function method (H_v) for analysis of biodynamic responses to uncorrelated multi-axis vibration;
- d) Analyses of cross-axis biodynamic responses of seated occupants single-axis vibration, and coupled effects of multi-axis vibration;
- e) Estimation of seated occupants response to multi-axis vibration from those measured under single axis vibration;
- f) Formulations of target biodynamic responses characterisations of the seated body exposed to multi-axis vibration in terms of measured APMS and STHT functions for applications in biodynamic modelling and developments in anthropo-dynamic manikins;
- g) A methodology for deriving an absorbed power-based frequency weightings for better evaluations of the vibration exposure risk; and
- h) Analysis of the primary contributory factors including the back and hands support conditions.

8.2 MAJOR CONCLUSIONS

The following are the major conclusions drawn from the methods explored and results obtained in the course in this dissertation research:

- a) The study of the seated body responses to multi-axis vibration, which is more representative of the vehicular vibration, is vital for enhancing our understating of health risks associated with multi-axis whole-body vibration exposure of the seated body.
- b) The apparent mass response magnitudes of the seated body derived from the driving-point force measured are substantially lower than those obtained from the total force measured at the seat structure base. This is attributed to lack of consideration of the upper body interactions with the backrest, when the driving-point force is measured directly at the buttock-seat interface. It is further shown that the total seated-body APMS response can be obtained from the vector sum of those measured at the two driving-points, the seat-pan and the backrest.
- c) The exposure to single-axis vibration yields substantial cross-axis apparent mass magnitudes suggesting coupled motions of the seated body. The application of the widely used H_1 frequency response function, however, suppresses the contributions of the cross-axis components and thereby the coupling effect under multi-axis vibration. This is attributable to uncorrelated nature of the multi-axis vibration synthesised in the laboratory.
- d) Power-spectral-density based H_v frequency response function is suggested for the analysis of seated-body responses to uncorrelated multi-axis vibration, which can adequately account for the coupling effect of multi-axis vibration. Greater coupling was observed in the fore-aft and vertical (sagittal plane) responses to dual (xz -) and three (xyz -) axis vibration. The multi-axis vibration induced mainly coupled upper-body sagittal-plane motions which were more clearly evident in the seat-to-head vibration transmissibility responses than in the apparent mass responses.
- e) Characterisation of both, to-the-body and through-the-body responses of the seated body exposed to vibration is thus vital in order to define target functions for developing biodynamic models of the seated body.
- f) The seated occupants responses to orthogonal uncorrelated multi-axis vibration can also be derived from super position of direct- and cross-axis responses obtained under single axis vibration. The results suggest approximately linear biodynamic responses under the excitations and sitting conditions considered in the study, although nonlinear effects of excitation magnitude are evident.
- g) Greater coupled effect of responses in the sagittal-plane is obtained, which is attributed to substantial cross-axis responses in the fore-aft and vertical biodynamic response.
- h) Back and hands supports resulted in higher fore-aft APMS magnitudes when compared to that obtained without the hands and back supports. This can be attributed to the fact that the hands and back supports constrain the upper body motions and impose additional vibration through the supports.
- i) Simultaneously measures of through-the-body (STHT) and to-the-body (APMS) responses revealed comparable primary modes along the lateral or vertical axis, while considerably different modes were under fore-aft vibration. This may be attributed to substantial fore-aft motions of the upper body, particularly of the low inertia body segments.

- j) The power absorbed by the seated body exposed to three-axis vibration can be obtained upon summation of absorbed power responses along the individual axes.
- k) The absorbed power responses of the seated occupants to whole-body vibration can be applied to derive the frequency weightings similar to those in ISO-2631-1. These weightings can further be employed to evaluate the vibration exposure risk factors in the vehicles.
- l) The frequency-weightings derived on the basis of the absorbed power data under fore-aft and lateral vibration were similar to the W_d -weightings defined in ISO-2631-1 for the back unsupported posture but differed considerably for the back supported condition. The results suggest that the standardised weighting W_d is applicable only for the back unsupported postures.

8.3 RECOMMENDATIONS FOR THE FUTURE WORK

The characterisation of the seated occupants responses to more realistic multi-axis vibration is vital for identifying improved frequency weightings and effective model developments, which could lead to improved designs of effective vibration attenuation devices. For this purpose, it is essential to define reliable target data sets involving the seated-body responses to multi-axis vibration. The present study provides the important methodology for characterising biodynamic responses of the seated body exposed to multi-axis vibration, and datasets obtained with a limited sample of subjects. Far more efforts are thus desirable for the advancement of knowledge and for defining reliable datasets. Following are some of the further works that would be most desirable:

- a) Subject pool: This research involved a relatively small sample of subjects with comparable body mass. It is essential to characterise seated body responses for larger subject population so as to clearly define the effects of body mass, anthropometry and the gender.
- b) The vehicular environments generally involve inclined backrest support and considerable correlations among the vibration along different axes, particularly between the vertical, pitch and fore-aft vibration, and between the vertical, roll and lateral vibration. It is thus essential to characterise seated body responses with back support under correlated multi-axis vibration.
- c) The study of vibration transmitted to different body segments is most important for injury prediction under multi-axis vibration, and for defining reliable biodynamic models.

- d) Multi-axis multi-body biomechanical models of the seated body are highly desirable not only for developments in improved vibration isolation systems but also for predicting injury potentials of vibration.
- e) The estimation of distributed absorbed power is also most essential for predicting body segment injuries. This can be obtained from multi-body models of the seated body.

REFERENCES

- [1] Bongers PM, Boshuizen, HC (1999) Back disorders and whole-body vibration at work. Thesis: Univ. of Amsterdam, Holland.
- [2] Fairley TE and Griffin MJ (1990) The apparent mass of the seated human body in the fore-and-aft and lateral directions. *J. of Sound and Vibration*, 139, 299-306.
- [3] Mandapuram S, Rakheja S, Ma S, Demont R (2005) Influence of back support conditions on the apparent mass of seated occupants under horizontal vibration. *Ind. Health*, 43, 421-35.
- [4] Hinz B and Seidel H (1987) The nonlinearity of human body's dynamic response during sinusoidal whole-body vibration. *Journal of Industrial Health*, 25, 169-181.
- [5] BS 6841, (1987) Guide to measurement and evaluation of human exposure to whole-body mechanical vibration and repeated shock.
- [6] ISO-2631-1 (1997) Evaluation of human exposure to whole-body vibration. Part 1: General requirements. International Organization for Standardization, Geneva.
- [7] International Organization for Standardization (1998) International Standard ISO 13090-1. Mechanical Vibration and Shock – Guidance on Safety Aspects and Experiments with People. Part I: Exposure to Whole-Body Mechanical Vibration and Repeated Shocks.
- [8] Boileau P-É, Wu X and Rakheja S (1998) Definition of a range of idealized values to characterize seated body biodynamic response under vertical vibration, *Journal of Sound and Vibration*, 215(4), 841-862.
- [9] Burström L (1990) Absorption of vibration energy in the human hand and arm. Ph.D. Thesis in the department of human work sciences, division of physical environment technology, Luleå University of Technology, Sweden.
- [10] Mansfield NJ, Holmlund P, Lundström R (2001) Apparent mass and absorbed power during exposure to whole-body vibration and repeated shocks. *J Sound Vib* 248 (3), 427-440.
- [11] Nawayseh N (2005) Absorbed power at the seat, backrest and feet of subjects exposed to whole-body vertical vibration. Proc. of the 40th UK Conf. on Human Response to Vibration, Liverpool (United Kingdom), 13-15 September.
- [12] Wang W, Rakheja S, Boileau P-E (2006), The role of seat geometry and posture on the mechanical energy absorption characteristics of seated occupants under vertical vibration. *Int. J Ind Ergon*, 36 (2), 171-184.
- [13] Lundström R, Holmlund P (1998) Absorption of energy during whole-body vibration exposure. *J Sound Vib* 215 (4), 789-799.
- [14] Wu X, Rakheja S and Boileau -É (1999) Analysis of relationships between biodynamic response functions. *J. Sound and Vibr.* 226 (3), 595-606.
- [15] Bendat JS, Piersol AG (1986) Random data: Analysis and measurement procedures, 2nd edition, John Wiley, New York.

- [16] Lee RA, Pradko F (1968) Analytical analysis of human vibration. SAE Transactions 77, Paper No.680091. Automotive Engineering Congress, Detroit, Michigan, 8-12 January.
- [17] Mehta CR, and Tewari VK (2000) Seating Discomfort for Tractor Operators - A Critical Review. International Journal of Industrial Ergonomics 25 661-674.
- [18] Kumar A, Mahajan P, Mohan D and Vargjese M (2001) Journal of Agricultural Engineering Research 80(4), 313-328. Tractor vibration severity and driver Health: a study from Rural India.
- [19] Paddan GS and Griffin MJ (1988) The transmission of translational seat vibration to the head – I. Vertical seat vibration. J. of Biomechanics, 21, 191-197.
- [20] Paddan GS and Griffin MJ (1988) The transmission of translational seat vibration to the head – II. Horizontal seat vibration. J. of Biomechanics, 21, 199-206.
- [21] Nawayseh N and Griffin MJ (2004) Tri-axial forces at the seat and backrest during whole-body vertical vibration, Journal of Sound and Vibration, 277, 309-326.
- [22] Bovenzi M and Hulshof CTJ (1999) An Updated Review of Epidemiologic Studies on the Relationship between Exposure to Whole-Body Vibration and Low Back Pain (1986-1997). International Archives of Occupational and Environmental Health 72: 351-365.
- [23] Magnusson M, Hansson T, Pope M (1994) The effect of seat back inclination on spine height changes. Applied Ergonomics, 25(5), 294-298.
- [24] Zimmermann CL, Cook TM, Goel VK (1993) Effects of seated posture on erector spinae EMG activity during whole body vibration. Ergonomics, 36(6), 667-675.
- [25] VIN: Vibration Injury Network (2001) Review of methods for evaluating human exposure to whole-body vibration. Appendix W4A to final report: BMH4-CT98-3291.
- [26] Anderson JS, Boughflower RAC (1978) Measurement of the energy dissipated in the hand and arm whilst using vibratory tools. Appl Acou 11, 219–24.
- [27] Demić M, Lukić J and Milić Ž (2002) Some Aspects of the Investigation of Random Vibration Influence on Ride Comfort. Journal of Sound and Vibration 253(1), 109-129.
- [28] Hinz B, Seidel H, Menzel G and Blüthner R (2002) Effects Related To Random Whole-Body Vibration And Posture On A Suspended Seat With And Without Backrest. Journal of Sound and Vibration 253 (1), 265-282.
- [29] Paddan GS and Griffin MJ (2002) Effect of Seating on Exposures to Whole-Body Vibration in Vehicles. Journal of Sound and Vibration 253(1), 215-241.
- [30] Paddan GS and Griffin MJ (2002) Evaluation of Whole-Body Vibration in Vehicles. Journal of Sound and Vibration 253(1), 195-213.
- [31] Programme for technical risk factors national institute for working life Research Network on Detection and Prevention of Injuries due to occupational vibration exposures (EU BIOMED 2 concerted Action Programme) October 13, 2003. Centralized European Database for Whole-Body Vibration in the Earth-Moving Vehicles. <http://umetech.niwl.se/vibration/WBVHome.html>.
- [33] Chris A. Marsili, L. Ragni, and G. Vassalini (1998) Journal of Agricultural Engineering Research 70, 295–306. Vibration and Noise of a Tracked Forestry Vehicle.

- [33] Marsili A, Ragni L, Santoro G, Servadio P and Vassalini G (2002) Innovative Systems to Reduce Vibrations on Agricultural Tractors: Comparative Analysis of Acceleration Transmitted Through the Driving Seat. *Biosystems Engineering* 81 (1), 35-47.
- [34] Donati P (2002) Survey of Technical Preventative Measures to Reduce Whole-Body Effects when Designing Mobile Machinery. *Journal of Sound and Vibration* 253(1), 169-183.
- [35] Scarlett AJ, Price JS and Stayner RM (2002) Whole-Body Vibration: Initial Evaluation of Emissions Originating from Modern Agricultural Tractors. Silsoe Research Institute and RMS Vibration Test Laboratory for the Health and Safety Executive (Contract Research Report 413/2002).
- [36] Boileau P-É (1995) A study of secondary suspensions and human driver response to whole-body vehicular vibration and shock, Ph.D. Thesis, (Concordia University).
- [37] Wang W, Rakheja S and Boileau P-É (2006) Effect of back support condition on seat to head transmissibilities of seated occupants under vertical vibration. *Journal of Low Freq. Noise, Vibration and Active Control*, 25(4), 239-259.
- [38] Paddan GS and Griffin MJ (1993) The transmission of translational floor vibration to the heads of standing subjects, *Journal of Sound and Vibration*, 160(3), 503-521.
- [39] Pope MH, Broman H, Hansson T (1990) Factors affecting the dynamic response of the seated subject. *J. Spinal Disorders*, 3, 135-142.
- [40] Matsumoto Y and Griffin MJ (2002) Effect of muscle tension on non-linearities in the apparent masses of seated subjects exposed to vertical whole-body vibration. *Journal of Sound and Vibration*, 253(1), 77-92.
- [41] Coermann RR (1962) The mechanical impedance of the human body in sitting and standing position at low frequencies, *Human Factors*, 4, 227-253.
- [42] Kim TH, Kim YT and Yoon YS (2005) Development of a biomechanical model of the human body in a sitting posture with vibration transmissibility in the vertical direction. *Int. J. of Industrial Ergonomics*, 35, 817-829.
- [43] Wu X (1998) Study of driver-seat interactions and enhancement of vehicular ride vibration environment. Ph.D. Thesis, Concordia University, Montreal, Canada.
- [44] Matsumoto Y and Griffin MJ (1998) Movement of the upper body of seated subjects exposed to vertical whole-body at the principal resonance frequency, *Journal of Sound and Vibration*, 215(4), 734-762.
- [45] Matsumoto Y and Griffin MJ (2000) Comparison of biodynamic responses in standing and seated human bodies. *Journal of Sound and Vibration*, 238(4), 691-704.
- [46] Mansfield NJ and Griffin MJ (2000) Nonlinearities in apparent mass and transmissibility during exposure to whole-body vertical vibration. *J. of Biomechanics*, 33, 933-941.
- [47] Wang W, Rakheja S and Boileau P-É (2008) Relationship between measured apparent mass and seat-to-head transmissibility responses of seated occupants exposed to vertical vibration. *J. of Sound and Vibration*, 314, 907-922.

- [48] Pranesh AM, Rakheja S and Demont R (2010) Influence of support conditions on vertical whole-body vibration of the seated human body. *Industrial Health*, 48, 682-697.
- [49] Kitazaki S. and Griffin M. J. (1997) A modal analysis of whole-body vertical vibration, using a finite element model of the human body. *J. Sound Vib.* 200 (1), 83-103.
- [50] Stein GJ, Múčka P, Chmúrny R, Hinz B and Blüthner R (2007) Measurement and modelling of x-direction apparent mass of the seated human body–cushioned seat system. *Journal of Biomechanics*, 40, 1493–1503.
- [51] Mansfield N. J. and Maeda S. (2007) The apparent mass of the seated human exposed to single axis and multi-axis whole-body vibration. *J. of Biomechanics*, 40, 2543-2551.
- [52] Hinz B, Blüthner R, Menzel G, Rützel S, Seidel H and Wölfel Horst P (2006) Apparent mass of seated men – Determination with single and multi-axis excitation at different magnitudes, *Journal of Sound and Vibration*, 298, 788-809.
- [53] Hinz B, Menzel G, Blüthner R and Seidel H, (2010) Seat-to-head transfer function of seated men – determination with single and Three-axis excitations at different magnitudes. *Industrial Health* 48, 565-583.
- [54] Edwards RG and Lange KO (1964) A mechanical impedance investigation of human response to vibration. AMRL-TR-64-91, Aerospace Medical Research Lab, Wright-Patterson Air Force Base, Ohio, USA.
- [55] Vykukal, HC (1968) Dynamic response of the human body to vibration when combined with various magnitudes of linear acceleration. *Aerospace Medicine*, 39, 1163-1166.
- [56] Vogt HL, Coermann RR and Fust HD (1968) Mechanical impedance of the sitting human under sustained acceleration. *Aerospace Medicine*, 39, 675-679.
- [57] Suggs CW, Abrams CF and Stikeleather LF (1969) Application of a damped spring-mass human vibration simulating vibration testing of vehicle seats. *Ergonomics*, 12, 79-90.
- [58] Miwa T (1975) Mechanical impedance of human body in various postures, *Industrial Health*, 13, 1-22.
- [59] Mertens H (1978) Nonlinear behaviour of sitting humans under increasing gravity. *Aviation Space and Environmental Medicine*, 49, 287-298.
- [60] Sandover J and Dupuis H (1987) A reanalysis of spinal motion during vibration. *Ergonomics*, 30, 975-985.
- [61] Donati PM and Bonthoux C (1983) Biodynamic response of the human body in the sitting position when subjected to vertical vibration, *Journal of Sound and Vibration*, 90, 423-442.
- [62] Fairley TE and Griffin MJ (1986) A test method for the prediction of seat transmissibility. Society of Automotive Engineers International Congress and Exhibition, Paper No. 860046.
- [63] Fairley TE and Griffin MJ (1983) Application of mechanical impedance methods to seat transmissibility. *Int. Conf. on Noise Control Engineering*, Edinburgh, UK, 533-536.
- [64] Fairley TE and Griffin MJ (1989) The apparent mass of the seated human body: vertical vibration. *Journal of Biomechanics*, 22, 81-94.

- [65] Mansfield NJ (1994) The apparent mass of the human body in the vertical direction – The effect of vibration magnitude, Proc. of the UK Group Meet on Human Response to Vibration, Gosport, Hants, UK, 19-21 September.
- [66] Matsumoto Y and Griffin MJ (1998) Movement of the upper body of seated subjects exposed to vertical whole-body at the principal resonance frequency, *Journal of Sound and Vibration*, 215(4), 734-762.
- [67] Kitazaki S. and Griffin M. J. (1998) Resonance behaviour of the seated human body and effects of posture. *J. of Biomechanics*, 31(2), 143-149.
- [68] Wu X (1998) Study of driver-seat interactions and enhancement of vehicular ride vibration environment. Ph.D. Thesis, Concordia University, Montreal, Canada.
- [69] Boileau P-É and Rakheja S (1998) Whole-body vertical biodynamic response characteristics of the seated vehicle driver: Measurement and model development. *International Journal of Industrial Ergonomics*, 22(6), 449-472.
- [70] Holmlund P (1999) Absorbed power and mechanical impedance of the seated human within a real vehicle environment compared with single-axis laboratory data. *J. of Low Freq. Noise, Vib. and Active Control*, 18(3), 97-110.
- [71] Holmlund P, Lundström R and Lindberg L (2000) Mechanical impedance of the human body in vertical direction. *Applied Ergonomics*, 31(4), 415-422.
- [72] Nawayseh N (2001) Non-linear behaviour and two dimensional movement of the human body in response to vertical vibration. Proc. of the 36th UK Conf. on Human Response to Vibration, Farnborough, UK, 12-14 September, 288-296.
- [73] Rakheja S, Stiharu I and Boileau, P-É (2002) Seated occupant apparent mass characteristics under automotive postures and vertical vibration, *Journal of Sound and Vibration*. 253(1), 57-75.
- [74] Matsumoto Y and Griffin MJ (2002) Effect of muscle tension on non-linearities in the apparent masses of seated subjects exposed to vertical whole-body vibration. *Journal of Sound and Vibration*, 253(1), 77-92.
- [75] Mansfield NJ and Griffin MJ (2002) Effects of posture and vibration magnitude on apparent mass and pelvis rotation during exposure to whole-body vertical vibration. *Journal of Sound and Vibration*, 253(1), 93-107.
- [76] Hinz B, Seidel H, Menzel G, Gericke L, Blüthner R and Keitel J (2004) Seated occupant apparent mass in automotive posture – examination with groups of subjects characterized by a representative distribution of body mass and body height. FIOSH Document 2004/4 Z.ARB.WISS.
- [77] Wang W, Rakheja S and Boileau P-É (2004) Effects of sitting postures on biodynamic response of seated occupants under vertical vibration. *International Journal of Industrial Ergonomics*, 34(4), 289-306.
- [78] Maeda S, Mansfield NJ (2005) Comparison of the apparent mass during exposure to whole-body vertical vibration between Japanese subjects and ISO-5982 standard. *Industrial Health*, 43, 413-420.

- [79] Mansfield NJ and Maeda S (2005) Comparison of the apparent mass of the seated human measured using random and sinusoidal vibration. *Industrial Health*, 43, 233-240.
- [80] Nawayseh N and Griffin MJ (2005) Effect of seat surface angle on forces at the seat surface during whole-body vertical vibration. *Journal of Sound and Vibration*, 284, 613-634.
- [81] Huang Y and Griffin MJ (2006) Effect of voluntary periodic muscular activity on nonlinearity in the apparent mass of the seated human body during vertical random whole-body vibration. *Journal of Sound and Vibration*, 298, 824-840.
- [82] Patra SK, Rakheja S, Nelisse H, Boileau P-É and Boutin J (2008) Determination of reference values of apparent mass responses of seated occupants of different body masses under vertical vibration with and without a back support. *Int. J. of Industrial Ergonomics*, vol. 38 5-6 p.483-498.
- [83] Mansfield NJ, Holmlund P, Lundström R, Lenzuni P and Nataletti P (2006) Effect of vibration magnitude, vibration spectrum and muscle tension on apparent mass and cross-axis transfer functions during whole-body vibration exposure, *J. of Biomechanics*, 39, 3062-3070.
- [84] Holmlund P and Lundström R (1998) Mechanical impedance of the human body in the horizontal direction. *J. of Sound and Vibration*, 215(4), 801-812.
- [85] Mansfield NJ and Lundström R (1999) The apparent mass of the human body exposed to non-orthogonal horizontal vibration, *J. of Biomechanics*, 32(12), 1269-1278.
- [86] Holmlund P and Lundström R (2001) Mechanical impedance of the sitting human body in single-axis compared to multi-axis whole-body vibration exposure. *Clinical Biomechanics*, 16(Supplement 1), S101-S110.
- [87] Nawayseh N and Griffin MJ. (2005) Non-linear dual-axis biodynamic response to fore-and-aft whole-body vibration, *Journal of Sound and Vibration*, 282, 831-862.
- [88] Griffin MJ, Lewis CH, Parsons KC and Whitham EM (1978) The biodynamic response of the human body and its application to standards Proceedings of the AGARD Conf., Proc. No. 253, Paris, France.
- [89] Zimmermann CL, Cook TM (1997) Effects of vibration frequency and postural changes on human responses to seated whole-body vibration. *Int. Arc. Of Occ. & Enf. Health*, 69: 165-179.
- [90] Wu X (1998) Study of driver-seat interactions and enhancement of vehicular ride vibration environment. Ph.D. Thesis, Concordia University, Montreal, Canada.
- [91] Hinz B, Menzel G, Blüthner R and Seidel H (2001) Transfer functions as a basis for the verification of models – variability and restraints. *Clinical Biomechanics*, 16(Suppl. 1), S93-S100.
- [92] Griffin MJ (1990) London: Academic Press. Handbook of Human Vibration.
- [93] Mansfield NJ and Maeda S (2006) Comparisons of the apparent masses and cross-axis apparent masses of seated body exposed to single and dual-axis whole-body vibration. *Journal of Sound and Vibration*, 298, 841-853.

- [94] Matsumoto Y and Griffin MJ (2002) Effect of muscle tension on non-linearities in the apparent masses of seated subjects exposed to vertical whole-body vibration. *Journal of Sound and Vibration*, 253(1), 77-92.
- [95] Nawayseh N and Griffin MJ (2005) Non-linear dual-axis biodynamic response to fore-and-aft whole-body vibration, *Journal of Sound and Vibration*, 282, 831-862.
- [96] Rakheja S, Stiharu I, Zhang H and Boileau P-É (2006) Seated occupant interactions with seat backrest and pan, and biodynamic responses under vertical vibration, *Journal of Sound and Vibration*, 298, 651-671.
- [97] Griffin MJ, Whitham EM, Parsons KC (1982) Vibration and comfort. II. Translational seat vibration. *Ergonomics*, 25, 603-630.
- [98] Magnusson M, Hansson T, Pope M (1994) The effect of seat back inclination on spine height changes. *Applied Ergonomics*, 25(5), 294-298.
- [99] White AA, Panjabi MM (1990) *Clinical Biomechanics of the Spine*. Lippincott-Raven Publishers, Philadelphia, USA.
- [100] Paddan GS and Griffin MJ (1994) Transmission of roll and pitch vibration to the head, *Ergonomics*, 37(9), 1513.
- [101] Holmlund P and Lundström R (1998) Mechanical impedance of the human body in the horizontal direction. *J. of Sound and Vibration*, 215(4), 801-812.
- [102] Nishiyama S, Uesugi N, Takeshima T, Kano Y and Togi H (2000) Research on vibration characteristics between human body and seat, steering wheel, and pedals (effects of seat position on ride comfort). *J. of Sound and Vibration*, 236(1), 1-21.
- [103] Pope MH, Broman H, Hansson T (1990) Factors affecting the dynamic response of the seated subject. *J. Spinal Disorders.*, 3, 135-142.
- [104] Mansfield Neil J and Griffin MJ (1998) Effect of magnitude of vertical whole-body vibration on absorbed power for the seated human body, *Journal of Sound and Vibration*, 215(4), 813-825.
- [105] Wong JY (1993) *Theory of ground vehicles*. John Wiley & Sons, Inc.
- [106] Paddan GS and Griffin MJ (1988) The transmission of translational seat vibration to the head – II. Horizontal seat vibration. *J. of Biomechanics*, 21, 199-206.
- [107] Qiu Y and Griffin MJ (2010) Biodynamic responses of the seated human body to single-axis and dual-axis vibration. *Industrial Health* 48, 615-627.
- [108] Rocklin GT, Crowley J and Vold H, (1985) A comparison of H_1 , H_2 , and H_v frequency response functions, *Proceedings of the 3rd international Modal Analysis Conference*, Orlando, FL, vol. 1 pp 272-278.
- [109] Dong RG, Wu JZ, and Welcome DE (2005) Recent advances in biodynamics of hand-arm system. *Industrial Health* 43, 449-471.

- [110] Bendat JS and Piersol AG (1993) Engineering applications of correlation and spectral analysis. John Wiley & Sons.
- [111] Griffin MJ and Whitham EM (1978) Individual variability and its effect on subjective and biodynamic response to whole-body vibration. *Journal of Sound and Vibration*, 58, 239-250.
- [112] Nélisse H, Patra S, Rakheja S, Boutin J, Boileau P-É (2008) Assessments of two dynamic manikins for laboratory testing of seats under whole-body vibration *Intl J Indus Ergonomics*, 38, 457-470.
- [113] Boileau P-É, Rakheja S, Yang X, Stiharu I (1997) Comparison of biodynamic response characteristics of various human body models as applied to seated vehicle drivers. *Noise and Vibration Worldwide*, 28 (9), 7-15.
- [114] Liang C-C, Chiang C-F (2006) A study of biodynamic models of seated human subjects exposed to vertical vibration. *Int. J. of Ind. Ergonomics*, 36, 869-890.
- [115] Fritz, Martin (2005) Dynamic properties of the biomechanical model of the human body – influence of posture and direction of vibration stress. *J. Low Freq. Noise, Vib. and Active Control*, 24(4), 233-249.
- [116] Rakheja S, Mandapuram S, Dong R (2008) Energy absorption of seated occupants exposed to horizontal vibration and role of back support. *Ind Health* 46, 550-66.
- [117] Nawayseh N and Griffin MJ (2005) Tri-axial forces at the seat and backrest during whole-body fore-aft vibration, *J Sound Vib* 281, 921-42.
- [118] Nawayseh N and Griffin MJ (2003) Non-linear dual-axis biodynamic response to vertical whole-body vibration, *J Sound Vib* 268, 503-23.
- [119] Winter DA (1990) *Biomechanics and motor control of human movement*. John Wiley & Sons, Toronto. 25)
- [120] Boileau P-É and Rakheja S (2000) Caractérisation de l'environnement vibratoire dans différentes catégories de véhicules : industriels, utilitaires et de transport urbain. IRSST Report R-242, Montréal, 162 p.
- [121] Mandapuram S, Rakheja S, Boileau P-É, Maeda S and Shibata N (2010) Apparent mass and seat-to-head transmissibility responses of seated occupants under single and dual axis horizontal vibration. *Industrial Health* 48, 698-714.
- [122] Mansfield NJ (2005) *Human Response to Vibration*, CRC Press.
- [123] Woodman PD (1996) The effect of the head-helmet coupling on the relative acceleration between head and helmet. *United Kingdom Conference on Human Response to Vibration* pp. 18-20.
- [124] Smith SD, Smith JA and Newman RJ (2000) Helmet system performance in vibration environments. *United Kingdom Conference on Human Response to Vibration* pp 13-15.
- [125] Pope MH, Svensson, Broman MH and Anderson GBJ (1986) Mounting of the transducer in measurement of segmental motion of the spine. *Journal of Biomechanics*, 19, 675-677.

- [126] Kitazaki S and Griffin MJ (1995) A data correction method for surface measurement of vibration of the human body. *Journal of Biomechanics* 28, 885–890.
- [127] Moschioni G, Saggin B, Tarabini M, Zappa E, 4th Whole-body injury conference proceedings, Montreal Canada, June 2009 (4) 49-50.
- [128] Cation S, Jack R, Oliver M, Dickey JP, Lee-Shee NK (2008) Six degree of freedom whole-body vibration during forestry skidder operations. *International Journal of Industrial Ergonomics*, 38 (9-10), 739-757.
- [129] Eger T, Stevenson J, Boileau P-É, Salmoni A and Vib RG (2008) Predictions of health risks associated with the operation of load-haul-dump mining vehicles: Part 1-Analysis of whole-body vibration exposure using ISO 2631-1 and ISO-2631-5 standards. *International Journal of Industrial Ergonomics* 38 (9-10), 726-738.
- [130] Mandapuram S, Rakheja S, Marcotte P and Boileau P-É (2011) Analyses of biodynamic responses of seated occupants to uncorrelated fore-aft and vertical whole-body vibration. *Journal of Sound and Vibration*, 330 (16) 4064-4079.
- [131] Rakheja S, Dong RG, Patra S, Boileau P-É, Marcotte P, Warren C (2010) Biodynamics of the human body under whole-body vibration: Synthesis of the reported. *International Journal of Industrial Ergonomics* 40, 710-732.
- [132] Burström L (1990) Measurement of the mechanical absorption in the hand and arm whilst using vibrating tools. *Journal of Low Frequency Noise and Vibration Control* 9, 1-14.
- [133] Mandapuram S, Rakheja S, Boileau P-É and Maeda S (2012) Apparent mass and head vibration transmission responses of seated body to three translational axis vibration. *International Journal of Industrial Ergonomics*, vol. 42, 268-277.
- [134] Boileau P-É, Rakheja S (1996) Évaluation et étude du comportement dynamique d'un système de suspension torsio-élastique pour véhicules tout terrain, Études et recherches / Rapport R-124, Montréal, IRSST.
- [135] Marsili A, Ragni L, Vassalini G (1998) Vibration and noise of a tracked forestry vehicle. *J Agric Eng Res* 70, 295-306.
- [136] Donati P (1998) A procedure for developing a vibration test method for specific categories of industrial trucks. *J Sound Vib* 215 (4), 947-957.
- [137] Bovenzi M, Pinto I, Stacchini N (2002) Low back pain in port machinery operators. *J Sound Vib* 235(1), 3-20.
- [138] Maeda S, Morioka M (1998) Measurement of whole-body vibration exposure from garbage trucks. *J Sound Vib* 215 (4), 959-964.
- [139] J. F. Golding, H. M. Markley, and J. R. R. Stott (1994) The effects of motion, body axis, and posture on motion sickness induced by low frequency linear oscillation. Proc. of the 29th UK Group Meeting on Human Response to Vibration, Alverstone, Gosport (United Kingdom), 19-21 September.
- [140] Lundström R, Holmlund P, Lindberg L (1998) Absorption of energy during vertical whole-body vibration exposure. *J Biomech* 31, 317-326.

[141] Mansfield NJ (2005) Impedance methods (apparent mass, driving point mechanical impedance and absorbed power) for assessment of the biomechanical response of the seated person to whole-body vibration. *Ind Health* 43, 378-389.

[142] Dong RG, Welcome DE, McDowell TW, Wu JZ, Schopper AW (2006) Frequency weighting derived from power absorption of fingers-hand-arm system under z_h -axis. *Journal of Biomechanics* 39, 2311-2324.